

University of Alberta

Black carbon in Quebec boreal black spruce forests

by

Laure Nalini Soucémarianadin

A thesis submitted to the Faculty of Graduate Studies and Research
in partial fulfillment of the requirements for the degree of

Doctor of Philosophy

in

Soil Science

Department of Renewable Resources

©Laure Nalini Soucémarianadin

Fall 2013

Edmonton, Alberta

Permission is hereby granted to the University of Alberta Libraries to reproduce single copies of this thesis and to lend or sell such copies for private, scholarly or scientific research purposes only. Where the thesis is converted to, or otherwise made available in digital form, the University of Alberta will advise potential users of the thesis of these terms.

The author reserves all other publication and other rights in association with the copyright in the thesis and, except as herein before provided, neither the thesis nor any substantial portion thereof may be printed or otherwise reproduced in any material form whatsoever without the author's prior written permission.

Abstract

Wildfires affect boreal forest carbon stocks through consumption of the vegetation and forest floor, and production of black carbon (BC). This by-product of organic matter's incomplete combustion is an important component of the global soil carbon pool. My thesis reveals how fire severity is related to BC chemical and physical properties and how it influences both soil organic carbon (SOC) and BC stocks in forest floors and mineral soils of fire-affected Quebec black spruce forests. This work also attempts to uncover BC storage mechanisms in mineral horizons.

I collected BC samples produced by 2005–2007 wildfires, and compared them to laboratory-produced samples. As indicated by ^{13}C NMR spectroscopy, elemental analysis, surface area analysis, and scanning electron microscopy, formation conditions – mostly maximum temperature – greatly affected BC properties, which in turn may determine its potential as a carbon sink. BC condensation increased with increasing fire severity, as shown by decreasing atomic H/C and O/C ratios. The fraction of aromatic carbon:total carbon of all these freshly-produced BC was low, suggesting that they may be susceptible to rapid physical alteration and chemical degradation. However, these BC were characteristic of early-season fires, which resulted in low temperatures ($\leq 250\text{ }^\circ\text{C}$) and overall, low fire severity, in forest floors.

Mineral horizons contained SOC stocks comparable to those in forest floors, but their BC stocks were significantly lower. In the fire sites I studied, forest floor's BC stocks were mostly influenced by past severe fires, with the deepest

layer containing most of the BC stocks. In mineral soils, SOC and BC concentrations were strongly correlated. To further explore the relationship between podzolization and BC storage mechanisms, I measured SOC and BC content in size and density fractions of podzolic B horizons. While some BC was found in unprotected particulate organic matter (POM), the rest was associated with organo-mineral and organo-metallic complexes in the micro-aggregate protected POM and fine fraction. Podzolization processes result in idiosyncratic patterns of SOC accumulation in the mineral subsoil; here I show that patterns of BC and SOC accumulation are similar, with the greater BC stocks being found in podzolic B horizons.

Acknowledgements

This PhD would not have been possible without the people mentioned on this page. I would never thank you enough, sincerely.

First and foremost, I'd like to thank Dr. Sylvie Quideau for her patience and always thorough comments (thanks for letting me stand on my own but keeping me on my feet when I needed it), and my committee members, Dr. Derek MacKenzie and Dr. Rod Wasylishen for their support and helpful feedback all along these four years.

I'd like to acknowledge Dr. Alison Munson for getting me on board with this project, for all the help with the fieldwork and for the feedback over the years, and also Dr. Guy Bernard for his patience while showing me the ropes with the spectrometers: thanks for working your magic on them so many times.

Thanks to Jeff Liu, Hawley Campbell, Luke Donnan, Cassandra MacKenzie, and Olga Kulikova for assisting in the lab with my endless samples. To all of you, thanks for your patience and your enthusiasm!

Un grand merci à Juliette Boiffin et Sylvain Pelletier-Bergeron pour leur collaboration et pour avoir rendu fun ces étés de terrain. Merci également à André Beaumont, Jérôme Bérubé, Mathieu Blanchette et Thomas Payer pour leur aide précieuse sur le terrain. Tous mes remerciements à Mawie et Jaja pour avoir fait de ces moments à Québec (presque) des vacances et pour leur amitié.

Merci Maman et Papa de votre soutien pendant ces quatre années, merci pour le skype dominical et tout l'amour dont vous avez fait preuve. Mimi et Jean-Rémi : merci d'avoir attendu... vous m'avez donné la motivation pour (presque) finir plus vite ! Merci Mally d'avoir été là depuis les balbutiements de ce projet de thèse et d'avoir cru en moi, comme tu le fais toujours, durant les moments difficiles.

Merci Martine pour ton soutien inconditionnel pendant ces quatre ans (et ces 21 années d'amitié !), pour toutes ces *paillettes* dont tu as saupoudré nos moments ensemble et pour ton inépuisable énergie et enthousiasme, qui font que la vie à tes côtés est toujours palpitante! Et dans le désordre : merci Val & Lolo pour le soutien, les random skypes et tout le reste... mais surtout Babichou/Alice ! Votre petit ange saura, sans doute, me faire garder les deux pieds sur terre ! Merci aux filles de La Source et plus particulièrement Kro, Marie, Alex, Cap'taine, JayGee (et Mémé aussi...) : merci d'avoir continué à me faire jeangéliner malgré les kilomètres !

I've met a lot of great people during these four years but I'd like to personally thank you, Dani, Gaby, Erin, Sanatan, Emily (and Rasmus) for all the good times, either spent talking about research, reinventing the world, playing crazy games, and/or attending weird fitness classes... but mostly for being there!

Almost last but definitely not least: MANY THANKS to the Rockers for letting me be part of your awesome family and for keeping me sane with all your craziness!

Finally, I would like to thank the Natural Sciences and Engineering Research Council of Canada and the Canadian Circumpolar Institute, for their funding and support.

Table of Contents

Chapter 1. Introduction

1.1. Carbon and carbon cycle.....	1
1.1.1. Carbon allotropes: the different forms of carbon.....	1
1.1.2. Carbon isotopes.....	2
1.1.3. Global carbon cycle.....	3
1.2. What is black carbon? – A definition.....	12
1.3. BC characterization and BC quantitation – solid-state ¹³ C nuclear magnetic resonance (NMR) spectroscopy.....	14
1.3.1. Fundamental properties.....	14
1.3.2. The cross polarization technique.....	16
1.3.3. The direct polarization technique and spin counting.....	18
1.3.4. Data analysis.....	19
1.4. Boreal forests.....	21
1.4.1. The different forest biomes.....	21
1.4.2. Boreal forests.....	22
1.5. BC storage and degradation.....	23
1.5.1. Is recalcitrance an appropriate notion?.....	23
1.5.2. BC degradation.....	25
1.6. Objectives and outline of the thesis.....	28
List of References.....	30

Chapter 2. Laboratory charring conditions affect black carbon properties: A case study from Quebec black spruce forest

2.1. Introduction.....	38
2.2. Material and methods.....	40
2.2.1. Creation of reference set.....	40
2.2.2. Charring conditions.....	41
2.2.3. BC characterization.....	42
2.2.4. Spectroscopic analysis.....	43
2.2.5. Data analysis.....	46
2.3. Results and discussion.....	47
2.3.1. Influence of MT.....	47
2.3.2. Influence of fuel type.....	51
2.3.3. Influence of charring duration.....	54
2.3.4. Influence of oxygen.....	55
2.3.5. Relative importance of various formation factors – example of the degree of aromatisation.....	57
2.4. Conclusions.....	58
Tables and Figures.....	60
List of References.....	70

Chapter 3. Early season fires in boreal black spruce forests produce black carbon with low aromatic content

3.1. Introduction.....	77
3.2. Materials and methods.....	80

3.2.1.	Site characteristics and selection.....	80
3.2.2.	Fire severity gradient.....	81
3.2.3.	Field collection of BC samples.....	83
3.2.4.	BC set produced under controlled laboratory conditions	84
3.2.5.	Characterization of BC chemical properties.....	84
3.2.6.	Characterization of BC physical properties.....	88
3.2.7.	Statistical analyses: influence of fire severity.....	88
3.3	Results.....	89
3.3.1.	Fire severity gradient.....	89
3.3.2.	Black carbon physical properties.....	89
3.3.3.	Black carbon elemental composition.....	90
3.3.4.	Black carbon molecular composition.....	91
3.3.5.	Comparison with the BC reference set.....	93
3.4	Discussion.....	94
3.4.1.	Formation conditions for the sampled BC.....	94
3.4.2.	BC properties and implications for their role in black spruce forests.....	98
3.5	Conclusion.....	100
	Tables and Figures.....	102
	List of References.....	112

Chapter 4. Total carbon and black carbon stocks in black spruce forest floors from eastern Canada: A quantitative study

4.1.	Introduction.....	120
4.2.	Materials and methods.....	123
4.2.1.	Site characteristics.....	123
4.2.2.	Sampling protocol.....	125
4.2.3.	Laboratory analyses.....	127
4.2.4.	Statistical analyses.....	131
4.3.	Results.....	131
4.3.1.	Forest floor carbon stocks.....	131
4.3.2.	Forest floor characteristics.....	133
4.3.3.	Black carbon content.....	135
4.4.	Discussion.....	137
4.4.1.	Fire effects on forest floor characteristics.....	137
4.4.2.	Carbon and black carbon stocks.....	139
4.5.	Conclusions.....	144
	Tables and Figures.....	146
	List of References.....	159

Chapter 5. Black carbon stocks and storage mechanisms in podzolic soils of fire-affected Quebec black spruce forests

5.1.	Introduction.....	168
5.2.	Materials and methods.....	171
5.2.1.	Site characteristics.....	171
5.2.2.	Soil sampling protocol.....	173
5.2.3.	Laboratory analyses.....	174

5.2.4.	BC quantitation.....	176
5.2.5.	Data analysis.....	177
5.3.	Results.....	178
5.3.1.	Calibration of the KMD digestion.....	178
5.3.2.	Bulk mineral soil.....	179
5.3.3.	Fractionated podzolic B horizons.....	184
5.4.	Discussion.....	185
5.4.1.	SOC and BC storage in the mineral soil.....	185
5.4.2.	BC stocks: mineral soil vs. forest floor.....	188
5.5.	Conclusions.....	191
	Tables and Figures.....	192
	List of References.....	203
Chapter 6. Conclusions		
6.1.	Main research objectives.....	208
6.2.	Specific research questions.....	209
6.3.	Research implications.....	212
6.4.	Study limitations and future research perspectives.....	215
6.5.	Conclusion.....	218
	List of References.....	219

List of Tables

Table 2-1. Yield (%) and characteristics of BC produced from three fuel-types, under varying maximum temperature, charring duration and pyrolysis type.	61
Table 3-1. Selected physical and elemental properties of BC samples produced by wildfire of the 6 severity classes observed in the field (0 to 5).....	103
Table 3-2. Distribution (% of total integrated spectral area from ¹³ C CPMAS NMR spectra) of the four main spectral regions for BC samples produced by wildfire of the 6 severity classes observed in the field (0 to 5).....	105
Table 4-1. Average organic matter (entire forest floor) thickness (cm) before fire (OMt), organic matter depth consumed by fire (OMc), residual organic matter thickness (ROM), and forest floor carbon stock after fire.....	147
Table 4-2. Thickness (cm) of each organic layer sampled after fire, pH of the F horizon, and nitrogen content (%) of the bulk forest floor.....	148
Table 4-3. C and BC stocks in the forest floor of the 23 soil profiles.....	149
Table 5-1. Mean physical and chemical properties of different mineral horizons, including particle size distribution, BC, SOC, pyrophosphate-extracted Al, Fe and total sesquioxides contents.....	192
Table 5-2. Influence of zones of homogeneous fire cycle and climatic conditions and stand types on (a) particle size distribution and pH of mineral horizons, and on POD Index and on (b) SOC and BC stocks of soil profiles.....	193
Table 5-3. Pearson and non-parametric rank correlation analyses between SOC, BC and various soil parameters for (a) all horizons; (b) soil profiles; (c) podzolic B horizons; (d) individual horizons.....	194
Table 5-4. BC and SOC stocks in organic and mineral horizons, and complete soil profiles.....	196

List of Figures

Figure 1-1. The global carbon cycle.....	4
Figure 1-2. The global black carbon cycle.....	12
Figure 1-3. The variable-amplitude cross polarization (VACP) pulse sequence with application of ten proton amplitudes.....	18
Figure 2-1. ¹³ C VACP NMR spectra of black spruce branch, Sphagnum and Rhododendron, submitted to different maximum temperatures (MTs) and charring durations.....	63
Figure 2-2. SEM micrographs of BC from black spruce (BSP) wood (bark and branches), Sphagnum and Rhododendron submitted to increasing MT.....	64
Figure 2-3. Distribution of total pore volume between micro, meso and macropores for BC produced from black spruce (BSP) branch and <i>Sphagnum</i> at various maximum temperatures.....	65
Figure 2-4. Main types of physisorption isotherms and hysteresis loops: (a) BC from Sphagnum at 75 °C; (b) BC from black spruce branch at 350 °C; (c) BC from Sphagnum at 800 °C.....	66
Figure 2-5. ¹³ C CP NMR spectra of three fuels after a thermal treatment at 75 °C for 24 h.....	67
Figure 2-6. Van Krevelen diagram showing the BC produced here and those from Keiluweit et al. (2010) and Baldock and Smernik (2002).....	68
Figure 2-7. Degree of aromatisation with increasing MT (75–600 °C) for BC formed under full (SB) or partial (Tin) pyrolysis conditions.....	69
Figure 3-1. Location of the 14 selected fires in the black spruce-moss domain of Quebec.....	106
Figure 3-2. Repartition of total pore volume between micro-, meso-, and macropores; and specific surface area for three BC samples produced by wildfires of different fire severity classes and two precursor materials.....	107
Figure 3-3. SEM micrographs of BC samples produced by wildfire of different fire severity classes (0, 2, 4, and 5).....	108
Figure 3-4. van Krevelen plot for BC samples produced by wildfire of the six severity classes observed in the field (0 to 5), and BC samples produced under controlled conditions in the laboratory.....	109
Figure 3-5. ¹³ C NMR CP spectra of (a) low severity BC (class 0) compared to unburnt Sphagnum and a fibric layer; (b) BC samples produced by wildfire of the six severity classes observed in the field (0 to 5); and (c) high severity BC (class 5) compared to Sphagnum and Rhododendron thermally treated at 250 °C.	110
Figure 3-6. The BC continuum.....	111

Figure 4-1. The 14 study sites and their corresponding homogeneous fire cycle and climatic conditions.....	151
Figure 4-2. (a) Mean organic matter (forest floor) thicknesses (cm) before (OMt) and after (ROM) fire and (b) mean C stocks after fire in the five zones of homogeneous fire cycle and climatic conditions.....	152
Figure 4-3. Frequency distribution of forest floor depth before fire (cm) for 44 plots with opposite topographic features (fire-prone vs. non fire-prone context).	154
Figure 4-4. van Krevelen diagram showing the different layers of the forest floor. Values are average (\pm SD) for the 23 soil profiles of the corresponding layer.	155
Figure 4-5. ^{13}C NMR CPMAS (top) and DPMAS (bottom) spectra of the different forest floor layers (fresh BC, F, H + historical BC, historical BC) developed under black spruce and jack pine.....	156
Figure 4-6. Distribution of the total signal intensity (%) between the 7 spectral regions for the different organic horizons.....	157
Figure 4-7. BC (% total SOC) estimated by the 3 different versions of the molecular mixing model and the data from the DP spectra in the various organic horizons (n = 15).....	158
Figure 5-1. The 14 fire sites and their corresponding 5 zones of homogeneous fire cycle and climatic conditions.	197
Figure 5-2. Fractionation scheme used to separate the podzolic B horizons into six fractions.....	198
Figure 5-3. Relationship between C-BC added to sample and C-BC measured with the KDM method from BC produced at various temperatures from <i>Pleurozium</i> and black spruce fuel.....	199
Figure 5-4. Influence of drainage on (a) SOC and (b) BC stocks.....	200
Figure 5-5. Carbon distribution (% of SOC) in podzolic horizons (n = 11).	201
Figure 5-6. Distribution of BC (% of total SOC) in fractionated podzolic horizons (n = 11).....	202

List of Equations

Equation 1: Prediction of BC content (% total SOC as estimated by DP+MMM) using BC content estimated by CP+MMM.....	150
Equation 2: Prediction of BC content (% total SOC) estimated by DP+MMM-1 using BC content estimated by DP+MMM.....	150
Equation 3: Prediction of BC content (% total SOC) estimated by DP+MMM-2 using BC content estimated by DP+MMM.....	150

List of Appendices

Table 2-A.1. Details of the charring experiments including the maximum temperature (MT), charring duration and the pyrolysis type (partial or complete)..	222
Table 2-B.1. Results from ^{13}C NMR direct polarization (DP) and variable-amplitude cross polarization (VACP) experiments, including spin counting and the relative intensity of carbonyl C, aromatic and phenolic C, O-alkyl C and alkyl C.....	223
Figure 2-C.1. ^{13}C VACP NMR spectra of <i>Sphagnum</i> BC produced at three MTs (250 °C; 425 °C; 600 °C) under two different pyrolysis treatments (partial O_2 – tin – and no O_2 – sand bath).....	224
Figure 2-C.2. ^{13}C VACP NMR spectra of black spruce (BSP) branch and <i>Rhododendron groenlandicum</i> BC produced at 250 °C with two charring durations (12 h vs. 24 h) under full pyrolysis (sand bath – SB).....	225
Table 3-A.1. Results of the spin counting obtained with a DP experiment for a subset of BC produced by wildfire.....	226
Table 4-A.1. Characteristics of the 23 soil profiles and their fire site.....	227
Table 4-B.1. Assignment of ^{13}C NMR signal intensity in the spectral regions associated with the char component of the molecular mixing model (default and adjusted models) and their properties.....	229
Table 4-C.1. Results of Pearson and non-parametric rank correlation analyses.	230
Table 4-D.1. Results from ^{13}C NMR direct polarization (DP) and variable-amplitude cross polarization (VACP) experiments, including spin counting, the relative intensity of alkyl C, N-alkyl and methoxyl C, O-alkyl C, di-O-alkyl C, aromatic C, phenolic C, and amide and carboxyl C, as well as the degree of aromatization and the polarity index.....	231
Table 5-A.1. Characteristics of the 23 soil profiles and their fire site, including BC stocks.....	233

List of Abbreviations

Al_p: pyrophosphate-extractable aluminum

BC: black carbon

BET: Brunauer–Emmett–Teller (method for the measurement of the specific surface area)

BPCA: benzenepolycarboxylic acid

BSP: black spruce – *Picea mariana* (Mill.)

C: carbon

CO₂: carbon dioxide

CP: cross-polarization

DP: direct polarization

Fe_p: pyrophosphate-extractable iron

H: hydrogen

JP: jack pine – *Pinus banksiana* (Lamb.)

LF: light fraction (density < 1.85 g·cm⁻³)

MT: maximum temperature (of BC formation)

N: nitrogen

NMR: nuclear magnetic resonance

O: oxygen

OC: organic carbon

OM: organic matter

OMc: organic matter consumed (forest floor consumed by the last fire event)

OMt: organic matter total (pre-fire forest floor)

Pg: petagram (10¹⁵ g)

POM: particulate organic matter

ROM: residual organic matter (forest floor left after fire)

SAA: surface area analysis

SEM: scanning electron microscopy

SOC: soil organic carbon

SOM: soil organic matter

Tg: teragram (10¹² g)

Chapter 1. Introduction

1.1. Carbon and carbon cycle

The word “Carbon” derives from Latin *carbo*, which means coal. Carbon is the fourth most abundant (by mass) element in the universe after hydrogen, helium, and oxygen, and the 15th most abundant element in the Earth's crust. It is a non-metallic and tetravalent chemical element, with an atomic number of 6. The most common oxidation state of carbon in inorganic compounds is +4, while +2 is found in carbon monoxide and other transition metal carbonyl complexes. Because of its abundance, and the unmatched diversity of organic compounds combined with their unique ability to form polymers, carbon is the building block of all life forms.

1.1.1. Carbon allotropes: the different forms of carbon

Atomic carbon is a very short-lived species and carbon is stabilized in multi-atomic structures with various molecular configurations called allotropes. All carbon allotropes are solids under normal conditions. They are all chemically resistant and require a high temperature to react even with oxygen. The three best known allotropes of carbon are amorphous carbon, graphite, and diamond; each allotropic form presents very distinctive physical properties.

Diamond is formed at very high pressures. Each carbon atom in diamond is covalently bonded to four other carbons in a tetrahedron. These tetrahedrons together form a three-dimensional network of six-membered carbon rings, in the

chair conformation. This stable network of covalent bonds and hexagonal rings is the reason that diamond is so incredibly strong.

Graphite is the most thermodynamically stable form of carbon under standard conditions. Each carbon atom is bonded trigonally to three others, in a plane composed of fused hexagonal rings. The resulting network is two-dimensional, where flat sheets of carbon are stacked and loosely bonded through weak van der Waals forces. Graphite conducts electricity, due to delocalization of the π bond electrons above and below the planes of the carbon atoms. The delocalised electrons are free to move but only in the plane of each covalently bonded sheet.

The amorphous form is a mixture of carbon atoms in a non-crystalline, irregular, glassy state, which is essentially graphite but not held in a crystalline macrostructure. Nevertheless most amorphous carbon actually contains microscopic crystals of graphite-like or even diamond-like carbon. Amorphous carbon is the main constituent of substances such as charcoal, coal, soot and activated carbon.

1.1.2. Carbon isotopes

Carbon isotopes are atomic nuclei that contain six protons plus a number of neutrons that varies from 2 to 16. There are 15 known isotopes of carbon, three of which are naturally occurring isotopes: carbon-12, 13, and 14. ^{12}C and ^{13}C are stable, occurring in a natural proportion of about 98.9:1.1.

1.1.3. Global carbon cycle

Under current terrestrial conditions, conversion of one element to another is very rare. Therefore, the amount of carbon on Earth (32×10^{23} g; Marty, 2012) is essentially constant. The global carbon cycle (GCC) is the biogeochemical cycle by which carbon (organic and inorganic forms) is exchanged among the following major carbon reservoirs (Figure 1-1): the biosphere (vegetation and other land living organisms; organic C), pedosphere (soils; organic and inorganic C), geosphere (geological reservoirs and fossil fuels; mostly inorganic C), hydrosphere (rivers and oceans; mainly dissolved CO_2), and atmosphere (CO_2). Carbon exchanges between reservoirs occur as the result of various chemical, physical, geological, and biological processes. The sum of the active carbon pools at the Earth's surface is about 40×10^{18} g C (Schlesinger and Bernhardt, 2013).

The examination of the balance of the carbon exchanges (incomes and losses) of a specific carbon pool or reservoir can provide information about whether the latter is functioning as a carbon source or sink.

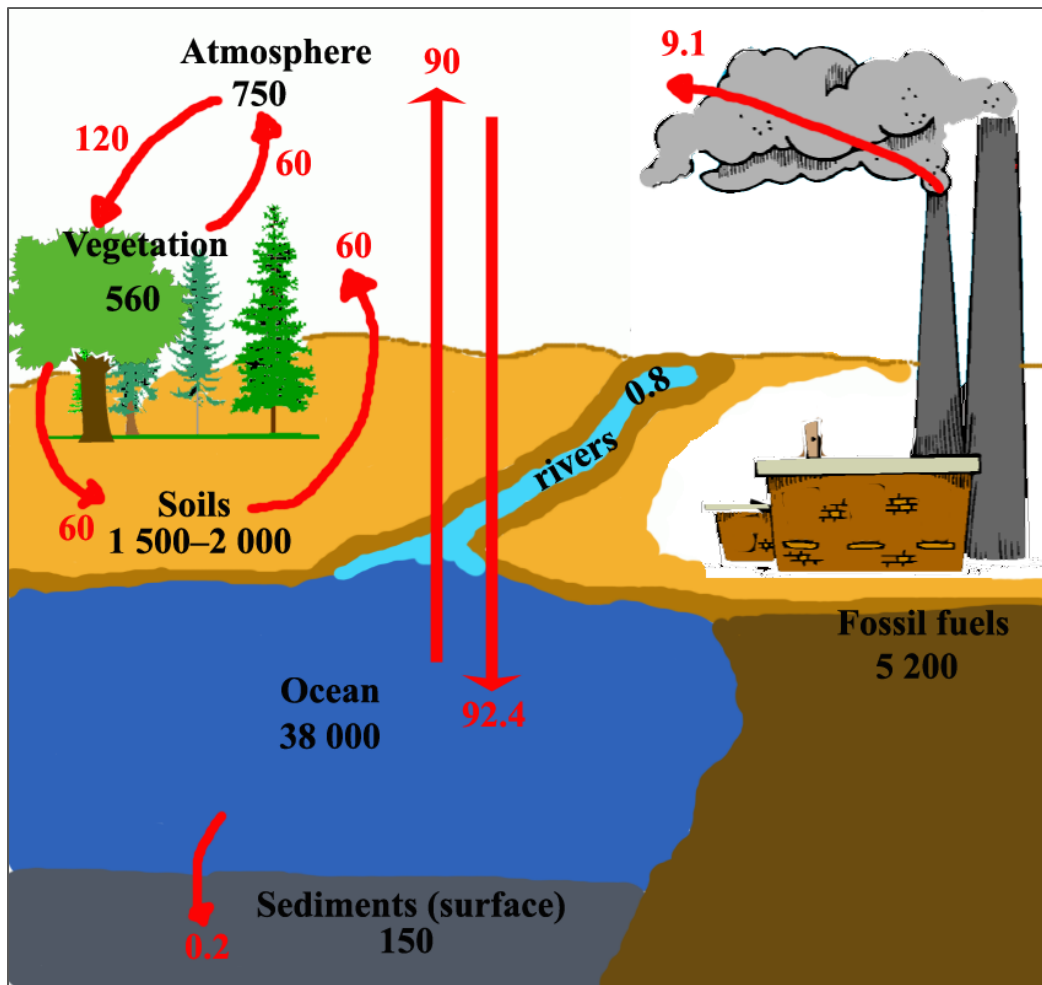


Figure 1-1. The global carbon cycle [adapted from Cole (2012) and Schlesinger and Bernhardt (2013)]. Reservoirs are in Pg C; fluxes in Pg C/year.

Soil organic carbon – importance for the Global Carbon Cycle

About a third of soil carbon is stored in inorganic forms, such as calcium carbonate (Lal, 2008); the rest is organic carbon. Soil organic carbon (SOC) is primarily composed of biomass and non-biomass carbon sources. Biomass carbon primarily includes various bacteria and fungi. Non-biomass carbon sources reflect the chemical composition of plant biomass and primarily include cellulose, hemicellulose, lignin and other diverse organic carbon compounds.

Soil organic carbon constitutes by far the most important carbon pool in terrestrial ecosystems. Globally, soils store around 1100–1600 Pg C (González-Pérez et al., 2004) in the top one meter, i.e., 3 times the amount found above ground in plants and in other living organisms and twice the amount present in the atmosphere (Batjes and Sombroek, 1997).

The main entry of C into the biosphere occurs through photosynthesis that results in the uptake of C from the atmosphere by plants (120 Pg/year). About 60 Pg annually becomes various types of soil organic matter including surface litter, creating a substrate, which decomposers respire (heterotrophic respiration) back to the atmosphere as carbon dioxide or methane depending on the availability of oxygen in the soil. Soils respire or oxidize about 60 Pg/year. Part of the C is also lost through plant respiration (autotrophic respiration); further C losses are caused by fires, drought, human activities, etc.

Soil carbon storage

Soil carbon storage is the balance between the input of dead plant material (leaf and root litter) and output from heterotrophic respiration. Carbon leaves the terrestrial biosphere in several ways and on different time scales. Under aerobic conditions, most of the C entering the soil is labile, and therefore respired back rapidly to the atmosphere as carbon dioxide (CO₂); in anaerobic conditions, methane production prevails. Combustion of soil carbon can also be responsible for its quick release (CO₂) back to the atmosphere. Generally, only one percent of the carbon entering the soil (0.4 Pg/year) accumulates in more stable fractions with long mean residence times (FAO, 2004).

Soil organic carbon is very heterogeneous (Batjes, 1996). The organic carbon can conceptually be divided into active and passive pools. The smaller active pool contains organic matter that decomposes in a time frame of years (fast pool) to decades (slow pool), whereas the larger passive pool comprises the stable carbon pool remaining in the soil for centuries to millennia (FAO, 2004; González-Pérez et al., 2004). These mean residence times, or potential decomposition rates, represent how fast the carbon is brought back into transferring inside the system.

The mean residence time is determined not only by soil organic matter (SOM) chemical composition but also by its stabilization (Marschner et al., 2008; Kleber, 2010; Schmidt et al., 2011). The stable carbon fraction is subjected to either physical or chemical protection. Carbon could bind to the mineral soil, becoming protected by occlusion into microaggregates, sorptive interactions with minerals, or it could experience chemical complexation (von Lützow et al., 2006). Multivalent metal cations, like Fe^{3+} or Al^{3+} , can indeed stabilize soil carbon by forming organo-metallic complexes that are more resistant to oxidation.

Because soils represent such a massive pool of carbon, it is crucial to identify the different carbon pools in the soil as well as the fluxes between them and the atmosphere or the oceans, to better understand the GCC. At the local scale, the relative importance of the different carbon pools matters because SOM constitutes a major factor in plant growth success (e.g., agriculture, silviculture, etc.). At the global scale, the fate of carbon is of particular importance in the context of climate change and there is an increasing pressure to sequester carbon so that it does not end up as CO_2 in the atmosphere, where it is contributing to global

warming. When considering long-term carbon sequestration potential it is primordial to not only consider the increase of C inputs into the soil but also the turnover time of the carbon pool where the storage occurs: C inputs must take place in large pools with slow turnover to maximise long-term carbon sequestration.

Local climatic conditions influence soil carbon sequestration and the latter is therefore contingent on climate change (FAO, 2004); conversely, changes in the size and the turnover rate of the soil carbon pools could possibly affect atmospheric CO₂ concentration and the global climate (von Lützow et al., 2006).

Influence of climate change

The GCC has been the focus of much attention in the recent past because of its association to global warming. In the past two centuries, with the industrial revolution, human activities have critically altered the GCC, and most significantly in the atmosphere. The increase in greenhouse gases in the latter has been recognized to contribute to climate change (IPCC, 2001). CO₂ is the most important anthropogenic greenhouse gas. Records from ice cores have shown that CO₂ levels cannot vary significantly without affecting global temperatures (Shakun et al., 2012). Changes in the amount of atmospheric CO₂ are considerably altering weather patterns and indirectly influencing oceanic chemistry.

The concentration of carbon dioxide in the atmosphere increased from a pre-industrial level of 285 ppm to about 397 ppm in February 2013

(<http://co2now.org/>). The magnitude of these levels, added to the fact that they are rising faster than ever recorded (Crowley, 2000), emphasize how critical a better understanding of the GCC and of its effects on the global climate is. Total annual carbon emissions from fossil fuel combustion (and cement production) are around 7.2 Pg and 2 Pg from land-use changes (IPCC, 2007). Half of these emissions remains in the atmosphere. The fraction absorbed by the atmosphere has increased in the past 50 years (Le Quéré et al., 2009). The remaining 50% is taken up by the oceans and the terrestrial biosphere, which act as important carbon sinks.

The biosphere constitutes a carbon sink that absorbs about 2 Pg/year (Cole, 2012): the increasing atmospheric CO₂ concentration stimulates photosynthesis and consequently plant growth (IPCC, 2000). Forests are most affected by this phenomenon, but their capacity to function as a carbon sink may be limited. First, C sequestration capacity is under the limitation of nutrient availability (Oren et al., 2001) and other biophysical factors. Second, photosynthesis may have a CO₂ saturation point. Third, climate change could induce ecosystem degradation, hence reducing C sequestration capacity. Finally, forests do not start sequestering carbon right after establishment and are under the threat of future disturbances. If boreal forests have been a steady average sink for two decades (0.5 ± 0.1 Pg C/year), it is actually the net result of divergent patterns in the different boreal regions caused by natural disturbances and forest management practices (Pan et al., 2011). While European Russia and northern Europe became a larger C sink, the sink in Canadian forests was reduced by half over the 1990–2007 period.

Biomass loss caused by intensified wildfires and insect outbreaks was determined as the principal cause of this reduction.

Uncertainties persist regarding some of the causes, consequences and extent of climate change. Whether the terrestrial biosphere will maintain its current role as a carbon sink or switch to a carbon source in the future, is highly controversial because it relies on the long-term sensitivity of heterotrophic respiration to global warming. Global warming could indeed lead to an increase in organic matter decomposition, and consequently reduce the capacity of terrestrial ecosystems to act as carbon sinks (Schimel et al., 2001). For instance, a study showed that forests would turn into carbon sources in the next 50–150 years (Cox et al., 2000). But there are also contradictory findings. Jarvis and Linder (2000) obtained results from long-term soil warming experiments in a boreal forest opposing the idea that heterotrophic respiration is very sensitive to increases in temperature. They concluded that forests that were currently carbon sinks would not become carbon sources in the near future.

Global warming-induced changes in the fire regime have raised specific concerns about the future evolution of C storage in boreal forests. An increase in fire frequency in the boreal region is suspected for the near future (Bergeron and Flannigan, 1995; Wotton et al., 2010), but uncertainty remains about the evolution of fire severity (Flannigan et al., 2005; van Bellen et al., 2010) and how this will affect organic carbon stocks in boreal forests soils, particularly with the production of black carbon by these wildfires.

Black carbon (BC) in soils and influence on the global carbon cycle

According to recent studies, BC is an important component of the stable soil carbon pool (Kasischke and Stocks, 2000; González-Pérez et al., 2004; Preston and Schmidt, 2006), although some other studies caution against assuming that all BC is recalcitrant (Harden et al., 2000; Hockaday et al., 2006; Czimczik and Masiello, 2007; Hammes et al., 2008; Preston, 2009).

In some soils, BC constitutes an important part of total organic matter. Skjemstad and colleagues (2002) showed that BC represents up to 35% of total SOC in American agricultural soils. Similarly BC amounted up to 45% of the total soil organic matter in European Chernozems (Schmidt et al., 1999; Schmidt et al., 2002) and the ratio BC/OC was as high as 60% in Black Chernozems of Saskatchewan (Ponomarenko and Anderson, 2001). If climate and relief have been shown to influence the stability of organic matter in Chernozems (Eckmeier et al., 2007), fire also plays an obvious role in the formation of these soils (Schmidt et al., 1999). In a review on boreal forests, where wildfire is a major natural disturbance, Preston and Schmidt (2006) reported BC stocks in boreal forest floors of the order of 1000–2000 kg/ha, but considered these numbers as likely underestimates of the real stocks. Moreover these estimates do not include BC stocks in mineral soils.

Natural BC accumulation in soil requires several essential factors (Czimczik and Masiello, 2007). First, BC production requires a fire, as well as the presence of an aromatic precursor, and appropriate combustion conditions, i.e., pyrolysis.

Then, mixing mechanisms are required to remove BC from the topsoil and to protect it from further oxidation, erosion and/or degradation processes.

BC production rate is dominated by burning of vegetation (Figure 1-2). Tropical forest fires produce around 5 Tg/year; whereas the boreal forest fires generate 9–20 Tg/year and savanna fires 4–40 Tg/year. The production rate varies widely and estimates also depend on the analytical technique used to measure BC (Forbes et al., 2006; Preston and Schmidt, 2006). Kuhlbusch and Crutzen (1995) estimated a global BC production of 50–270 Tg BC/year (40–240 Tg BC/year for the solid residues; 10–30 Tg BC/year for aerosols). More than 80% of BC produced by wildfires remains in solid residues and less than 20% is released with smoke (Kuhlbusch and Crutzen, 1995). Shift to agriculture associated with permanent deforestation have the largest influence in the global BC cycle and contributes to about 50% to the annual BC formation. BC produced by fossil fuel combustion accounts for 6–9 Tg C/year (Forbes et al., 2006).

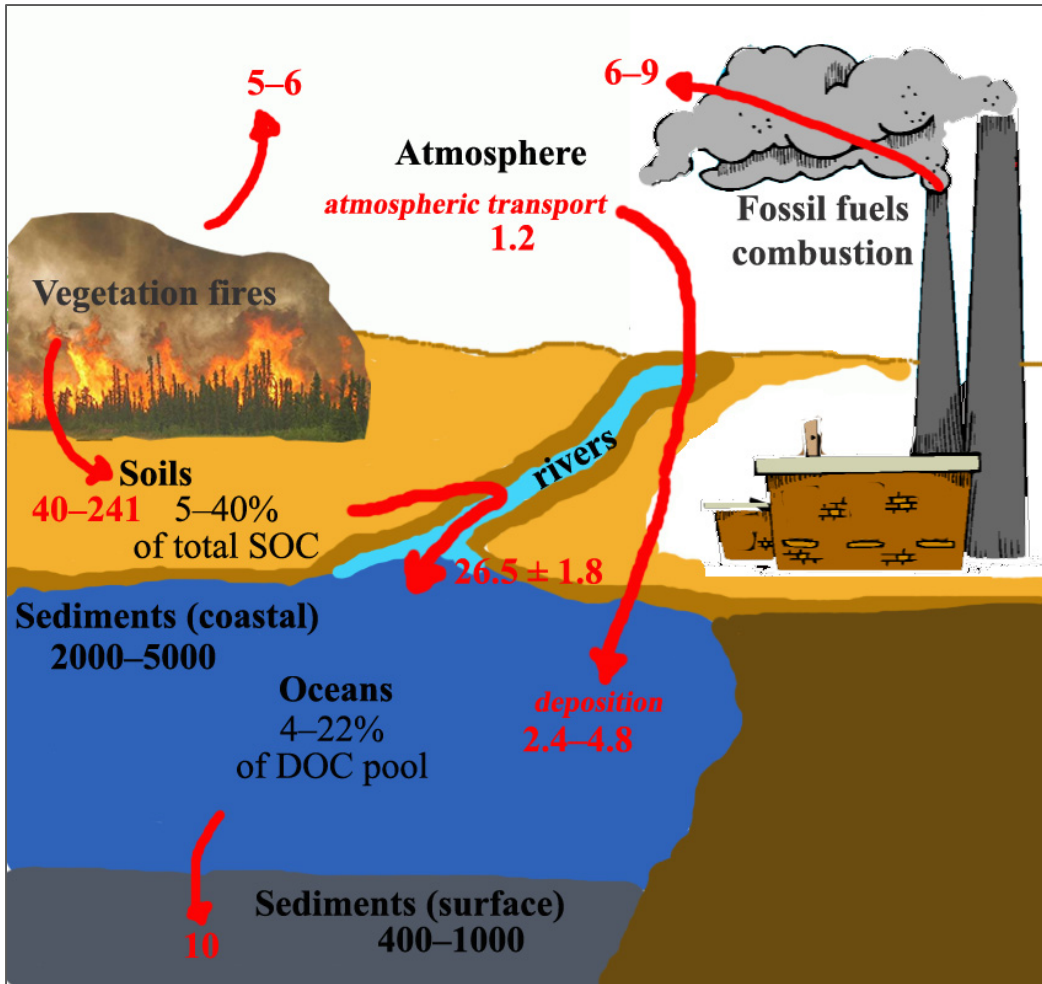


Figure 1-2. The global black carbon cycle [adapted from Schmidt et al. (1999), using data from Forbes et al. (2006) and Jaffé et al. (2013)]. BC pools are in Pg; BC fluxes in Tg/year.

Fire events affect both the composition and quantity of the terrestrial carbon pool. The effect is dependent on different factors such as fire type, maximal temperature, and duration of the event (González-Pérez et al., 2004).

1.2. What is black carbon? – A definition

Black carbon is commonly defined as the highly condensed carbonaceous residue produced from the incomplete combustion of biomass (Baldock and

Smernik, 2002). Hereafter we will focus on the solid residues. The volatiles later solidify to form highly aromatic combustion condensates like soot, which is structurally very close to graphite. These often airborne particles have received a lot of attention in air quality and other and atmospheric sciences but they constitute a different product that is outside the focus in this study. Important defining properties of BC are its relative inertness, ubiquity in pyrogenic ecosystems (Schmidt and Noack, 2000) and high content of aromatic structures (Lehmann and Joseph, 2009). However, an ambiguity persists in determining what constitutes BC, as no standard analytical method exists. Masiello (2004) proposed to define BC as a continuum. The idea was further explored by Hammes et al. (2007) with an inter-laboratory ring trial that aimed to resolve which techniques best assessed each part of the continuum. BC is extremely variable and it is almost impossible to define clear numerical cut-offs to the BC continuum (Lehmann and Joseph, 2009).

In addition to its potential contribution to the overall SOC pool, the amount of BC left on site after fire may affect ecosystem recovery through modification of plant community dynamics and by stimulation of the nitrogen cycle (DeLuca et al., 2006). BC plays a central role in soil fertility, in particular by stimulating microbial activity and nutrient cycling after fire (Wardle et al., 1998; DeLuca et al., 2006). Although BC composition and morphological features may contribute to the rejuvenating effects of wildfire on soil properties (Certini, 2005), these properties, and the extent to which they are affected by formation conditions, remain largely unknown.

1.3. BC characterization and BC quantitation – solid-state ^{13}C nuclear magnetic resonance (NMR) spectroscopy

Characterization of BC chemical and physical properties is critical for the purpose of its quantification (e.g., Hammes et al., 2007; Keiluweit et al., 2010). Solid-state NMR spectroscopy is one of the few methods allowing for both qualitative and quantitative analysis of soil organic matter samples (Knicker, 2011); it is also a non-destructive technique.

1.3.1. *Fundamental properties* (Hore, 1995)

Both ^{13}C and ^1H are nuclei with a spin quantum number (I) of $1/2$, which makes them magnetically active as opposed to ^{12}C that has $I = 0$. The magnetic moment of a nucleus is defined by:

$$\boldsymbol{\mu} = \gamma_{\text{N}} \boldsymbol{I}$$

where \boldsymbol{I} is the spin angular momentum and γ_{N} is the magnetogyric ratio. When an external magnetic field, B_0 , is applied, the nuclear spin vectors align themselves with, or opposed to, the external field. For spin-1/2 nuclei with positive magnetogyric ratios, the low energy configuration or state has the spin vectors parallel to \boldsymbol{B}_0 and the high energy state has the spin vectors antiparallel to \boldsymbol{B}_0 . In the NMR experiment one observes transitions between these so-called Zeeman states. The frequency of the transition is proportional to the applied magnetic field and the magnetogyric ratio of the nuclei:

$$\nu = \gamma_{\text{N}} B_0 / 2\pi.$$

In practice a short intense electromagnetic radio frequency (RF) pulse, perpendicular to B_0 , is applied and its frequency has to correspond to the resonance frequency, also called Larmor frequency.

As already mentioned, when a group of spin-1/2 nuclei are placed in a magnetic field, each spin aligns in one of the two possible orientations. If n_{upper} is the number of spins in the upper level and n_{lower} the number in the lower energy level, Boltzmann statistics tells us that

$$(n_{\text{upper}} / n_{\text{lower}}) = \exp (-\Delta E/kT)$$

where k is the Boltzmann's constant, 1.3805×10^{-23} J/Kelvin, and T is the absolute temperature in Kelvin. ΔE is the energy difference between the two states, and is related to the frequency, ν , by Planck's constant, $h = 6.63 \times 10^{-34}$ J s: $\Delta E = h \nu$. Because ΔE is very small, this ratio is close to one at room temperature. The intensity of the NMR signal is proportional to the population difference between the states; therefore it is advantageous to work at high magnetic field strengths and low temperature.

The “electron cloud” present around a nucleus creates a magnetic field that generally opposes the external field and therefore shields the nucleus of interest. The effective magnetic field experienced by the nucleus is reduced, and this results in a shift of the specific resonance frequency; the frequency then becomes:

$$\nu_i = \gamma B_0/2\pi (1-\sigma_i)$$

with σ_i , the shielding constant. Nuclei in different local environments have different and particular resonance conditions. The RF pulse generates a symmetric frequency band around the transmitter frequency (set approximately to ν_i).

Following excitation by the RF pulse, the spin system returns to thermal equilibrium by re-emitting the absorbed energy. The relaxation process is described by two time constants T_1 and T_2 . T_1 is the spin-lattice relaxation time and describes how the z -component of the nuclear spin magnetization, M_Z , returns to its thermal equilibrium value M_0 :

$$M_Z = M_0 (1 - \exp(-t/T_1))$$

T_2 , the spin-spin relaxation time, describes the return to equilibrium of the transverse magnetization, M_{XY} :

$$M_{XY} = M_{XY0} \exp(-t/T_2)$$

In general, T_2 is less than or equal to T_1 .

All ^{13}C NMR experiments in the present study were conducted with magic-angle (54.74°) spinning (MAS) to average chemical shielding anisotropy to zero. Resonance frequencies of the nuclei are expressed as chemical shifts (δ_i) in parts per million (ppm), with

$$\delta_i/\text{ppm} = (v_i - v_{\text{ref}}) / v_{\text{ref}}$$

In this study, chemical shifts were externally referenced to tetramethylsilane using the adamantane peak at 38.56 ppm (Earl and VanderHart, 1982).

1.3.2. The cross polarization technique

The abundance (1.1%) and magnetogyric ratio ($6.728284 \cdot 10^7 \text{ rad}\cdot\text{s}^{-1}\cdot\text{T}^{-1}$) of ^{13}C make its detection by NMR spectroscopy much harder than is the case for ^1H . The cross polarization (CP) technique uses the large natural abundance (99.99%) and relatively large magnetic moment of protons to enhance the NMR signals of

“rare” or “dilute” spins such as ^{13}C . To establish magnetisation transfer between two spins the RF pulses that are applied on the two frequency channels must fulfill the Hartmann-Hahn condition (Axelson, 2012):

$$\gamma_{\text{H}} \times B_{1\text{H}} = \gamma_{\text{C}} \times B_{1\text{C}}$$

This can be achieved by applying adjusted RF fields $B_{1\text{H}}$ and $B_{1\text{C}}$ during a contact time (t_{c}). The spin-lattice relaxation time of hydrogen, T_1^{H} , being much shorter than T_1^{C} , CP allows for shorter pulse delay (Axelson, 2012), hence shorter total acquisition times. This, added to the transfer of magnetisation from ^1H to ^{13}C , increases the signal-to-noise ratio. Because of its principle, CP becomes impractical when the number of hydrogen present in the sample becomes too low. In that case, the experiment will likely not be quantitative. Similarly the ^{13}C signal will be most intense if the following condition is fulfilled:

$$T_{\text{CH}} \ll t_{\text{c}} \ll T_{1\text{p}}^{\text{H}}$$

where T_{CH} is the cross-relaxation time. It ensures that proton spin-lattice relaxation in the rotating frame is slow during the time cross polarization is taking place. T_{CH} generally increases with molecular motion (Hore, 1995) and the distance between the ^{13}C nucleus and the protons (Axelson, 2012). Finally the spin system must be totally returned to thermal equilibrium before a new RF pulse is applied, to avoid saturation. In practice, the pulse delay should be in the order of $5 \times T_{1\text{p}}^{\text{H}}$ (Smernik).

In the different chapters of this thesis, I used a modified version of the CP technique: the variable-amplitude cross polarization (VACP; Peersen et al., 1993). This specific pulse sequence (Figure 1-3) optimizes the cross polarization by

restoring a broad matching profile to the Hartmann Hahn conditions (Axelson, 2012). This is achieved by modulating the proton field power during the contact time. High-power ^1H decoupling (TPPM sequence) was used to suppress heteronuclear spin coupling between ^1H and ^{13}C .

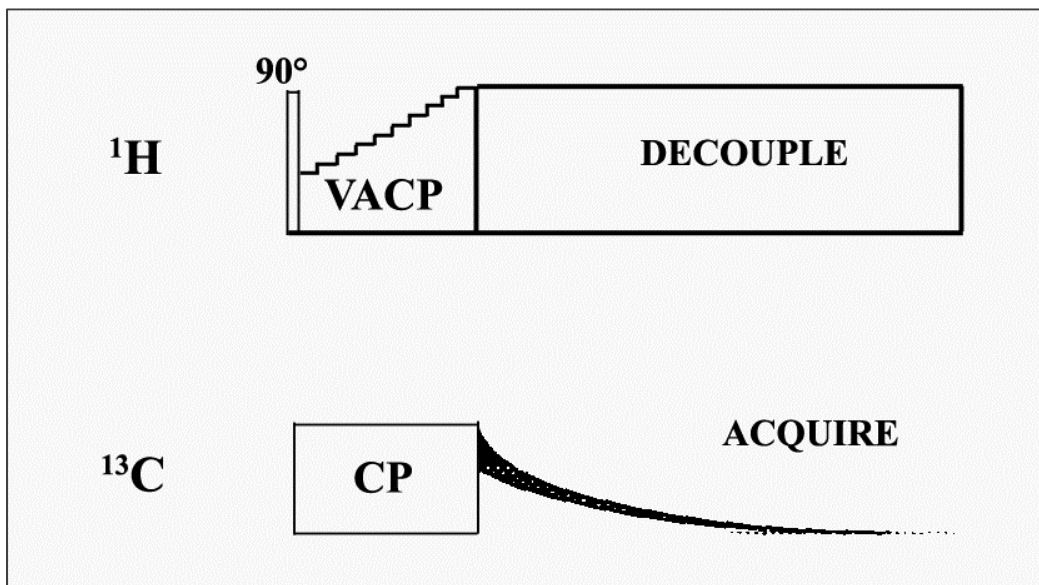


Figure 1-3. The variable-amplitude cross polarization (VACP) pulse sequence with application of ten proton amplitudes [adapted from Peersen et al. (1993)].

1.3.3. The direct polarization technique and spin counting

With the direct polarization (DP), also called Bloch-decay, technique, ^{13}C nuclei are exposed to short and intense pulses of radiofrequency radiation to bring ^{13}C magnetisation into the transverse plane (Axelson, 2012). Because it directly excites the ^{13}C nuclei, DP experiment is in theory quantitative. However, relaxation of ^{13}C magnetisation back to equilibrium is particularly slow (i.e., long relaxation time T_1^{C}), necessitating long recycle delays and resulting in particularly long acquisition times.

The potential to determine quantitative distributions of functional groups is a major advantage of solid-state ^{13}C NMR spectroscopy. Following Smernik and Oades' (2000a) methodology, I used spin counting to determine if the DP spectra were representative of all the carbon moieties in the samples. Spin counting relies on comparing the ^{13}C NMR integrated signal intensity of a sample for which the mass and carbon content are known with that of a standard, which is known to provide a quantitative signal. In this study, I used glycine as external reference material. I determined how much of the expected signal was actually detected in the NMR spectra. The C observability, C_{obs} , corresponds to the fraction of the expected NMR intensity actually observed. It is assumed that the intensity of the NMR resonances quantitatively reflects the distribution of ^{13}C environments in the sample if $C_{\text{obs}} = 100\%$ (Smernik and Oades, 2000b). A value $< 100\%$ implies that part of the potential signal was not detected. By further comparing the distribution of the total intensity between the CP and DP spectra I was able to determine if the CP experiments were quantitative.

1.3.4. Data analysis

For each set of samples (series of samples that was to be compared), the same processing steps needs to be applied. First the probe background signal needs to be subtracted. Background signal can arise from rotors, rotor end-caps and the probe itself if these components contain carbon. The rotors I used were made from zirconium oxide which contain no carbon and hence do not give rise to any background signal. The rotor end-caps were made from a fluoro-polymer (e.g.,

Kel-F) and can be a significant source of background signal. The stator of a MAS probe does not usually contain carbon, but plastics or glues that are sometimes present in the probe can generate a significant background signal (Smernik). I acquired spectra on an empty rotor, under the same acquisition conditions than the rest of the samples to assess the background signal. I then subtracted the background free induction decay (FID) from the sample FID.

The ^{13}C NMR spectra are typically divided into different spectral regions, each corresponding to a major type of carbon, as described for instance in Baldock & Smernik (2002): ketone (215–190 ppm), carbonyl and amide (190–165 ppm), O-aryl (165–145 ppm), aryl and unsaturated (145–110 ppm), di-O-alkyl (110–90 ppm), O-alkyl (90–65 ppm), methoxyl and N-alkyl (65–45 ppm), alkyl (45–0 ppm).

Another concern regarding quantification is the presence of spinning side bands (ssbs). The latter occur in solid-state NMR spectra when the rate of magic angle spinning (MAS) is lower than the chemical shift anisotropy. The latter is proportional to field strength. First order ssbs are most important for carbonyl and aromatic resonances; for alkyl and O-alkyl, ssbs are negligible. There are three principal ways to handle the spinning side bands. First, the use of high MAS rates can remove the ssbs from the region of interest. Second, some pulse sequences (e.g., TOSS) can be used to suppress the ssbs. However, this can generate quantification problems and I thus chose not to use these pulse sequences. Third, ssbs can be corrected for during integration (e.g., Baldock and Smernik, 2002). First order ssbs are approximately of equal intensity, and appear on either side of

the central band at frequencies shifted by the MAS rate. On a 200 MHz spectrometer ($B_0 = 4.70 \text{ T}$), with a MAS speed of 5 kHz, ^{13}C ssbs emerge 100 ppm from the central bands. The high ppm ssbs resulting from the aromatic and carbonyl resonances generally do not overlap with any resonances in OM samples. Signal loss from the central band of these resonances can be corrected for by adding twice the intensity of ssbs. However, the low ppm ssbs resulting from the aromatic and carbonyl resonances overlap with resonances in the O-alkyl and alkyl regions, respectively. To correct for ssbs, the intensity of the high ppm ssbs needs to be subtracted.

1.4. Boreal forests

1.4.1. The different forest biomes

Forest biomes occupy approximately a third of Earth's land area, and contain about 70% of carbon present in living organisms. Based on latitude, three major forest types are identified: tropical, temperate and boreal forests. Carbon sequestration and release vary substantially by forest, but generalization can be made following these forest types.

Tropical forests are located around the equator. Soils of these forests are nutrient-poor and acidic (e.g., Ferralsols in tropical rain forests); they are also subject to heavy leaching, in relation to the heavy rains that most of these forests are receiving. Decomposition and nutrient cycling occur rapidly, and half of the total carbon ($270 \times 10^3 \text{ kg/ha}$) is stored in the aboveground vegetation. Species diversity is very high.

Temperate forests occur in mid-latitudes of both hemispheres. Some are dominated by coniferous trees while others are dominated by broadleaf trees; there are also a few mixed forests. Overall, temperate forests have much lower plant species diversity than tropical forests. Soil characteristics are very dependent on parent geological material, precipitation and vegetation types. More than one-third of the total carbon (170×10^3 kg/ha) is stored in the vegetation, and nearly two-thirds in the soil. Most of these forests are managed.

1.4.2. Boreal forests

Boreal ecosystems cover 24×10^7 km², 17% of the Earth terrestrial land area but account for 30% of the world soil carbon; they include boreal forests in the southern range and treeless tundras in the north. The boreal forest biome is restricted to the northern hemisphere and forms a circumpolar belt through northern Eurasia and North America, which consists of a broad complex of forested and partially-forested ecosystems (Apps et al., 1993). The boundary between boreal and temperate forests is not sharp, but occurs instead as a transitional zone with mixed forests or as a mosaic of temperate deciduous species established on favorable soils while conifers occupy colder sites. Boreal forest soils represent a massive global carbon pool estimated at 272 ± 23 Pg (Pan et al., 2011). Podzols are very common soils in boreal forests: part of the carbon pool is found in the podzolic B horizons, while the rest is stored in forest floors. Because of the short growing season and low mean temperatures (responsible for slow decomposition), boreal forests are often dominated by conifers, and are

unproductive compared to forests located in less constraining climates: vegetation stores less than one-sixth of total carbon (450×10^3 kg/ha).

Boreal forests are exposed to large-scale and recurrent natural disturbances (e.g., wildfires, insect outbreaks) as opposed to tropical forests where local natural disturbances prevail. These major disturbances significantly affect the carbon cycle. And because boreal forests constitute the largest carbon pool of terrestrial carbon – they generally contain more carbon than temperate or tropical forests – it is particularly relevant to study how changes in disturbance regimes triggered by climate change/global warming will affect carbon sequestration in these forests.

Quebec's boreal forest covers 1.2 million km², 21% of Canada's boreal forest. With about 800–1000 mm of annual precipitation (at least in the southern range of the boreal domain, i.e., in the closed crown forests), Quebec boreal forests are amongst the more humid boreal forests. These abundant precipitations are, at least partially, responsible for less frequent fires in eastern Canada compared to continental Canada, and generally thick forest floors.

1.5. BC storage and degradation

1.5.1. Is recalcitrance an appropriate notion?

In ecology, recalcitrance is often associated with variations in decomposition rates experienced by different SOM moieties, and is therefore tightly linked to microbial decomposition. But agreeing on a common definition is challenging. Some frequently used definitions include: recalcitrance as a material property (molecular level); recalcitrance as a characteristic of old organic compounds with

slow turnover time; recalcitrance as an operational characteristic of organic materials that would be decomposed in the latest stages of an incubation experiment and/or would resist a chemical treatment (Kleber, 2010). The accepted idea is that those three things are tied up together in the following reasoning: organic matter with particular molecular properties (like a high proportion of aromatics) would be decomposed in the latest stages of an incubation experiment and would therefore achieve long residence time in the system.

Recalcitrant compounds are resistant to biodegradation for reasons that could be biological, environmental or chemical. Biological and environmental reasons include: the absence of required nutrients (limiting nutrients); presence of unfavourable environmental conditions (e.g., pH, redox potentials, temperature, etc.); presence of a substance at high concentration (toxicity); the compound may be at too low a concentration; the compound may not be bioavailable (e.g., entrapment into microaggregates, complexation, etc.); the microbial population does not produce the correct enzymes, or the microorganisms capable of degrading the substance are missing from the environment. For chemical factors, it is mostly based on structure-function relationships: some chemical structures and molecules are resistant to the range of enzymes produced by microorganisms. It is often the case with xenobiotic compounds.

Intrinsic recalcitrance may not exist, rather it is more likely that the fate of organic matter in an ecosystem and its residence time may be more controlled by the interactions between the nature (chemical properties/molecular structure) of organic material, the microbial communities present and abiotic conditions

(Kleber, 2010). For instance, Kleber (2010) argues that decomposition rates are not directly linked, or at least not only and surely not primarily, to intrinsic features of the organic material but rather are dependant on the microbes present in the system as well as the additional environmental and abiotic conditions (e.g., low temperatures, lack of oxygen, etc.). SOM preservation is therefore probably not a molecular property (i.e., recalcitrance), but more an ecosystem property (Schmidt et al., 2011). To conclude, it might be time to abandon the concept of recalcitrance, especially for carbon cycling modeling purposes, and conceive SOM preservation as primarily dependant on environmental conditions (biotic and abiotic). Nevertheless, in the context of recalcitrance of soil organic matter, fire-derived SOM constitutes a special case. Because of its intrinsic variability – resulting from fire variability – adequate micro-organisms capable of achieving a complete degradation of those products may be missing from the environment. More importantly, the decomposition pathways of fire-derived organic matter are still uncertain (Schmidt et al., 2011).

1.5.2. BC degradation

Stability has often been part of BC definition, and because of its supposed resistance to oxidation, BC was first believed to be systematically part of the passive carbon pool (e.g., Goldberg, 1985; Kuhlbusch and Crutzen, 1995; Schmidt and Noack, 2000; González-Pérez et al., 2004). However, to account for discrepancies between BC production and available BC pools, natural degradation processes of BC must take place (Masiello, 2004; Czimczik and Masiello, 2007).

Considering the estimated production rate proposed by Kuhlbusch and Crutzen (1995; 0.05–0.27 Pg/year), and assuming that BC produced by biomass burning has been accumulating since the Last Glacial Maximum, BC pool in the pedosphere would account for 25–125% of total soil carbon (Masiello and Druffel, 2003). This does not match the reported BC contents (maximum observed in Chernozemic soils is 35%; cf. p10), suggesting that BC must be abiotically or biotically degradable. BC degradation has been observed both in incubation experiments and in natural environment, suggesting that under the right conditions at least part of the BC could be degraded by fungi and/or bacteria. Knowing that pyrogenic ecosystems have been around since the Late Silurian period (Paleozoic era), it is likely that some microorganisms have developed the appropriate enzymes to degrade BC (Kleber, 2010).

Many studies have pointed out possible losses through biotic or abiotic degradation. The discussion about possible microbial degradation of thermally altered biomass has been ongoing for over a century now. Potter (1908) was the first to report oxidation of coal and charcoal by microorganisms (bacteria). Shneour (1966) ran a 96-day incubation experiment in which a sterilized and an untreated soils were mixed with ^{14}C labeled graphite and proved that bacteria were actively involved in the degradation of the graphite. Hamer et al. (2004) reported a positive priming effect of glucose addition on the mineralization of charred biomass and hypothesized that co-metabolism is an important process in BC decomposition.

The amount and the storage of BC in soils are controlled by a large number of variables, such as BC chemical composition (e.g., H/C and O/C atomic ratios influenced by the formation temperature) but also the soil and climate conditions. These factors also affect BC degradation rate. Baldock and Smernik (2002) tested the influence of temperature on the bioavailability of thermally altered red pine trees. The chemical changes resulting from the thermal treatment significantly reduced the ability of the microbes to mineralise the carbon contained in the charred residues. The C mineralisation rate constants decreased by an order of magnitude for wood heated to ≥ 200 °C, dropping from 13% with the wood treated at 150 °C to below 2%.

Both Bird et al. (1999) and Hockaday et al. (2007) reported a change in color and consistency with ageing of the BC in natural conditions, suggesting that microbial degradation processes had altered the nature of the carbon compounds. A lower specific surface area and a higher BC/OC ratio were also observed (Hockaday et al., 2007). The presence of fungi on the older particles in that study could explain BC decomposition: the oxidation of BC to water-soluble compounds has been hypothesized to be accelerated by fungal co-metabolism (Hockaday et al., 2006). In these two studies (Bird et al., 1999; Hockaday et al., 2007), BC bigger particles were rapidly degraded into smaller particles, the latter becoming more resistant to oxidation. Bird and colleagues (1999) also calculated the half-life for BC in a savanna grassland sandy soil and found that under well-aerated conditions in a seasonal subtropical climate it was less than a century.

Cheng et al. (2006) investigated the relative importance of biotic and abiotic processes in BC oxidation. They concluded that abiotic processes played a more important role than biotic processes in oxidizing BC. In natural conditions, abiotic degradation processes are certainly occurring, with for instance, BC oxidation by subsequent fires. Other abiotic processes include transport from the system with wind and/or water erosion. Chemical oxidation increases the water solubility hence promoting abiotic BC loss through water erosion.

Despite all these proofs, it remains very difficult to tease apart which factors are more influential in BC degradation, because of the various settings of these experiments, with both lab and field experiments looking at both naturally- and artificially-produced BC.

1.6. Objectives and outline of the thesis

The main objective of my PhD project was to evaluate the amount and the fate of black carbon in podzolic soils of fire-affected Quebec black spruce forests, along with variable fire severity. Hence, this thesis focuses on the following three research objectives: (i) To characterize black carbon chemical and physical properties and to assess how the latter are influenced by formation conditions, in relation to fire severity, (ii) To determine black carbon stocks and distribution in soil profile and investigate possible storage mechanisms in the mineral soil.

As an opening chapter, this introduction reviews some of the literature available on black carbon and looks at some of the important concepts tackled later in the thesis. It is followed by four chapters, which address the research

objectives, and a final chapter summarizing and concluding this work. The second and third chapters focus on the first research objective. Chapter 2 concentrates on alterations in fuels submitted to thermal treatment under controlled conditions, and the creation of a BC reference set. This experiment was devised to relate the observed fire severity to actual formation conditions, a posteriori. In chapter 3, I used the methodology developed in the previous chapter to look at variations in chemical and physical properties of BC collected in the field, and determine their formation conditions. This insight on BC production by wildfire was then used in chapter 4 to study BC stocks in forest floors. Chapter 5 completed the work on BC stocks by focusing on the mineral soil. Lastly the concluding chapter synthesizes and connects all the results from the previous chapters. It also indicates some limitations of this study and some future research perspectives.

List of references

- Apps, M.J., Kurz, W.A., Luxmoore, R.J., Nilsson, L.O., Sedjo, R.A., Schmidt, R., Simpson, L.G., Vinson, T.S., 1993. Boreal forests and tundra. *Water, Air, & Soil Pollution* 70, 39-53.
- Axelsson, D.E., 2012. *Solid State Nuclear Magnetic Resonance. A Practical Introduction*, 1st Edition. MRI_Consulting, Lexington, KY.
- Baldock, J.A., Smernik, R.J., 2002. Chemical composition and bioavailability of thermally altered *Pinus resinosa* (Red pine) wood. *Organic Geochemistry* 33, 1093-1109.
- Baldock, J.A., Masiello, C.A., Gélinas, Y., Hedges, J.I., 2004. Cycling and composition of organic matter in terrestrial and marine ecosystems. *Marine Chemistry; New Approaches in Marine Organic Biogeochemistry: A Tribute to the Life and Science of John I.Hedges* 92, 39-64.
- Batjes, N.H., 1996. Total carbon and nitrogen in the soils of the world. *European Journal of Soil Science* 47, 151-163.
- Batjes, N.H., Sombroek, W.G., 1997. Possibilities for carbon sequestration in tropical and subtropical soils. *Global Change Biology* 3, 161-173.
- Bergeron, Y., Flannigan, M.D., 1995. Predicting the effects of climate change on fire frequency in the southeastern Canadian boreal forest. *Water, Air and Soil Pollution* 82, 437-444.
- Bird, M.I., Moyo, C., Veenendaal, E.M., Lloyd, J., Frost, P., 1999. Stability of elemental carbon in a savanna soil. *Global Biogeochemical Cycles* 13, 923-932.
- Certini, G., 2005. Effects of fire on properties of forest soils: a review. *Oecologia* 143, 1-10.
- Cheng, C., Lehmann, J., Thies, J.E., Burton, S.D., Engelhard, M.H., 2006. Oxidation of black carbon by biotic and abiotic processes. *Organic Geochemistry* 37, 1477-1488.

- Cole, J.J., 2012. The Carbon Cycle, with a brief Introduction to Global Biogeochemistry. In: Weathers, K.C., Strayer, D.L., Likens, G.E., (Eds.), Fundamentals of Ecosystem Science. Academic Press, Inc, San Diego, USA, 109-135.
- Cox, P.M., Betts, R.A., Jones, C.D., Spall, S.A., Totterdell, I.J., 2000. Acceleration of global warming due to carbon-cycle feedbacks in a coupled climate model. *Nature* 408, 184-187.
- Crowley, T.J., 2000. Causes of climate change over the past 1000 years. *Science* 289, 270-277.
- Czimczik, C.I., Masiello, C.A., 2007. Controls on black carbon storage in soils. *Global Biogeochemical Cycles* 21,
- DeLuca, T.H., MacKenzie, M.D., Gundale, M.J., Holben, W.E., 2006. Wildfire-produced charcoal directly influences nitrogen cycling in ponderosa pine forests. *Soil Science Society of America Journal* 70, 448-453.
- Earl, W.L., VanderHart, D.L., 1982. Measurement of ^{13}C chemical shifts in solids. *Journal of Magnetic Resonance* 48, 35-54.
- Eckmeier, E., Gerlach, R., Gehrt, E., Schmidt, M.W.I., 2007. Pedogenesis of Chernozems in central Europe - A review. *Geoderma* 139, 288-299.
- Flannigan, M.D., Logan, K.A., Amiro, B.D., Skinner, W.R., Stocks, B.J., 2005. Future area burned in Canada. *Climatic Change* 72, 1-16.
- Food and Agriculture Organization of the United Nations, 2004. Carbon Sequestration in Dryland Soils, FAO, Rome, Italy.
- Forbes, M.S., Raison, R.J., Skjemstad, J.O., 2006. Formation, transformation and transport of black carbon (charcoal) in terrestrial and aquatic ecosystems. *Science of The Total Environment* 370, 190-206.
- Goldberg, E.D., 1985. Black Carbon in the Environment: Properties and Distribution, John Wiley Edition. John Wiley and Sons, New York, NY.

- González-Pérez, J.A., González-Vila, F.J., Almendros, G., Knicker, H., 2004. The effect of fire on soil organic matter - a review. *Environment international* 30, 855-870.
- Hamer, U., Marschner, B., Brodowski, S., Amelung, W., 2004. Interactive priming of black carbon and glucose mineralisation. *Organic Geochemistry* 35, 823-830.
- Hammes, K., Schmidt, M.W.I., Smernik, R.J., Currie, L.A., Ball, W.P., Nguyen, T.H., Louchouart, P., Houel, S., Gustafsson, Ö., Elmquist, M., Cornelissen, G., Skjemstad, J.O., Masiello, C.A., Song, J., Peng, P., Mitra, S., Dunn, J.C., Hatcher, P.G., Hockaday, W.C., Smith, D.M., Hartkopf-Fröder, C., Böhmer, A., Luer, B., Huebert, B.J., Amelung, W., Brodowski, S., Huang, L., Zhang, W., Gschwend, P.M., Flores-Cervantes, D., Largeau, C., Rouzau, J., Rumpel, C., Guggenberger, G., Kaiser, K., Rodionov, A., González-Vila, F.J., González-Pérez, J.A., De la Rosa, J.M., Manning, D.A.C., Lopez-Capél, E., Ding, L., 2007. Comparison of quantification methods to measure fire-derived (black/elemental) carbon in soils and sediments using reference materials from soil, water, sediment and the atmosphere. *Global Biogeochemical Cycles* 21, 2-18.
- Hammes, K., Torn, M.S., Lapenas, A.G., Schmidt, M.W.I., 2008. Centennial black carbon turnover observed in a Russian steppe soil. *Biogeosciences* 5, 1339-1350.
- Harden, J.W., Trumbore, S.E., Stocks, B.J., Hirsch, A., Gower, S.T., O'Neill, K.P., Kasischke, E.S., 2000. The role of fire in the boreal carbon budget. *Global Change Biology* 6, 174-184.
- Hockaday, W.C., Grannas, A.M., Kim, S., Hatcher, P.G., 2006. Direct molecular evidence for the degradation and mobility of black carbon in soils from ultrahigh-resolution mass spectral analysis of dissolved organic matter from a fire-impacted forest soil. *Organic Geochemistry* 37, 501-510.

- Hockaday, W.C., Grannas, A.M., Kim, S., Hatcher, P.G., 2007. The transformation and mobility of charcoal in a fire-impacted watershed. *Geochimica et Cosmochimica Acta* 71, 3432-3445.
- Hore, P.J., 1995. *Nuclear Magnetic Resonance*, Oxford University Press, Oxford, UK.
- Intergovernmental Panel on Climate Change, 2000. *Land Use, Land-Use Change and Forestry - A Special Report of the IPCC*, Cambridge University Press, Cambridge, UK.
- Intergovernmental Panel on Climate Change, 2001. *Climate Change 2001: Synthesis Report. A Contribution of Working Groups I, II, and III to the Third Assessment Report of the IPCC*, Cambridge University Press, Cambridge, United Kingdom.
- Intergovernmental Panel on Climate Change, 2007. *Climate Change 2007: The Physical Science Basis, Contribution of Working Group I to the Fourth Assessment Report of the IPCC*, Cambridge University Press, Cambridge, UK.
- Jaffé, R., Ding, Y., Niggemann, J., Vähätalo, A.V., Stubbins, A., Spencer, R.G.M., Campbell, J., Dittmar, T., 2013. Global charcoal mobilization from soils via dissolution and riverine transport to the oceans. *Science* 340, 345-347.
- Jarvis, P., Linder, S., 2000. Botany: Constraints to growth of boreal forests. *Nature* 405, 904-905.
- Kasischke, E.S., Stocks, B.J., 2000. *Fire, Climate Change, and Carbon Cycling in the Boreal Forest*, 1st Edition. Springer-Verlag, New-York.
- Keiluweit, M., Nico, P.S., Johnson, M.G., Kleber, M., 2010. Dynamic molecular structure of plant biomass-derived black carbon (biochar). *Environmental Science & Technology* 44, 1247-1253.
- Kleber, M., 2010. What is recalcitrant soil organic matter? *Environmental Chemistry* 7, 320-332.

- Knicker, H., 2011. Solid state CPMAS ^{13}C and ^{15}N NMR spectroscopy in organic geochemistry and how spin dynamics can either aggravate or improve spectra interpretation. *Organic Geochemistry*; 42, 867-890.
- Kuhlbusch, T.A.J., Crutzen, P.J., 1995. Toward a global estimate of black carbon in residues of vegetation fires representing a sink of atmospheric CO_2 and a source of O_2 . *Global Biogeochemical Cycles* 9, 491-501.
- Lal, R., 2008. Sequestration of atmospheric CO_2 in global carbon pools. *Energy & Environmental Science* 1, 86-100.
- Le Quéré, C., Raupach, M.R., Canadell, J.G., Marland, G., Bopp, L., Ciais, P., Conway, T.J., Doney, S.C., Feely, R.A., Foster, P., Friedlingstein, P., Gurney, K., Houghton, R.A., House, J.I., Huntingford, C., Levy, P.E., Lomas, M.R., Majkut, J., Metzl, N., Ometto, J.P., Peters, G.P., Prentice, I.C., Randerson, J.T., Running, S.W., Sarmiento, J.L., Schuster, U., Sitch, S., Takahashi, T., Viovy, N., van der Werf, G.R., Woodward, F.I., 2009. Trends in the sources and sinks of carbon dioxide. *Nature Geoscience* 2, 831-836.
- Lehmann, J., Joseph, S., 2009. Biochar for environmental management - An introduction. In: Lehmann, J., Joseph, S., (Eds.), *Biochar for Environmental Management: Science and Technology*. Earthscan Publications Ltd, London, UK, 1-12.
- Marschner, B., Brodowski, S., Dreves, A., Gleixner, G., Gude, A., Grootes, P.M., Hamer, U., Heim, A., Jandl, G., Ji, R., Kaiser, K., Kalbitz, K., Kramer, C., Leinweber, P., Rethemeyer, J., Schäffer, A., Schmidt, M.W.I., Schwark, L., Wiesenberg, G.L.B., 2008. How relevant is recalcitrance for the stabilization of organic matter in soils? *Journal of Plant Nutrition and Soil Science* 171, 91-110.
- Marty, B., 2012. The origins and concentrations of water, carbon, nitrogen and noble gases on Earth. *Earth and Planetary Science Letters* 313-314, 56-66.

- Masiello, C.A., Druffel, E.R.M., 2003. Organic and black carbon ^{13}C and ^{14}C through the Santa Monica Basin sediment oxic-anoxic transition. *Geophysical Research Letters* 30, 1185.
- Masiello, C.A., 2004. New directions in black carbon organic geochemistry. *Marine Chemistry* 92, 201-213.
- Oren, R., Ellsworth, D., Johnsen, K., Phillips, N., Ewers, B., Maier, C., Schafer, K., McCarthy, H., Hendrey, G., McNulty, S., Katul, G., 2001. Soil fertility limits carbon sequestration by forest ecosystems in a CO_2 -enriched atmosphere. *Nature* 411, 469-472.
- Pan, Y., Birdsey, R.A., Fang, J., Houghton, R., Kauppi, P.E., Kurz, W.A., Phillips, O.L., Shvidenko, A., Lewis, S.L., Canadell, J.G., Ciais, P., Jackson, R.B., Pacala, S.W., McGuire, A.D., Piao, S., Rautiainen, A., Sitch, S., Hayes, D., 2011. A large and persistent carbon sink in the world's forests. *Science* 333, 988-993.
- Peersen, O.B., Wu, X.L., Kustanovich, I., Smith, S.O., 1993. Variable-amplitude cross-polarization MAS NMR. *Journal of Magnetic Resonance, Series A* 104, 334-339.
- Ponomarenko, E.V., Anderson, D.W., 2001. Importance of charred organic matter in Black Chernozem soils of Saskatchewan. *Canadian Journal of Soil Science* 81, 285-297.
- Potter, M.C., 1908. Bacteria as agents in the oxidation of amorphous carbon. *Proceedings of the Royal Society of London. Series B*, 80, 239-259.
- Preston, C.M., Schmidt, M.W.I., 2006. Black (pyrogenic) carbon in boreal forests: a synthesis of current knowledge and uncertainties. *Biogeosciences* 3, 397-420.
- Preston, C.M., 2009. Biogeochemistry: Fire's black legacy. *Nature Geoscience* 2, 674-675.
- Schimel, D.S., House, J.I., Hibbard, K.A., Bousquet, P., Ciais, P., Peylin, P., Braswell, B.H., Apps, M.J., Baker, D., Bondeau, A., Canadell, J., Churkina, G., Cramer, W.,

- Denning, A.S., Field, C.B., Friedlingstein, P., Goodale, C., Heimann, M., Houghton, R.A., Melillo, J.M., Moore, B., Murdiyarso, D., Noble, I., Pacala, S.W., Prentice, I.C., Raupach, M.R., Rayner, P.J., Scholes, R.J., Steffen, W.L., Wirth, C., 2001. Recent patterns and mechanisms of carbon exchange by terrestrial ecosystems. *Nature* 414, 169-172.
- Schlesinger, W.H., Bernhardt, E.S., 2013. Chapter 11 - The Global Carbon Cycle. In: Schlesinger, W.H., Bernhardt, E.S. (Eds.), *Biogeochemistry (Third Edition)*. Academic Press, Boston, 419-444.
- Schmidt, M.W.I., Skjemstad, J.O., Gehrt, E., Kögel-Knabner, I., 1999. Charred organic carbon in German chernozemic soils. *European Journal of Soil Science* 50, 351-365.
- Schmidt, M.W.I., Noack, A.G., 2000. Black carbon in soils and sediments: Analysis, distribution, implications, and current challenges. *Global Biogeochemical Cycles* 14, 777-793.
- Schmidt, M.W.I., Skjemstad, J.O., Jäger, C., 2002. Carbon isotope geochemistry and nanomorphology of soil black carbon: Black chernozemic soils in central Europe originate from ancient biomass burning. *Global Biogeochemical Cycles* 16,
- Schmidt, M.W.I., Torn, M.S., Abiven, S., Dittmar, T., Guggenberger, G., Janssens, I.A., Kleber, M., Kögel-Knabner, I., Lehmann, J., Manning, D.A.C., Nannipieri, P., Rasse, D.P., Weiner, S., Trumbore, S.E., 2011. Persistence of soil organic matter as an ecosystem property. *Nature* 478, 49-56.
- Shakun, J.D., Clark, P.U., He, F., Marcott, S.A., Mix, A.C., Liu, Z., Otto-Bliesner, B., Schmittner, A., Bard, E., 2012. Global warming preceded by increasing carbon dioxide concentrations during the last deglaciation. *Nature* 484, 49-54.
- Shneour, E.A., 1966. Oxidation of graphitic carbon in certain soils. *Science* 151, 991-992.

- Skjemstad, J.O., Reicosky, D.C., Wilts, A.R., McGowan, J.A., 2002. Charcoal carbon in U.S. agricultural soils. *Soil Science Society of America Journal* 66, 1249-1255.
- Smernik, R.J. (n.d.). Quantitation in solid state ^{13}C NMR spectroscopy of NOM. In *Solid state ^{13}C NMR characterisation of natural organic matter (NOM)*. Retrieved February 15, 2010, from <http://www.waite.adelaide.edu.au/NMR/nmr/NMR%20quantitation.html>.
- Smernik, R.J., Oades, J.M., 2000a. The use of spin counting for determining quantitation in solid state ^{13}C NMR spectra of natural organic matter: 1. Model systems and the effects of paramagnetic impurities. *Geoderma* 96, 101-129.
- Smernik, R.J., Oades, J.M., 2000b. The use of spin counting for determining quantitation in solid state ^{13}C NMR spectra of natural organic matter: 2. HF-treated soil fractions. *Geoderma* 96, 159-171.
- van Bellen, S., Garneau, M., Bergeron, Y., 2010. Impact of climate change on forest fire severity and consequences for carbon stocks in boreal forest stands of Quebec, Canada: A synthesis. *Fire Ecology* 6, 16-44.
- von Lützow, M., Kögel-Knabner, I., Ekschmitt, K., Matzner, E., Guggenberger, G., Marschner, B., Flessa, H., 2006. Stabilization of organic matter in temperate soils: mechanisms and their relevance under different soil conditions - a review. *European Journal of Soil Science* 57, 426-445.
- Wardle, D.A., Zackrisson, O., Nilsson, M., 1998. The charcoal effect in boreal forests: Mechanisms and ecological consequences. *Oecologia* 115, 419-426.
- Wotton, B.M., Nock, C.A., Flannigan, M.D., 2010. Forest fire occurrence and climate change in Canada. *International Journal of Wildland Fire* 19, 253-271.

Chapter 2. Laboratory charring conditions affect black carbon properties:

A case study from Quebec black spruce forest

A version of this chapter has been submitted for publication to *Organic Geochemistry*.

2.1. Introduction

Black carbon (BC) is commonly defined as the highly condensed carbonaceous residue produced from the incomplete combustion of organic matter (Baldock and Smernik, 2002). Important defining properties of BC are its relative inertness, ubiquity in pyrogenic ecosystems, and high content of aromatic structures (Schmidt and Noack, 2000) although BC produced by wildfires tend to be composed of small aromatic clusters (Preston and Schmidt, 2006). However, an ambiguity persists in determining what constitutes BC, as no standard analytical method exists. Masiello (2004) proposed to define BC as a continuum. The idea was further explored by Hammes et al. (2007) with an inter-laboratory ring trial that aimed to resolve which techniques best assessed each part of the continuum.

Soil organic carbon (SOC) constitutes by far the most important carbon stock in terrestrial ecosystems. Globally, soils store around 1.5×10^{15} kg C (Schlesinger and Bernhardt, 2013), i.e. 3-fold the amount found above ground in plants and in other living organisms. The C reservoir in boreal forest soils is particularly significant; it is estimated at 227×10^{12} kg (Kasischke and Stocks, 2000), which represents 17% of all terrestrial C. Studies showed that BC may be a significant component of the SOC pool (e.g., Schmidt et al., 1999; Ponomarenko and

Anderson, 2001; Skjemstad et al., 2002). Preston and Schmidt (2006) reported BC stocks in boreal forest floors of the order of 1000–2000 kg/ha, and considered these numbers as likely underestimates of the real stocks. Indeed, in boreal forests, the combustion of the thick forest floor layers by wildfire is often incomplete and BC is a major outcome.

In addition to its potential importance in contributing to the overall SOC pool, the amount of BC left on site after fire may affect ecosystem recovery through modification of plant community dynamics and by stimulation of the N cycle (DeLuca et al., 2006). BC plays a notable role in soil microbial activity and nutrient cycling after fire (Wardle et al., 1998; DeLuca et al., 2006). Unfortunately, there is a lack of knowledge with regards to its composition and morphological features, although these may contribute to the rejuvenating effects of wildfire on soil properties (Certini, 2005). For instance, porosity directly affects the role BC plays in retaining water, nutrients and/or tannins, and its potential to provide habitats for microorganisms (Zackrisson et al., 1996; Hockaday et al., 2006; Hockaday et al., 2007). Characterization of BC chemical and physical properties is moreover critical for the purpose of its quantification, as demonstrated by e.g., Hammes et al. (2007) and Keiluweit et al. (2010). At the same time, there is an immediate need to introduce the BC pool into global carbon models under future climate change conditions (Bergeron and Flannigan, 1995), especially since an increase in fire frequency is expected for the boreal region.

In this study, we focussed on BC properties that directly affect its ability to impact on soil functioning after fire, including its elemental and macromolecular

composition, and several key physical characteristics, such as porosity and surface area. We produced BC samples under controlled conditions and analyzed them using a set of diverse methods to (i) identify the range of chemical and physical properties of BC as it might be produced in boreal forests and (ii) identify the different influences of the formation conditions on these properties under a range of fire severity. This study is unique in its attempt to investigate the effects of thermal treatments simulating different wildfire conditions on major fuels from boreal forests.

2.2. Material and methods

2.2.1. Creation of reference set

We created a reference set of laboratory-produced BC samples (n = 88) by controlling several key variables, namely: the type of fuel (Hammes et al., 2006), the maximum temperature reached during combustion (Baldock and Smernik, 2002; Brown et al., 2006) and the duration of charring (Baldock and Smernik, 2002). We also explored the influence of the abundance of O₂ available during the thermal treatment on BC chemical properties.

We selected biomass representing the most common fuels available in Quebec black spruce-moss forests. These included fresh (L) and partially humified (F) layers of *Sphagnum* sp. and *Pleurozium shreberi* dominated forest floor, bark, branches and needles from black spruce (*Picea mariana*), cones, branches and needles from jack pine (*Pinus banksiana* Lamb.) and twigs and leaves from

Labrador tea (*Rhododendron groenlandicum*). Similar fuel types are available in many boreal forests throughout Eurasia and North America.

2.2.2. Charring conditions

We chose the temperature and duration of charring associated with each charcoalification (Orvis et al., 2005) experiment to mimic, as close as possible, a range of plausible wildfire conditions, as they might occur in boreal forests (Miyaniishi, 2001; Ryan, 2002; Taylor et al., 2004; Rein et al., 2008). Specifically, we varied the maximum temperature (MT) from 75 to 800 °C and the duration of charring from 0.5 to 24 h. We paired the charring conditions (MT, duration and O₂) to further analyze their influence (Table 2-A.1). The experiments were performed with a muffle furnace under controlled temperature and charring duration. The amount of O₂ was varied by either placing the fuels in a tin with a cap pierced with tiny holes (limited O₂ input, i.e. partial pyrolysis) or by tightly wrapping them in Al foil before putting them in a sand bath (full pyrolysis). The objective of this O₂ treatment was to simulate variations in pyrolysis conditions as they are likely to occur during a wildfire [BC forms both during the flaming and smoldering stages (Schmidt and Noack, 2000)]. However our experimental set-up did not allow us to measure differences in O₂ content between the SB and T experiments. The charring duration refers to the time during which the fuel was held at MT. The time taken to reach MT was not included as one of the variables, and total time in the furnace varied among charcoalification experiments. The higher MTs (≥ 600 °C) were associated with short charring duration (Table 2-A.1)

as, during a wildfire, those temperatures are not likely to persist for long periods of time. With our muffle furnace, there was no possible adjustment of the heating rate. However, the latter was recorded and proved to be relatively constant among the different batches (13–19 °C·min⁻¹), so we considered it a fixed parameter. Sufficient amount of fuel was used for each BC production to give at least 4 g of BC samples.

2.2.3. BC characterization

The BC samples were finely ground using a mortar and pestle or a mortar grinder (RM 100 mortar grinder, Retsch, Haan, Germany). The total amounts of C, H and N were determined from dry combustion using a CHN Analyzer (CEC – Control Equipment Corporation – Model 440 Elemental Analyzer with auto-injector). The O content was estimated by difference from the ash free mass of the sample obtained after 6 h at 750 °C in a muffle furnace, in accord with ASTM Standard D1762-84 (ASTM, 2007). The procedure also provided the total ash content. All results reported for carbon, hydrogen, nitrogen and oxygen have been normalized to a dry and ash-free basis.

Physical properties were characterized as follow. The BET (Brunauer et al., 1938) specific surface area (multipoint) and the size pore distribution were characterised from N adsorption and desorption isotherms measured at 77.3 K with an Autosorb 1MP surface area analyzer (Quantachrome Instruments Corp., Boynton Beach, FL). Prior to analysis, samples were degassed at room temperature up to 150 °C (depending on the MT of formation) for 3 to 27 h

(average degassing time 20 h). BET surface area was derived from a multipoint plot over a range of relative pressure, $P/P_0 = 0.05\text{--}0.35$ (Sing et al., 1985). Calculation of the different pore volumes was done using the pore volume data with Autosorb 1 for Windows 1.52.

BC heterogeneity, notably the size and shape of pores, was assessed using scanning electron microscopy (SEM). High-resolution digital images of the surface of different BC samples were obtained using a field emission SEM instrument (JEOL 6301F – JEOL Ltd.) with magnification ranging from 20 x to 50000 x. Before being imaged through the SEM instrument, samples were coated with Au (Nanotech SEMPRep 2 sputter coater) to increase conductivity.

2.2.4. Spectroscopic analysis

To characterize BC macromolecular structure, we used a non-destructive method: solid-state ^{13}C NMR spectroscopy with magic angle spinning (MAS). The ^{13}C nuclei (1.1% natural abundance) provided information about the various functional groups in the samples (Axelson, 2012). Usually studies focussing on organic matter use cross-polarization (CP) as it generally allows acquisition of ^{13}C NMR spectra in less time. However, the CP efficiency for chars is reduced (Baldock and Smernik, 2002) because of the absence of particularly mobile ^1H nuclei (Freitas et al., 1999; Smernik et al., 2002). To verify that our CP spectra were representative we used the more quantitative Bloch decay (BD) also called direct polarisation (DP) technique (Preston and Schmidt, 2006) on a subset of samples.

The ^{13}C NMR experiments were conducted with a Chemagnetics CMX Infinity 200 Spectrometer. A 7.5 mm Chemagnetics double resonance MAS probe was used to spin the samples at 5 kHz at the magic angle (54.7°). Samples were packed into a 7.5 mm o.d. zirconium oxide rotor equipped with a Kel-F® drive tip and Teflon end cap and spacer. Chemical shifts (ppm) were externally referenced to tetramethylsilane (TMS) by setting the high frequency peak for adamantane to 38.56 ppm (Earl and VanderHart, 1982). Spectra were acquired at 50.3 MHz.

We used a variable-amplitude CP (VACP) pulse sequence (Peersen et al., 1993) to obtain the free induction decays (FIDs) of the CP spectra, using a spectral width of 30 kHz; 1024 data points were collected over an acquisition time of 34.1 ms. All spectra were then zero-filled to 8192 data points. The background ^{13}C NMR signal, obtained by the acquisition of the spectrum of an empty rotor, was subtracted before processing the FIDs. The number of scans acquired for the CP spectra ranged from 8432 to 9468. We used a 1 ms contact time, a 90° ^1H pulse of 4.5 μs duration and a recycle delay of 10 s. Finally, we applied Lorentzian line broadening of 60 to 100 Hz before performing the Fourier Transform. The spectra were divided into eight spectral regions, each corresponding to a major C type, as described by Baldock and Smernik (2002). Briefly, the intensity associated with the following regions was quantified by integration: ketone C (215–190 ppm), carbonyl and amide C (190–165 ppm), O-aryl C (165–145 ppm), aryl and unsaturated C (145–110 ppm), di-O-alkyl C (110–90 ppm), O-alkyl C (90–65 ppm), methoxyl and N-alkyl C (65–45 ppm), alkyl C (45–0 ppm), while using the regions with high chemical shift (290–

215 ppm) to correct for the spinning side bands. In doing so, we assumed that the side bands were of equal intensity on either side of the isotropic peak. While likely accurate for the aromatics, this may not be so true for the carbonyls. Because our spectra did not show any large carbonyl peak, we decided that it was safe to apply this methodology. For part of the statistical analysis, the regions were simplified into four regions: carbonyl C (215–165 ppm); aromatic and phenolic C (165–110 ppm); O-alkyl C (110–45 ppm); alkyl C (45–0 ppm).

For the DP spectra, 884 to 888 scans were acquired using a 90° ^{13}C pulse of 4.5 μs . To allow complete relaxation, the recycle delay was set to 100 s. The FID of the background signal was subtracted from the FID of the sample before processing; all spectra were zero-filled to 8192 data points and a Lorentzian line broadening of 60 to 100 Hz was applied to the FID. Applying Smernik and Oades' (2000a) methodology, we used spin counting to determine if the DP spectra were representative of all the C moieties in the samples. Glycine (Fisher Scientific, reagent grade) was used as external reference material. The C observability, C_{obs} , corresponds to the fraction of the expected NMR intensity actually observed. It is assumed that the intensity of the NMR resonances quantitatively reflects the distribution of ^{13}C environments in the sample if $C_{\text{obs}} = 100\%$ (Smernik and Oades, 2000b). A value $< 100\%$ implies that part of the potential signal was not detected.

Even though CP experiments are not commonly considered as quantitative, we concluded, based on comparison with the respective DP spectra, that they represented the distribution of the total intensity quite accurately, further

indicating that the majority of the aromatic/quaternary carbons efficiently cross-polarized. The results (Table 2-B.1) are similar to previous observations (Baldock and Smernik, 2002; Knicker et al., 2005). We therefore used the results from the VACP spectra for the remainder of the study.

2.2.5. Data analysis

The analytical methods described above were applied to different subsets of samples in order to reduce the cost and time of analysis. Elemental analysis was performed on 67 of the 88 samples. The ^{13}C NMR VACP experiment was performed on 40 samples [*Sphagnum* spp.; black spruce (bark; branches + twigs; needles); *Rhododendron* g.], while only a subset of ten BC samples was subjected to both VACP and DP associated with spin counting ^{13}C NMR experiments. We were not able to acquire ^{13}C NMR spectra for the BC produced at 800 °C because of our inability to properly tune the probe containing these samples. This phenomenon has been related to the high electrical conductivity associated with the alignment of aromatic sheets (Freitas et al., 1999) in such samples. Because surface area analysis is time-consuming, only a subset of 14 samples (*Sphagnum*; black spruce branch; *Rhododendron* g. at specific MTs) was examined. Finally, scanning electron micrographs were obtained for 20 samples [*Sphagnum* spp.; black spruce (branch + bark); *Rhododendron* g. at specific MTs].

The different biomass types were grouped into the following four main fuel types for part of the statistical analysis: moss (*Sphagnum* spp. and *Pleurozium*

shreberi), ericaceous shrub (*Rhododendron groenlandicum*), “wood” (branches and bark) and needles from black spruce (*Picea mariana*).

We conducted analysis of variance (one- and two- ways) and paired t-tests to isolate the influence of the different formation factors, using SAS 9.2 (SAS Institute Inc., Cary, North Carolina). The influence of duration of charring and O₂ abundance on BC physical properties was not tested because of time limitations; for these two variables, the results presented below only cover chemical properties.

2.3. Results and discussion

2.3.1. Influence of MT

Yield and chemical composition

The yield of BC decreased with increasing MT (Table 2-1). Most of the distinct decrease in yield (36–50%) between 75 °C and 250 °C can be attributed to moisture loss (Melkior et al., 2012). There was another steep decrease between 250 °C and 350 °C, likely due to the decomposition of hemicellulose and release of CO and CO₂ (Miyanishi, 2001). The remaining yield decrease for MT ≥ 350 °C can be explained by cellulose degradation followed by lignin degradation (Antal and Grønli, 2003; Belderok, 2007; Melkior et al., 2012). The additional weight loss > 425 °C was smaller (5–13% decrease) and likely caused by the final stages of lignin degradation and release of volatile matter (including tar).

For all fuel types, we observed a progressive increase in C content and a decrease in O and H contents with increasing MT (Table 2-1). The atomic H/C

ratio values generally agreed with observations from Hammes et al. (2006), who reported that an atomic H/C ratio > 0.5 seemed to characterize chars which experienced temperatures < 500 °C, whereas chars with H/C < 0.5 were mostly formed at higher temperature (≥ 500 °C). For all fuels, N concentration first slightly increased up to 425 °C and then decreased back to initial level (Table 2-1). The trend agrees with previous studies (Baldock and Smernik, 2002; Lang et al., 2005; Calvelo Pereira et al., 2011), and suggests that at low to intermediate temperature (≤ 425 °C), N is included in newly formed unsaturated heterocyclic compounds (Knicker, 2007) and is not volatilized until higher temperature. The BC ash content also increased with increasing MT and BC produced at 800 °C contained significantly more ash than BC formed at lower MT (Table 2-1).

For temperatures as low as 250 °C, a change in the NMR spectra was observed for all fuels (Figure 2-1), with a relative decrease in the signals characteristic of carbohydrates (105 ppm, 74 ppm, etc.) compared with the materials treated at 75 °C. As MT increased from 250 to 350 °C, there was a shift from BC spectra dominated by O-alkyl functional groups (related to cellulose and hemicelluloses) to aryl and alkyl dominated spectra. The NMR spectra confirmed results from the elemental analysis in that the transition between 250 and 350 °C was a key point for the evolution of the samples along the temperature gradient. At 350 °C, the relative increase and appearance of broad peaks around 130 ppm and 20–25 ppm matched the beginning of char formation (Inari et al., 2007).

The distinct shoulder around 150 ppm in spectra acquired at MT ≥ 250 °C is due to aromatic C linked to O, such as phenols and derivatives (Freitas et al.,

1999). Above 350 °C, the ^{13}C NMR spectra are dominated by aromatic non-oxygenated carbons (130 ppm), the latter peak becoming narrower with increasing MT.

The dominance of aryl groups with increasing MT (Figure 2-1) reflects the conversion of the fuel macromolecules into small aromatic O-containing heterocyclics (Baldock and Smernik, 2002; Chatterjee et al., 2012). Using the spectroscopic data, we calculated the degree of aromatisation, which corresponds to the ratio of aromatic C (165–110 ppm) to aliphatic and O-containing C (110–0 ppm) (Keiluweit et al., 2010). When comparing BC formed under strictly pyrolytic conditions (SB), the degree of aromatisation significantly increased with increasing MT, corresponding to decreasing H/C and O/C atomic ratios (Table 2-1). This increase in the relative proportion of aryl-C structures is an indicator of the increasingly condensed nature of chars (Keiluweit et al., 2010). At 800 °C, the formation of structures containing unsaturated carbons such as aromatic rings associated with the increase in condensation was indirectly noticeable by our inability properly tune the probe containing BC formed at this MT, as reported by (Freitas et al., 1999).

The increase in aromatic content and decrease in atomic ratios observed with increasing MT have been associated with increasing resistance to biotic degradation (e.g., Baldock and Smernik, 2002; Zimmerman, 2010; Harvey et al., 2012). This is an important result regarding BC potential as a valuable carbon sink after wildfires.

Physical properties

With increasing temperature, we observed an increase in specific surface area (by two orders of magnitude between 75 °C and 600 °C) for the black spruce and the *Sphagnum* BC (Table 2-1). Similar observations were made by Hammes et al. (2006) in an investigation of grass and wood chars. From comparison with other BC studies, they deduced that BC formed at low temperature tends to have low surface area ($< 25 \text{ m}^2\cdot\text{g}^{-1}$), while BC formed at high temperatures usually has a large surface area (214–336 $\text{m}^2\cdot\text{g}^{-1}$). As illustrated from SEM, samples produced at 75 °C and 250 °C showed little porosity (Figure 2-2). In these samples cell structures were also preserved, with the membrane of the bordered pits clearly present for the *Rhododendron* and black spruce branch BC. The largest increase in specific SA (both for black spruce branch and *Sphagnum*) occurred between 600 °C and 800 °C, and was particularly marked for the wood BC (Table 2-1). With this range of MT, we also observed a partial or total destruction of fuel cell structure (Figure 2-2). At 600 °C, there was evidence of intermediate melt in the structure of BC from black spruce branch. This was likely formed by the decomposition and softening of some volatile fractions (Lua et al., 2004), which could explain the relatively lower BET surface area vs. the BC from *Sphagnum* (Table 2-1).

The increase in MT resulted in changes in the distribution of BC porosity (Figure 2-3). The shape of the adsorption and desorption isotherms and their associated hysteresis loops (Figure 2-4) also helped characterize the type and shape of the pores (Han et al., 2006). Type II isotherms with a very small closed

hysteresis loop (Figure 2-4a) included BC from *Sphagnum* at 75 °C, black spruce branch at 75 °C and 250°C, and *Rhododendron* at 250 °C), and was characteristic of a porosity dominated by macropores (Figure 2-3). BC from *Rhododendron* at 425 °C, black spruce branch, *Sphagnum* and *Rhododendron* at 350 °C engendered a type H3 non-closed hysteresis loop (Figure 2-4b), indicative of narrow slit-shaped pores (Bourke et al., 2007). Finally, BC from black spruce branch and *Sphagnum* at 425 °C and 600 °C, and black spruce branch and *Sphagnum* at 800 °C generated a type H4 hysteresis loop. The 800 °C BC had a closed loop (Figure 2-4c) while BC formed at lower temperatures presented a non-closed loop. Slit-like pores are frequently the cause of a type H4 hysteresis loop, and these samples, exhibiting the highest measured specific surface areas, were dominated by micropores (Figure 2-3). In a review including studies of BC produced under controlled conditions from various fuels and at a broad range of temperature, Downie et al. (2009) similarly reported an increase in specific SA, mostly related to an increase in microporosity with high MTs.

2.3.2. *Influence of fuel type*

Yield and chemical composition

There were no significant differences in BC yield between the various types of fuel when considering the entire temperature gradient, and comparing analogous charring conditions (Table 2-1). Similarly, atomic ratios and C content were not significantly influenced by the type of fuel. BC from black spruce branches generated less ash than the BC from other precursor materials. This could be

explained by the fact that the non-photosynthetic parts of softwood trees have a relatively low ash content vs. other fuels (Ponomarenko and Anderson, 2001). However, there was no significant difference in ash content over the whole thermal gradient between the various types of fuel.

The ^{13}C NMR spectra illustrate how fuel type affected the composition of the samples exposed to low thermal treatment (Figure 2-5). When only dried (75 °C), the different types of fuel gave distinctive spectra exhibiting representative peaks attributed to cellulose, hemicelluloses and lignin (Wikberg and Maunu, 2004; Inari et al., 2007; Melkior et al., 2012). Based on the relative intensity of the different peaks in the *Sphagnum* spectrum (Figure 2-5), it could be concluded that this particular fuel contained a higher proportion of carbohydrates than the black spruce wood or the ericaceous shrub. This can be explained by the reduced lignin fraction in this particular fuel type.

Differences among fuel types persisted until a MT of 250 °C to 350 °C (Figure 2-1). At 250 °C, the spectrum of black spruce BC looked far more complex than the one from *Rhododendron* and *Sphagnum*. For all fuels, there was a distinct increase in the aromatic and phenolic C content, compared with results obtained at 75 °C. The black spruce and *Rhododendron* had a smaller increase in carbonyl C. The appearance of a broad peak centered around 20–25 ppm for all fuels indicated a higher alkyl content. This signal was most intense for the *Rhododendron*, and also sharper, suggesting less heterogeneity in the functional groups present. Peaks at 65, 74, 84 and 89 ppm in the black spruce BC clearly revealed the persistence of the cellulose. Peaks related to cellulose decreased

substantially for the *Rhododendron* and were totally absent from the *Sphagnum* BC spectrum (Figure 2-1). Hemicellulose (173 ppm) and lignin (56 ppm) structures were still visible in the black spruce and *Rhododendron* BC spectra. The near disappearance of the other hemicellulose signals (20 ppm and 102 ppm), paralleled by the increase in relative intensity of the peak at 173 ppm, suggests carbohydrate degradation with concurrent acetic acid release (Sivonen et al., 2005).

At 350 °C, the spectra began to look similar for all fuels, with the broad peak in the aromatic and phenolic C region (130 ppm) becoming predominant (Figure 2-1). The BC from *Sphagnum* differed from BC produced from other fuels, with significant char formation that began at lower temperature (250 °C) than for the two other precursor materials (around 350 °C). Once again, this could be related to the reduced amount of the more thermally resistant lignin fraction. This result is important since this type of fuel represents a large C input to black spruce ecosystems as shown previously (Harden et al., 1997; Harden et al., 2000; Yu et al., 2002). For MT > 350 °C, there was no difference in the composition of BC produced from the different fuels. This is a slightly lower MT than that reported by Krull et al. (2009) in their review (500 to 600 °C), but the difference could be a result of the different duration of charring in the various studies.

Physical properties

Here we focus on the differences and/or changes in physical properties that are fuel-specific. We observed large differences in BC specific surface area

produced from the different feedstocks (Table 2-1). Considering analogous thermal treatments (MT, duration of charring, O₂ abundance), the black spruce wood led to BC with a smaller specific surface area than the one created from the ericaceous shrub, which in turn had a smaller specific SA than that *Sphagnum* origin. BC from wood usually had higher SA than BC of grass origin (e.g. Keiluweit et al., 2010), as the original vascular structure and the pores created by escaping gas combined to produce a porous BC. On the SEM micrographs, the carbonaceous skeleton of the former wood capillary structure was clearly visible (pores in the range of 10 µm) for the black spruce wood BC produced at high MT (Figure 2-2). The higher values for the *Sphagnum* BC might be more related to the higher proportion of very small and rough particles in these samples rather than actual porosity. Pore volume distribution was also influenced by fuel type (Figure 2-3), with a higher proportion of micropores in the BC from *Sphagnum*. Based on the importance of mosses in boreal forests, the distinctive physical characteristics of moss BC are likely to be important for post-fire forest floor properties.

2.3.3. *Influence of charring duration*

Overall BC yield did not appear to be affected by the differences in charring duration. Lua et al. (2004) reported similar results and observed that once charring exceeded 2 h, the yield did not decrease further. Duration of charring only appeared to significantly influence the H/C ratio for the 600 °C charcoification experiment. Shorter exposure (0.5 h vs. 6 h) did not influence the O/C atomic

ratio but resulted in higher H/C atomic ratio (Figure 2-6). Although there was no significant difference, BC produced with longer exposure to the MT had a higher ash content than BC exposed for shorter time. The evolution of the atomic ratios between the BC formed at 600 °C for 6 h with the BC formed at 800 °C for 0.5 h indicates that dehydrogenation was the only reaction occurring for the latter (Figure 2-6). On the other hand, the main reactions between 600 °C and 800 °C, when the charring duration was kept at 0.5 h for both MTs, followed a condensation pathway.

The trend in the evolution of the atomic ratios with increasing MT (Figure 2-6) is the same as that observed in two independent studies (Baldock and Smernik, 2002; Keiluweit et al., 2010); however there are some differences worthy of discussion. The atomic ratios for our samples differed from those of Baldock and Smernik (2002) and Keiluweit et al. (2010) especially at low and intermediate temperatures (Figure 2-6). The main difference between the formation conditions of all the BC samples was the duration of charring: 1 h for Keiluweit et al. (2010), 24 h to 72 h (until BC reached a constant mass) for Baldock and Smernik (2002) and 0.5 h to 24 h in our study. Charring duration is likely responsible for the discrepancy in atomic ratios; our results are indeed much closer to those obtained by Baldock and Smernik (2002), as were the charring durations we used.

2.3.4. Influence of oxygen

The presence of O₂ significantly decreased BC yield at 250 °C. At the other MT, yield of BC produced in a tin or sand bath were not significantly different

(data not shown). This can be explained by the fact that O₂ favours more complete combustion, reducing the production of char while producing more gas; this is exacerbated at lower temperatures. CO₂ is indeed one of the most abundant gaseous products at the early stages of combustion (Degroot et al., 1988; Behar and Hatcher, 1995).

BC samples produced in tins (with O₂) at low temperature appeared as outliers from the main trend for a given fuel (Figure 2-6). At 250 °C, the presence of O₂ gave BC with significantly lower H/C values (2 to 3-fold) than those of BC produced under fully anoxic conditions (Figure 2-6). On the other hand, the influence of O₂ on BC produced at higher temperatures was minimal (Figure 2-6). Further, its presence did not appear to significantly alter the O/C ratio, or the N content or ash content. The latter was unexpected as a more efficient charring process (in the presence of O₂) should have increased the ash content of the residue (Krull et al., 2009). This might be related to the MT as well as the duration of charring. During thermal treatment, the fuel experienced two of the three following processes: drying (up to 150 °C); pyrolysis (in the absence of O₂); and oxidation (when O₂ was present). Under total pyrolysis conditions, condensation was the main pathway along the increasing thermal treatment gradient, whereas when O₂ was at least partially available, oxidation prevailed (Figure 2-6).

2.3.5. Relative importance of various formation factors – example of the degree of aromatisation

The degree of aromatisation illustrates the relative influence of the various formation factors (Figure 2-7). When there was only dehydration (75 °C; 24 h), the degree of aromatisation was very low under both conditions of pyrolysis (with or without O₂). It increased for BC produced at 250 °C (24 h). At that temperature, the presence of O₂ greatly favoured condensation (5-fold). If one compares the atomic O/C and H/C ratios for these samples (Figure 2-6), in the presence of O₂ our values were close to those obtained by Baldock and Smernik (2002), implying that maximum condensation had been reached. Similarly, increasing the duration of charring from 12 to 24 h allowed a greater condensation as shown by the decrease in H/C ratio (0.83) (Knicker et al., 2005); although the decrease was smaller than in the presence of O₂ (H/C = 0.40). From the ¹³C NMR results (Figure 2-C.1), it appears that the presence of O₂ preferentially reduced the contribution of the O-alkyl C, methoxyl and N-alkyl C, and alkyl C regions. Increasing charring duration intensified the contribution of the regions located at higher ppm (ketone C, carbonyl and amide C, O-aryl C and aryl and unsaturated C; Figure 2-C.2). At 425 °C, the presence of O₂ did not have a significant influence on the degree of aromatisation (Figure 2-7), which suggests that at 425 °C a shorter duration of charring (6 h) was enough to achieve maximum condensation. Finally, BC formed at 600 °C (0.5 h) was even more aromatic when O₂ was present, but plateaued under full pyrolysis. Figure 2-6 shows the increase in condensation when the charring duration was extended. This suggests a similar

behaviour as for the BC formed at 250 °C: short exposure to 600 °C was insufficient to reach maximum condensation but the presence of O₂ was able to compensate.

2.4. Conclusions

Thermal treatment had a significant influence on both the chemical and physical properties of BC originating from various types of fuel. Results obtained for this reference set, produced under controlled thermal treatments, confirmed the importance of maximum temperature and fuel type as factors influencing the composition and physical properties of the resulting BC. Duration of charring and abundance of O₂ also influenced BC chemical properties.

As for the chemical properties, the type of fuel was most important for temperatures < 250 °C to 350 °C. Then, the main fuel components – namely cellulose, hemicelluloses and lignin – started to degrade and the maximum temperature became the dominant formation factor. Charring duration affected the composition at both low (250 °C) and high (\geq 600 °C) temperature. The presence of O₂ affected BC composition mainly at low temperature, i.e. 250 °C, and resulted in accelerated alkyl C degradation. The H content and yield of BC were the two attributes most sensitive to other formation factors besides maximum temperature. With increasing temperature, we observed a decrease in yield, although at 250 °C, the presence of O₂ also provoked a drastic decrease in yield.

MT was the most influential factor with respect to physical properties. There was an important increase in BC porosity (specific surface area and total pore

volume) with the more severe thermal treatments. Nevertheless, BC physical features appeared to also be under the control of the type of fuel.

Tables and Figures

Table 2-1. Yield (%) and characteristics of BC produced from three fuel-types [*Sphagnum* spp., black spruce (BSP) branch and *Rhododendron g.*], under varying maximum temperature (MT), charring duration and pyrolysis type [sand bath (SB) without O₂; tin (T) with limited O₂; nd, not determined].

Fuel	MT (°C)	Charring duration (h)	Pyrolysis type	Yield ^a (%)	Moisture content (%)	Ash content (%)	C ^{b, c} (%)	H ^{b, c} (%)	N ^{b, c} (%)	O ^b (%)	C/N	Atomic H/C ^b	Atomic O/C ^b	SSA ^d (m ² /g)	Degree of aromatisation ^e
<i>Sphagnum</i>	75	24	SB	99.4	7.3	1.55	46.5 (0.7)	5.66 (0.09)	0.61 (0.01)	47.2	76.3	1.46	0.76	2.5	0.41
<i>Sphagnum</i>	250	24	SB	53.4	2.5	6.17	70.5	4.25	1.43	23.8	49.2	0.72	0.25	nd	1.78
<i>Sphagnum</i>	350	12	SB	41.5	1.2	9.02	70.9	4.07	1.45	23.6	48.9	0.69	0.25	13.8	3.27
<i>Sphagnum</i>	425	6	SB	31.5	6.2	8.87	74.2	2.77	1.59	21.5	46.7	0.45	0.22	231.1	5.59
<i>Sphagnum</i>	600	0.5	T	27.7	1.3	5.02	88.0 (0.3)	2.52 (0.31)	1.14 (0.05)	8.3	77.3	0.34	0.07	315.0	21.51
<i>Sphagnum</i>	600	0.5	SB	30.3	1.0	7.61	86.2	2.85	1.27	9.7	67.9	0.40	0.08	nd	8.59
<i>Sphagnum</i>	800	0.5	SB	18.3	2.5	26.98	84.3 (5.4)	1.35 (0.08)	1.13 (0.04)	13.3	74.6	0.19	0.12	502.9	nd
BSP branch	75	24	SB	100.2	4.6	1.02	49.5 (1.4)	5.80 (0.25)	0.51 (0.10)	44.2	98.0	1.41	0.67	2.2	0.23
BSP branch	250	24	SB	63.5	2.1	1.41	64.1 (1.6)	5.08 (0.22)	0.50 (0.11)	30.3	129.0	0.95	0.36	0.6	0.74
BSP branch	350	12	SB	40.1	0.8	2.73	77.4	4.16	0.72	17.8	107.6	0.65	0.17	5.2	2.65
BSP branch	425	6	SB	30.6	2.9	3.22	76.2 (8.0)	3.10 (0.53)	0.57 (0.20)	20.1	133.0	0.49	0.20	18.3	10.57
BSP branch	600	0.5	SB	28.2	2.6	3.30	72.9 (10.6)	2.93 (0.77)	0.53 (0.14)	23.7	137.0	0.48	0.24	89.5	5.91
BSP branch	800	0.5	SB	23.0	2.6	7.82	89.9 (0.6)	1.47 (0.05)	0.82 (0.01)	7.8	109.0	0.20	0.06	365.7	nd
<i>Rhododendron</i>	75	24	SB	100.3	4.6	2.28	53.5 (0.1)	6.50 (0.07)	1.65 (0.07)	38.3	32.5	1.46	0.54	nd	0.39

<i>Rhododendron</i>	250	24	SB	62.1	1.4	3.74	66.2 (1.658)	4.64 (0.22)	2.31 (0.10)	26.8	28.7	0.84	0.30	1.0	0.90
<i>Rhododendron</i>	350	12	SB	41.4	2.0	5.45	77.8 (0.1)	4.49 (0.04)	2.03 (0.01)	15.7	38.3	0.69	0.15	12.8	2.53
<i>Rhododendron</i>	425	6	SB	32.6	0.6	6.23	77.5 (3.3)	3.32 (0.38)	2.55 (0.33)	16.7	30.4	0.52	0.16	3.7	11.33
<i>Rhododendron</i>	600	0.5	SB	30.5	1.0	6.85	72.3 (12.6)	3.11 (0.36)	2.35 (0.44)	22.2	30.7	0.52	0.23	nd	8.52
<i>Rhododendron</i>	800	0.5	SB	22.3	6.8	18.44	82.5 (0.2)	1.37 (0)	1.62 (0.03)	14.5	50.8	0.20	0.13	nd	nd

^a dry wt. basis; ^b dry wt. and ash-free basis; ^c average (\pm SD), n = 3; ^d multi-point BET specific surface area (SAA) obtained by nitrogen adsorption at 77.3 K (7–8 data points); ^e degree of aromatisation defined by aromatic C/(aliphatic + O-containing C) ratio from ¹³C NMR CP spectra (i.e. ratio of the [165–110 ppm]/[110–0 ppm] regions).

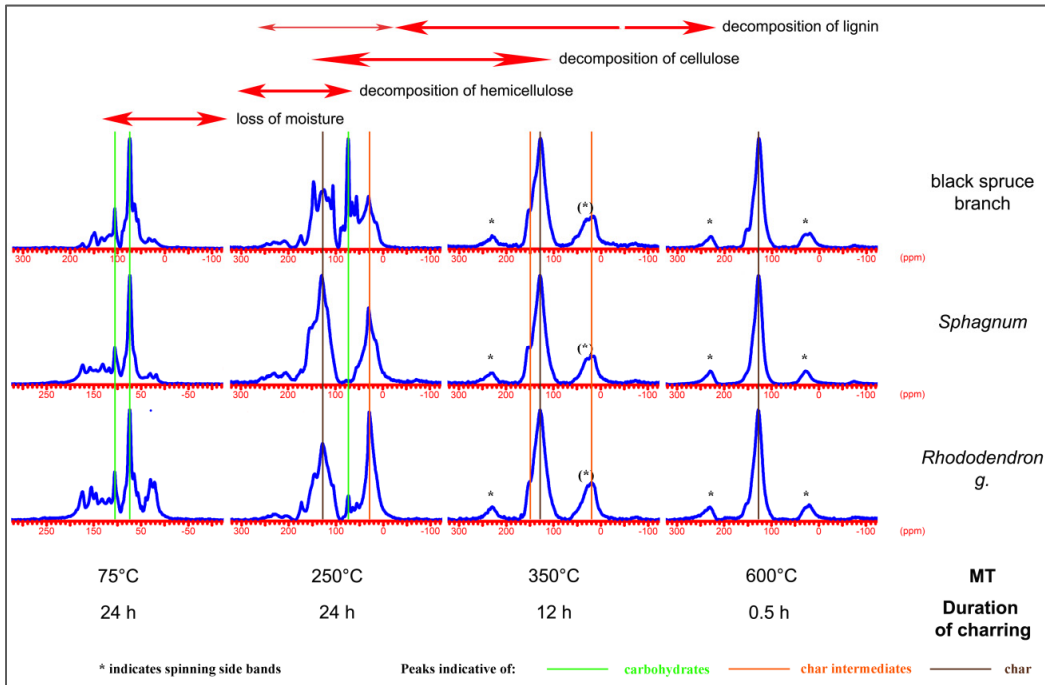


Figure 2-1. ^{13}C VACP NMR spectra of black spruce branch, *Sphagnum* and *Rhododendron*, submitted to different maximum temperatures (MTs) and charring durations.

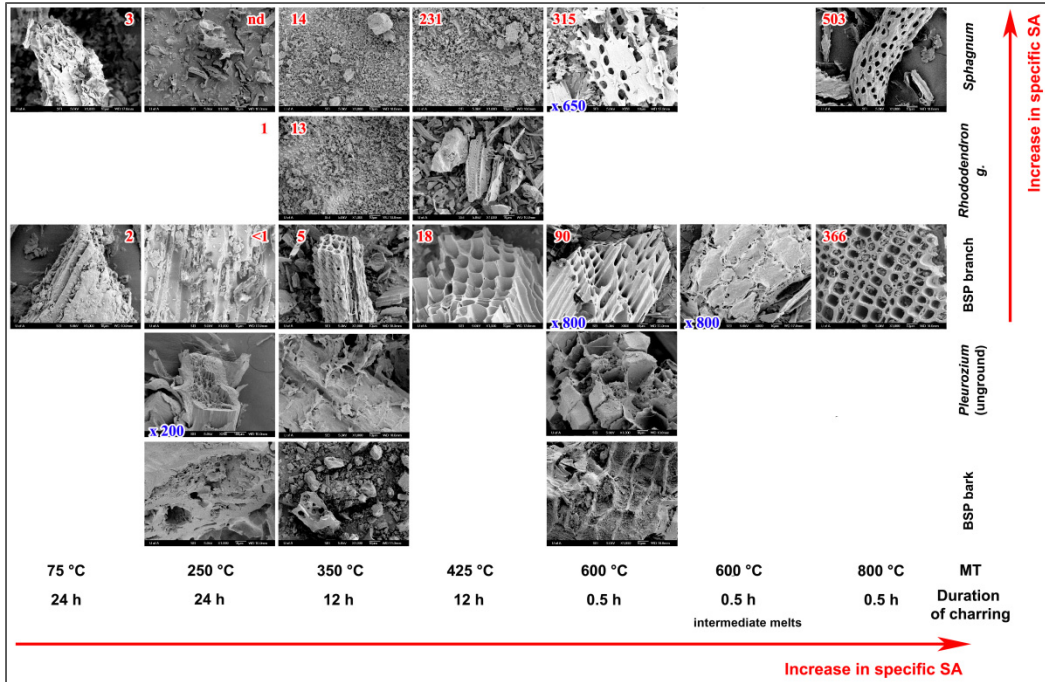


Figure 2-2. SEM micrographs of BC from black spruce (BSP) wood (bark and branches), *Sphagnum* and *Rhododendron* submitted to increasing MT. The associated duration of charring is indicated. Magnification is 1000 x unless otherwise specified. The specific surface area (SA) in m^2g^{-1} obtained from N_2 BET multipoint is also shown.

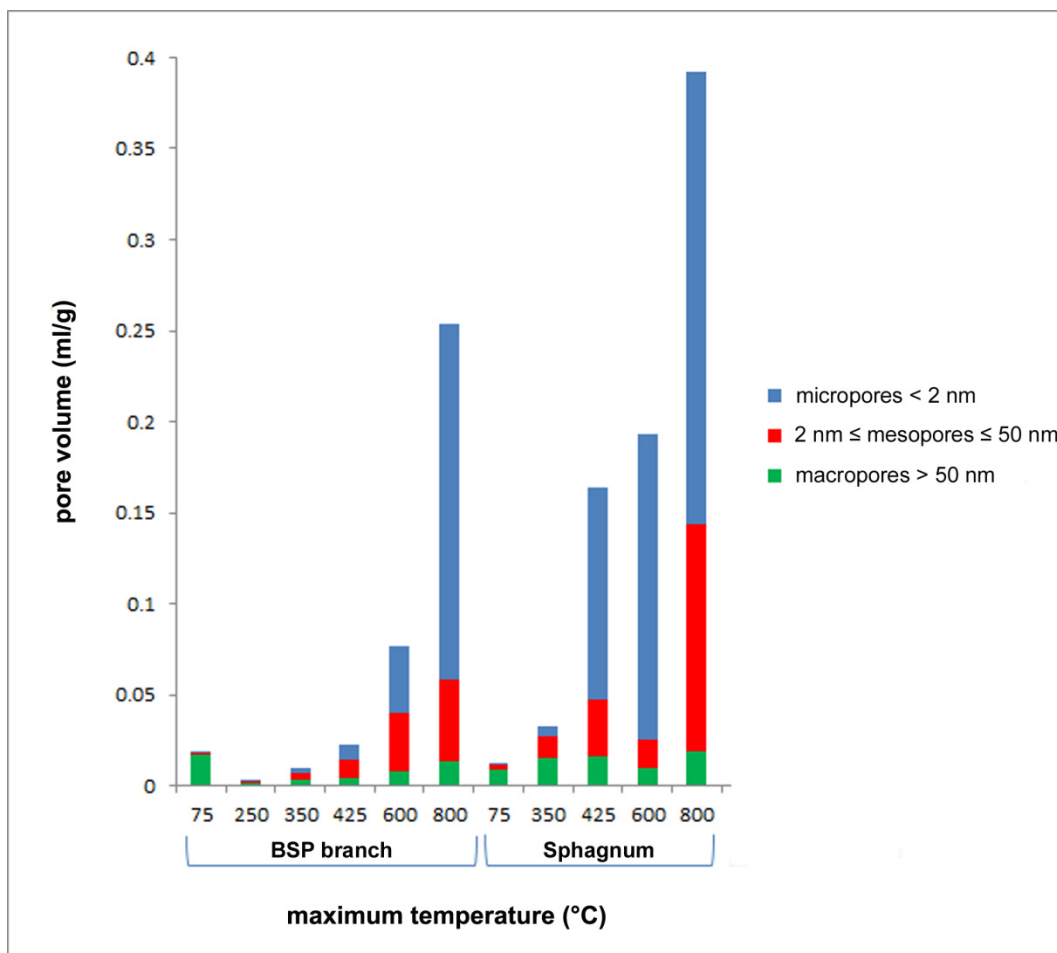


Figure 2-3. Distribution of total pore volume (ml/g) between micro, meso and macropores for BC produced from black spruce (BSP) branch and *Sphagnum* at various MT values.

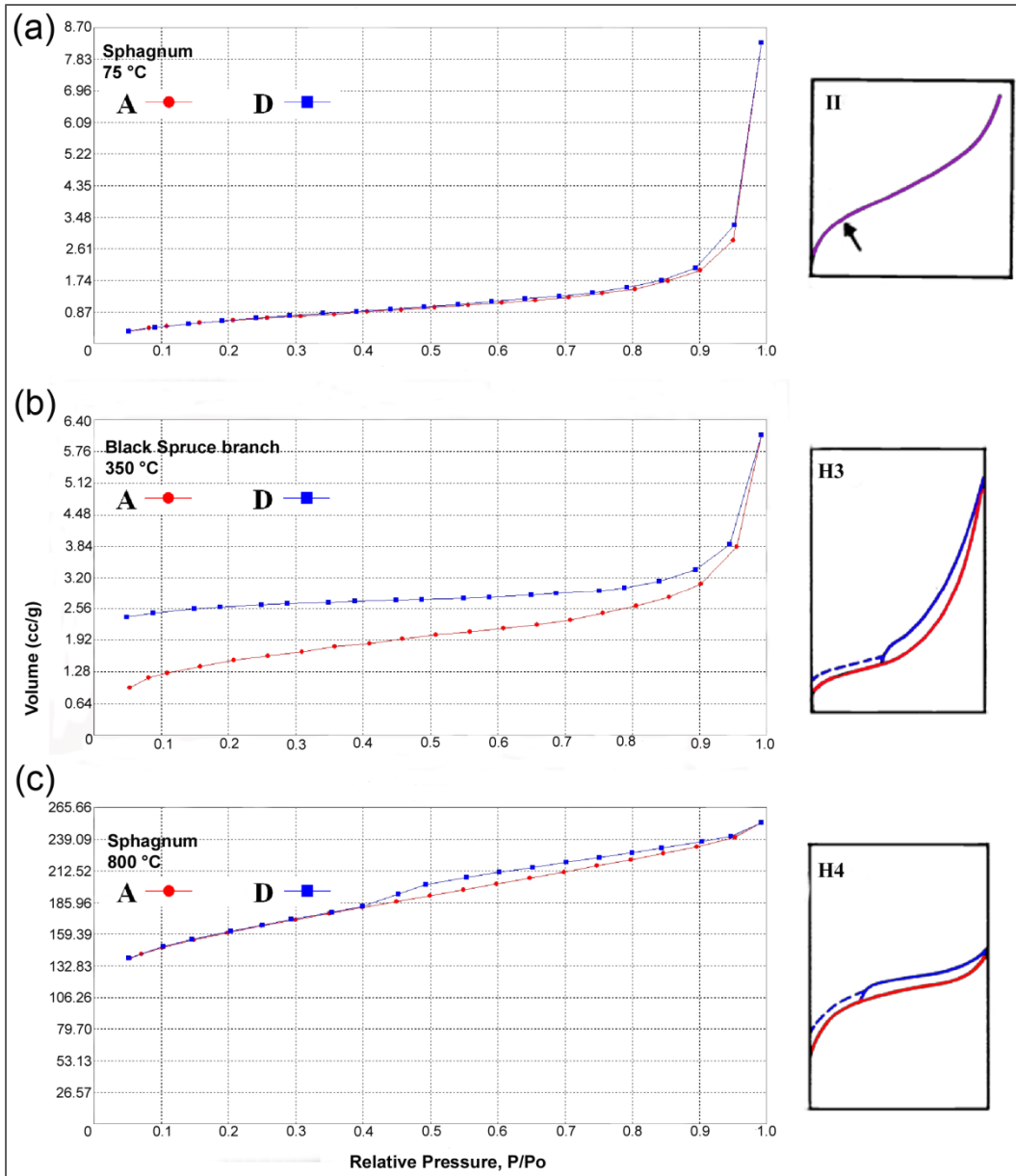


Figure 2-4. Main types of physisorption isotherms and hysteresis loops: (a) BC from *Sphagnum* at 75 °C, with a type II isotherm; (b) BC from black spruce branch at 350 °C, with a type H3 hysteresis loop (indicative of narrow slit-shaped pores); (c) BC from *Sphagnum* at 800 °C, with a type H4 hysteresis loop (indicative of micropores). A, adsorption; D, desorption. The inserts on the right are ideal representations of types of physisorption isotherms or types of hysteresis loops.

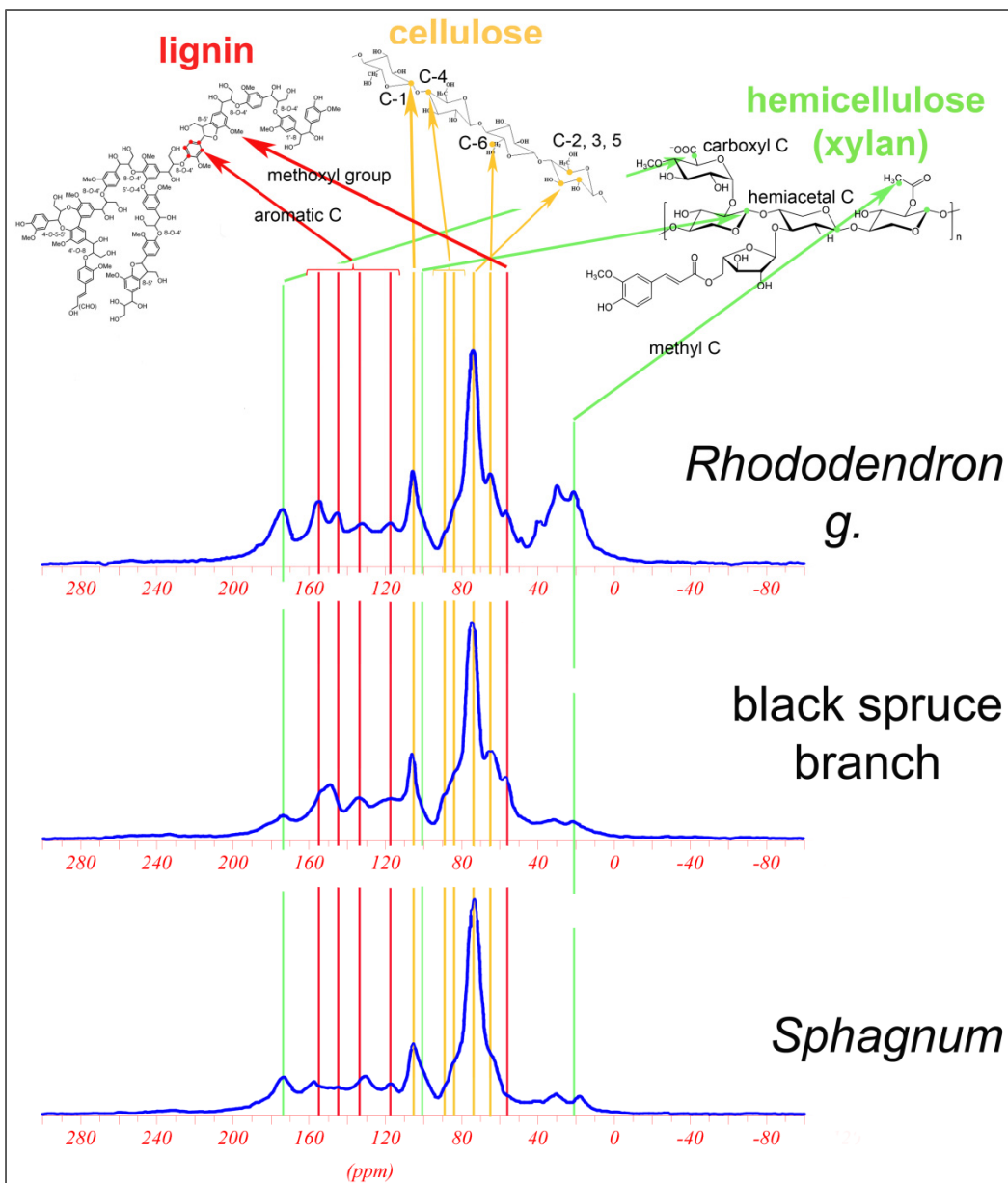


Figure 2-5. ^{13}C CP NMR spectra of three fuels after a thermal treatment at $75\text{ }^\circ\text{C}$ for 24 h. Functional groups of the constituent macromolecules (cellulose, hemicelluloses and lignin) are tentatively assigned to the main peaks.

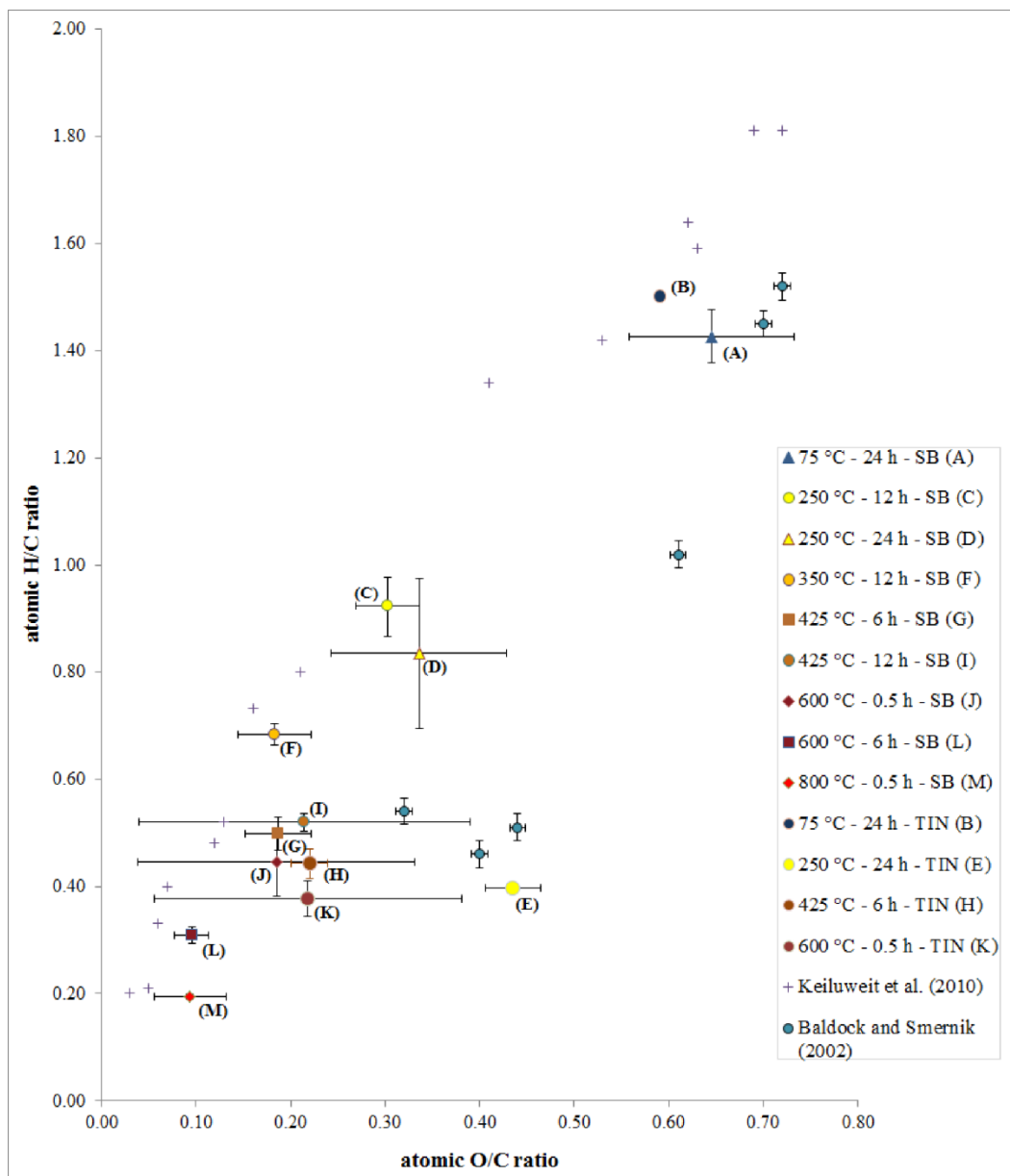


Figure 2-6. Van Krevelen diagram showing the BC produced here and those from Keiluweit et al. (2010) and Baldock and Smernik (2002). Our BC produced in full (SB) and partial (TIN) pyrolysis conditions is reported. Values represent an average (\pm standard deviation) for the types of fuel for a given MT and duration of charring.

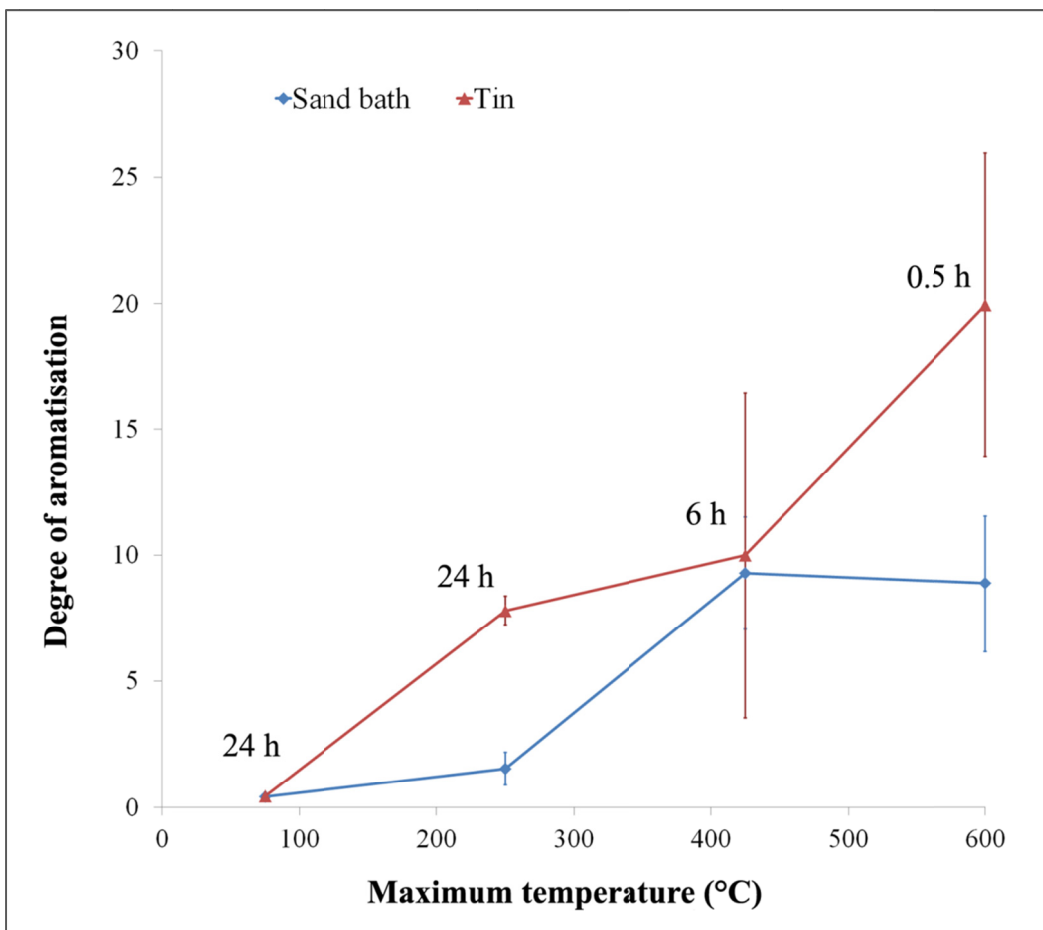


Figure 2-7. Degree of aromatisation with increasing MT (75 °C to 600 °C) for BC formed under full (SB) or partial (Tin) pyrolysis conditions. The degree of aromatisation is the ratio of aromatic C to aliphatic and O-containing C [(165–110 ppm)/(110–0 ppm)]. Data are mean (\pm standard deviation) for all available fuels. Charring durations (h) for each MT are specified.

List of References

- Antal, M.J., Grønli, M., 2003. The Art, Science, and Technology of Charcoal Production. *Industrial & Engineering Chemistry Research* 42, 1619-1640.
- ASTM, 2007. D1762-84 Standard Test Method for Chemical Analysis of Wood Charcoal. American Society for Testing and Materials International, West Conshohocken, PA.
- Axelsson, D.E., 2012. Solid State Nuclear Magnetic Resonance. A Practical Introduction, 1st Edition. MRi_Consulting, Lexington, KY.
- Baldock, J.A., Smernik, R.J., 2002. Chemical composition and bioavailability of thermally altered *Pinus resinosa* (Red pine) wood. *Organic Geochemistry* 33, 1093-1109.
- Behar, F., Hatcher, P.G., 1995. Artificial coalification of a fossil wood from brown coal by confined system pyrolysis. *Energy Fuels* 9, 984-994.
- Belderok, H.J.M., 2007. Experimental Investigation and Modeling of the Pyrolysis of Biomass MSc Thesis. Eindhoven University of Technology, Eindhoven, The Netherlands.
- Bergeron, Y., Flannigan, M.D., 1995. Predicting the effects of climate change on fire frequency in the southeastern Canadian boreal forest. *Water, Air and Soil Pollution* 82, 437-444.
- Bourke, J., Manley-Harris, M., Fushimi, C., Dowaki, K., Nunoura, T., Antal, M.J., 2007. Do all carbonized charcoals have the same chemical structure? 2. A Model of the chemical structure of carbonized charcoal. *Industrial & Engineering Chemistry Research* 46, 5954-5967.
- Brown, R.A., Kercher, A.K., Nguyen, T.H., Nagle, D.C., Ball, W.P., 2006. Production and characterization of synthetic wood chars for use as surrogates for natural sorbents. *Organic Geochemistry* 37, 321-333.

- Brunauer, S., Emmett, P.H., Teller, E., 1938. Adsorption of Gases in Multimolecular Layers. *Journal of the American Chemical Society* 60, 309-319.
- Calvelo Pereira, R., Kaal, J., Camps Arbestain, M., Pardo Lorenzo, R., Aitkenhead, W.P., Hedley, M., Macías, F., Hindmarsh, J., Maciá-Agulló, J.A., 2011. Contribution to characterisation of biochar to estimate the labile fraction of carbon. *Organic Geochemistry* 42, 1331-1342.
- Certini, G., 2005. Effects of fire on properties of forest soils: a review. *Oecologia* 143, 1-10.
- Chatterjee, S., Santos, F., Abiven, S., Itin, B., Stark, R.E., Bird, J.A., 2012. Elucidating the chemical structure of pyrogenic organic matter by combining magnetic resonance, mid-infrared spectroscopy and mass spectrometry. *Organic Geochemistry* 51, 35-44.
- Degroot, W.F., Pan, W., Rahman, M.D., Richards, G.N., 1988. First chemical events in pyrolysis of wood. *Journal of Analytical and Applied Pyrolysis* 13, 221-231.
- DeLuca, T.H., MacKenzie, M.D., Gundale, M.J., Holben, W.E., 2006. Wildfire-Produced Charcoal Directly Influences Nitrogen Cycling in Ponderosa Pine Forests. *Soil Science Society of America Journal* 70, 448-453.
- Downie, A., Crosky, A., Munroe, P., 2009. Physical properties of biochar. In: Lehmann, J., Joseph, S., (Eds.), *Biochar for Environmental Management: Science and Technology*. Earthscan Publications Ltd, London, UK, 13-32.
- Earl, W.L., VanderHart, D.L., 1982. Measurement of ^{13}C chemical shifts in solids. *Journal of Magnetic Resonance* 48, 35-54.
- Freitas, J.C.C., Bonagamba, T.J., Emmerich, F.G., 1999. ^{13}C High-Resolution Solid-State NMR Study of Peat Carbonization. *Energy Fuels* 13, 53-59.
- Hammes, K., Smernik, R.J., Skjemstad, J.O., Herzog, A., Vogt, U.F., Schmidt, M.W.I., 2006. Synthesis and characterisation of laboratory-charred grass straw (*Oryza sativa*)

and chestnut wood (*Castanea sativa*) as reference materials for black carbon quantification. *Organic Geochemistry* 37, 1629-1633.

Hammes, K., Schmidt, M.W.I., Smernik, R.J., Currie, L.A., Ball, W.P., Nguyen, T.H., Louchouart, P., Houel, S., Gustafsson, Ö., Elmquist, M., Cornelissen, G., Skjemstad, J.O., Masiello, C.A., Song, J., Peng, P., Mitra, S., Dunn, J.C., Hatcher, P.G., Hockaday, W.C., Smith, D.M., Hartkopf-Fröder, C., Böhmer, A., Lüer, B., Huebert, B.J., Amelung, W., Brodowski, S., Huang, L., Zhang, W., Gschwend, P.M., Flores-Cervantes, D., Largeau, C., Rouzaud, J., Rumpel, C., Guggenberger, G., Kaiser, K., Rodionov, A., González-Vila, F.J., González-Pérez, J.A., De la Rosa, J.M., Manning, D.A.C., Lopez-Capél, E., Ding, L., 2007. Comparison of quantification methods to measure fire-derived (black/elemental) carbon in soils and sediments using reference materials from soil, water, sediment and the atmosphere. *Global Biogeochemical Cycles* 21, 2-18.

Han, X., Jiang, X., Yu, L., Cui, Z., 2006. Change of Pore Structure of Oil Shale Particles during Combustion. Part 1. Evolution Mechanism. *Energy & Fuels* 20, 2408-2412.

Harden, J.W., O'Neill, K.P., Trumbore, S.E., Veldhuis, H., Stocks, B.J., 1997. Moss and soil contributions to the annual net carbon flux of a maturing boreal forest. *Journal of Geophysical Research* 102, 28,805-28,816.

Harden, J.W., Trumbore, S.E., Stocks, B.J., Hirsch, A., Gower, S.T., O'Neill, K.P., Kasischke, E.S., 2000. The role of fire in the boreal carbon budget. *Global Change Biology* 6, 174-184.

Harvey, O.R., Kuo, L., Zimmerman, A.R., Louchouart, P., Amonette, J.E., Herbert, B.E., 2012. An index-based approach to assessing recalcitrance and soil carbon sequestration potential of engineered black carbons (biochars). *Environmental Science & Technology* 46, 1415-1421.

- Hockaday, W.C., Grannas, A.M., Kim, S., Hatcher, P.G., 2006. Direct molecular evidence for the degradation and mobility of black carbon in soils from ultrahigh-resolution mass spectral analysis of dissolved organic matter from a fire-impacted forest soil. *Organic Geochemistry* 37, 501-510.
- Hockaday, W.C., Grannas, A.M., Kim, S., Hatcher, P.G., 2007. The transformation and mobility of charcoal in a fire-impacted watershed. *Geochimica et Cosmochimica Acta* 71, 3432-3445.
- Inari, G.N., Mounquengui, S., Dumarçay, S., Pétrissans, M., Gérardin, P., 2007. Evidence of char formation during wood heat treatment by mild pyrolysis. *Polymer Degradation and Stability* 92, 997-1002.
- Kasischke, E.S., Stocks, B.J., 2000. *Fire, Climate Change, and Carbon Cycling in the Boreal Forest*, 1st Edition. Springer-Verlag, New-York.
- Keiluweit, M., Nico, P.S., Johnson, M.G., Kleber, M., 2010. Dynamic molecular structure of plant biomass-derived black carbon (biochar). *Environmental Science & Technology* 44, 1247-1253.
- Knicker, H., Totsche, K.U., Almendros, G., González-Vila, F.J., 2005. Condensation degree of burnt peat and plant residues and the reliability of solid-state VACP MAS ¹³C NMR spectra obtained from pyrogenic humic material. *Organic Geochemistry* 36, 1359-1377.
- Knicker, H., 2007. How does fire affect the nature and stability of soil organic nitrogen and carbon? A review. *Biogeochemistry* 85, 91-118.
- Krull, E.S., Baldock, J.A., Skjemstad, J.O., Smernik, R.J., 2009. Characteristics of biochar - organo-chemical properties. In: Lehmann, J., Joseph, S., (Eds.), *Biochar for Environmental Management: Science and Technology*. Earthscan Publications Ltd, London, UK, pp. 53-66.

- Lang, T., Jensen, A.D., Jensen, P.A., 2005. Retention of organic elements during solid fuel pyrolysis with emphasis on the peculiar behavior of nitrogen. *Energy Fuels* 19, 1631-1643.
- Lua, A.C., Yang, T., Guo, J., 2004. Effects of pyrolysis conditions on the properties of activated carbons prepared from pistachio-nut shells. *Journal of Analytical and Applied Pyrolysis* 72, 279-287.
- Masiello, C.A., 2004. New directions in black carbon organic geochemistry. *Marine Chemistry* 92, 201-213.
- Melkior, T., Jacob, S., Gerbaud, G., Hediger, S., Le Pape, L., Bonnefois, L., Bardet, M., 2012. NMR analysis of the transformation of wood constituents by torrefaction. *Fuel* 92, 271-280.
- Miyanishi, K., 2001. Duff consumption. In: Johnson, E.A., Miyanishi, K., (Eds.), *Forest Fires: Behavior & Ecological Effects*. Academic Press, San Diego, pp. 437-475.
- Orvis, K.H., Lane, C.S., Horn, S.P., 2005. Laboratory production of vouchered reference charcoal from small wood samples and non-woody plant tissues. *Palynology* 29, 1-11.
- Peersen, O.B., Wu, X.L., Kustanovich, I., Smith, S.O., 1993. Variable-amplitude cross-polarization MAS NMR. *Journal of Magnetic Resonance, Series A* 104, 334-339.
- Ponomarenko, E.V., Anderson, D.W., 2001. Importance of charred organic matter in Black Chernozem soils of Saskatchewan. *Canadian Journal of Soil Science* 81, 285-297.
- Preston, C.M., Schmidt, M.W.I., 2006. Black (pyrogenic) carbon in boreal forests: a synthesis of current knowledge and uncertainties. *Biogeosciences* 3, 397-420.
- Rein, G., Cleaver, N., Ashton, C., Pironi, P., Torero, J.L., 2008. The severity of smouldering peat fires and damage to the forest soil. *Catena* 74, 304-309.
- Ryan, K.C., 2002. Dynamic interactions between forest structure and fire behavior in boreal ecosystems. *Silva Fennica* 36, 13-39.

- Schlesinger, W.H., Bernhardt, E.S., 2013. The Global Carbon Cycle. In: Schlesinger, W.H., Bernhardt, E.S., (Eds.), *Biogeochemistry - An Analysis of Global Change*. Academic Press, Boston, 419-444.
- Schmidt, M.W.I., Noack, A.G., 2000. Black carbon in soils and sediments: Analysis, distribution, implications, and current challenges. *Global Biogeochemical Cycles* 14, 777-793.
- Schmidt, M.W.I., Skjemstad, J.O., Gehrt, E., Kögel-Knabner, I., 1999. Charred organic carbon in German chernozemic soils. *European Journal of Soil Science* 50, 351-365.
- Sing, K.S.W., Everett, D.H., Haul, R.A.W., Moscou, L., Pierotti, R.A., Rouquérol, J., Siemieniowska, T., 1985. Reporting physisorption data for gas/solid systems with special reference to the determination of SA and porosity (Recommendations 1984). *Pure and Applied Chemistry* 57, 603-619.
- Sivonen, H., Maunu, S.L., Sundholm, F., Jämsä, S., Viitaniemi, P., 2005. Magnetic resonance studies of thermally modified wood. *Holzforschung* 56, 648-654.
- Skjemstad, J.O., Reicosky, D.C., Wilts, A.R., McGowan, J.A., 2002. Charcoal carbon in U.S. agricultural soils. *Soil Science Society of America Journal* 66, 1249-1255.
- Smernik, R.J., Oades, J.M., 2000a. The use of spin counting for determining quantitation in solid state ^{13}C NMR spectra of natural organic matter: 1. Model systems and the effects of paramagnetic impurities. *Geoderma* 96, 101-129.
- Smernik, R.J., Oades, J.M., 2000b. The use of spin counting for determining quantitation in solid state ^{13}C NMR spectra of natural organic matter: 2. HF-treated soil fractions. *Geoderma* 96, 159-171.
- Smernik, R.J., Baldock, J.A., Oades, J.M., Whittaker, A.K., 2002. Determination of $T_{1\rho}^H$ relaxation rates in charred and uncharred wood and consequences for NMR quantitation. *Solid State Nuclear Magnetic Resonance* 22, 50-70.

- Taylor, S.W., Wotton, B.M., Alexander, M.E., Dalrymple, G.N., 2004. Variation in wind and crown fire behaviour in a northern jack pine - Black spruce forest. *Canadian Journal of Forest Research* 34, 1561-1576.
- Wardle, D.A., Zackrisson, O., Nilsson, M., 1998. The charcoal effect in boreal forests: Mechanisms and ecological consequences. *Oecologia* 115, 419-426.
- Wikberg, H., Maunu, S.L. 2004. Characterisation of thermally modified hard- and softwoods by ¹³C CPMAS NMR. *Carbohydrate Polymers* 58, 461-466.
- Yu, Z., Apps, M.J., Bhatti, J.S., 2002. Implications of floristic and environmental variation for carbon cycle dynamics in boreal forest ecosystems of central Canada. *Journal of Vegetation Science* 13, 327-340.
- Zackrisson, O., Nilsson, M., Wardle, D.A., 1996. Key ecological function of charcoal from wildfire in the boreal forest. *Oikos* 77, 10-19.
- Zimmerman, A.R., 2010. Abiotic and microbial oxidation of laboratory-produced black carbon (biochar). *Environmental Science & Technology* 44, 1295-1301.

Chapter 3. Early season fires in boreal black spruce forests produce black carbon with low aromatic content.

A version of this chapter has been submitted for publication to *Global Biogeochemical Cycles*.

3.1 Introduction

Worldwide, boreal ecosystems cover $24 \times 10^7 \text{ km}^2$, and the associated boreal forest soils, which store more carbon per unit area than permafrost soils [*Deluca and Boisvenue, 2012*] represent an immense global carbon pool estimated at $227 \times 10^{12} \text{ kg}$ [*Kasischke, 2000*]. The boreal forest is characterized by recurring wildfires that produce significant amounts of CO_2 ; these forests subsequently turn into carbon sources for at least a decade [*Bond-Lamberty et al., 2007; Hatten and Zabowski, 2009; van Bellen et al., 2010*]. The combustion of the thick organic forest floor layers by wildfire is often incomplete and black carbon (BC) residues are a major by-product. Current climate models predict an increase in fire frequency and a potential shift in fire seasonality toward the spring in Canada [*Flannigan et al., 2005; Wotton et al., 2010*]. How present and future environmental conditions may affect the stability of boreal soil carbon pools, including that of BC residues, is currently poorly understood.

Differences in biophysical conditions create spatial variation in wildfire intensity [*Sousa, 1984*]. Fire thus results in a mosaic of vegetation and soils burned to varying degrees [*Turner and Romme, 1994*], and consequently produces BC residues whose properties vary across the stand and the landscape. Fire severity, a component of the fire regime, refers to fire impacts on the terrestrial

ecosystem, including both vegetation and soil [e.g., *Brown and DeByle*, 1987; *Turner and Romme*, 1994; *van Wagtenock*, 2006]. However, an absolute scale of fire severity does not exist, since the degree of severity depends on the local ecosystem, where particular environmental and weather conditions further define fire behavior. Most fire severity assessments follow Ryan's [2002] suggestions to consider the burn mosaic on three-dimensional levels: (i) the pattern of the burnt area over the entire fire perimeter; fire impacts (ii) on the aboveground compartment (vegetation) and (iii) on the belowground compartment (soil). Furthermore, the environmental conditions responsible for the spatial variation in fire regime appear at various scales: broad-scale climatic and weather conditions [*Flannigan and Wotton*, 2001], meso-scale environmental characteristics such as surficial geology [*Kafka et al.*, 2001] and topography [*Ryan*, 2002], and local features such as vegetation/fuel conditions [*Johnson and Miyanishi*, 2001]. Spatial variability in fire severity therefore occurs at variable scales, ranging from thousands of km² to small patches of a few dm².

Black carbon is the highly condensed carbonaceous residue from incomplete combustion processes of biomass. Because of its intrinsic variability, *Masiello* [2004] proposed that BC is a continuum of material. However, BC consists of so many end-products that it is almost impossible to define distinctive classes with quantitative boundaries [*Lehmann and Joseph*, 2009]. BC is generally considered an important component of the stable soil carbon pool [*Kasischke*, 2000; *González-Pérez et al.*, 2004; *Preston and Schmidt*, 2006], although some studies caution against assuming that all BC is recalcitrant [*Harden et al.*, 2000;

Hockaday et al., 2006; *Czimczik and Masiello*, 2007; *Hammes et al.*, 2008; *Preston*, 2009]. In addition to its potential importance as a global carbon sink, there is evidence that BC plays a central role in soil fertility, in particular by stimulating microbial activity and nutrient cycling after fire [*Wardle et al.*, 1998; *DeLuca et al.*, 2006]. A detailed knowledge of chemical composition and physical properties is a prerequisite to determine BC fate and functions [*Keiluweit et al.*, 2010] in terrestrial ecosystems.

In the present study we focused on properties of BC that directly affect soil functions, including its elemental and macromolecular composition, as well as several key physical characteristics, including porosity and surface area. As pointed out by *Preston et al.* [2006], the entire BC continuum does not present chemical properties (e.g., condensed aromatic structures) associated with long-term stability that would allow it to enter the slow carbon pool. Moreover, porosity and surface area directly affect the role BC plays in retaining water, nutrients and/or tannins, and its potential to provide habitats for microorganisms [*Saito*, 1990; *Zackrisson et al.*, 1996; *Hockaday et al.*, 2006, 2007].

This study aims to provide a more complete characterization of wildfire-produced BC, knowledge that is scarce in boreal ecosystems), and to explore how formation conditions influence BC properties and hence ecosystem function. We hypothesized that fire severity would directly affect BC properties, creating a continuum of BC. Sites affected by higher fire severity would present more aromatic and more porous BC, while BC produced in sites affected by low fire severity would have chemical and physical characteristics more similar to the

unburned forest floor. In 2005–2007, high fire activity in Northern Quebec caused over 1.2 Mha to be burned from the southern Baie-James to the Manicouagan regions. This provided the opportunity to study the influence of these early season wildfires on BC properties. We collected BC samples and analyzed them using a set of analytical methods to: (i) identify the range of variation in their chemical (aromaticity) and physical properties (porosity) and (ii) determine how these properties may be related to fire severity.

3.2 Materials and methods

3.2.1. Site characteristics and selection

The province of Quebec is divided into ten bioclimatic domains, characterized by distinct vegetation and climatic conditions [Saucier *et al.*, 2001]. The black spruce feathermoss bioclimatic domain covers a third of the provincial territory and is divided into the eastern and western subdomains (Figure 3-1). The western subdomain is characterized by an average precipitation of 850 mm/year (north) to 900 mm/year (south), whereas the eastern subdomain receives 1020 mm evenly distributed through the year [Bergeron *et al.*, 2004; Cyr *et al.*, 2007]. Mean annual temperature [Carrier, 1996] ranges from $-2\text{ }^{\circ}\text{C}$ in the north to just above $0\text{ }^{\circ}\text{C}$ in the south. The western sector of the domain forms a transition zone between a continental climate (southern range) and a subpolar continental climate (northern range), while the eastern subdomain experiences a cooler, more humid maritime climate, at least in its southern range. The majority of the black spruce feathermoss domain is characterized by humo-ferric podzols [Soil Classification Working Group, 1998], which have developed on glacio-fluvial sediments/till

deposits and generally contain a high proportion of coarse fragments (> 2 mm diameter). Veins of clay are occasionally present in the western part of the domain, because of the proximity to the Clay Belt [Robitaille and Saucier, 1998]. Both subdomains are dominated by black spruce (*Picea mariana* (Mill.) Britton, Sterns & Poggenb.) with ericaceous shrubs (*Rhododendron groenlandicum* (Oeder) Kron & Judd; *Kalmia angustifolia* L.; *Vaccinium angustifolium* Ait.), feathermoss (*Pleurozium schreberi* (Brid.) Mitt.) and/or *Sphagnum* moss (*Sphagnum* sp.) constituting the majority of the understory vegetation. Locally, lichens (*Cladina rangiferina* (L.) Weber) associated with fire moss (*Ceratodon purpureus* (Hedw.) Brid.) and haircap moss (*Polytrichum* sp.) are present. On drier sites, jack pine (*Pinus banksiana* Lamb.) is often associated with black spruce in mixed stands and becomes dominant under the driest conditions.

A total of 14 fires, ranging in size from 330 to 56000 ha, were selected for the present study (Figure 3-1). Sites description and samples collection took place in summer 2010.

3.2.2. Fire severity gradient

Within each fire site, two to four topographic gradients were established inside unsalvaged areas. Three 20 m x 20 m square plots were positioned on each topographic gradient, and within each plot, nine round microplots of 1.5 m diameter were investigated. We created a mixed “vegetation x soil” severity scale, designed to assess both the aboveground (aerial severity) and belowground (soil severity) impacts of fire at the plot and microplot scale.

To estimate aerial fire severity, we evaluated three burn characteristics of the trees remaining on the plot: scorch height, abundance of twigs, and presence of bark splitting. To quantify the degree of canopy consumption, we rated each element based on the magnitude of fire damage, and added the individual ratings to obtain an index of aerial fire severity at the plot level. To estimate soil fire severity, we evaluated the impact of fire on the consumption of the forest floor organic layers (i.e., burning class), and assessed the nature of the main substrate present within each microplot. We used four burning classes (unburnt/scorched; slightly, moderately and severely burnt; Table 3-1) and five substrate classes (burnt forest floor; mineral soil; dead wood; rock; unburnt forest floor). We used an additional method to estimate fire severity based on the measurement of the amount of forest floor that was consumed during the last fire event. To do so, we measured the thickness of the residual organic matter. On five microplots, we located the uppermost adventitious root of the black spruce tree taller than 2 m and closest to the center of the microplot. In the few cases where no adventitious root was found – e.g., well drained sites with shallow organic layers – the top of the basal root was used. The distance between the adventitious or basal root and the mineral soil surface was used to estimate the thickness of the pre-fire organic layer [*Kasischke et al.*, 2008]. Lastly, thickness of the forest floor that was consumed by the last fire event was calculated as the difference between the latter and the thickness of the residual organic matter. Six soil fire severity classes (0 – low – to 5 – high) combining the various burning class x substrate class options were created and attributed to each sample (Table 3-1).

3.2.3. Field collection of BC samples

All soils within the selected fires presented a surface layer containing black carbon (BC). This thin (around 2 cm) burnt forest floor, which was produced during the last fire event, overlaid partially decomposed fibric and unburnt humus (F or FH horizons); the sampled material is referred to as fresh BC hereafter. For each plot, three fresh BC samples (approximately 20 cm x 20 cm) representative of the overall plot soil fire severity, were collected close to the center of a microplot. The depth of burn was recorded for each sample and the substrate type was also identified where possible (*Pleurozium*; *Sphagnum*; Lichen; duff – when the forest floor was too decomposed and the main species could not be identified anymore). The latter is an important parameter, as it provides information about the type of fuel from which the BC was produced. Since the focus of our research was on the forest floor, only the following three substrates: burnt forest floor, burnt forest floor < 2 cm, and scorched forest floor were sampled for BC (Table 3-1).

A subset of the 267 fresh BC samples were collected and characterized. The selection process was designed to encompass the entire range of fire severity at the sampling locations. Triplicates (or duplicates) of each soil fire severity class, as previously defined, were randomly chosen among the collected samples and further analyzed. This led to a total of 33 fresh BC samples for detailed analysis (Table 3-1).

3.2.4. *BC set produced under controlled laboratory conditions*

Fresh BC samples collected in the field were compared to a BC reference set produced under controlled laboratory conditions [L. N. Soucémarianadin, S. A. Quideau, M. D. MacKenzie, G. M. Bernard, R. E. Wasylishen, Laboratory charring conditions affect black carbon properties: A case study from Quebec black spruce forest, submitted to *Organic Geochemistry*, 2013]. To produce the controlled BC set, we selected biomass representing the most common fuels available in Quebec black spruce-feathermoss forests, including *Sphagnum* sp. and *Pleurozium shreberi* dominated forest floors, bark, branches and needles from black spruce, cones, branches and needles from jack pine and twigs and leaves from Labrador tea (*Rhododendron groenlandicum*). The charcoalification experiments were performed in a muffle furnace under controlled maximum temperature (MT), which varied between 75 and 800 °C for charring durations between 0.5 to 24 hours. The amount of oxygen present during BC formation was adjusted by either placing the fuels in a moisture tin with a cap pierced with tiny holes (tin = partial pyrolysis) or by tightly wrapping them in tinfoil before putting them in a sand bath (SB = full pyrolysis). Samples from the BC reference set were submitted to the same analyses as the fresh BC.

3.2.5. *Characterization of BC chemical properties*

Prior to analysis, the BC samples were finely ground using a mortar and pestle or a mortar grinder (RM 100 mortar grinder, Retsch, Haan, Germany). Carbon, hydrogen, and nitrogen concentrations were determined by dry combustion using

a CE440 Elemental Analyzer (Exeter Analytical, Inc., Chelmsford, MA, USA). The oxygen content was estimated by difference from the sample ash-free mass obtained after 6 hours at 750 °C in accordance with ASTM Standard D1762-84 [ASTM, 2007]. This procedure also provided total ash content.

To characterize BC macromolecular structure, we used a non-destructive method: solid-state ^{13}C NMR spectroscopy with magic angle spinning (MAS). The ^{13}C nuclei (1.1% natural abundance) provided information about the various functional groups present in our samples [Kögel-Knabner, 1997; Axelson, 2012]. Usually studies focusing on organic matter employ the cross-polarization (CP) technique, as it generally allows for the acquisition of ^{13}C NMR spectra in less time. However the CP efficiency for chars is reduced [Baldock and Smernik, 2002] because of the absence of particularly mobile ^1H nuclei [Freitas *et al.*, 1999; Smernik *et al.*, 2002]. To verify that spectra acquired with CP were representative, we used the more quantitative direct polarization (DP) technique also called the Bloch decay (BD) technique [Preston and Schmidt, 2006] on a subset of samples.

The ^{13}C NMR experiments were carried out using a Chemagnetics CMX Infinity 200 Spectrometer. A 7.5 mm Chemagnetics double resonance MAS probe was used to spin the samples at 5 kHz. Samples were packed into 7.5 mm od zirconium oxide rotors equipped with Kel-F® drive tips and Teflon end-caps and spacers. Chemical shifts in parts per million (ppm) were externally referenced to tetramethylsilane (TMS) by setting the high-frequency peak for adamantane to

38.56 ppm [Earl and VanderHart, 1982]. Spectra were acquired at a frequency of 50.3 MHz.

To acquire ^{13}C NMR spectra with ^1H CP, a variable-amplitude cross-polarization (VACP) pulse sequence [Peersen *et al.*, 1993] was used. A spectral width of 30 kHz was used and 1024 real data points were collected over an acquisition time of 34.1 ms. All spectra were then zero-filled to 8192 data points. The probe background ^{13}C NMR signal, obtained by acquiring a spectrum of an empty rotor, was subtracted before processing the free induction decays (FIDs). 8580–8624 scans were acquired for the CP spectra. We used a 1 ms contact time, a 90° ^1H pulse of 4.5 μs duration and a recycle delay of 10 s. Finally, we applied Lorentzian line broadening of 60 to 100 Hz before performing the Fourier transform. The ^{13}C NMR spectra were divided into eight spectral regions, each corresponding to a major type of carbon, as described in Baldock and Smernik [2002]: ketone (215–190 ppm), carbonyl and amide (190–165 ppm), O-aryl (165–145 ppm), aryl and unsaturated C (145–110 ppm), di-O-alkyl (110–90 ppm), O-alkyl (90–65 ppm), methoxyl and N-alkyl (65–45 ppm), alkyl (45–0 ppm); corrections for the spinning side-bands were made using the regions with large chemical shifts (290–215 ppm), following the same methodology as Baldock and Smernik [2002]. For part of the statistical analysis, the above regions were combined and simplified into the following four carbon regions: carbonyl (215–165 ppm); aromatic & phenolic (165–110 ppm); O-alkyl (110–45 ppm); alkyl (45–0 ppm).

For the DP spectra, 888 scans were acquired using a 90° ^{13}C pulse of 4.5 μs . To allow for complete relaxation the recycle delay was set to 100 s. The FID of the background signal was subtracted from the FID of the sample before processing; all spectra were zero-filled to 8192 data points while a Lorentzian line-broadening of 80 Hz was applied to the FID. Applying *Smernik and Oades'* [2000a] methodology, we used spin counting to determine if the DP spectra were quantitative for the various carbons present in the samples. Glycine (Fisher Scientific, reagent grade) was used as an external reference material. The carbon observability, C_{obs} , corresponds to the fraction of the expected NMR intensity that is actually observed; intensities of the NMR resonances quantitatively reflect the distribution of ^{13}C environments present in the sample if $C_{\text{obs}} = 100\%$ [*Smernik and Oades*, 2000b]. A value of less than a 100% for C_{obs} implies that part of the potential signal is not detected.

Even though CP experiments are not commonly considered quantitative, we concluded, based on the comparison to their respective DP spectra, that they represented the distribution of the total intensity quite accurately ($\pm 7\%$), further indicating that the CP efficiency for the aromatic/quaternary carbons was about the same as for the aliphatic carbons. These results (Table 3-A1) are in agreement with previous observations [*Baldock and Smernik*, 2002; *Knicker et al.*, 2005]. Therefore, we used the results derived from the VACP spectra for the remainder of the study.

3.2.6. *Characterization of BC physical properties*

The BET [Brunauer *et al.*, 1938] specific surface area (multipoint) and the size pore distribution were characterized from nitrogen adsorption and desorption isotherms measured at 77.3 K on an Autosorb 1MP surface area analyzer (Quantachrome Instruments Corp., Boynton Beach, FL). Prior to analysis, samples were outgassed at room temperature or 105 °C for 19 to 26 hours. BET surface areas (SA) were derived from a multipoint plot over a range of relative pressure, $P/P_0 = 0.05-0.35$. Calculation of the different pore volumes was performed using Autosorb 1 for Windows 1.52.

Black carbon heterogeneity, notably the size and shape of pores, was assessed by Scanning Electron Microscopy (SEM). High-resolution digital images of the surfaces of different BC samples were obtained using a field emission SEM (JEOL 6301F – JEOL Ltd.) with magnifications ranging from 25 x to 50000 x. Before being imaged through the SEM, samples were coated with gold (Nanotech SEMPrep 2 sputter coater) to increase their conductivity.

3.2.7. *Statistical analyses: influence of fire severity*

A 1-way ANOVA was used to analyze the ^{13}C NMR and elemental results of the 33 fresh BC samples and evaluate the influence of fire severity estimation on BC chemical characteristics. When the data were not following the ANOVA assumptions a Mood's median test- and a Kruskal-Wallis 1-way ANOVA were used. The experimental units were the microplots and their associated fire severity classes. To test for differences in the distribution of the total signal intensity

between the ^{13}C CP and DP NMR experiments, a Wilcoxon signed-rank test was used because the data did not follow a normal distribution. All comparisons, Wilcoxon signed-rank test, and ANOVA were considered significant at an alpha value of 0.05. For the significant ANOVAs, the alpha was adjusted with a Bonferroni correction when exploring all possible comparisons. All the statistical analyses were performed with SAS 9.2 (SAS Institute Inc., Cary, North Carolina).

3.3 Results

3.3.1. Fire severity gradient

Field observations indicated that aboveground fire severity was fairly homogeneous across and within sites, in that most trees were completely burned and dead. On the other hand, at the soil level, the amount of organic matter left post-fire varied greatly both along topographic gradients as well as among microplots at each given topographic position. The visual appearance of post-fire organic matter also varied.

There was no significant relationship between aerial fire severity and soil fire severity when determined at the microplot scale. Soil fire severity was linked to the aerial fire severity when plot averages were considered, although only when the soil fire severity was high (\geq class 4).

3.3.2. Black carbon physical properties

The analyzed samples exhibited very low specific surface area, and porosity was dominated by macropores (Figure 3-2). Results further indicated that the BC

corresponding to a fuel that was only scorched (class 0) had a higher surface area ($2.3 \text{ m}^2\text{g}^{-1}$) than that associated with a high fire severity (class 5; $\text{SA} = 1.6 \text{ m}^2\text{g}^{-1}$). Moreover, these values were similar to results obtained for dry (exposed to $75 \text{ }^\circ\text{C}$ for 24 hours in the laboratory) but unburnt fuels ($\text{SA} = 2.2\text{--}2.5 \text{ m}^2\text{g}^{-1}$). Finally, as can be seen on the SEM micrographs (Figure 3-3), the bulk of the original fuel cell structures remained unaltered (Figure 3-3). Microorganisms were still visible in most samples; in particular, we were able to observe bacteria as well as various fungal structures (e.g., hyphae; hyphal tubes) in these samples.

3.3.3. *Black carbon elemental composition*

The carbon content of the samples varied from 47.0 to 60.4% (Table 3-1) and increased with increasing fire severity. The BC collected on the low fire severity sites (classes 0 and 1) showed a significantly lower carbon content when compared to the BC collected on the high fire severity sites (classes 4 and 5). The increase in carbon percentage occurred with a concomitant decrease of the atomic H/C and O/C ratios. The oxygen content steadily decreased with the increase in fire severity (46.3 to 35.6%). On the other hand, the hydrogen content remained constant (5.4%) when fire severity ranged between classes 0 to 2, before decreasing steadily to 4.0% for class 5. The nitrogen content was only weakly related to fire severity; it increased slightly up to class 3 (1.1 to 1.8%) and then appeared to plateau (Table 3-1). The C/N ratio tended to decrease with increasing fire severity; the C/N values for BC associated with fire severity classes 3 to 5

were lower (around 35:1) than for BC of classes 0, 1, and 2 (40:1 or higher), although values were not significantly different. The ash content ranged from 3.6% to 35.9%; it increased slightly from class 0 to 3, then more importantly from class 4 (11.0%) to class 5 (Table 3-1). The atomic H/C and O/C ratios both decreased with increasing fire severity (Figure 3-4). BC from classes 0 and 1 had significantly higher atomic ratios than BC from classes 4 and 5 (H/C ratio) and classes 2, 4, and 5 (O/C ratio).

3.3.4. *Black carbon molecular composition*

The variable amplitude cross-polarization ^{13}C NMR spectra acquired for the BC samples associated with low fire severity showed a distribution of carbon groups very similar to that in unburnt fuels (Figure 3-5a). Spectra were dominated by carbohydrates, as confirmed by the presence of peaks representative of cellulose and hemicelluloses; i.e., at 62, 72–75, and 105 ppm [Wikberg and Maunu, 2004; Inari et al., 2007; Melkior et al., 2012], and showed limited presence of lignin. Lignin was identified by the presence of peaks between 110 and 165 ppm, the aromatic carbons appearing in various weak intensity (and generally broad) peaks (Figure 3-5a). Peaks in that region could also have been due to humification products from the forest floor material, similar to the peak centered at 30 ppm in the alkyl region [Kögel-Knabner et al., 1992] for the fibric layer (Figure 3-5a).

Spectra from fresh BC collected on sites affected by fire severity classes 2 and 3 were very similar (Figure 3-5b). Their main difference arises from an increase

in the contribution of the alkyl carbons (peaks at ≈ 30 ppm) and the emergence of two peaks characteristic of aromatic carbons: one at 130 ppm assigned to polyaromatic hydrocarbons [Baldock and Smernik, 2002], and one at 150 ppm ascribable to O-substituted aromatic carbons (furans). In the spectra of fresh BC associated with class 4 fire severity, the relative contribution of the two peaks in the aromatic region as well as the one in the alkyl region continued to increase (Figure 3-5b). Conversely, the contribution of signals relative to cellulose (72 and 105 ppm) decreased. The broad peak centered at 30 ppm also became slightly narrower, suggesting that the variability in the composition of the alkyl groups was decreasing. In contrast, the ^{13}C NMR spectra obtained for the BC associated with high fire severity (class 5) was dominated by broad peaks related to aromatic and phenolic carbons. They were similar to spectra of fuels thermally treated at 250 °C in pyrolytic conditions (Figure 3-5c). These spectra were dominated by two broad peaks: one in the aromatic and phenolic regions and the other one in the alkyl region. Peaks associated with cellulose (centered at 84 ppm and 89 ppm but also at 74 ppm and 65 ppm) were almost absent for the BC produced from *Rhododendron* and *Sphagnum* at 250 °C, and had all disappeared for the BC produced under oxic conditions. On the other hand, hemicelluloses (173 ppm) and lignin (56 ppm) structures were still clearly visible. Finally, for the class 5 fresh BC, carbohydrates and lignin biomolecules were still present even though their relative contribution had substantially decreased (Figure 3-5b).

With increasing fire severity, we observed an increase in the aromatic and phenolic carbon contributions (Table 3-2). There was also a small increase in the

contribution of the carbonyl carbons. Furthermore, BC exhibited a higher proportion of alkyl carbons, corresponding with the emergence of the broad peak centered at 30 ppm (Figure 3-5a). Overall, from low to high fire severity, the ^{13}C NMR spectra shifted from intensity dominated by O-alkyl and di-O-alkyl signals (cellulose and hemicelluloses) to intensity dominated by peaks associated with aryl and alkyl functional groups. The contributions of the aforementioned carbon types were significantly different between fire severity classes 0–1, and class 5. These observations are consistent with those from the calculated atomic ratios, that is, an increase in aromatic content (Figure 3-4).

3.3.5. *Comparison with the BC reference set*

We incorporated the results of the BC produced under controlled conditions on the BC continuum (Figure 3-6) to match changes in chemical and physical properties along the gradient of increasing maximum temperature of formation. Values and observations summarized in Figure 3-6 are derived entirely from results of BC produced in the laboratory under full pyrolysis [L. N. Soucémariadin, S. A. Quideau, M. D. MacKenzie, G. M. Bernard, R. E. Wasylshen, Laboratory charring conditions affect black carbon properties: A case study from Quebec black spruce forest, submitted to *Organic Geochemistry*, 2013]. With increasing maximum temperature, we observed a degradation of the fuel macromolecules (cellulose, hemicelluloses, and lignin) and formation of aromatic structures, with a concomitant increase in BC carbon content and a decrease in H/C and O/C ratios, consistent with the NMR results, i.e., an increase

in carbon condensation. As for BC physical properties, an increase in the maximum temperature induced an increase in BC specific surface area, with a shift from a porosity dominated by macropores to a porosity dominated by micropores. This was accompanied by a progressive destruction of the cell structures of the fuel. Overall, the physical and chemical properties of the wildfire BC matched the properties of the laboratory BC produced at low temperatures ranging between 75 and 250 °C (Figures 3-4 and 3-6). Hence, wildfire BC appears to be composed of transition and amorphous chars; i.e., low in aromatic structures.

3.4 Discussion

3.4.1. Formation conditions for the sampled BC

Hammes et al. [2006] reported that an atomic H/C ratio > 0.5 characterizes chars experiencing temperatures < 500 °C. When compared to results obtained for BC produced under controlled conditions, the high atomic ratio values obtained for the BC produced by wildfires (Table 3-1) were characteristic of a low temperature of formation (Figure 3-4). Results from both elemental analysis and ^{13}C NMR spectroscopy confirmed that all fresh BC samples collected on black spruce sites affected by variable fire severity were the products of forest floor exposed to temperatures ranging from 75 °C to 250 °C. Results also suggested that pyrolysis conditions prevailed during the production of this BC, indicating formation by smouldering fire. Wildfires usually go through different phases [*DeBano et al.*, 1998]; a crown fire associated with flaming combustion generally

transitions to a smouldering fire, affecting the forest floor through glowing combustion. If the forest floor is dry, the combustion is more complete and almost all the organic layer is consumed, which was not the case in the present study. The absence of a relationship between aerial fire severity and soil fire severity further suggests that fire behavior in the canopy and at soil level was disconnected under these conditions. In this situation, fire severity at the soil level is driven by microscale patterns, such as differences in microtopography rather than flammability of the canopy. The C content of the BC produced by wildfire (Table 3-1) was slightly lower (< 60%) than the values obtained for the BC produced under controlled conditions at similar temperatures (Figure 3-6), suggesting a more complete combustion in the former context [Krull *et al.*, 2009].

Under conditions of the highest severity in the field (class 5), ^{13}C NMR spectra indicate that the forest floor underwent thermal alterations. Specifically, there was a visible decrease in peaks associated with the cellulose and hemicellulose, accompanied by a relative increase in the contribution of peaks associated with lignin. A potential explanation is that while cellulose and hemicellulose were subject to (thermal) degradation, the temperature remained below the pyrolysis temperatures of lignin (280–500 °C; [Miyaniishi, 2001]), consequently increasing its relative contribution. With increasing fire severity, significant changes in the distribution of signal intensity occurred, including: a decrease in O-alkyl and di-O-alkyl, an increase in aryl and O-aryl, and a slight increase followed by a slight decrease of the alkyl carbons (Table 3-2). These modifications were triggered by the degradation of hemicelluloses in the

precursor material. For the highest fire severity class, aromatic non-oxygenated carbons (130 ppm) dominated the ^{13}C NMR spectra, suggesting that at this stage, condensation of the original macromolecules into aromatic polymers had begun. This suggests an increase in condensation with severity, which agrees with the observed decrease in atomic H/C and O/C ratios along the same severity gradient. To illustrate this phenomenon, we calculated the degree of aromatization, which corresponds to the ratio [aromatic & phenolic C (165–110 ppm)] to [O-alkyl C + alkyl C (110–0 ppm)], and is an indicator of the increasingly condensed nature of chars (Keiluweit *et al.*, 2010). As expected, there was an increase in the degree of aromatization with increasing fire severity (Table 3-2).

Surface area and pore volume have been shown to be principally controlled by maximum temperature [Brown *et al.*, 2006] and duration of charring [Rutherford *et al.*, 2005; Hilscher *et al.*, 2009]; both are expected to increase with harsher formation conditions, including higher maximum temperature and/or longer charring duration. Hammes *et al.* [2006] reported BC surface areas less than $25 \text{ m}^2\text{g}^{-1}$ for low temperatures of formation ($< 500 \text{ }^\circ\text{C}$), while high temperatures ($500\text{--}1000 \text{ }^\circ\text{C}$) led to surface areas of $214\text{--}336 \text{ m}^2\text{g}^{-1}$. Rutherford *et al.* [2005] also reported a very small micropore volume ($\leq 0.001 \text{ cm}^3\text{g}^{-1}$) for pine wood and pine bark treated at $250 \text{ }^\circ\text{C}$. The low values we measured on our samples confirm the low temperatures of formation, corroborating the observed chemical composition. The higher specific surface area of BC produced at high fire severity (class 5; $\text{SA} = 1.6 \text{ m}^2\text{g}^{-1}$) compared to the BC associated with moderate fire severity (class 2; $\text{SA} = 1.1 \text{ m}^2\text{g}^{-1}$) could be related to higher temperatures of

formation. The latter create new pores, especially mesopores (Figure 3-2), by degradation of the initial macromolecules. The absence of major destruction of the fuel cell structures, as observed on the SEM micrographs (Figure 3-3), confirms an average low formation temperature across the severity gradient. The relative contribution of microporosity did not increase with increasing fire severity, suggesting that the temperature of BC formation was too low to create new microporosity. These results match changes in chemical structure suggested by the ^{13}C NMR spectra (Figure 3-4b), where it is obvious that the conversion of alkyl to aromatic carbon remained incomplete. The rigid structure that fused-ring aromatic carbons provide and in which micropores develop is not fully established yet [Rutherford *et al.*, 2005]. In addition, at low temperatures, a certain proportion of the porosity – especially the microporosity – could have been occluded by tars and other condensed volatiles [Downie *et al.*, 2009]. This process can also disrupt pore continuity, leading to small specific surface areas and pore volumes. Finally, low surface area could also be associated with low thermal ramping [Brown *et al.*, 2006]. Wildfire thermal rates are typically low, characterized by values between 2 and 17 $^{\circ}\text{C}\cdot\text{min}^{-1}$ for natural smoldering combustion [Miyaniishi, 2001]. A slow thermal ramping rate (0.5–3.3 $^{\circ}\text{C}\cdot\text{min}^{-1}$) tends to produce chars with low surface area ($< 0.5 \text{ m}^2\cdot\text{g}^{-1}$). Because the thermal ramping rate used to produce the reference set BC was high (13–20 $^{\circ}\text{C}\cdot\text{min}^{-1}$), it may not be appropriate to compare results obtained for the physical/structural characteristics of the artificially-produced BC those of BC produced by wildfire.

The chemical characteristics, as observed with ^{13}C NMR spectroscopy, of BC produced in Quebec boreal black spruce forests during the 2005–2007 wildfires are quite different from characteristics of BC produced by wildfires in other ecosystems. For example, a Mediterranean wildfire that affected a stone pine (*P. pinea* L.) forest and qualified by *Nocentini et al.* [2010] as moderate intensity produced BC that was much more condensed; even the highest class 5 fire severity BC in our study is less dominated by aromatic C than BC characterized by this latter study, as indicated by the ^{13}C NMR spectrum. In a more comparable boreal ecosystem; i.e., a Siberian Scots pine forest (*Pinus sylvestris* ssp. *sibirica* Lebed) affected by a surface fire, *Czimczik et al.* [2003] obtained ^{13}C NMR spectra comparable to the spectra of class 5 fire severity BC from the present study.

3.4.2. BC properties and implications for their role in black spruce forests

NMR spectroscopy and elemental analyses indicate that BC produced in the Quebec black spruce forests by 2005–2007 wildfires was not composed of carbon moieties with intrinsic chemical properties (molecular structures) known to resist microbial degradation. One important factor to consider is that all fires sampled occurred early in the fire season; relatively low fire severity was observed at the soil level, validated by low organic matter consumption [*Boiffin and Munson, 2013*]. Nonetheless, BC properties proved to vary predictably according to changes in fire severity observed at the soil level.

BC porosity may play a role in ecosystem successional processes through adsorption of phenolic compounds that may depress natural regeneration. As shown by *Joanisse et al.* [2007], condensed tannins found in high concentration in the *Kalmia* litter inhibit microbial enzyme activity and decrease nitrogen mineralization. As nitrogen is one of the most limiting nutrients in boreal forests, black carbon porosity could thus play an important role in post-fire tree re-establishment. As shown for the reference set, the increase in BC porosity is related to the temperature of formation (Figure 3-6), although thermal ramping rate and charring duration are important factors [e.g., *Brown et al.*, 2006]. The potential for tannin adsorption (i.e., average measured specific surface area) was already relatively low for the BC sampled in the field. However, these BC samples were collected 4 to 5 years after wildfires, hence, it is possible that the original porosity was higher but decreased over time. Indeed, phenols interacting with activated carbon undergo an irreversible adsorption [*Grant and King*, 1990]. Measuring surface area on samples collected immediately after fire occurrence could improve our understanding of rates of loss of porosity.

The 3–5 °C mean annual increase in temperature projected for the end of the century [*Lemprière et al.*, 2008] is predicted to result in an increase in fire frequency all over the boreal zone, although there will be regional differences. By the end of the century (2090), the black spruce feathermoss domain is expected to experience a 4–5 °C increase in summer temperature, and an increase in summer precipitation, although in the southern sector the precipitation increase (0–10%) is less than in the northern sector (25–50%). Overall, fire seasons are expected to be

longer (averaging +30 days) and fires to be more severe [Wotton *et al.*, 2010], and the southern sectors are more prone to an increase in fire frequency and severity. On the other hand, fire seasonality is expected to shift toward an earlier fire season, which would favor lower fire severity at the soil level, producing the same low condensed BC as is reported here for the 2005–2007 fires. In all cases, there will be years when low-intensity fires will continue to dominate in the black spruce domain.

3.5 Conclusion

In Quebec black spruce forests, 2005–2007 wildfires produced forest floor BC that was composed of transition and amorphous chars displaying a relatively low degree of aromatization, and not very condensed. The BC chemical properties were related to fire severity, an increase in fire severity inducing an increase in aromatization. The aromatic content of the collected BC was low when compared to the range of known values along the BC continuum, suggesting a low intrinsic potential for recalcitrance. In addition, the porosity of the analyzed samples was low. However, the importance of BC in ecosystem functioning, e.g., as a habitat for microorganisms involved in nutrient cycling, should not be dismissed. Overall, these results are representative of BC produced during early season wildfires, resulting in a relatively low fire severity at the soil level. They provide insight on the type of BC that would be produced in the scenario where early season fires were to become dominant. Furthermore, the results can help inform carbon modeling efforts for black spruce boreal forests by providing key

information on the influence of low fire severity on relative recalcitrance of BC pools, as well as on the post-disturbance regeneration potential of these forests.

Tables and Figures

Table 3-1. Selected physical and elemental properties of BC samples produced by wildfire of the 6 severity classes observed in the field (0 to 5); na: not available; nd: not determined.

fire severity class	burning class ^a	substrate class ^b	substrate type	moisture content (%)	ash content (%) ^c	N content (%) ^{d, e}		C content (%) ^{d, e}		H content (%) ^{d, e}		O content (%) ^d	C/N ratio	atomic H/C ratio ^d	atomic O/C ratio ^d	specific SA (m ² ·g ⁻¹) ^f
0	0	5	<i>Sphagnum</i>	9.7	4.4	1.26	(0.04)	47.6	(0.3)	5.30	(0.19)	45.8	37.7	1.34	0.72	nd
0	0	5	<i>Sphagnum</i>	6.2	3.0	0.94	(0.08)	47.0	(1.9)	5.33	(0.34)	46.7	49.8	1.36	0.74	2.32
1	1	1	Lichen	6.7	3.0	0.69	(0.15)	46.1	(0.5)	5.75	(0.22)	47.5	67.2	1.50	0.77	nd
1	1	1	Lichen	5.1	24.0	0.94	(0.09)	48.2	(1.4)	5.02	(0.39)	45.8	51.2	1.25	0.71	nd
1	1	1	Lichen	5.6	2.3	0.92	(0.10)	49.8	(0.8)	5.62	(0.28)	43.7	54.0	1.36	0.66	nd
1	1	1	<i>Pleurozium</i>	6.5	4.7	1.47	(0.05)	52.7	(2.4)	4.86	(0.11)	41.0	35.8	1.11	0.58	nd
1	1	1	<i>Pleurozium</i>	6.6	3.7	1.32	(0.02)	51.8	(0.3)	5.26	(0.14)	41.6	39.1	1.22	0.60	nd
1	1	1	<i>Pleurozium</i>	6.4	5.7	1.21	(0.02)	50.3	(0.8)	5.38	(0.13)	43.1	41.6	1.28	0.64	nd
1	1	1	<i>Pleurozium</i>	6.1	12.5	1.28	(0.03)	52.4	(0.3)	5.13	(0.14)	41.2	40.8	1.17	0.59	nd
1	1	1	<i>Sphagnum</i>	7.3	5.4	1.18	(0.05)	50.6	(0.3)	5.13	(0.15)	43.1	43.0	1.22	0.64	nd
1	1	1	<i>Sphagnum</i>	6.7	4.8	1.36	(0.06)	51.1	(0.6)	5.39	(0.12)	42.2	37.5	1.26	0.62	nd
1	1	1	<i>Sphagnum</i>	6.0	3.8	1.13	(0.12)	49.6	(1.4)	5.50	(0.19)	43.8	43.9	1.33	0.66	nd
2	2	1	Lichen	6.3	4.0	1.19	(0.03)	47.9	(0.2)	6.06	(0.15)	44.9	40.3	1.52	0.70	nd
2	2	1	Lichen	5.9	5.1	1.13	(0.07)	50.8	(0.2)	5.56	(0.04)	42.5	44.8	1.31	0.63	nd
2	2	1	Lichen	6.5	2.9	1.08	(0.03)	49.2	(0.4)	5.86	(0.20)	43.9	45.5	1.43	0.67	nd
2	2	1	Lichen	4.7	5.2	1.37	(0.04)	55.6	(0.5)	5.41	(0.06)	37.6	40.5	1.17	0.51	nd
2	2	1	duff	6.1	7.4	1.55	(0.05)	55.9	(0.5)	4.94	(0.08)	37.6	36.0	1.06	0.50	nd
2	2	1	duff	5.7	4.8	1.63	(0.09)	55.6	(1.0)	5.21	(0.04)	37.6	34.0	1.12	0.51	nd
2	2	1	duff	5.6	6.2	1.13	(0.03)	52.7	(0.8)	5.20	(0.04)	41.0	46.8	1.18	0.58	nd

2	2	1	<i>Pleurozium</i>	6.2	5.7	1.48	(0.08)	54.5	(1.8)	4.96	(0.16)	39.1	36.7	1.09	0.54	nd
2	2	1	<i>Pleurozium</i>	5.8	2.9	1.41	(0.02)	53.9	(0.1)	5.24	(0.02)	39.5	38.1	1.17	0.55	nd
2	2	1	<i>Pleurozium</i>	5.6	5.5	1.36	(0.10)	55.1	(2.7)	4.97	(0.10)	38.5	40.5	1.08	0.52	nd
2	2	1	<i>Pleurozium</i>	5.4	5.0	1.62	(0.11)	52.5	(2.0)	5.29	(0.22)	40.6	32.3	1.21	0.58	1.05
3	2	2	+ <i>Polytrichum</i>	7.0	4.9	1.57	(0.03)	53.0	(0.1)	5.15	(0.10)	40.3	33.7	1.17	0.57	nd
3	2	2	<i>Polytrichum</i>	6.9	7.8	2.07	(0.17)	54.0	(2.9)	4.72	(0.02)	39.2	26.1	1.05	0.55	nd
4	3	1	duff	6.1	4.0	1.40	(0.04)	55.2	(0.3)	5.13	(0.04)	38.3	39.5	1.12	0.52	nd
4	3	1	duff	5.6	4.9	1.50	(0.01)	56.2	(0.2)	4.97	(0.09)	37.3	37.4	1.06	0.50	nd
4	3	1	duff	5.0	10.3	2.06	(0.01)	57.8	(0.3)	4.50	(0.13)	35.6	28.1	0.93	0.46	nd
4	3	1	<i>Pleurozium</i>	6.4	5.1	1.60	(0.00)	54.2	(1.6)	5.06	(0.05)	39.2	33.9	1.12	0.54	nd
4	3	1	<i>Pleurozium</i>	5.8	4.2	1.49	na	53.7	na	4.98	na	39.9	36.0	1.11	0.56	nd
4	3	1	<i>Pleurozium</i>	5.8	16.1	1.52	(0.07)	51.4	(3.2)	4.62	(0.06)	42.5	33.9	1.08	0.62	nd
4	3	1	<i>Pleurozium</i>	4.5	28.8	1.49	(0.02)	60.4	(9.5)	4.35	(0.07)	33.8	40.4	0.87	0.42	nd
5	3	2	duff	4.2	34.0	1.63	(0.05)	58.7	(0.8)	4.02	(0.05)	35.6	35.9	0.82	0.45	1.59

^a class 0 (unburnt/scorched): plant parts are green and unchanged/moss is yellow, but species are identifiable; class 1 (slightly burnt): moss and duff are scorched or charred but not altered over the entire depth of duff, the original form of mosses and twigs is visible; class 2 (moderately burnt): organic layer partially consumed, duff charred or consumed, parts of woody twigs and roots remaining; class 3 (severely burnt): forest-floor material deeply consumed (almost to mineral soil), no discernible plant parts remaining; ^b class 5: scorched forest floor; class 1: burnt forest floor; class 2: deeply burnt forest floor (residual forest floor < 2 cm); ^c dry weight basis; ^d dry weight and ash-free basis; ^e values are averages with their associated standard deviations indicated in parentheses (n = 1–5); ^f multi-point BET specific surface area obtained by nitrogen adsorption at 77.3 K (7–8 data points).

Table 3-2. Distribution (% of total integrated spectral area from ^{13}C CPMAS NMR spectra) of the four main spectral regions for BC samples produced by wildfire of the 6 severity classes observed in the field (0 to 5).

fire severity class	carbonyl C	aromatic & phenolic C	O-alkyl C	alkyl C	DoA ^a
0	6.7	15.5	58.8	19.1	0.20
0	7.2	17.4	61.8	13.6	0.23
1	2.8	9.8	70.8	16.6	0.11
1	7.7	16.1	57.8	18.3	0.21
1	4.1	12.5	64.6	18.7	0.15
2	8.1	27.9	36.0	28.1	0.44
2	8.8	26.9	42.5	21.9	0.42
2	8.2	22.4	45.9	23.5	0.32
3	9.2	22.7	44.3	23.7	0.33
3	8.0	28.8	36.5	26.7	0.46
4	10.7	34.3	34.7	20.2	0.63
4	6.8	28.6	41.1	23.5	0.44
5	11.3	47.7	21.6	19.5	1.16

^a Degree of aromatization (DoA) = (aromatic & phenolic C) / (O-alkyl C + alkyl C)

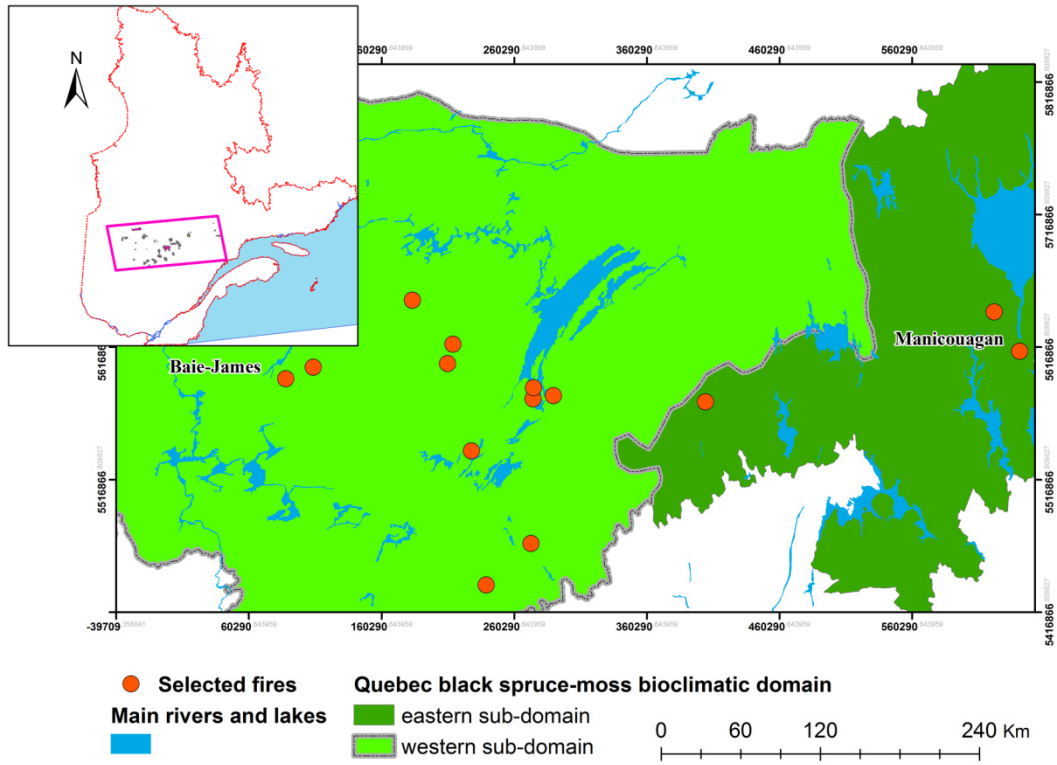


Figure 3-1. Location of the 14 selected fires in the black spruce-moss domain of Quebec.

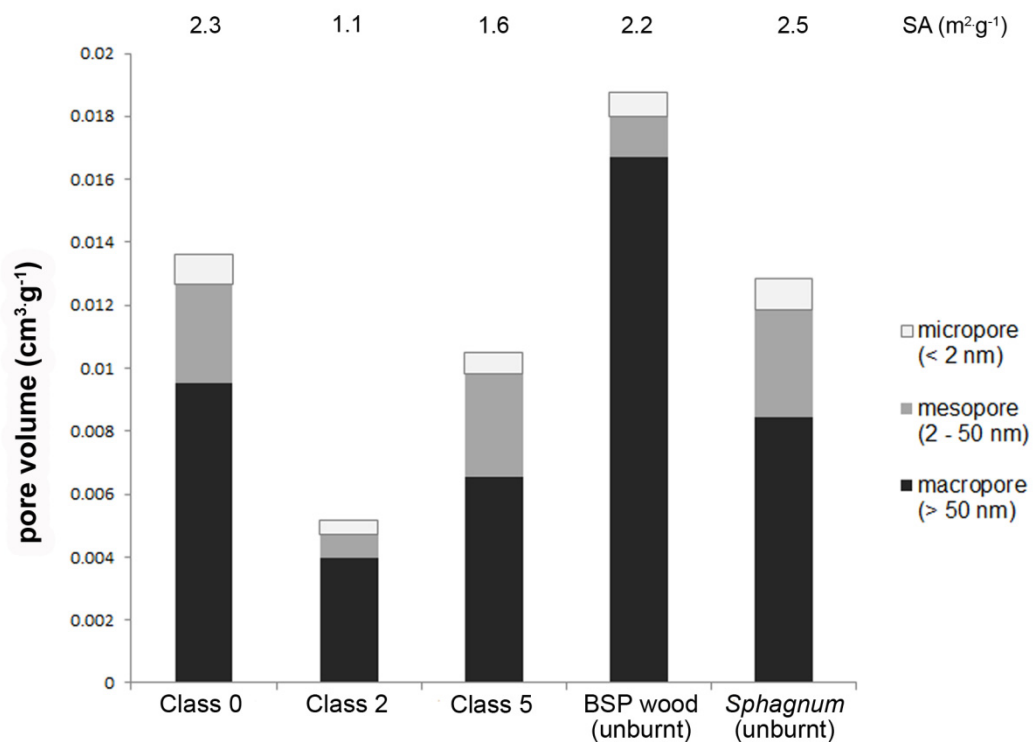


Figure 3-2. Repartition of total pore volume (cm³·g⁻¹) between micro-, meso-, and macropores; and specific surface area (SA) for three BC samples produced by wildfires of different fire severity classes (0, 2 and 5) and two precursor materials (black spruce – BSP – wood and *Sphagnum*).

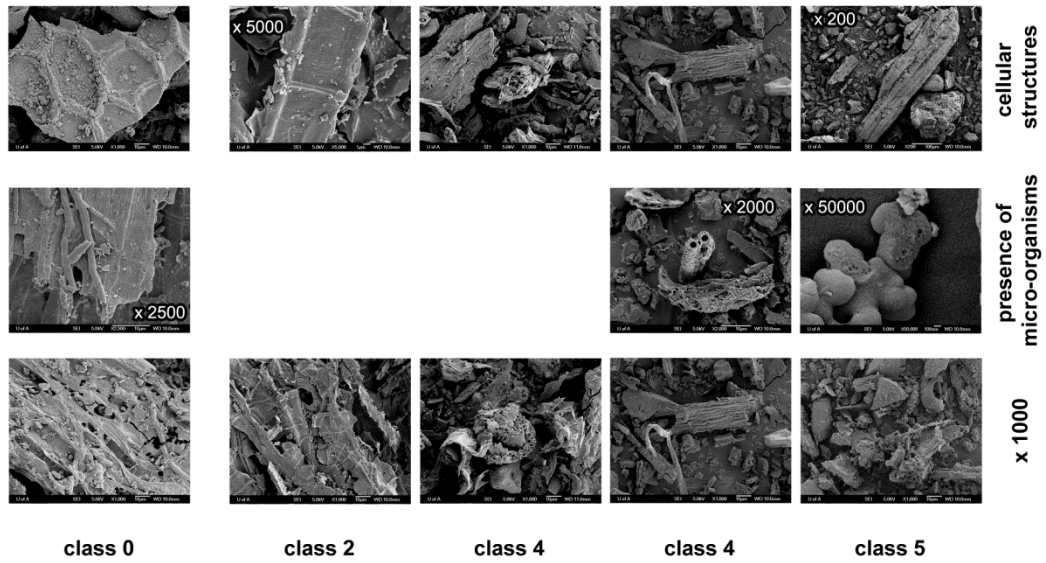


Figure 3-3. SEM micrographs of BC samples produced by wildfire of different fire severity classes (0, 2, 4, and 5). Magnification is x 1000 unless otherwise specified.

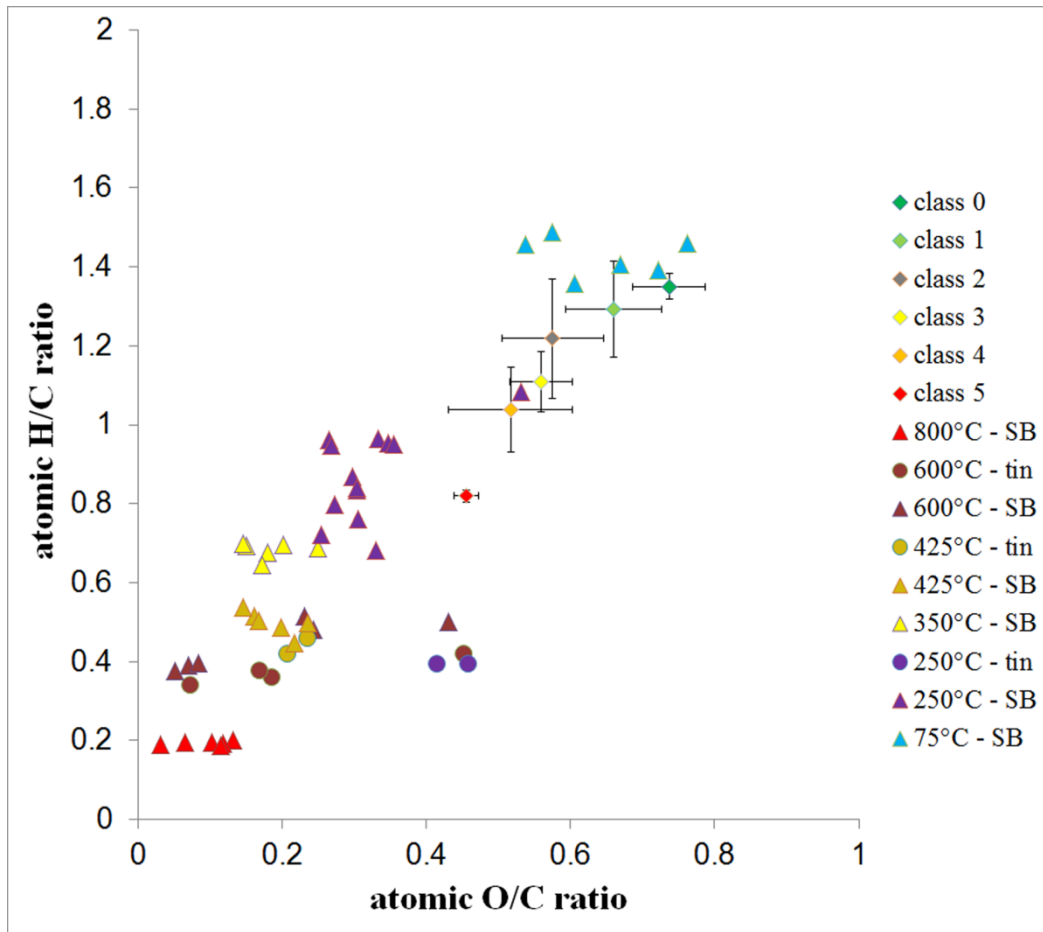


Figure 3-4. van Krevelen plot for BC samples produced by wildfire of the six severity classes observed in the field (0 to 5), and BC samples produced under controlled conditions in the laboratory (full pyrolysis, SB; partial pyrolysis, tin).

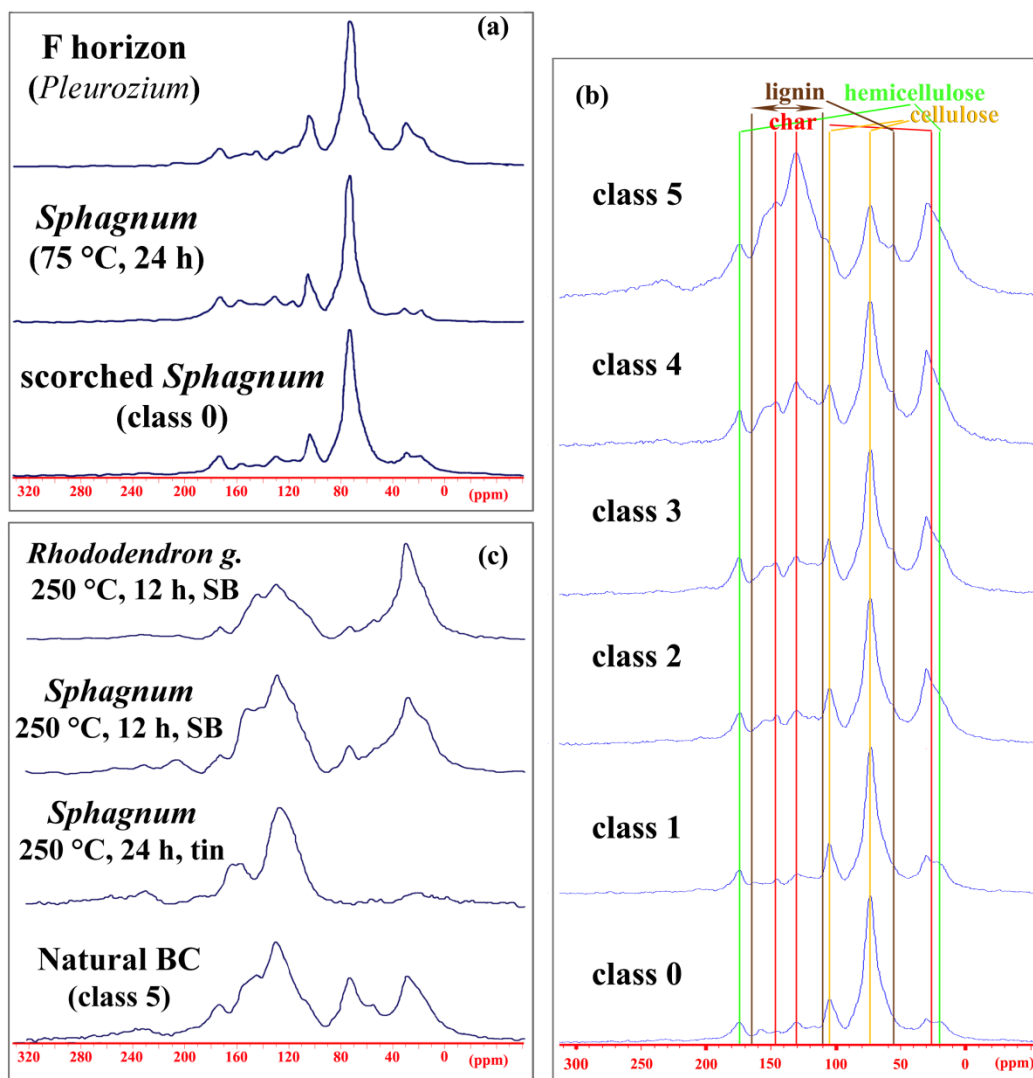


Figure 3-5. ^{13}C NMR CP spectra of (a) low severity BC (class 0) compared to unburnt *Sphagnum* and a fibric layer; (b) BC samples produced by wildfire of the six severity classes observed in the field (0 to 5); and (c) high severity BC (class 5) compared to *Sphagnum* and *Rhododendron* thermally treated at 250 °C.

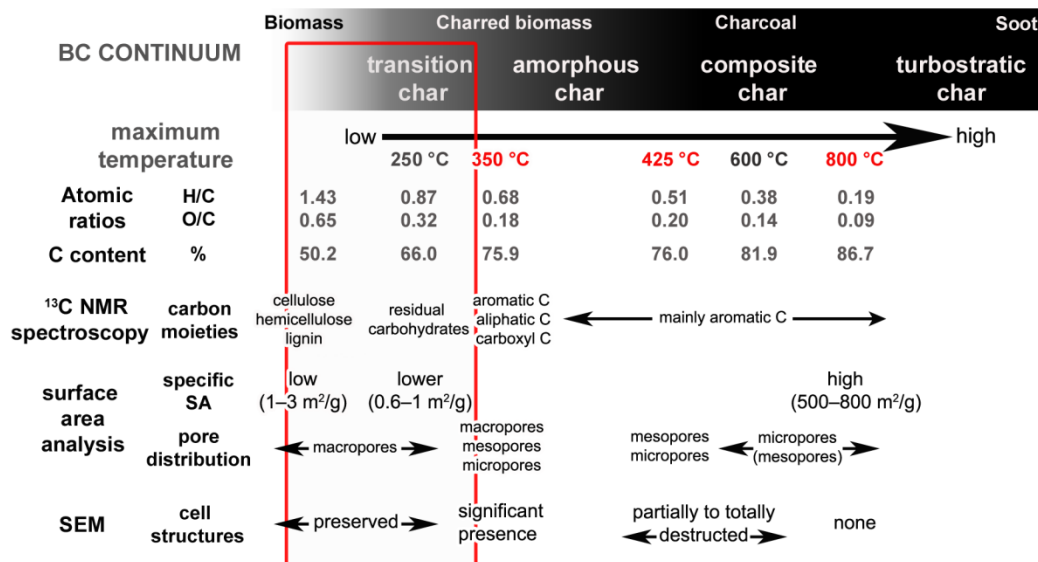


Figure 3-6. The BC continuum. Specific numbers and derived BC characteristics were obtained for BC samples formed under controlled laboratory conditions. Samples produced by wildfires of the six severity classes observed in the field (0 to 5) are contained within the red square.

List of References

- ASTM (2007), D1762-84 Standard test method for chemical analysis of wood charcoal, *American Society for Testing and Materials International*, 2010, doi:10.1520/D1762-84R07.
- Axelsson, D. E. (2012), *Solid State Nuclear Magnetic Resonance. A Practical Introduction*, vol. 1, 1st ed., 471 pp., MRi_Consulting, Lexington, KY.
- Baldock, J. A. and R. J. Smernik (2002), Chemical composition and bioavailability of thermally altered *Pinus resinosa* (Red pine) wood, *Org. Geochem.*, 33, 1093-1109, doi:10.1016/S0146-6380(02)00062-1.
- Bergeron, Y., S. Gauthier, M. D. Flannigan, and V. Kafka (2004), Fire regimes at the transition between mixedwood and coniferous boreal forest in northwestern Quebec, *Ecology*, 85, 1916-1932.
- Boiffin, J. and A. D. Munson (2013), Three large fire years threaten resilience of closed crown black spruce forests in eastern Canada, *Ecosphere*, 4(5):56, doi:10.1890/ES13-00038.1.
- Bond-Lamberty, B., S. D. Peckham, D. E. Ahl, and S. T. Gower (2007), Fire as the dominant driver of central Canadian boreal forest carbon balance, *Nature*, 450, 89-92.
- Brown, J. K. and N. V. DeByle (1987), Fire damage, mortality, and suckering in aspen, *Can. J. For. Res.*, 17, 1100-1109, doi:10.1139/x87-168.
- Brown, R. A., A. K. Kercher, T. H. Nguyen, D. C. Nagle, and W. P. Ball (2006), Production and characterization of synthetic wood chars for use as surrogates for natural sorbents, *Org. Geochem.*, 37, 321-333, doi:10.1016/j.orggeochem.2005.10.008.
- Brunauer, S., P. H. Emmett, and E. Teller (1938), Adsorption of gases in multimolecular layers, *J. Am. Chem. Soc.*, 60, 309-319, doi:10.1021/ja01269a023.

- Carrier, A. (1996), Contribution de l'imagerie satellitaire NOAA à la cartographie des grands feux de forêt du Québec boréal : 1972 à 1994, M.S. thesis, 1-115 pp., Université du Québec à Chicoutimi, Chicoutimi, Québec, Canada.
- Cyr, D., S. Gauthier, and Y. Bergeron (2007), Scale-dependent determinants of heterogeneity in fire frequency in a coniferous boreal forest of eastern Canada, *Landscape Ecol.*, 22, 1325-1339.
- Czimczik, C. I. and C. A. Masiello (2007), Controls on black carbon storage in soils, *Global Biogeochem. Cycles*, 21, doi:10.1029/2006GB002798.
- Czimczik, C. I., C. M. Preston, M. W. I. Schmidt, and E. Schulze (2003), How surface fire in Siberian Scots pine forests affects soil organic carbon in the forest floor: Stocks, molecular structure, and conversion to black carbon (charcoal), *Global Biogeochem. Cycles*, 17, doi:10.1029/2002GB001956.
- DeBano, L. F., D. G. Neary, and P. F. Ffolliott (Eds.) (1998), *Fire's Effects on Ecosystems*, 352 pp., John Wiley & Sons, Inc, New York, New York, USA.
- DeLuca, T. H. and C. Boisvenue (2012), Boreal forest soil carbon: distribution, function and modelling, *Forestry*, 85, 161-184.
- DeLuca, T. H., M. D. MacKenzie, M. J. Gundale, and W. E. Holben (2006), Wildfire-produced charcoal directly influences nitrogen cycling in ponderosa pine forests, *Soil Sci. Soc. Am. J.*, 70, 448-453, doi:10.2136/sssaj2005.0096.
- Downie, A., A. Crosky, and P. Munroe (2009), Physical properties of biochar, in *Biochar for Environmental Management: Science and Technology*, 1st edn., edited by Johannes Lehmann and Stephen Joseph, pp. 13-32, Earthscan Publications Ltd, London, UK.
- Earl, W. L. and D. L. VanderHart (1982), Measurement of ^{13}C chemical shifts in solids, *J. Magn. Reson.*, 48, 35-54, doi:10.1016/0022-2364(82)90236-0.

- Flannigan, M. D., K. A. Logan, B. D. Amiro, W. R. Skinner, and B. J. Stocks (2005), Future area burned in Canada, *Clim. Change*, *72*, 1-16, doi:10.1007/s10584-005-5935-y.
- Flannigan, M. D. and B. M. Wotton (2001), Climate, weather, and area burned, in *Forest Fires: Behavior & Ecological Effects*, edited by E. A. Johnson and Kiyoko Miyanishi, pp. 351-373, Academic Press, San Diego, CA.
- Freitas, J. C. C., T. J. Bonagamba, and F. G. Emmerich (1999), ¹³C high-resolution solid-state NMR study of peat carbonization, *Energ. Fuel*, *13*, 53-59, doi:10.1021/ef980075c.
- González-Pérez, J. A., F. J. González-Vila, G. Almendros, and H. Knicker (2004), The effect of fire on soil organic matter - a review, *Environ. Int.*, *30*, 855-870, doi:10.1016/j.envint.2004.02.003.
- Grant, T. M. and C. J. King (1990), Mechanism of irreversible adsorption of phenolic compounds by activated carbons, *Ind Eng Chem Res*, *29*, 264-271, doi:10.1021/ie00098a017.
- Hammes, K., R. J. Smernik, J. O. Skjemstad, A. Herzog, U. F. Vogt, and M. W. I. Schmidt (2006), Synthesis and characterisation of laboratory-charred grass straw (*Oryza sativa*) and chestnut wood (*Castanea sativa*) as reference materials for black carbon quantification, *Org. Geochem.*, *37*, 1629-1633, doi:10.1016/j.orggeochem.2006.07.003.
- Hammes, K., M. S. Torn, A. G. Lapenas, and M. W. I. Schmidt (2008), Centennial black carbon turnover observed in a Russian steppe soil, *Biogeosciences*, *5*, 1339-1350, doi:10.5194/bg-5-1339-2008.
- Harden, J. W., S. E. Trumbore, B. J. Stocks, A. Hirsch, S. T. Gower, K. P. O'Neill, and E. S. Kasischke (2000), The role of fire in the boreal carbon budget, *Global Change Biol.*, *6*, 174-184.

- Hatten, J. A. and D. Zabowski (2009), Changes in soil organic matter pools and carbon mineralization as influenced by fire severity, *Soil Sci. Soc. Am. J.*, *73*, 262-273, doi:10.2136/sssaj2007.0304.
- Hilscher, A., K. Heister, C. Siewert, and H. Knicker (2009), Mineralisation and structural changes during the initial phase of microbial degradation of pyrogenic plant residues in soil, *Org. Geochem.*, *40*, 332-342, doi:10.1016/j.orggeochem.2008.12.004.
- Hockaday, W. C., A. M. Grannas, S. Kim, and P. G. Hatcher (2006), Direct molecular evidence for the degradation and mobility of black carbon in soils from ultrahigh-resolution mass spectral analysis of dissolved organic matter from a fire-impacted forest soil, *Org. Geochem.*, *37*, 501-510, doi:10.1016/j.orggeochem.2005.11.003.
- Hockaday, W. C., A. M. Grannas, S. Kim, and P. G. Hatcher (2007), The transformation and mobility of charcoal in a fire-impacted watershed, *Geochim. Cosmochim. Acta*, *71*, 3432-3445, doi:10.1016/j.gca.2007.02.023.
- Inari, G. N., S. Mounquengui, S. Dumarçay, M. Pétrissans, and P. Gérardin (2007), Evidence of char formation during wood heat treatment by mild pyrolysis, *Polym. Degrad. Stab.*, *92*, 997-1002, doi:10.1016/j.polymdegradstab.2007.03.003.
- Joanisse, G. D., R. L. Bradley, C. M. Preston, and A. D. Munson (2007), Soil enzyme inhibition by condensed litter tannins may drive ecosystem structure and processes: the case of *Kalmia angustifolia*, *New Phytol.*, *175*, 535-546.
- Johnson, E. A. and K. Miyanishi (Eds.) (2001), *Forest Fires: Behavior and Ecological Effects*, Forest Fires, 594 pp., Academic Press, San Diego, CA.
- Kafka, V., S. Gauthier, and Y. Bergeron (2001), Fire impacts and crowning in the boreal forest: study of a large wildfire in western Quebec, *Int. J. Wildland Fire*, *10*, 119-127.
- Kasischke, E. S., M. R. Turetsky, R. D. Ottmar, N. H. F. French, E. E. Hoy, and E. S. Kane (2008), Evaluation of the composite burn index for assessing fire severity in Alaskan black spruce forests, *Int. J. Wildland Fire*, *17*, 515-526.

- Kasischke, E. (2000), Boreal ecosystems in the global carbon cycle, in *Fire, Climate Change, and Carbon Cycling in the Boreal Forest*, vol. 138, edited by Eric S Kasischke and Brian J Stocks, pp. 19-30, Springer-Verlag, New-York.
- Keiluweit, M., P. S. Nico, M. G. Johnson, and M. Kleber (2010), Dynamic molecular structure of plant biomass-derived black carbon (biochar), *Environ. Sci. Technol.*, *44*, 1247-1253, doi:10.1021/es9031419.
- Knicker, H., K. U. Totsche, G. Almendros, and F. J. González-Vila (2005), Condensation degree of burnt peat and plant residues and the reliability of solid-state VACP MAS ^{13}C NMR spectra obtained from pyrogenic humic material, *Org. Geochem.*, *36*, 1359-1377, doi:10.1016/j.orggeochem.2005.06.006.
- Kögel-Knabner, I. (1997), ^{13}C and ^{15}N NMR spectroscopy as a tool in soil organic matter studies, *Geoderma*, *80*, 243-270, doi:10.1016/S0016-7061(97)00055-4.
- Kögel-Knabner, I., J. W. de Leeuw, and P. G. Hatcher (1992), Nature and distribution of alkyl carbon in forest soil profiles: implications for the origin and humification of aliphatic biomacromolecules, *Sci. Total Environ.*, *117-118*, 175-185, doi:10.1016/0048-9697(92)90085-7.
- Krull, E. S., J. A. Baldock, J. O. Skjemstad, and R. J. Smernik (2009), Characteristics of biochar - organo-chemical properties, in *Biochar for Environmental Management: Science and Technology*, 1st edn., edited by Johannes Lehmann and Stephen Joseph, pp. 53-66, Earthscan Publications Ltd, London, UK.
- Lehmann, J. and S. Joseph (2009), Biochar for environmental management - an introduction, in *Biochar for Environmental Management: Science and Technology*, 1st edn., edited by Johannes Lehmann and Stephen Joseph, pp. 1-12, Earthscan Publications Ltd, London, UK.
- Lemprière, T. C., P. Y. Bernier, A. L. Carroll, M. D. Flannigan, R. P. Gilsean, D. W. McKenney, E. H. Hogg, J. H. Pedlar, and D. Blain (2008), The Importance of Forest

- Sector Adaptation to Climate Change, *Information Report, NOR-X-416E*, Natural Resources Canada, Edmonton, Alberta.
- Masiello, C. A. (2004), New directions in black carbon organic geochemistry, *Mar. Chem.*, *92*, 201-213, doi:10.1016/j.marchem.2004.06.043.
- Melkior, T., S. Jacob, G. Gerbaud, S. Hediger, L. Le Pape, L. Bonnefois, and M. Bardet (2012), NMR analysis of the transformation of wood constituents by torrefaction, *Fuel*, *92*, 271-280, doi:10.1016/j.fuel.2011.06.042.
- Miyanishi, K. (2001), Duff consumption, in *Forest Fires: Behavior & Ecological Effects*, edited by E. A. Johnson and Kiyoko Miyanishi, pp. 437-475, Academic Press, San Diego, CA.
- Nocentini, C., G. Certini, H. Knicker, O. Francioso, and C. Rumpel (2010), Nature and reactivity of charcoal produced and added to soil during wildfire are particle-size dependent, *Org. Geochem.*, *41*, 682-689, doi:10.1016/j.orggeochem.2010.03.010.
- Peersen, O. B., X. L. Wu, I. Kustanovich, and S. O. Smith (1993), Variable-amplitude cross-polarization MAS NMR, *J. Magn. Reson. Ser. A*, *104*, 334-339, doi:10.1006/jmra.1993.1231.
- Preston, C. M. (2009), Biogeochemistry: Fire's black legacy, *Nature Geosci*, *2*, 674-675.
- Preston, C. M. and M. W. I. Schmidt (2006), Black (pyrogenic) carbon in boreal forests: a synthesis of current knowledge and uncertainties, *Biogeosciences*, *3*, 397-420, doi:10.5194/bg-3-397-2006
- Robitaille, A. and J. Saucier (1998), *Paysages Régionaux Du Québec Méridional*, 213 pp., Les Publications du Québec, Sainte-Foy, Québec.
- Rutherford, D. W., R. L. Wershaw, and L. G. Cox (2005), Changes in Composition and Porosity Occurring During the Thermal Degradation of Wood and Wood Components, *Scientific Investigations Report, 2004-5292*, U.S. Dept. of the Interior, U.S. Geological Survey, Reston, VA.

- Ryan, K. C. (2002), Dynamic interactions between forest structure and fire behavior in boreal ecosystems, *Silva Fenn.*, 36, 13-39.
- Saito, M. (1990), Charcoal as a micro-habitat for VA mycorrhizal fungi, and its practical implication, *Agric. , Ecosyst. Environ.*, 29, 341-344.
- Saucier, J., P. Grondin, A. Robitaille, and J. Bergeron (2001), *Zones De Végétation Et Les Domaines Bioclimatiques Du Québec*, 3^e ed., 2 pp., Gouvernement du Québec, Ministère des Ressources naturelles, Québec.
- Smernik, R. J., J. A. Baldock, J. M. Oades, and A. K. Whittaker (2002), Determination of $T_{1\rho}^H$ relaxation rates in charred and uncharred wood and consequences for NMR quantitation, *Solid State Nucl. Magn. Reson.*, 22, 50-70, doi:10.1006/snmr.2002.0064.
- Smernik, R. J. and J. M. Oades (2000a), The use of spin counting for determining quantitation in solid state ^{13}C NMR spectra of natural organic matter: 1. Model systems and the effects of paramagnetic impurities, *Geoderma*, 96, 101-129, doi:10.1016/S0016-7061(00)00006-9.
- Smernik, R. J. and J. M. Oades (2000b), The use of spin counting for determining quantitation in solid state ^{13}C NMR spectra of natural organic matter: 2. HF-treated soil fractions, *Geoderma*, 96, 159-171, doi:10.1016/S0016-7061(00)00007-0.
- Soil Classification Working Group (Ed.) (1998), *The Canadian System of Soil Classification - Third Edition*, vol. 1646 (Revised), Research Branch, Agriculture and Agri-Food Canada ed., 187 pp., NRC Research Press, Ottawa.
- Sousa, W. P. (1984), The role of disturbance in natural communities, *Ann. Rev. Ecol. Syst.*, 15, 353-391, doi:0066-4162/8411120-0353\$02. 00.
- Turner, M. G. and W. H. Romme (1994), Landscape dynamics in crown fire ecosystems, *Landscape Ecol.*, 9, 59-77.

- van Bellen, S., M. Garneau, and Y. Bergeron (2010), Impact of climate change on forest fire severity and consequences for carbon stocks in boreal forest stands of Quebec, Canada: A synthesis, *Fire Ecology*, 6, 16-44, doi:10.4996/fireecology.0603016.
- van Wagtenock, J. W. (2006), Fire as a physical process, in *Fire in California's Ecosystems*, edited by Neil G. Sugihara, Jan W. van Wagtenock, Kevin E. Shaffer, Joann Fites-Kaufman, and Andrea E. Thode, pp. 38-57, University of California Press, Berkeley, CA.
- Wardle, D. A., O. Zackrisson, and M. Nilsson (1998), The charcoal effect in boreal forests: Mechanisms and ecological consequences, *Oecologia*, 115, 419-426.
- Wikberg, H. and S. L. Maunu (2004), Characterisation of thermally modified hard- and softwoods by ¹³C CPMAS NMR, *Carbohydr. Polym.*, 58, 461-466, doi:10.1016/j.carbpol.2004.08.008.
- Wotton, B. M., C. A. Nock, and M. D. Flannigan (2010), Forest fire occurrence and climate change in Canada, *Int. J. Wildland Fire*, 19, 253-271.
- Zackrisson, O., M. Nilsson, and D. A. Wardle (1996), Key ecological function of charcoal from wildfire in the boreal forest, *Oikos*, 77, 10-19.

Chapter 4. Total carbon and black carbon stocks in black spruce forest floors from eastern Canada: A quantitative study

A version of this chapter has been submitted for publication to Journal of Geophysical Research (Biogeosciences).

4.1. Introduction

Surficial accumulation of organic material is one of the most distinctive features of boreal forests; large amounts of carbon (C) are stored in thick forest floors overlying the mineral soils. Although the boreal zone covers less than 17% of the earth's land surface, boreal ecosystems contain more than 30% of the C stored in terrestrial ecosystems on a global basis. Boreal forest soils alone contain two thirds of the soil organic C stored in forest soils worldwide (227×10^{12} kg; [Kasischke, 2000]). Increasing concerns about climate change and its impacts on fire regimes have brought global attention to boreal ecosystems, including Canada's boreal forest region, representing 21% of the world's boreal forest (<http://cfs.nrcan.gc.ca/pages/256>). An increase in fire frequency is hypothesized in the near future for the boreal region, but uncertainties remain about the evolution of fire severity [Flannigan *et al.*, 2005; van Bellen *et al.*, 2010] and how changes in severity will affect both total organic C stocks and black carbon (BC) stocks in boreal forest soils.

As well as being a major natural and recurring disturbance in boreal forests, wildfire is also a main driver of the C cycle [Bond-Lamberty *et al.*, 2007; Hatten and Zabowski, 2009]. In parts of the boreal where forest floor accumulation is less important, such as pine-lichen forests or mixedwood boreal forests, wildfire is

prone to consume most of the forest floor [e.g., *Kasischke et al.*, 2000; *Shvidenko and Nilsson*, 2000; *Czimczik et al.*, 2005]. However, in boreal black spruce forests of Quebec, combustion of the thick forest floor layers by wildfire is often incomplete and BC is a major product. Typical properties of BC are its relative inertness, its ubiquity in pyrogenic ecosystems [*Schmidt and Noack*, 2000], and its high content of aromatic molecular structures [*Lehmann and Joseph*, 2009].

An ambiguity persists in determining the intrinsic nature of BC, as no standard analytical method exists. *Masiello* [2004] defined BC as the continuum of thermally-altered organic materials. This idea was further explored by *Hammes et al.* [2007] with an inter-laboratory ring trial that aimed to resolve which analytical techniques were best used to assess each part of the continuum. Most of these methods are better adapted to quantify BC in mineral soil. Indeed, the abundance and diversity of C structures present in a well-developed boreal forest floor constitutes a challenge in terms of BC quantification. The commonly used oxidation methods, such as thermal digestion [*Kuhlbusch and Crutzen*, 1995], nitric acid and peroxide [*Kurth et al.*, 2006], oxidation with sodium hypochlorite or acid dichromate [*Hammes et al.*, 2007] may not be able to degrade all of the non-BC carbon, hence leading to overestimates of BC stocks. Another issue common to many protocols used for BC quantitation, such as the BPCA method [*Czimczik et al.*, 2005; *Brodowski et al.*, 2005; *Guggenberger et al.*, 2008], is that only the condensed BC is detected [*Hammes et al.*, 2007]. Nuclear magnetic resonance spectroscopy is the only direct non-destructive method that can adequately estimate BC in organic horizons, and this may be accomplished

independently of the degree of condensation of the material. Other non-destructive spectroscopic methods exist (e.g., Fourier transform infrared/near-infrared, mid-infrared spectroscopy) but they are indirect methods, requiring a calibration set and multivariate data analysis [*Viscarra Rossel et al.*, 2006; *Janik et al.*, 2007; *Bornemann et al.*, 2008].

According to recent studies, BC may be a significant component of the SOC pool. The review by *Preston and Schmidt* [2006] reported BC stocks in boreal forest floors on the order of 1000–2000 kg/ha. Significant BC accumulation was observed in certain North American boreal forests [e.g., *Harden et al.*, 2000; *Bélanger and Pinno*, 2008] but BC stocks appear to vary greatly among boreal ecosystems [*Czimczik et al.*, 2005; *Preston and Schmidt*, 2006; *Kane et al.*, 2007; *Kane et al.*, 2010]. To correctly introduce BC into C models as a slow or passive pool, test its response to future climate conditions, there is a strong need to better understand of its physical and chemical characteristics. As well, better estimates of BC stocks and their distribution in soil profiles are needed for adequate modeling of this pool.

The present study had two main objectives. First, we estimated forest floor C stocks in a range of fire-affected black spruce forests (mesic sites with varying components of jack pine) representative of eastern Canada. Second, we quantified BC stocks in the distinct forest floor layers using solid-state ^{13}C nuclear magnetic resonance (NMR) spectroscopy. Specifically, we quantified BC stocks in the forest floors of 11 soil profiles distributed over the entire northern black spruce-*feathermoss* domain of Quebec. Finally we investigated the influence of regional

variation in fire frequency and climate, and local variation in topography and stand type, on these stocks. This is the first quantitative investigation of BC stocks and wildfire effects on these stocks, in eastern Canada, which represents a large proportion of the boreal forest of North America.

4.2. Materials and methods

4.2.1. Site characteristics

The province of Quebec is divided into ten bioclimatic domains, characterized by distinct vegetation and climatic conditions [*Saucier et al.*, 2001]. The black spruce-feathermoss bioclimatic domain covers a third of the provincial territory and is divided into the eastern and western subdomains, characterized by different precipitation regimes. The west subdomain receives an average precipitation of 850 mm/year in its northern range, and 900 mm/year in its southern range, whereas the eastern subdomain receives 1020 mm evenly distributed throughout the year [*Bergeron et al.*, 2004; *Cyr et al.*, 2007]. Mean annual temperature [*Carrier*, 1996] ranges from -2°C in the north to just above 0°C in the south. The western sector of the domain forms a transition zone between a continental climate (southern range) and a subpolar continental climate (northern range), while the eastern subdomain experiences a cooler, more humid maritime climate, at least in its southern range.

Humo-ferric podzols are found in the majority of the black spruce-feathermoss domain [*Soil Classification Working Group*, 1998]. With the exception of some of the drier sites, forest floors are thick, typically ranging from

10 to more than 120 cm. These podzolic soils have developed on glacio-fluvial sediments/till deposits and therefore have a sandy texture and generally contain a high proportion of coarse fragments (> 2 mm diameter). Veins of clay are occasionally present in the western part of the gradient, because of the proximity to the Clay Belt [Robitaille and Saucier, 1998]. Both subdomains are largely dominated by black spruce (*Picea mariana* (Mill.) Britton, Sterns & Poggenb.) with ericaceous shrubs (*Rhododendron groenlandicum* (Oeder) Kron & Judd, *Kalmia angustifolia* L., and *Vaccinium angustifolium* Ait.), feathermoss (*Pleurozium schreberi* (Brid.) Mitt.) and/or *Sphagnum* moss (*Sphagnum* sp.) constituting most of the understory. Locally, lichens (*Cladina rangiferina* (L.) Weber) associated with fire moss (*Ceratodon purpureus* (Hedw.) Brid.) and haircap moss (*Polytrichum* sp.) were present. On well-drained sites, jack pine (*Pinus banksiana* Lamb.) is often associated with black spruce in mixed stands and becomes dominant under the driest conditions.

In 2005–2007, high fire activity in Northern Quebec caused 1.2 Mha to be burned over these three years. Large fires occurred even in regions that do not experience fires often, i.e., with long fire cycles. These fires provided us with potential study sites spread over a 600-km gradient, with decreasing fire frequency along a west-east axis. Only those fire sites that were accessible by road and that presented a large enough unsalvaged area were selected. A total of 14 fires, ranging in size from 330 to 56000 ha, were selected. Most of the fires occurring during those three years took place at the beginning of the fire season [Kasischke et al., 2010; Turetsky et al., 2011]. In the province of Quebec, fire

regime has been regionalized by landscape units of relative homogeneous environmental conditions, including vegetation, temperature, and precipitation [Lefort *et al.*, 2004; Chabot *et al.*, 2009], using two descriptors of fire frequency: fire occurrence and fire cycle. To test for the influence of fire frequency on SOC and BC stocks, we divided our study area into five zones of homogeneous fire cycle and similar climatic conditions using these landscape units (Figure 4-1). Each zone included 2 to 4 fire sites. All sites were outside the permafrost zone and were sampled in summer 2010.

4.2.2. Sampling protocol

Topographic gradients and plots

We positioned two to four topographic gradients within each selected fire site, for a total of 46 gradients. Two to three 20 m x 20 m plots were situated on each of the gradients (total plot number = 133). For each plot, we defined its slope position (upper, mid, lower), and measured the aspect. We estimated the amount of biomass that was consumed during the last fire event by measuring the depth of the residual organic matter (ROM) following *Kasischke and colleagues'* [2008] methodology. On five microplots, we located the uppermost adventitious root of the black spruce tree taller than 2 m and closest to the center of the microplot. In the few cases where no adventitious roots were found – e.g., well drained sites with shallow organic layers – the top of the basal root was used. The distance between the adventitious or basal root and the mineral soil surface was determined to estimate the thickness of the pre-fire organic layer (OMt). Lastly,

the thickness of the forest floor that was consumed by the last fire event (OMc) was calculated as the difference between the latter and the thickness of the ROM.

In Quebec coniferous boreal forests some topographic positions, including S, SW, and W facing aspects, are more fire-prone than others dominated by N, NE or E facing slopes [Cyr *et al.*, 2007]. Similarly, soils located upslope tend to have better drainage than downslope soils, and their forest floor is more likely to be drier and therefore more prone to consumption by fire. To study the frequency distribution of forest floor thickness before fire, we used the following two combinations of slope position and aspect: 1. Upslope position on S, SW or W facing slope, and 2. Downslope position on N, NE or E facing slope. Forty-two plots (21 plots for each of the 2 position+aspect combinations) met these conditions.

Soil profiles

A total of twenty-three soil profiles were described and sampled to capture each of the five zones of homogeneous fire cycle and climatic conditions of the black spruce domain (n= 4–5 for each zone; Table 4-A.1). For each soil profile, the entire forest floor was sampled using a shovel to delimit an approximate 20 cm x 20 cm square. The exact measurements of the square were recorded. The forest floors usually presented the following distinct layers that were individually sampled: a thin – averaging 2 cm – superficial burnt layer produced by the last fire event (referred to hereafter as fresh BC), a partially decomposed litter horizon (F), and a highly humified organic matter horizon (H). The latter was generally

associated with a thin layer of BC produced by previous fire events (historical BC, which was sitting right at the interface with the mineral soil). In some instances, the historical BC layer was thick enough that we were able to separate it from the rest of the H horizon.

4.2.3. Laboratory analyses

Elemental content

Organic samples were placed at 65 °C in a drying oven for 3 to 5 days, and weighed to determine dry mass and to estimate bulk density. Prior to elemental analysis, samples were finely ground using a mortar grinder (RM 100 mortar grinder, Retsch, Haan, Germany). Carbon, hydrogen, and nitrogen contents were determined by dry combustion using a CHN Analyzer (CEC – Control Equipment Corporation – Model 440 Elemental Analyzer with auto-injector). The oxygen content was estimated by difference from the ash free mass of the sample obtained after 6 hours at 750 °C in a muffle furnace in accordance with ASTM Standard D1762-84 [ASTM, 2007]. This procedure also provided total ash content.

Solid-state ¹³C Nuclear Magnetic Resonance spectrometry

For a subset of 11 soil profiles (n = 33 horizons), the BC content of the forest floor horizons (fresh BC, F, and H + historical BC or H horizon and historical BC layer) was determined using solid-state ¹³C NMR spectroscopy with magic angle spinning (MAS). The ¹³C nuclei (1.1% natural abundance) provided information

about the various functional groups present in our samples [Kögel-Knabner, 1997; Axelson, 2012]. Studies focusing on organic matter usually employ the cross-polarization (CP) technique as it allows for acquisition of ^{13}C NMR spectra in less time. However, the CP efficiency for chars is reduced [Baldock and Smernik, 2002] because of the absence of mobile ^1H nuclei [Freitas et al., 1999; Smernik et al., 2002]. To verify that our CP spectra were representative, we used the more quantitative direct polarization (DP) technique, also called Bloch decay (BD) technique [Preston and Schmidt, 2006] on a subset of horizons ($n = 15$).

The CP experiments were conducted on a Chemagnetics CMX Infinity 200 spectrometer. A 5.0 mm Chemagnetics triple-resonance MAS probe was used to spin the samples at the magic angle (54.7°), with a spinning frequency of 10 kHz (± 10 Hz). This is fast enough to move the spinning side bands out from the region of interest at this field strength (4.7 T). Samples were packed in 5.0 mm od zirconium oxide rotors equipped with Kef-F® drive tips and Teflon end-cap and spacer. Chemical shifts in parts per million (ppm) were externally referenced to tetramethylsilane (TMS) using the adamantane peak at 38.56 ppm [Earl and VanderHart, 1982]. Spectra were acquired at a frequency of 50.3 MHz, using a variable-amplitude cross-polarization (VACP) pulse sequence [Peersen et al., 1993]. A spectral width of 30 kHz was used and 1024 real data points were collected over an acquisition time of 34.1 ms. All spectra were then zero-filled to 8192 data points. The background ^{13}C NMR signal, obtained by the acquisition of the spectrum of an empty rotor, was subtracted before processing the free induction decays (FIDs). The number of scans acquired for the CP spectra ranged

from 8432 to 9468. We used a 1 ms contact time, a 90° ^1H pulse of 4.5 μs duration and a pulse delay of 10 s. Finally, we applied Lorentzian line-broadening of 60 to 100 Hz before performing the Fourier transform. The spectra were divided into seven spectral regions, each corresponding to a major type of C, as described in *Baldock et al.* [2004]: amide and carboxyl (215–165 ppm), phenolic (165–145 ppm), aromatic (145–110 ppm), di-O-alkyl (110–95 ppm), O-alkyl (95–60 ppm), methoxyl and N-alkyl (60–45 ppm), and alkyl (45–0 ppm).

The DP experiments were conducted on a Bruker Avance 300 spectrometer using a 4.0 mm Bruker double-resonance MAS probe with a spinning frequency of 13 kHz (\pm 10 Hz). 1800 scans were acquired using a 90° ^{13}C pulse of 4.5 μs duration at a frequency of 75.5 MHz. To allow for complete relaxation of all C nuclei [*Baldock and Smernik*, 2002], the pulse delay was set to 100 s. The background signal was removed using a background suppression program [*Cory and Ritchey*, 1988]. All spectra were zero-filled to 8192 data points and a Lorentzian line-broadening of 100 Hz was applied to the FID. Applying *Smernik and Oades'* [2000a] methodology, we used spin counting to determine if the DP spectra were representative of all the C moieties present in the samples. Spin counting relies on comparing the ^{13}C NMR integrated signal intensity of a sample for which the mass and C content are known with that of a standard, which is known to provide a quantitative signal. Glycine (Fisher Scientific, reagent grade) was used as an external standard. We determined how much of the expected signal was in fact detected in the NMR spectra. The C observability, C_{obs} , corresponds to the fraction of the expected NMR intensity that was actually

observed. It is assumed that the intensities of the NMR resonances quantitatively reflect the distribution of ^{13}C environments present in the sample if $C_{\text{obs}} = 100\%$ [Smernik and Oades, 2000b]. A value of less than a 100% for C_{obs} implies that part of the potential signal is not detected.

Molecular mixing model

To estimate the BC content of each sample, we used a molecular mixing model (MMM) as described in *Baldock et al.* [2004]. The molecular model predicts sample composition by targeting the four major classes of organic compounds (carbohydrates; proteins; lignins; lipids) as well as carbonyl C and char, which represent the organic matter altered by oxidation and fire, respectively. The integrated areas (% of the total signal intensity) corresponding to the seven spectral regions from the CP spectra – and DP spectra when available – were entered into the molecular mixing model to estimate the percentage of BC in the samples. We refer to these results as CP+MMM and DP+MMM, respectively, in the rest of the manuscript. For the following 5 model components: carbohydrate; protein; lignin; lipid, and carbonyl C, we used the assigned percentage of total ^{13}C NMR signal intensity to the seven spectral regions as reported in *Baldock et al.* [2004]. For the char component we used the default value proposed by *Baldock* (personal communication; Table 4-B.1) as well as values obtained for a fresh BC layer that was not very aromatic (MMM-1; Table 4-B.1) and a BC produced in the laboratory at 600 °C under controlled conditions (MMM-2; Table 4-B.1). We used these two adjusted models to estimate how

much slightly-aromatic and highly-aromatic BC the samples contained. BC content is expressed as a percentage of the total organic C present in the sample.

4.2.4. Statistical analyses

We used a 1-way ANOVA – or Mood's median test and a Kruskal-Wallis when needed – to analyze the ^{13}C NMR and elemental data of the selected organic horizons of the soil profiles. The same analysis was used to evaluate the effect of the five zones of homogeneous fire cycle and climatic conditions on bulk forest floor characteristics. When performing analyses to test for the effects of stand type (i.e., black spruce-dominated vs. jack pine-dominated) or topographic features, we used the five zones of homogeneous fire cycle and climatic conditions as blocks. Differences linked to stand type and aspect were tested using an unequal variance Welch t-test. Relationships between variables were estimated using Pearson correlation and Spearman rank correlation when needed. All comparisons and ANOVA were considered significant at an alpha value of 0.05. For the significant ANOVAs, we adjusted the alpha with a Bonferroni correction when exploring all possible comparisons. All statistical analyses were performed with SAS 9.2 (SAS Institute Inc., Cary, North Carolina).

4.3. Results

4.3.1. Forest floor carbon stocks

Forest floor thickness in undisturbed black spruce forests averaged 27.2 cm (Table 4-1). During the high fire activity episode of 2005–2007, the average depth

of forest floor consumed by fire was 10.6 cm, and the residual organic matter (ROM) thickness was 16.6 cm. A reduced fire frequency appeared to favor the accumulation of organic material (Figure 4-2a). A significant difference in forest floor thickness before fire (OMt) was observed between the two zones with shorter fire cycle (FC) (East Baie-James – FC < 200 years and Chibougamau – FC between 200–500 years, where depths were 23.6 and 26.0 cm, respectively), and the zone with the longest fire cycle (North-Shore – FC > 1000 years, which had a forest floor thickness of 33.3 cm; Figure 4-2a). This translated into a significant difference in forest floor depth after fire (ROM): the North-Shore region had a deeper ROM than the other zones (Figure 4-2a). There was also a significant difference in C stocks after fire (Figure 4-2b); forest floors of the three zones with an intermediate fire cycle, Saguenay-Ashuapmushuan, West Baie-James, and Chibougamau, stored more C than that of the zone with the shortest fire cycle, East Baie-James.

The mean pre-fire forest floor thickness in black spruce-dominated stands was significantly greater (29.5 cm) than that of jack pine-dominated stands (19.9 cm; Table 1). This difference persisted after fire (Table 4-1). C stocks were significantly higher in black spruce-dominated stands ($6.4 \pm 2.8 \text{ kg m}^{-2}$) compared to stocks in stands dominated by jack pine ($3.4 \pm 1.8 \text{ kg m}^{-2}$).

The plots located on N and E facing slopes (i.e., non-fire prone slopes) had significantly deeper organic horizons before fire (29.3 cm) than those located on S and W facing slopes, i.e., fire prone slopes (average of 25.8 cm; Table 4-1). The ratio of forest floor consumed by the last fire event over the initial forest floor

depth (OMc/OMt), was also significantly smaller in plots located on N facing slopes (35.8%) compared to plots located on S facing slopes (44%; Table 4-1). In addition, slope position affected forest floor depth before fire; downslope positions were characterized by a significantly deeper forest floor (30.7 cm) than midslope (26.1 cm) or upslope (25.3 cm) positions (Table 4-1). Finally, upslope plots exhibited a significantly higher ratio of forest floor consumption (OMc/OMt; 45.1%) than the downslope plots (36.0%; Table 4-1). Figure 4-3 clearly illustrates the greater accumulation of organic material on the northern slopes and downslope positions.

4.3.2. *Forest floor characteristics*

Forest floor quality as defined by N content and C/N ratio did not vary significantly as a function of stand type (Table 4-2). The deepest organic layer (H + historical BC) was significantly less developed in jack pine stands (2.7 ± 1.7 cm) compared to black spruce stands (5.5 ± 2.2 cm; Table 4-2). The humic layer was generally thin, and sometimes absent, in recently fire-affected forest floors of jack pine stands. The fresh BC layer had a significantly higher pH than the underlying F, H or H + historical BC layers. The fresh BC layer also had a significantly higher C content ($52.4 \pm 2.9\%$) than the F layer ($50.1 \pm 1.9\%$). However, the C/N ratios of these two layers were not significantly different. Fire had an effect on atomic ratios, with the H/C and O/C ratios generally decreasing in the fire-affected layers (Figure 4-4). The atomic H/C ratio in the F layer was significantly higher than in the H + historical BC layer, which was significantly

higher than for the historical BC. On the other hand, atomic O/C ratio differences among the forest floor layers were not statistically significant.

The ^{13}C NMR spectra revealed chemical composition differences among the different organic horizons (fresh BC, F, H + historical BC, historical BC). Figure 4-5 presents CP and DP spectra of forest floor horizons of two soil profiles typical of black spruce- and jack pine- dominated stands.

Spectra from the fresh BC and F layers were very similar and exhibited peaks representative of cellulose, hemicelluloses and lignin [Wikberg and Liisa Maunu, 2004; Inari et al., 2007; Melkior et al., 2012]. The dominant peak at 72–75 ppm (O-alkyl spectral region) can be attributed to cellulose, as can the smaller peak at 105 ppm. The third most important peak was located at 30 ppm in the alkyl region, and is characteristic of long-chain CH_2 . It was particularly broad, suggesting a large heterogeneity in the functional groups present (CH , CH_2 and CH_3 structures). The aromatic, phenolic, and carboxyl regions were very weak in the CP spectra but the DP spectra presented detectable peaks. The signal at 173 ppm was assigned to the hemicellulose carboxyl groups, although that peak was rather broad and could also be associated with the amide C of proteins as well as the carboxyl groups of microbial and plant lipids [Preston et al., 2006]. Peaks arising from lignin are mainly present between 110 and 165 ppm, and at 56 ppm for the lignin methoxyl groups. Lignin content was minor as suggested by the weak signals obtained for these regions; the signal at 155 ppm is likely ascribable to tannins [Lorenz et al., 2000]. The small signal at 130 ppm is related to black carbon [Inari et al., 2007].

There were major differences in the H + historical BC spectra with an important loss of intensity in the O-alkyl and di-O-alkyl regions counterbalanced by an increase in the aromatic and phenolic regions. The intensity in the other regions remained relatively constant. The broad alkyl peak at 25 ppm and the strong and broad signal at 130 ppm indicated the presence of a significant amount of BC in this layer. The historical BC layer was clearly dominated by aromatic C with a characteristic broad peak centered at 130 ppm. The small residual peaks in the O-alkyl (73 ppm) and carboxyl regions (173 ppm) are the remains of carbohydrate structures, while the small signal in the alkyl region could be related to BC formation [Inari *et al.*, 2007]. Figure 4-6 illustrates the shift in dominance in the ^{13}C NMR spectra from the O-alkyl and di-O-alkyl regions (fresh BC and F) to the aromatic region (H + historical BC and historical BC).

4.3.3. *Black carbon content*

Calibration of the Molecular Mixing Model (MMM)

Results of the spin counting showed that the DP experiments were quantitative, whereas the CP experiments were not. Hence, to obtain accurate BC content, only the DP spectra data should be used with the molecular mixing model. BC concentrations estimated by CP+MMM were strongly correlated to those estimated by DP+MMM, which allowed us to derive a predictive equation (Equation 1; $R^2 = 0.89$) to obtain more accurate BC concentrations for all analyzed samples.

We applied the different versions of the molecular model to the 15 samples for which we acquired both a CP and a DP spectrum. BC contents estimated with the 3 MMM were strongly correlated (Table 4-C.1) and we derived equations to predict BC contents estimated with DP+MMM-1 ($R^2 = 0.92$; Equation 2) and DP+MMM-2 ($R^2 = 0.99$; Equation 4-3) from the BC content estimated with DP+MMM. Figure 4-7 summarizes the BC content estimated from the DP data for the different horizons using the 3 models. There was significantly more BC (40.8%) in the historical BC layer than in all other horizons, as estimated by MMM-2. BC contents estimated by MMM-1 were significantly higher than those estimated by the two other models (Figure 4-7). Similarly to the default model (MMM), there was a strong and significant relationship between the BC concentrations estimated by CP+model and those estimated by DP+model for MMM-1 and MMM-2 ($R^2 = 0.88$ and $R^2 = 0.85$ respectively; Table 4-C.1).

Estimation of forest floor BC stocks

Using the mixing model with the ^{13}C NMR CP and DP spectra data, we found that the organic layers were characterized by variable BC concentrations. There was a significant difference in BC content (expressed as % of total SOC) among the organic layers. The historical BC layer contained the highest amount of BC ($67.7 \pm 5.2\%$). The H + historical BC contained more BC ($26.0 \pm 13.3\%$) than the fresh BC ($13.4 \pm 7.1\%$) and F ($6.2 \pm 2.9\%$) horizons. The F horizon was thicker than the other organic horizons, representing 50% ($\pm 3\%$) of the total forest floor thickness; comparatively the H + historical BC horizon accounted for only 36%

($\pm 3\%$) of the total depth. Despite this, most of the BC stock was present within the H + historical BC layer. BC stock in the latter horizon was significantly higher ($0.188 \pm 0.242 \text{ kg C m}^{-2}$) than that of the fresh BC layer ($0.014 \pm 0.012 \text{ kg C m}^{-2}$). Total C content of individual forest floor horizons was not strongly related to its BC content ($R^2 = 0.34$; Table 4-C.1). However, the atomic H/C ratio explained a large part of the variability in BC content ($R^2 = 0.80$; Table 4-C.1).

BC stocks for the 11 profiles, as well as their corresponding C stocks, are presented in Table 4-3. They range between 0.24 and 1.23 kg C m^{-2} . We could not detect any significant difference in BC stocks in relation to environmental conditions (stand type, zone, slope aspect and position, fire-prone context).

4.4. Discussion

4.4.1. Fire effects on forest floor characteristics

Stand type influenced the chemical composition and depth of the forest floor, thereby affecting its vulnerability to complete combustion by wildfire (Tables 4-1, 4-2). Partial consumption of the forest floor by wildfire results in BC layers, which are ubiquitous in Quebec black spruce forests [Simard *et al.*, 2007]. At our study sites, BC was often absent from the H horizon if the forest floor was thin, and its absence may indicate that the forest floor had been entirely consumed by fire in the past. This situation is more probable in rapidly or well-drained stands and where the canopy is dominated by jack pine. The deeper organic layers present on north-facing slopes suggests that moister and cooler slopes are less

likely to burn. *Kane et al.* [2010] made similar observations in Alaskan black spruce forests.

The presence of BC affected the ^{13}C NMR spectra, as indicated by a characteristic and broad peak at 130 ppm (Figure 4-5). Previous studies conducted in various ecosystems have reported similar results [e.g., *Czimczik et al.*, 2003; *González-Pérez et al.*, 2004; *Preston et al.* 2006]. For the H + historical BC layer, and in particular for the historical BC layer itself, the ^{13}C NMR spectra were dominated by aromatic non-oxygenated C (130 ppm), suggesting that condensation of the original macromolecules into aromatic polymers had occurred. This suggests an increase in condensation, which agrees with the decrease in the atomic H/C, and to a lesser extent O/C, ratios in the layers that have been more affected by fire. To illustrate this phenomenon, we calculated the degree of aromatization, which corresponds to the ratio of aromatic & phenolic C (165–110 ppm) to O-alkyl C + alkyl C (110–0 ppm), and is an indicator of the increasingly condensed nature of chars [*Keiluweit et al.*, 2010]. As expected, there was an increase in the degree of aromatization in the organic layers where the effect of fire was more important (Table 4-D.1). We derived another index from the ^{13}C NMR spectra: the polarity index, which corresponds to the ratio of (Carboxyl/Amide C + O/N-alkyl C) to (phenolic C + aromatic C + alkyl C) and illustrates the water repellency potential of BC [*Knicker et al.*, 2006]. The polarity index decreased in the layers most affected by fire (Table 4-D.1), which supports increasing hydrophobicity with more BC [e.g., *Kinney et al.*, 2012]. This could be significant in the case of soil mixing after salvage harvesting. This form of

scarification is a common silvicultural practice in Quebec and could lead to increased water repellency in the post-fire soil environment.

In forest floors, the major structural components of soil organic C are generally divided as follows: O-alkyl (40–55%), aromatic (15–25%), alkyl (20–30%) and carboxyl (5–10%). The percentage of alkyl C generally increases during humification [Kögel-Knabner *et al.*, 1992]. The presence of BC in the H horizon completely changed this trend, with aromatic and phenolic C representing up to 35–55% while O-alkyl C dropped to 15–25% (Figure 4-6). These differences indicate that the deeper layers of the forest floor in these boreal black spruce forests (H + historical BC and historical BC; located just above the mineral-organic interface) are more chemically complex, hence likely less susceptible to decomposition than non fire-affected forest floors.

4.4.2. Carbon and black carbon stocks

Carbon stocks

Average SOC stocks after fire ($5.70 \pm 0.29 \text{ kg m}^{-2}$ in the 133 plots and $5.49 \pm 0.54 \text{ kg m}^{-2}$ in the 23 profiles) were higher than results obtained by Czimczik *et al.* [2005] in Siberian Scot pine (*Pinus sylvestris*) forests (max = 2.19 kg m^{-2}), or by Nalder and Wein [1999] in jack pine forests of western Canada (1.17 ± 0.27 to $1.52 \pm 0.49 \text{ kg m}^{-2}$). When considering only jack pine stands, SOC stocks were similar to the latter values ($3.40 \pm 0.18 \text{ kg m}^{-2}$). The higher SOC stocks we observed are likely the result of higher annual precipitation in our forests, favoring feathermoss over lichen cover in the forest. Neff *et al.* [2005] reported C

stocks in recently burned Alaskan black spruce forests that were similar to our values ($3.12 \pm 0.58 \text{ kg m}^{-2}$). In organic horizons of Alaskan black spruce forests, *Kane et al.* [2010] also reported C stocks that were in the same range as we observed, with $4.09 (\pm 0.64) \text{ kg m}^{-2}$ in the south facing sites and $5.73 (\pm 0.64) \text{ kg m}^{-2}$ in the organic horizons of north facing sites.

The difference in C stocks after fire between black spruce-dominated stands ($6.4 \pm 2.8 \text{ kg m}^{-2}$) and those dominated by jack pine ($3.4 \pm 1.8 \text{ kg m}^{-2}$) is an important finding in the context of possible species compositional shifts associated with low fire severity and large fire years [*Boiffin and Munson, 2013*]. The influence of canopy composition on forest floor C stocks was likely due to preferential position in the landscape: black spruce dominate in moderately- to poorly-drained sites whereas jack pine occupies driest uplands that are more fire-prone. This favors moss accumulation in black spruce stands [*Boiffin and Munson, 2013* and references therein]. Moreover, high tannin concentrations in forest floors of black spruce stands are prone to reduce N availability and inhibit decomposition [e.g., *Lorenz et al., 2000; Preston et al., 2006*]. Lastly, differences in understory vegetation could explain differences in C stocks. Notably *Sphagnum* mosses, which have been connected to sites with high C storage [e.g., *Hollingsworth et al., 2008*], were preferentially associated with black spruce, whereas jack pine was mostly associated with lichen and/or feathermosses that produce thinner forest floor layers.

In our study, we were able to show that shorter fire cycles tended to reduce C storage in the forest floors. We suspect that the difference in C stocks is also

related to the climatic conditions and the soil physical characteristics of this zone. First, even if the time since last fire was shorter in the East Baie-James zone, it was close from the four other zones (Table 4-A.1). Second, the lower C stocks in the East Baie-James zone were principally associated with lower C storage in the black spruce stands ($4.8 \pm 1.8 \text{ kg m}^{-2}$) compared to similar stands in the other zones (6.1 ± 2.1 to $7.6 \pm 3.1 \text{ kg m}^{-2}$). Reduced precipitation in this zone (Table 4-A.1) and a frequent and quite abundant stoniness on the sites may reduce stand productivity. Alternatively, the second to last fire events may have been exceptionally severe in this zone, partially consuming the H + historical BC, and consequently removing an important portion of the historical C stock.

Black carbon stocks

As expected the slightly-aromatic BC content (BC estimated by MMM-1) was significantly higher than the highly-aromatic BC content (BC estimated by MMM-2). The absence of a significant difference between the default MMM (*Baldock*) and MMM-2 confirms that the default model provides an estimate for BC that is already highly aromatic (Figure 4-7; Table 4-B.1). The use of the adjusted model MMM-1 can be particularly relevant to estimate BC content in the fresh layers after low severity fires, and/or to assess how much BC transfers to the F layer following low severity surface fires. Equations 2 and 3 could be used to quickly provide higher and lower boundaries to BC stocks present in the forest floor layers, respectively.

The BC stocks we measured ($608 \pm 314.1 \text{ g C m}^{-2}$) were much higher than those reported in previous studies. For instance, in similar ecosystems (Alaskan black spruce forests), *Kane et al.* [2010] observed BC stocks (estimated by DP+MMM) of $260 (\pm 1) \text{ g C m}^{-2}$ in the organic horizons of south facing forests but only $140 (\pm 4) \text{ g C m}^{-2}$ in the organic horizons of north facing forests. In the organic layers of a forest tundra in northern Siberia, *Guggenberger et al.* [2008] reported BC stocks, estimated by BPCA, ranging between $8 (\pm 3)$ in SSW slopes and $103 (\pm 23) \text{ g m}^{-2}$ in intact raised bogs. In a chronosequence of 12 forest sites in northern Sweden, *Zackrisson et al.* [1996] found soil charcoal mass, estimated by hand sorting, to vary from 98.4 to 207.4 g m^{-2} . Using a similar methodology, *Bélanger et al.* [2004] reported char stocks of 34.3– 129.5 g m^{-2} in the forest floor of a deciduous forest of Southern Quebec, 75 years after fire. Finally, comparing burned and unburned forest floor of Siberian scots pine forests, *Czimczik et al.* [2003] reported BC stocks, estimated by BPCA, of $14.1 (\pm 7.7) \text{ g m}^{-2}$ and $20.2 (\pm 11.0) \text{ g m}^{-2}$ for the unburned and burned sites respectively. Because of the different analytical methods employed to measure BC, it is not necessarily acceptable to compare these estimates [*Hammes et al.*, 2007]. However *Kane et al.* [2010] adopted a similar methodology to ours and estimated C stocks that were comparable. The difference in BC stocks we observed could be due to the presence of the H + historical BC horizon, which was quite deep in half of the profiles and contributed importantly to the total BC stock of the forest floor. This horizon was apparently absent from the sites studied by *Kane et al.* [2010].

This study highlights the importance of the forest floor in Quebec black spruce forests in terms of BC storage. In contrast to other forest ecosystems, e.g., temperate forests or less productive boreal ecosystems, complete forest floor consumption by fire does not appear to be the norm in these forests. Part of the forest floor usually survives fire events and the fresh BC produced likely gets diluted in the F layer over time, as new moss accumulates on top of it. In this situation, BC does not generally come into direct contact with the mineral soil, and instead accumulates in the organic horizons. In our study, past accumulation of BC represented an important contribution to total BC stocks, as shown by the large amount of BC stored in the H + historical BC layers. On the other hand, contribution of the fresh BC layer (i.e., from the last fire event) to the BC stocks already present in the F and H horizons averaged only 6%. This could be because the recent fires we studied were not severe at the forest floor level [*Boiffin and Munson, 2013*]. *Czimczik et al. [2005]* made similar observations in Siberian scots pine forests and concluded that BC accumulation in the organic horizons was under the control of fire severity.

As discussed earlier, the ^{13}C NMR spectroscopic signature of the historical BC indicates that it was formed at high temperature ($> 450\text{ }^{\circ}\text{C}$). This temperature seems high for a smoldering fire [e.g., *Miyanishi, 2001*; *Ryan, 2002*]. The historical BC layer more likely originated from very rare and intense fires at ground level, which consumed most of the forest floor; but left the BC formed on trees, i.e., carbonized bark and wood, covering the ground. A new moss layer, and

eventually a new forest floor, then formed over that BC layer, which remained at the interface with the mineral soil.

4.5. Conclusions

Fires affect the quantity and quality of the forest floors in Quebec black spruce forests. Fire appears to be a driving factor of the carbon cycle in these forests. First it oxidized some organic carbon; this complete combustion was influenced by environmental features, including slope position and aspect. Second, fire affected part of the remaining C stocks through production of more or less condensed black carbon. The recent low severity fires at the forest floor level, which affected our study sites, left part of the carbon pool and much of the historical black carbon legacy intact, with the persistence of the H + historical BC layer, as well as part of the F horizon, which on occasion constituted a substantial BC reservoir. In this study, fire history seemed to control BC stocks, as the H + historical BC layer contained the biggest BC reservoir in most profiles.

We were able to determine BC content in the various forest floors layers by applying the molecular mixing model on the ^{13}C NMR DP spectra data. This method of BC quantitation for organic samples is not only accurate but also flexible, with the possibility of calibrating the molecular model for different ecosystems and various scenarios of fire severity by choosing the degree of condensation of the BC. But if sample preparation for NMR analysis is minimal, acquisition times, and access to a spectrometer are prohibitive when analyzing a large number of samples. This study highlights the need to find a standard method

of BC quantitation for this type of samples that will be less time consuming. This improved knowledge on BC pools is urgently needed in fire-affected ecosystems where organic materials represent a large part of the carbon pool (e.g., boreal forests, peatlands, etc.).

Tables and Figures

Table 4-1. Average organic matter (entire forest floor) thickness (cm) before fire (OMt), organic matter depth consumed by fire (OMc), residual organic matter thickness (ROM), and forest floor carbon stock after fire.

		N	OMt (cm)		OMc (cm)		OMc/OMt		ROM (cm)		C stock (kg m ⁻²)	
stand type	all plots	133	27.2	(8.5)	10.6	(5)	0.406	(0.12)	16.6	(8.2)	5.7	(2.9)
	Black spruce	102	29.5 ^c	(7.7)	10.6	(5)	0.37 ^c	(0.15)	18.9 ^c	(7.8)	6.4 ^c	(2.8)
	Jack pine	31	19.9 ^d	(6.7)	10.6	(4.9)	0.524 ^d	(0.15)	9.1 ^d	(3.7)	3.4 ^d	(1.8)
topography (aspect)	Non fire-prone (N and E aspects)	56	29.3 ^e	(8.3)	9.8	(4.4)	0.358 ^e	(0.16)	17.7	(9.1)	6.6 ^e	(2.9)
	Fire-prone (S and W aspects)	77	25.8 ^f	(8.4)	11.2	(5.2)	0.440 ^f	(0.16)	15.7	(7.3)	5.1 ^f	(2.7)
topography (position)	downslope	42	30.7 ^g	(8.2)	10.7	(5.8)	0.36 ^g	(0.18)	19.8	(8.6)	7.0 ^g	(3.5)
	midslope	50	26.1 ^h	(7.9)	10.1	(4.5)	0.40 ^{gh}	(0.16)	15.8	(7.5)	5.4 ^h	(2.2)
	upslope	41	25.3 ^h	(8.8)	11.1	(4.6)	0.45 ^h	(0.16)	14.3	(7.7)	4.8 ^h	(2.4)

Values for each parameter are mean (SD)

Means with a different letter are significantly different from one another (with Bonferroni adjustment for the ANOVA/position on the slope) in similar subsets (columns: year = a, b; stand type = c, d; aspect = e, f; position = g, h)

Table 4-2. Thickness (cm) of each organic layer sampled after fire, pH of the F horizon, and nitrogen (N) content (%) of the bulk forest floor. The number of samples considered (n) is reported.

		stand type			
		black spruce (BSP)	jack pine (JP)	n (BSP)	n (JP)
	fresh BC	1.4 ^a (0.3)	1.3 ^a (0.5)	16	6
horizon depth (cm)	F	6.9 ^a (4.4)	6.5 ^a (2.6)	16	6
	H	6.7 ^a (2.9)	2.7 ^a (1.8)	3	3
	H + historical BC	5.5 ^a (2.2)	2.7 ^b (1.7)	14	4
pH	F	3.1 ^a (0.2)	3.1 ^a (0.2)	16	6
N content (%)	bulk forest floor	1.21 ^a (0.26)	1.18 ^a (0.19)	16	7
C/N ratio	bulk forest floor	40.2 ^a (8.2)	41.2 ^a (4.9)	16	7

Values for each parameter are mean (SD)

Means with a different letter in similar subsets (rows) indicate significant differences between the two stand types (calculated with unequal variance Welch t-test).

Table 4-3. C and BC stocks in the forest floor of the 23 soil profiles. We calculated the BC stocks for only 11 profiles (nd: not determined) using the BC estimated with Baldock MMM (associated with the data from the DP experiment or when needed, the data from the CP experiment plotted in equation 1).

Profile	Fire site	Zone of homogeneous fire cycle and climatic conditions	Stand type	C stock (kg m⁻²)	BC stock (kg C m⁻²)
1	8	Saguenay-Ashuapmushuan	jack pine	11.86	nd
2	8	Saguenay-Ashuapmushuan	black spruce	8.11	nd
3	9	Saguenay-Ashuapmushuan	jack pine	3.07	0.35
4	9	Saguenay-Ashuapmushuan	jack pine	6.75	0.48
5	10	Saguenay-Ashuapmushuan	black spruce	9.36	nd
6	14	North-Shore	black spruce	8.68	nd
7	14	North-Shore	black spruce	2.29	nd
8	13	North-Shore	jack pine	4.44	0.64
9	13	North-Shore	black spruce	4.81	0.89
10	7	Chibougamau	jack pine	2.74	nd
11	7	Chibougamau	jack pine	2.42	nd
12	6	Chibougamau	black spruce	5.93	nd
13	6	Chibougamau	black spruce	8.40	nd
14	1	East Baie-James	black spruce	6.16	nd
15	1	East Baie-James	black spruce	3.65	nd
16	2	East Baie-James	black spruce	3.52	0.84
17	3	East Baie-James	black spruce	3.95	0.45
18	3	East Baie-James	black spruce	6.71	0.85
19	4	Chibougamau	black spruce	3.76	0.47
20	12	West Baie-James	black spruce	2.68	nd
21	12	West Baie-James	black spruce	3.21	0.24
22	11	West Baie-James	jack pine	7.11	0.24
23	11	West Baie-James	black spruce	6.73	1.23

Equations

Equation 1: Prediction of BC content (% total SOC as estimated by DP+MMM)
using BC content estimated by CP+MMM.

$$BC_{DP+MMM} = 6.98 + 1.12 \times BC_{CP+MMM}$$

Equation 2: Prediction of BC content (% total SOC) estimated by DP+MMM-1
using BC content estimated by DP+MMM.

$$BC_{DP+MMM-1} = 10.80 + 1.49 \times BC_{DP+MMM}$$

Equation 3: Prediction of BC content (% total SOC) estimated by DP+MMM-2
using BC content estimated by DP+MMM.

$$BC_{DP+MMM-2} = -1.02 + 0.62 \times BC_{DP+MMM}$$

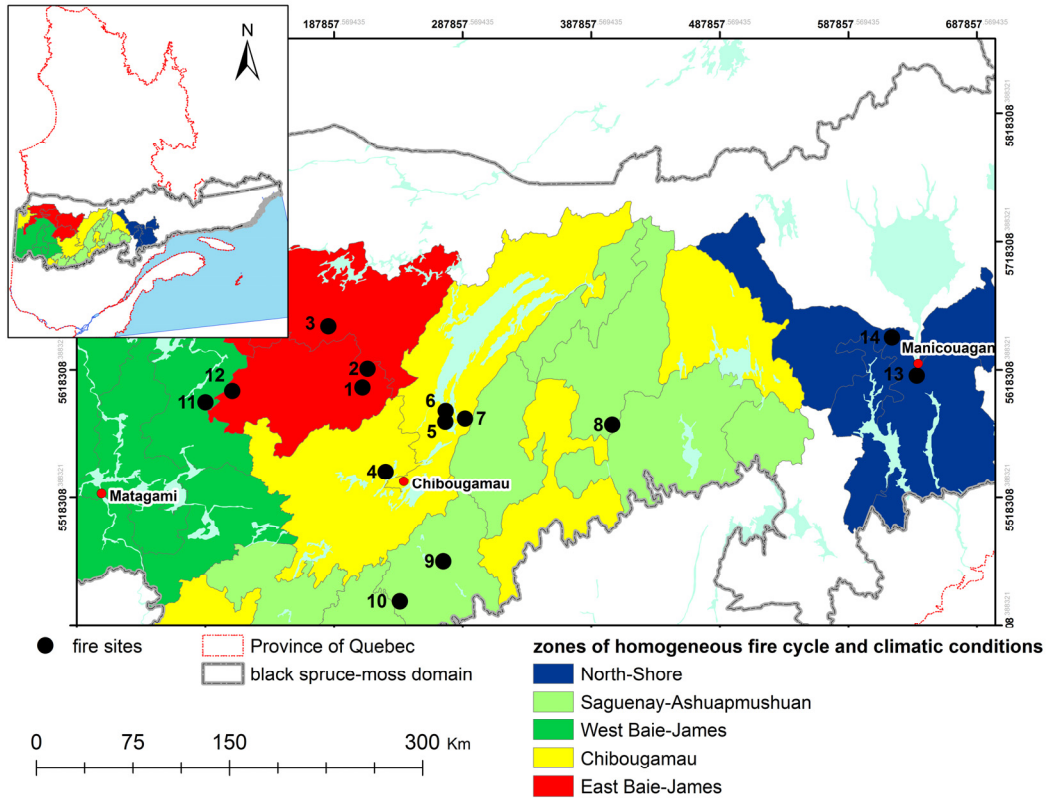


Figure 4-1. The 14 study sites and their corresponding homogeneous fire cycle and climatic conditions zones.

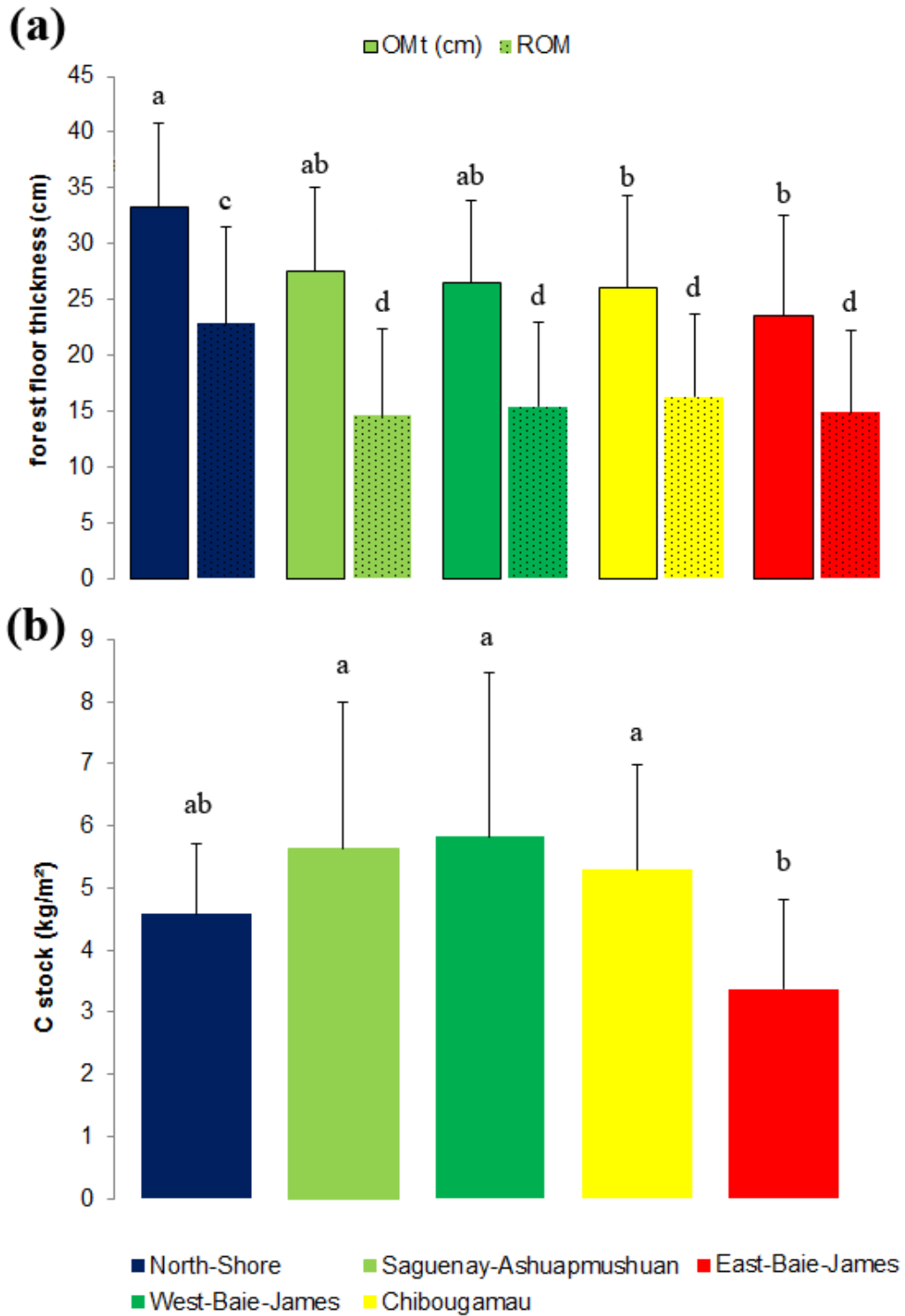


Figure 4-2. (a) Mean organic matter (forest floor) thicknesses (cm) before (OMt) and after (ROM) fire and (b) mean C stocks (kg·m⁻²) after fire in the five zones of

homogeneous fire cycle and climatic conditions. Different letters indicate significant differences among zones (p-value < 0.005 with Bonferroni adjustment).

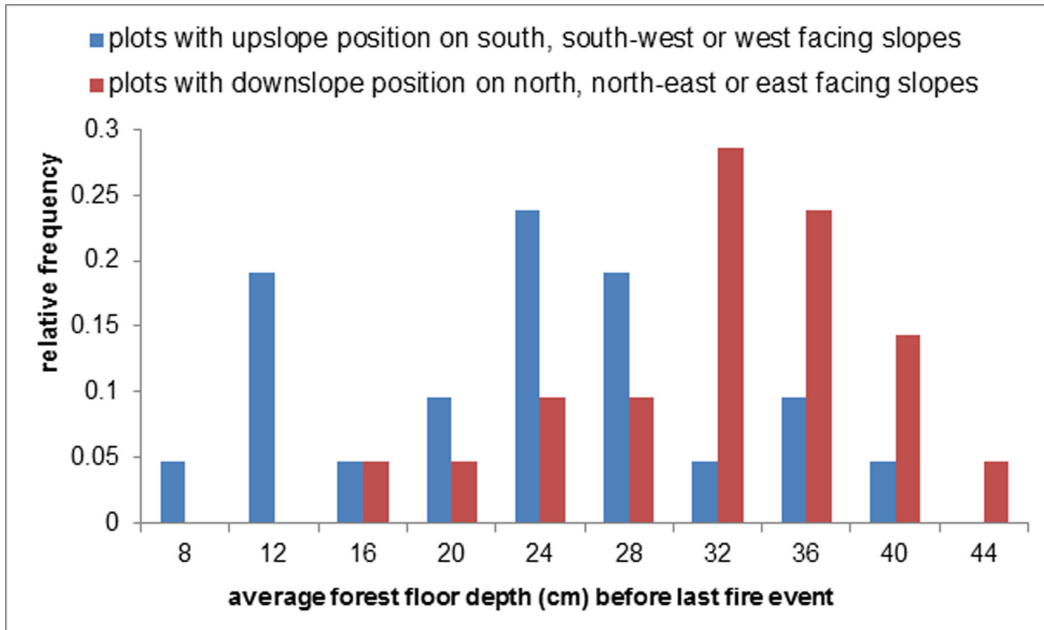


Figure 4-3. Frequency distribution of forest floor depth before fire (cm) for 44 plots with opposite topographic features (fire-prone vs. non fire-prone context).

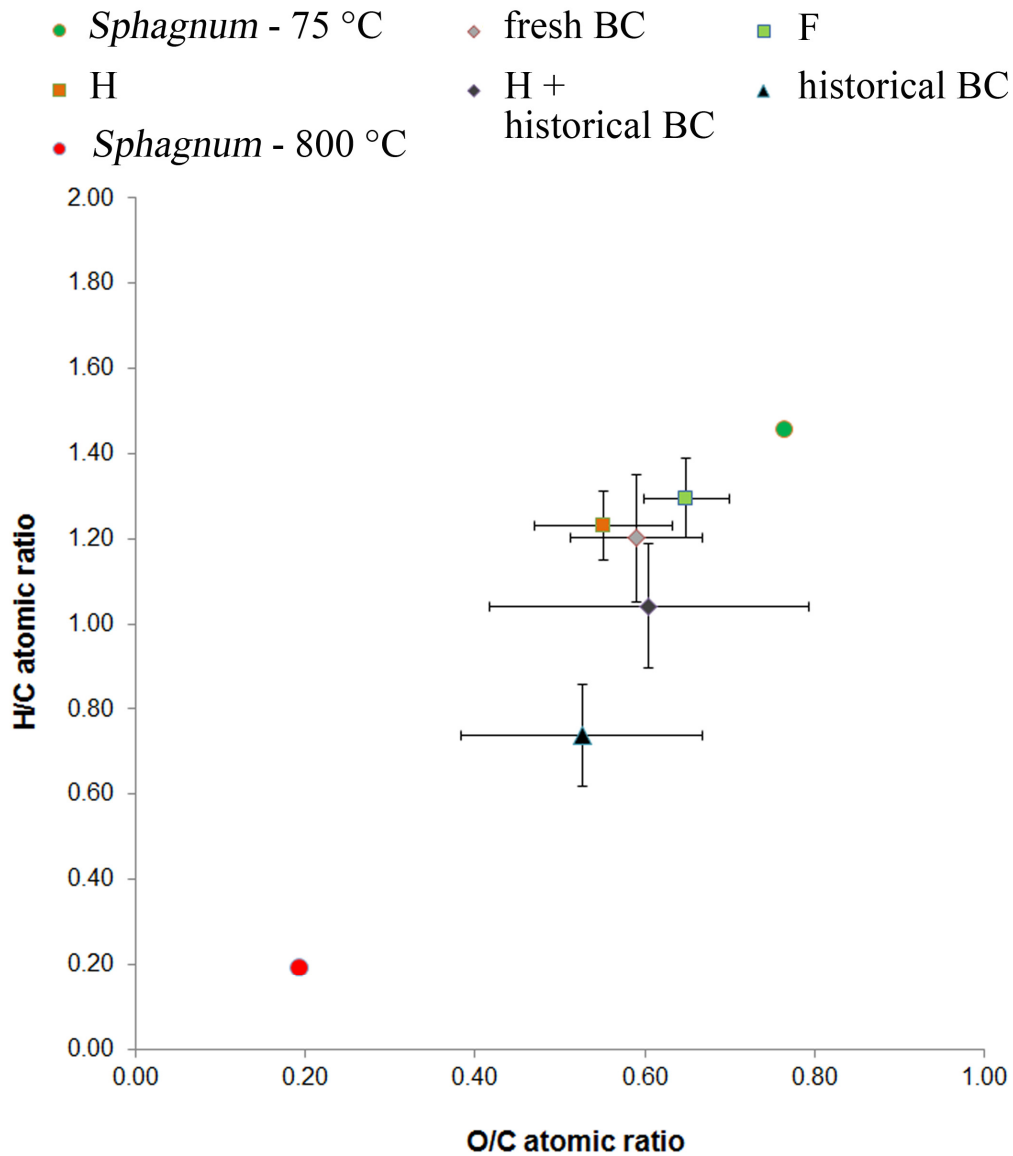


Figure 4-4. van Krevelen diagram showing the different layers of the forest floor. Values are average (\pm SD) for the 23 soil profiles of the corresponding layer. For comparison, values for *Sphagnum* samples heated at 75 °C for 24 hours and at 800 °C for 30 minutes as well as for the BC used for the calibration of the molecular models (class 5 fresh BC and lab BC 15 for MMM-1 and MMM-2 respectively) are plotted.

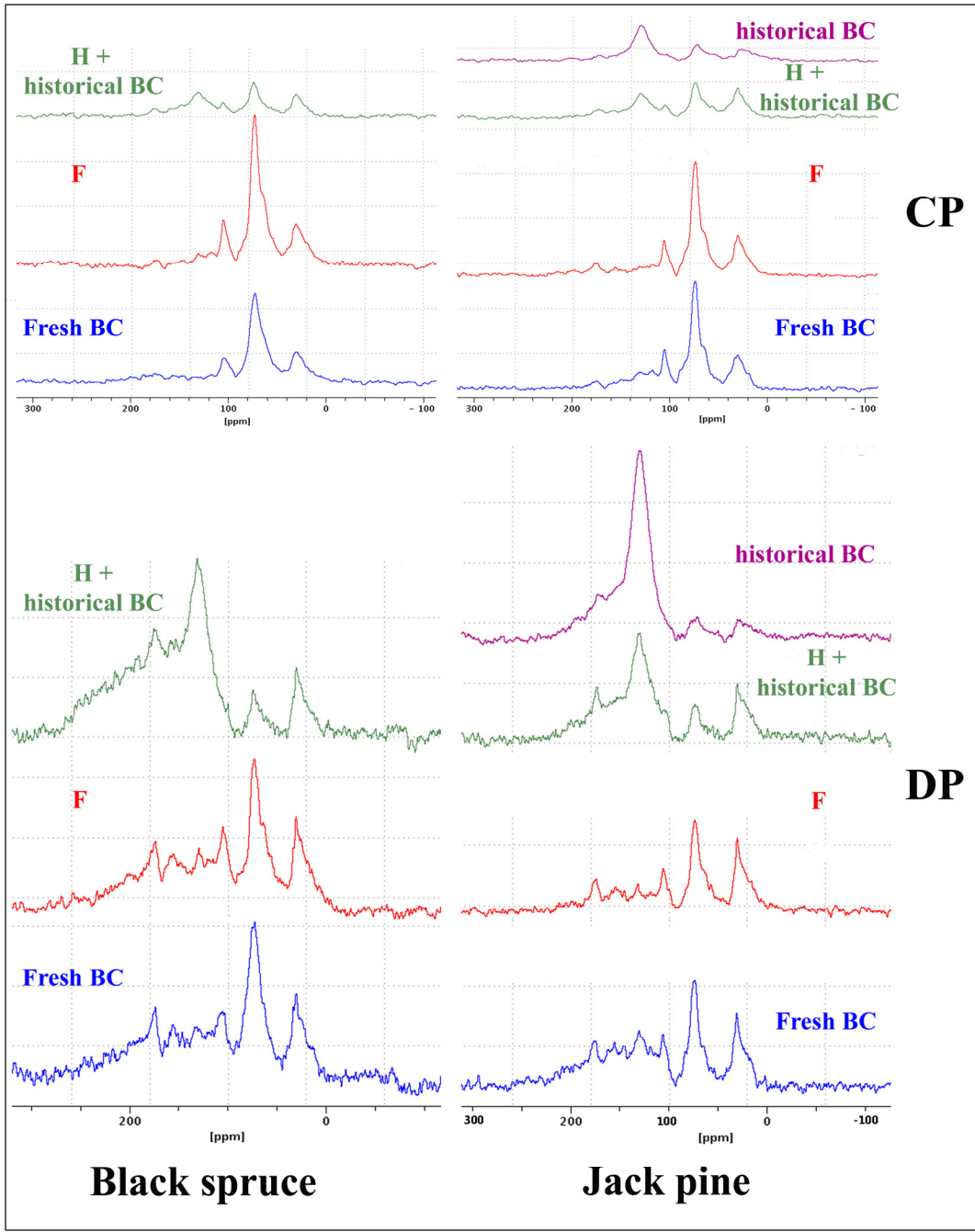


Figure 4-5. ¹³C NMR CPMAS (top) and DPMAS (bottom) spectra of the different forest floor layers (fresh BC, F, H + historical BC, historical BC) developed under black spruce and jack pine.

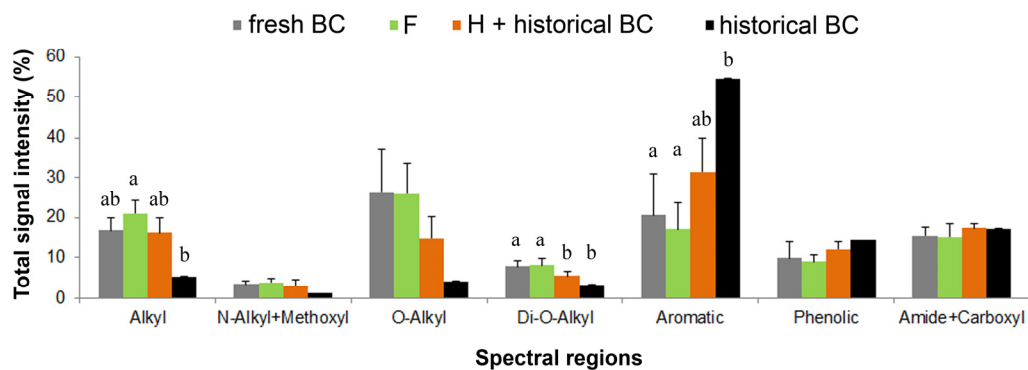


Figure 4-6. Distribution of the total signal intensity (%) between the 7 spectral regions (obtained from the DP NMR experiment) for the different organic horizons. Values are mean (\pm SD). For each spectral region, means with a different letter are significantly different from one another (with Bonferroni adjustment).

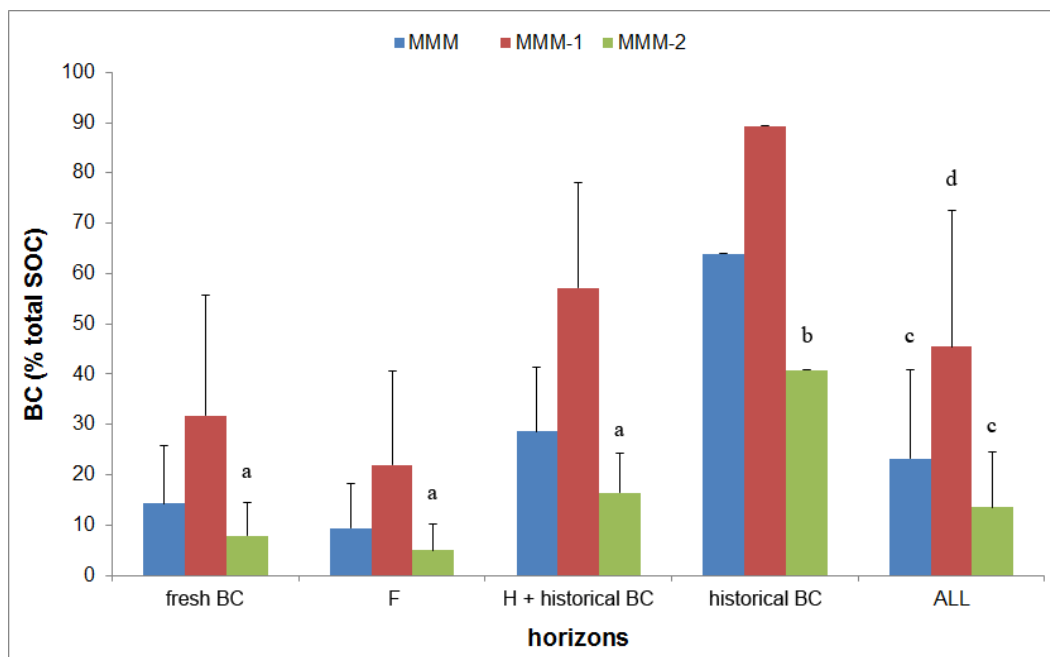


Figure 4-7. BC (% total SOC) estimated by the 3 different versions of the molecular mixing model (MMM) and the data from the DP spectra in the various organic horizons (n = 15). MMM is the default model, while MMM-1 estimates the proportion of slightly condensed BC and MMM-2 estimates the proportion of highly condensed BC. Values are mean (\pm SD). Different letters for the various horizons (a, b) or models (c, d) indicate means that are significantly different from one another (with Bonferroni adjustment).

List of references

- ASTM (2007), D1762-84 Standard test method for chemical analysis of wood charcoal, *American Society for Testing and Materials International*, West Conshohocken, PA, doi:10.1520/D1762-84R07.
- Axelson, D. E. (2012), *Solid State Nuclear Magnetic Resonance. A Practical Introduction*, 1st ed., MRi_Consulting, Lexington, KY.
- Baldock, J. A., C. A. Masiello, Y. G elinas, and J. I. Hedges (2004), Cycling and composition of organic matter in terrestrial and marine ecosystems, *Mar. Chem.*, **92**(1), 39-64, doi:10.1016/j.marchem.2004.06.016.
- Baldock, J. A. and R. J. Smernik (2002), Chemical composition and bioavailability of thermally altered *Pinus resinosa* (Red pine) wood, *Org. Geochem.*, **33**(9), 1093-1109, doi:10.1016/S0146-6380(02)00062-1.
- B elanger, N. and B. D. Pinno (2008), Carbon sequestration, vegetation dynamics and soil development in the Boreal Transition ecoregion of Saskatchewan during the Holocene, *Catena*, **74**(1), 65-72, doi:10.1016/j.catena.2008.03.005.
- B elanger, N., B. C ot e, J. Fyles, F. Courchesne, and W. Hendershot (2004), Forest regrowth as the controlling factor of soil nutrient availability 75 years after fire in a deciduous forest of Southern Quebec, *Plant Soil*, **262**(1-2), 363-272, doi:10.1023/B:PLSO.0000037054.21561.85.
- Bergeron, Y., S. Gauthier, M. D. Flannigan, and V. Kafka (2004), Fire regimes at the transition between mixedwood and coniferous boreal forest in northwestern Quebec, *Ecology*, **85**(7), 1916-1932, doi:10.1890/02-0716.
- Boiffin, J. and A. D. Munson (2013), Three large fire years threaten resilience of closed crown black spruce forests in eastern Canada, *Ecosphere*, **4**(5):56, doi:10.1890/ES13-00038.1.

- Bond-Lamberty, B., S. D. Peckham, D. E. Ahl, and S. T. Gower (2007), Fire as the dominant driver of central Canadian boreal forest carbon balance, *Nature*, **450**(7166), 89-92, doi:10.1038/nature06272.
- Bornemann, L. C., G. Welp, S. Brodowski, A. Rodionov, and W. Amelung (2008), Rapid assessment of black carbon in soil organic matter using mid-infrared spectroscopy, *Org. Geochem.*, **39**(11), 1537-1544, doi:10.1016/j.orggeochem.2008.07.012.
- Brodowski, S., A. Rodionov, L. Haumaier, B. Glaser, and W. Amelung (2005), Revised black carbon assessment using benzene polycarboxylic acids, *Org. Geochem.*, **36**(9), 1299-1310, doi:10.1016/j.orggeochem.2005.03.011.
- Carrier, A. (1996), Contribution de l'imagerie satellitaire NOAA à la cartographie des grands feux de forêt du Québec boréal : 1972 à 1994, M.S. thesis, Université du Québec à Chicoutimi, Chicoutimi, Quebec, Canada.
- Chabot, M. et al. (2009), Le feu en milieu forestier, in *Manuel De Foresterie*, edited by R. Doucet and M. Côté, pp. 1037-1090, Éditions MultiMondes, Québec, Quebec, Canada.
- Cory, D. G. and W. M. Ritchey (1988), Suppression of signals from the probe in Bloch decay spectra, *J. Magn. Reson.*, **80**(1), 128-132, doi:10.1016/0022-2364(88)90064-9.
- Cyr, D., S. Gauthier, and Y. Bergeron (2007), Scale-dependent determinants of heterogeneity in fire frequency in a coniferous boreal forest of eastern Canada, *Landscape Ecol.*, **22**(9), 1325-1339, doi:10.1007/s10980-007-9109-3.
- Czimczik, C. I., C. M. Preston, M. W. I. Schmidt, and E. Schulze (2003), How surface fire in Siberian Scots pine forests affects soil organic carbon in the forest floor: Stocks, molecular structure, and conversion to black carbon (charcoal), *Global Biogeochem. Cycles*, **17**(1), doi:10.1029/2002GB001956.

- Czimeczik, C. I., M. W. I. Schmidt, and E. Schulze (2005), Effects of increasing fire frequency on black carbon and organic matter in Podzols of Siberian Scots pine forests, *Eur. J. Soil Sci.*, **56**(3), 417-428, doi:10.1111/j.1365-2389.2004.00665.x.
- Earl, W. L. and D. L. VanderHart (1982), Measurement of ^{13}C chemical shifts in solids, *J. Magn. Reson.*, **48**(1), 35-54, doi:10.1016/0022-2364(82)90236-0.
- Flannigan, M. D., K. A. Logan, B. D. Amiro, W. R. Skinner, and B. J. Stocks (2005), Future area burned in Canada, *Clim. Change*, **72**(1), 1-16, doi:10.1007/s10584-005-5935-y.
- Freitas, J. C. C., T. J. Bonagamba, and F. G. Emmerich (1999), ^{13}C high-resolution solid-state NMR study of peat carbonization, *Energy Fuels*, **13**(1), 53-59, doi:10.1021/ef980075c.
- González-Pérez, J. A., F. J. González-Vila, G. Almendros, and H. Knicker (2004), The effect of fire on soil organic matter - a review, *Environ. Int.*, **30**(6), 855-870, doi:10.1016/j.envint.2004.02.003.
- Guggenberger, G., A. Rodionov, O. Shibistova, M. Grabe, O. A. Kasansky, H. Fuchs, N. Mikheyeva, G. Zrazhevskaya, and H. Flessa (2008), Storage and mobility of black carbon in permafrost soils of the forest tundra ecotone in Northern Siberia, *Global Change Biol.*, **14**(6), 1367-1381, doi:10.1111/j.1365-2486.2008.01568.x.
- Hammes, K. et al. (2007), Comparison of quantification methods to measure fire-derived (black/elemental) carbon in soils and sediments using reference materials from soil, water, sediment and the atmosphere, *Global Biogeochem. Cycles*, **21**, 2-18, doi:10.1029/2006GB002914.
- Harden, J. W., S. E. Trumbore, B. J. Stocks, A. Hirsch, S. T. Gower, K. P. O'Neill, and E. S. Kasischke (2000), The role of fire in the boreal carbon budget, *Global Change Biol.*, **6**(S1), 174-184, doi:10.1046/j.1365-2486.2000.06019.x.

- Hatten, J. A. and D. Zabowski (2009), Changes in soil organic matter pools and carbon mineralization as influenced by fire severity, *Soil Sci. Soc. Am. J.*, **73**(1), 262-273, doi:10.2136/sssaj2007.0304.
- Hollingsworth, T. N., E. A. G. Schuur, F. S. Chapin III, and M. D. Walker (2008), Plant community composition as a predictor of regional soil carbon storage in Alaskan boreal black spruce ecosystems, *Ecosystems*, **11**(4), 629-642, doi:10.1007/s10021-008-9147-y.
- Inari, G. N., S. Mounquengui, S. Dumarçay, M. Pétrissans, and P. Gérardin (2007), Evidence of char formation during wood heat treatment by mild pyrolysis, *Polym. Degrad. Stab.*, **92**(6), 997-1002, doi:10.1016/j.polymdegradstab.2007.03.003.
- Janik, L. J., J. O. Skjemstad, K. D. Shepherd, and L. R. Spouncer (2007), The prediction of soil carbon fractions using mid-infrared-partial least square analysis, *Aust. J. Soil Res.*, **45**(2), 73-81, doi:10.1071/SR06083.
- Kane, E. S., W. C. Hockaday, M. R. Turetsky, C. A. Masiello, D. W. Valentine, B. Finney, and J. A. Baldock (2010), Topographic controls on black carbon accumulation in Alaskan black spruce forest soils: implications for organic matter dynamics, *Biogeochemistry*, **100**(1-3), 39-56, doi:10.1007/s10533-009-9403-z.
- Kane, E. S., E. S. Kasischke, D. W. Valentine, M. R. Turetsky, and A. D. McGuire (2007), Topographic influences on wildfire consumption of soil organic carbon in interior Alaska: Implications for black carbon accumulation, *J. Geophys. Res.*, **112**, doi:10.1029/2007JG000458.
- Kasischke, E. S., M. R. Turetsky, R. D. Ottmar, N. H. F. French, E. E. Hoy, and E. S. Kane (2008), Evaluation of the composite burn index for assessing fire severity in Alaskan black spruce forests, *Int. J. Wildland Fire*, **17**(4), 515-526, doi:10.1071/wf08002.

- Kasischke, E. S. et al. (2010), Alaska's changing fire regime – Implications for the vulnerability of its boreal forests, *Can. J. For. Res.*, **40**(7), 1313-1324, doi:10.1139/X10-098.
- Kasischke, E. (2000), Boreal ecosystems in the global carbon cycle, in *Fire, Climate Change, and Carbon Cycling in the Boreal Forest*, vol. 138, edited by E. S. Kasischke and B. J. Stocks, pp. 19-30, Springer-Verlag, New-York, NY.
- Kasischke, E., K. P. O'Neill, N. H. F. French, and L. L. Bourgeau-Chavez (2000), Controls on patterns of biomass burning in alaskan boreal forests, in *Fire, Climate Change, and Carbon Cycling in the Boreal Forest*, vol. 138, edited by E. S. Kasischke and B. J. Stocks, pp. 173-196, Springer-Verlag, New-York, NY.
- Keiluweit, M., P. S. Nico, M. G. Johnson, and M. Kleber (2010), Dynamic molecular structure of plant biomass-derived black carbon (biochar), *Environ. Sci. Technol.*, **44**(4), 1247-1253, doi:10.1021/es9031419.
- Kinney, T. J., C. A. Masiello, B. Dugan, W. C. Hockaday, M. R. Dean, K. Zygourakis, and R. T. Barnes (2012), Hydrologic properties of biochars produced at different temperatures, *Biomass Bioenerg.*, **41**(0), 34-43, doi:10.1016/j.biombioe.2012.01.033.
- Knicker, H., G. Almendros, J. A. González-Pérez, F. J. González-Vila, and O. Polvillo (2006), Characteristic alterations of quantity and quality of soil organic matter caused by forest fires in continental Mediterranean ecosystems: a solid-state ^{13}C NMR study, *Eur. J. Soil Sci.*, **57**(4), 558-569, doi:10.1111/j.1365-2389.2006.00814.x.
- Kögel-Knabner, I. (1997), ^{13}C and ^{15}N NMR spectroscopy as a tool in soil organic matter studies, *Geoderma*, **80**(3), 243-270, doi:10.1016/S0016-7061(97)00055-4.
- Kögel-Knabner, I., J. W. de Leeuw, and P. G. Hatcher (1992), Nature and distribution of alkyl carbon in forest soil profiles: implications for the origin and humification of aliphatic biomacromolecules, *Sci. Total Environ.*, **117-118**(0), 175-185, doi:10.1016/0048-9697(92)90085-7.

- Kuhlbusch, T. A. J. and P. J. Crutzen (1995), Toward a global estimate of black carbon in residues of vegetation fires representing a sink of atmospheric CO₂ and a source of O₂, *Global Biogeochem. Cycles*, **9**, 491-501, doi:10.1029/95GB02742.
- Kurth, V. J., M. D. MacKenzie, and T. H. DeLuca (2006), Estimating charcoal content in forest mineral soils, *Geoderma*, **137**(1-2), 135-139, doi:10.1016/j.geoderma.2006.08.003.
- Lefort, P., A. Leduc, S. Gauthier, and Y. Bergeron (2004), Recent fire regime (1945-1998) in the boreal forest of western Quebec, *Ecoscience*, **11**(4), 433-445.
- Lehmann, J. and S. Joseph (2009), Biochar for environmental management - An introduction, in *Biochar for Environmental Management: Science and Technology*, 1st edn., edited by J. Lehmann and S. Joseph, pp. 1-12, Earthscan Publications Ltd, London, UK.
- Lorenz, K., C. M. Preston, S. Raspe, I. K. Morrison, and K. H. Feger (2000), Litter decomposition and humus characteristics in Canadian and German spruce ecosystems: information from tannin analysis and ¹³C CPMAS NMR, *Soil Biol. Biochem.*, **32**(6), 779-792, doi:10.1016/S0038-0717(99)00201-1.
- Masiello, C. A. (2004), New directions in black carbon organic geochemistry, *Mar. Chem.*, **92**(1-4), 201-213, doi:10.1016/j.marchem.2004.06.043.
- Melkior, T., S. Jacob, G. Gerbaud, S. Hediger, L. Le Pape, L. Bonnefois, and M. Bardet (2012), NMR analysis of the transformation of wood constituents by torrefaction, *Fuel*, **92**(1), 271-280, doi:10.1016/j.fuel.2011.06.042.
- Miyaniishi, K. (2001), Duff consumption, in *Forest Fires: Behavior & Ecological Effects*, edited by E. A. Johnson and K. Miyaniishi, pp. 437-475, Academic Press, San Diego, CA.

- Nalder, I. A. and R. W. Wein (1999), Long-term forest floor carbon dynamics after fire in upland boreal forests of western Canada, *Global Biogeochem. Cycles*, **13**(4), 951-968, doi:10.1029/1999GB900056.
- Neff, J. C., J. W. Harden, and G. Gleixner (2005), Fire effects on soil organic matter content, composition, and nutrients in boreal interior Alaska, *Can. J. For. Res.*, **35**, 2178-2187, doi:10.1139/X05-154.
- Peersen, O. B., X. L. Wu, I. Kustanovich, and S. O. Smith (1993), Variable-amplitude cross-polarization MAS NMR, *J. Magn. Reson. Ser. A*, **104**(3), 334-339, doi:10.1006/jmra.1993.1231.
- Preston, C. M., J. S. Bhatti, L. Flanagan, and C. E. Norris (2006), Stocks, chemistry, and sensitivity to climate change of dead organic matter along the Canadian boreal forest transect case study, *Clim. Change*, **74**(1), 223-251, doi:10.1007/s10584-006-0466-8.
- Preston, C. M. and M. W. I. Schmidt (2006), Black (pyrogenic) carbon in boreal forests: a synthesis of current knowledge and uncertainties, *Biogeosciences*, **3**(1), 397-420, doi:10.5194/bg-3-397-2006.
- Robitaille, A. and J. Saucier (1998), *Paysages Régionaux Du Québec Méridional*, Les Publications du Québec, Sainte-Foy, Québec, Canada.
- Ryan, K. C. (2002), Dynamic interactions between forest structure and fire behavior in boreal ecosystems, *Silva Fenn.*, **36**(1), 13-39.
- Saucier, J., P. Grondin, A. Robitaille, and J. Bergeron (2001), *Zones De Végétation Et Les Domaines Bioclimatiques Du Québec*, 3^e ed., Ministère des Ressources naturelles, Québec, Québec, Canada.
- Schmidt, M. W. I. and A. G. Noack (2000), Black carbon in soils and sediments: Analysis, distribution, implications, and current challenges, *Global Biogeochem. Cycles*, **14**(3), 777-793, doi:10.1029/1999GB001208.

- Shvidenko, A. Z. and S. Nilsson (2000), Fire and the carbon budget of russian forests, in *Fire, Climate Change, and Carbon Cycling in the Boreal Forest*, vol. 138, edited by E. S. Kasischke and B. J. Stocks, pp. 289-311, Springer-Verlag, New-York, NY.
- Simard, M., N. Lecomte, Y. Bergeron, P. Y. Bernier, and D. Paré (2007), Forest productivity decline caused by successional paludification of boreal soils, *Ecol. Appl.*, **17**(6), 1619-1637, doi:10.1890/06-1795.1.
- Smernik, R. J., J. A. Baldock, J. M. Oades, and A. K. Whittaker (2002), Determination of $T_{1\rho}^H$ relaxation rates in charred and uncharred wood and consequences for NMR quantitation, *Solid State Nucl. Magn. Reson.*, **22**(1), 50-70, doi:10.1006/snmr.2002.0064.
- Smernik, R. J. and J. M. Oades (2000a), The use of spin counting for determining quantitation in solid state ^{13}C NMR spectra of natural organic matter: 1. Model systems and the effects of paramagnetic impurities, *Geoderma*, **96**(1-2), 101-129, doi:10.1016/S0016-7061(00)00006-9.
- Smernik, R. J. and J. M. Oades (2000b), The use of spin counting for determining quantitation in solid state ^{13}C NMR spectra of natural organic matter: 2. HF-treated soil fractions, *Geoderma*, **96**(3), 159-171, doi:10.1016/S0016-7061(00)00007-0.
- Soil Classification Working Group (Eds.) (1998), *The Canadian System of Soil Classification - Third Edition*, vol. 1646 (Revised), NRC Research Press, Ottawa, Ontario, Canada.
- Turetsky, M. R., E. S. Kane, J. W. Harden, R. D. Ottmar, K. L. Manies, E. E. Hoy, and E. S. Kasischke (2011), Recent acceleration of biomass burning and carbon losses in Alaskan forests and peatlands, *Nature Geosci.*, **4**(1), 27-31, doi:10.1038/ngeo1027.
- van Bellen, S., M. Garneau, and Y. Bergeron (2010), Impact of climate change on forest fire severity and consequences for carbon stocks in boreal forest stands of Quebec, Canada: A synthesis, *Fire Ecology*, **6**(3), 16-44, doi:10.4996/fireecology.0603016.

- Viscarra Rossel, R. A., D. J. J. Walvoort, A. B. McBratney, L. J. Janik, and J. O. Skjemstad (2006), Visible, near infrared, mid infrared or combined diffuse reflectance spectroscopy for simultaneous assessment of various soil properties, *Geoderma*, **131**(1), 59-75, doi:10.1016/j.geoderma.2005.03.007.
- Wikberg, H. and S. L. Maunu (2004), Characterisation of thermally modified hard- and softwoods by ¹³C CPMAS NMR, *Carbohydr. Polym.*, **58**(4), 461-466, doi:10.1016/j.carbpol.2004.08.008.
- Zackrisson, O., M. Nilsson, and D. A. Wardle (1996), Key ecological function of charcoal from wildfire in the boreal forest, *Oikos*, **77**(1), 10-19.

Chapter 5. Black carbon stocks and storage mechanisms in podzolic soils of fire-affected Quebec black spruce forests

A version of this chapter has been submitted for publication to Geoderma.

5.1. Introduction

Boreal ecosystems cover 24×10^7 km², which corresponds to 17% of the Earth land surface. Boreal forest soils cover a smaller area of the boreal biome than permafrost soils but represent an almost equally large carbon pool estimated at 227×10^{12} kg (Kasischke, 2000). Boreal forests are exposed to recurring wildfires, which act as a major driver of the carbon cycle (Bond-Lamberty et al., 2007; Hatten and Zabowski, 2009). Fires result in the production of significant amounts of CO₂, and temporarily turn these forests into carbon sources (e.g., Harden et al., 2000; Neff et al., 2005). The often large boreal fires occurring in North America are thought to be relatively homogeneous with stand-replacing, high intensity crown fires. However, in Quebec boreal black spruce forests, combustion of the thick forest floor layers by wildfire is often incomplete and black carbon (BC) residues are a major by-product. Forest floor BC stocks may increase over successive fires as long as fire severity is not high enough that fire consumes all organic layers. Some BC may also be translocated and accumulate into mineral soils, although the extent of this process is currently poorly understood and likely varies from one ecosystem to another (Czimczik and Masiello, 2007).

According to some studies, BC is an important component of the stable soil carbon pool (Kasischke and Stocks, 2000; González-Pérez et al., 2004; Preston

and Schmidt, 2006), although several studies caution against assuming that all BC is recalcitrant (Harden et al., 2000; Hockaday et al., 2006; Czimeczik and Masiello, 2007; Hammes et al., 2008; Preston, 2009). Significant BC accumulation has been observed in some Canadian boreal forest soils (e.g., Harden et al., 2000; Bélanger and Pinno, 2008) but the amount accumulated appears to greatly vary among ecosystems (Czimeczik et al., 2005; Preston and Schmidt, 2006; Kane et al., 2007; Kane et al., 2010). To introduce BC into carbon models, and to test its potential as a passive carbon pool under future climate change conditions, there is an urgent need for a better understanding of its storage mechanisms, as well as for better estimates of overall soil stocks.

Podzolic soils occur in various regions of the world but boreal podzols generally contain more iron and aluminum oxides, as well as less soil organic carbon (SOC) in their podzolic B horizons than non-boreal podzols (Buurman and Jongmans, 2005). Two main SOC reservoirs are present in boreal podzols: first, the humified forest floor, dominated by mor humus, which often shows a clear/abrupt boundary with the mineral soil; and second the subsoil B horizons, which accumulate illuvial SOC (Sanborn et al., 2011). In poorly drained podzolic B horizons and ortstein, SOC appears to accumulate predominantly through mobilization, transport, and subsequent precipitation. However this mechanism may not be as significant in well-drained B horizons, where roots may also represent an important carbon input to the subsoil (Buurman and Jongmans, 2005). Consequently, for our experimental area, we hypothesized that poorly drained and ortstein podzols would store more BC in their podzolic B horizons

than well-drained podzols. Strong correlations between BC and SOC have been observed in different fire-affected ecosystems (e.g., Eckmeier et al., 2010; Cusack et al., 2012). Mineral interactions between oxides and clay minerals have also been shown to play a significant role in SOC stabilization, through the formation of complexes or aggregates, which help protect SOC from mineralization (Wiseman and Püttmann, 2006). The same stabilization mechanisms could apply to BC (Rodionov et al., 2006; Eckmeier et al., 2010; Cusack et al., 2012).

Previous work conducted at the same Quebec black spruce forest sites estimated that total C stocks in forest floors averaged $5.5 (\pm 2.6) \text{ kg C m}^{-2}$, while BC stocks in the same organic horizons ranged from 0.2 to 1.2 kg C m^{-2} (Soucémariadin et al., submitted). Here we focused on mineral soils and investigated their relative importance in terms of total C and BC stocks. There were three specific objectives in this study. We first estimated total BC amounts in various soil profiles. Then we identified the different BC pools in physically fractionated horizons and explored the relationship between pedogenetic processes, more specifically podzolization, and BC storage. Finally, we compared BC stocks in mineral soils to forest floor stocks and investigated the potential influence of environmental conditions on these stocks. To do so, we considered the following permanent environmental features and site characteristics: slope position and aspect, stand type, and climatic conditions. This is the first investigation of BC stocks in complete soil profiles from Canadian black spruce boreal forests.

5.2. Materials and methods

5.2.1. Site characteristics

The province of Quebec is divided into ten bioclimatic domains, characterized by distinct vegetation and climatic conditions (Saucier et al., 2001). The black spruce-feathermoss bioclimatic domain covers a third of the province territory and is divided into the eastern and western subdomains. The west subdomain is characterized by an average precipitation of 850 mm/year in its northern range and 900 mm/year in its southern range, whereas the eastern subdomain receives 1020 mm evenly distributed through the year (Bergeron et al., 2004; Cyr et al., 2007). Mean annual temperature (Carrier, 1996) ranges from $-2\text{ }^{\circ}\text{C}$ in the north to just above $0\text{ }^{\circ}\text{C}$ in the south. The western sector of the domain forms a transition zone between a continental climate in its southern range, and a subpolar continental climate in its northern range, while the eastern subdomain experiences a cooler, more humid maritime climate, at least in its southern range.

Both subdomains are largely dominated by black spruce (*Picea mariana* (Mill.) Britton, Sterns & Poggenb.) with ericaceous shrubs (*Rhododendron groenlandicum* (Oeder) Kron & Judd, *Kalmia angustifolia* L., and *Vaccinium angustifolium* Ait.), feathermoss (*Pleurozium schreberi* (Brid.) Mitt.) and/or *Sphagnum* moss (*Sphagnum* sp.) constituting most part of the understory. Locally lichens (*Cladina rangiferina* (L.) Weber) associated with fire moss (*Ceratodon purpureus* (Hedw.) Brid.) and haircap moss (*Polytrichum* sp.) are present. On drier sites, jack pine (*Pinus banksiana* Lamb.) is often associated to black spruce in mixed stands and becomes dominant on the driest conditions. The majority of

the black spruce-feathermoss domain is covered by humo-ferric and ferro-humic podzols (Soil Classification Working Group, 1998), with a typically thin (< 10 cm) Ae eluviated horizon. Underneath lays a podzolic B horizon, enriched in Fe and Al and more (Bhf) or less (Bf) organic matter. Ortstein humo-ferric/ferro-humic Podzols are found locally. They contain a strongly cemented Bfc or Bhfc horizon, at least 3 cm thick. All of these podzolic soils have developed on glacio-fluvial sediments/till deposits and generally contain a high proportion of coarse fragments (> 2 mm). Their texture is largely dominated by sands, locally enriched with loams. Except for some of the drier sites, organic horizons (L, F, H) are thick, from 10 to more than 120 cm. Veins of clay are occasionally present in the western part of the gradient, because of the proximity to the Clay Belt (Robitaille and Saucier, 1998). There, the proportion of coarse fragments is greatly reduced and drainage may be impaired.

In 2005–2007, high fire activity in Northern Quebec burned 1.2 Mha in the black spruce-feathermoss domain. Large fires occurred even in regions that do not experience fires often, i.e., with long fire cycles. These fires provided us with potential study sites spread over a 600-km gradient, with decreasing fire frequency along a west-east axis. Only those fire sites that were accessible by road and that presented a large enough unsalvaged area were selected, which led to a total of 14 fires, ranging in size from 330 to 56000 ha. Most of the fires occurring during those three years took place at the beginning of the fire season. Over the province of Quebec, fire regime has been regionalized by landscape units of relatively homogeneous environmental conditions, including vegetation,

temperature, and precipitation (Lefort et al., 2004; Chabot et al., 2009). To test for the influence of fire frequency on total C and BC stocks, we divided our study area into five zones of homogeneous fire cycle and similar climatic conditions (Figure 5-1). Each zone included two to four study sites. All sites were outside the permafrost zone and were sampled in summer 2010.

5.2.2. Soil sampling protocol

For each study site, one or two topographic gradients were established inside unsalvaged areas. Two to three 20 m x 20 m plots were positioned on each topographic gradient. Initial survey with a hand auger was conducted to select the plot where podzolization was best expressed, i.e., where an indurated layer was present and/or the podzolic B horizon(s) were the most developed. A total of 23 soil profiles was described and sampled to capture the variability within each of the five zones of homogeneous fire cycle and climatic conditions of the black spruce domain. For each soil profile, drainage was estimated based on the classification of Saucier et al. (1994). In soils with a good drainage, the water table and mottles, are absent from the first meter, and the water in excess drains easily but slowly. In opposition, in imperfectly to poorly drained soils, the water table and/or mottles are present in the first 50 cm and water is in excess all year round. In addition, aspect and slope position (crest; upslope; midslope; downslope; toe; depression) were recorded for each profile.

Soil pits were dug until the parent material (C horizon) was reached except for three profiles where the presence of the water table, rocks or a thick induration

prevented us from achieving that goal. Forest floors usually presented the following profile development (Soucémariadin et al., submitted): a thin, about 2-cm-thick, superficial burnt layer produced by the last fire event referred to as fresh BC hereafter; the partially decomposed litter (F); and the highly humified organic matter (H). The latter was generally associated with a thin BC layer produced by previous fire events (historical BC) and sitting right at the interface with the mineral soil (H + historical BC). Mineral horizons were fully described and sampled for the present study. When possible (horizons at least 3 cm thick and not too many coarse fragments), a core was taken for bulk density determination.

5.2.3. Laboratory analyses

Chemical and physical properties

Bulk density was determined by weighing the collected cores before and after drying at 105 °C, and correcting for the presence of coarse fragments. For the few horizons for which a bulk density sample could not be collected, bulk density was estimated using the model proposed by Périé and Ouimet (2008). The rest of the mineral samples was air-dried and sieved (≤ 2 mm). Texture was determined with the Bouyocos hydrometer method (Kalra and Maynard, 1991). Subsamples were finely ground using an Angstrom ring and puck shatterbox, and carbon, hydrogen, and nitrogen contents were determined by dry combustion using a CE440 Elemental Analyzer (Exeter Analytical, Inc., Chelmsford, MA, USA). The pH of

every mineral horizon was determined with an Ag/AgCl pH electrode in a soil to 0.01 M CaCl₂ solution ratio of 1:2 (Kalra and Maynard, 1991).

The degree of podzolization of each soil profile was determined using the POD index (Schaetzl and Mokma, 1988), which is based on Munsell hue and value differences between the eluviated Ae horizon and the podzolic B horizons. Pyrophosphate-extractable iron (Fe_p) and aluminum (Al_p) contents of the B horizons (n = 48) were determined according to McKeague's (1967) methodology to identify different Great Groups (Soil Classification Working Group, 1998). Ground samples were extracted with a solution of 0.1 M sodium pyrophosphate (30 ml), and Fe and Al concentrations were measured by atomic absorption spectrophotometry (AAS) using a Varian SpectrAA 880 (Varian Inc, Mulgrave, Victoria Australia). Ferro-Humic Podzols are characterized by the presence of a Bhf horizon, at least 10 cm thick with organic C > 5%, and Fe_p+Al_p ≥ 0.6% (0.4% for sands); for Humo-Ferric Podzols, a Bf horizon, possibly combined to a thin Bhf, is at least 10 cm thick with organic C = 0.5–5%, and Fe_p+Al_p ≥ 0.6% (0.4% when soil is sandy).

Soil physical fractionation

A combination of particle-size and density fractionation was applied to a subset of podzolic B horizons (n = 11). The fractionated horizons were separated into three groups: Bhf(c), podzolic Bhf horizons with partial cementation (c); Bf, podzolic B horizons; B/C, transitional (gradual) podzolic B horizons. Several existing procedures (Six et al., 1998; Six et al., 2000; Six et al., 2002) were

combined to generate the following six fractions (Figure 5-2): heavy ($d > 1.85 \text{ g cm}^{-3}$), coarse (250–2000 μm) particulate organic matter (POM); coarse (250–2000 μm) light ($d < 1.85 \text{ g cm}^{-3}$) fraction (LF); fine sand and micro-aggregate protected (53–250 μm) POM; fine (53–250 μm) light ($d < 1.85 \text{ g cm}^{-3}$) fraction; silt (2–53 μm); and clay ($< 2 \mu\text{m}$). Details of the procedure are available on Figure 5-2. All fractions were oven-dried overnight at 40 °C and further weighed to calculate their relative distribution, as well as particle-size distribution among sand ($> 53 \mu\text{m}$), silt (2–53 μm) and clay ($< 2 \mu\text{m}$). We recovered 97 to 99% of the soil samples. We further looked at overall SOC distribution by regrouping the six initial fractions into the three following fractions: unprotected POM (heavy coarse POM + coarse and fine light fractions), protected POM (fine sand and micro-aggregate protected POM) and fine fraction carbon (silt + clay). For BC distribution, the same horizons were used, and fractions were modified as follow: unprotected POM (heavy coarse POM only), protected POM (fine sand and micro-aggregate protected POM) and fine fraction carbon (silt only).

5.2.4. *BC quantitation*

Sampling, preparation, bulk density, elemental analyses and BC quantification for the organic horizons were conducted as previously described (Soucémariadin et al., submitted). All mineral samples ($< 2 \text{ mm}$; $n = 107$) were analyzed for BC content using the Kurth-MacKenzie-DeLuca (KMD) digestion technique developed by Kurth et al. (2006) to estimate charcoal content of forest mineral soils. Finely ground sub-samples were exposed to this weak $\text{H}_2\text{O}_2\text{--HNO}_3$

digestion and further analyzed for total C by dry combustion, with the assumption that the carbon left over after the digestion corresponds to BC. To evaluate BC recovery using the KMD method, we selected a C horizon sample originally free of BC and added BC at seven different concentrations (0, 0.05, 0.1, 0.5, 1.0, 2.0 and 5.0% (w/w) soil/BC) before performing the digestion. To investigate further the potential association of BC with other soil moieties (SOC, mineral fractions, iron and aluminum oxides) we applied the KMD digestion to the mineral fractions (coarse sand, fine sand/microaggregates, silt) obtained from the fractionation scheme. The clay quantities yielded by the fractionation were too small and this fraction was not submitted to the digestion.

The amount of coarse BC particles (> 2 mm) was estimated during the sieving step. We applied a BC-C content of 55% (Bélanger and Pinno, 2008) and used that value to estimate the BC stocks (g C m^{-2}) originating from the coarse BC particles in each horizon.

5.2.5. Data analysis

A 1-way ANOVA, or Mood's median test and a Kruskal-Wallis when needed, were used to analyze differences among horizons in various properties. The same analysis was used to evaluate the effect of the 5 zones of homogeneous fire cycle and climatic conditions on bulk mineral soil characteristics. Differences linked to stand types and aspect were tested using an unequal variance Welch t-test. Relationships between variables were estimated using Pearson correlation, and Spearman rank correlation when needed. All comparisons and ANOVA were

considered significant at an alpha value of 0.05. For the significant ANOVAs, the alpha was adjusted with a Bonferroni correction when exploring all possible comparisons. For all the regression analyses, outliers were determined using Cook's distance and subsequently removed from the analysis. All the statistical analyses were performed with SAS 9.2 (SAS Institute Inc., Cary, North Carolina).

5.3. Results

5.3.1. Calibration of the KMD digestion

Results from the calibration step showed that the KMD digestion was a conservative method that tended to underestimate BC contents, especially when aromaticity was low (Figure 5-3). When this digestion was performed on a slightly aromatic BC produced from *Pleurozium* at 250 °C, the percentage recovery was only 20%; it reached 70% when using more aromatic BC produced from *Pleurozium* and black spruce needles at 425 °C. The KMD digestion yielded the most accurate estimate of BC content for the very aromatic BC that was produced from needles exposed to 600 °C. Results from the calibration were used to estimate the range of BC present in each mineral horizon, namely by using two correction factors for the KMD results: a multiplicative factor of 1.43 for the lower limit, which would correspond to moderately condensed BC, and a corrective factor of 5 for the highest plausible BC content, which would correspond to slightly condensed BC.

5.3.2. Bulk mineral soil

Soil characteristics and environmental factors

Texture of all soils was clearly dominated by sand, which averaged 70% (Table 5-1). Coarse fragments (> 2 mm) averaged 8% ($\pm 11\%$). Carbon and N contents in all mineral horizons were quite low, with the exception of podzolic B horizons. Soil profiles under jack pine were significantly sandier ($80 \pm 14\%$) than those found under black spruce ($67 \pm 18\%$). There was a minor effect of vegetation on pH, with a slightly lower pH under black spruce (4.4 ± 0.7) than under jack pine (4.7 ± 0.8). Silt content further varied among climatic zones. Soils from West Baie-James contained significantly more silt ($31 \pm 14\%$) than those in the North-Shore zone ($14 \pm 11\%$), which corresponded to parent material differences since West Baie-James is in closer proximity to the Clay belt. Finally, the POD Index was significantly higher for the profiles located in the Saguenay-Ashuapmushuan zone (28.6 ± 10.3) than in Chibougamau and East Baie-James (6.7 ± 4.4 and 7.5 ± 7.3 respectively; Table 5-2a). On the other hand, no significant relationship was observed between slope position and aspect and any of the measured soil characteristics.

Total SOC and BC contents

We observed a trend of increasing BC stocks in mineral soil of profiles with decreasing drainage (Figure 5-4). In the profiles with good drainage, the mean BC stocks were 1.7 times smaller than in profiles with imperfect drainage and 2.8

times smaller than in profiles with poor drainage. However the variability within the same drainage class was important.

We looked at relationships between bulk density, SOC, BC, and pH in bulk horizons (n = 107). Both SOC and BC contents were significantly and negatively correlated to bulk density and pH (Table 5-3a), indicating that both were higher in more acidic and lower density horizons. In particular, pH was significantly lower in Ae and podzolic horizons than in B/C and C horizons. Total SOC content was better explained by bulk density than pH, as opposed to BC content. Total SOC content explained 51.2% of the variation in BC content (Table 5-3a), and the two were positively correlated. The BC/SOC ratio was significantly different from the ratio of black carbon:organic carbon (BC/OC; where $OC = SOC - BC$), which measures the relative abundance of BC. This suggests that BC significantly contributes to SOC. When looking at variations of these ratios between horizons, the biggest difference between BC/SOC and BC/OC occurred in Ae and C horizons (Table 5-1).

Relationships between SOC and BC stocks and other soil characteristics were considered, including $Fe_p + Al_p$ maximal content, cumulative thickness of the podzolic horizons, thickness of the H (+ historical BC) horizon, as well as total forest floor thickness (Table 5-3b). Mineral C stocks were significantly and positively correlated to mineral BC stocks, cumulative thickness of podzolic horizons, and thickness of H + historical BC horizon. Mineral BC stocks were only correlated to the latter. Interestingly, there was no relationship between total C or BC contents in the mineral soils and total forest floor thickness. Furthermore,

there was no significant difference among the five zones or the two forest types in terms of total mineral soil C and BC stocks (Table 5-2b).

Total C content of the podzolic B horizons was strongly correlated to Fe_p+Al_p content, more so than to Fe_p content or Al_p content separately (Table 5-3c). For these horizons, correlation between total C and BC contents was also strong, and was comparable to the one observed for the entire soil profiles (Table 5-3a). The BC content was also significantly correlated to sesquioxides although the coefficients of determination were not as high as with SOC. Another interesting difference was the higher correlation of BC content with Fe_p content than with Al_p content or with Fe_p+Al_p content (Table 5-3c). The 48 podzolic horizons were further separated into three groups: Bf, Bfc and B/C to look at these relationships more closely. Sesquioxide contents were significantly higher in the Bfc horizons than in the Bf or B/C horizons (Table 5-1). The B/C horizons presented a different pattern from the two podzolic horizons; their black C content was not correlated to sesquioxides or total C content, which may be related to the very low concentrations in these horizons ($0.03 \pm 0.02\%$ for black C). Despite the low sesquioxide contents ($Fe_p+Al_p = 2.68 \pm 1.37\%$), SOC content was strongly correlated to Fe_p+Al_p and slightly less to Al_p (Table 5-3c); there was no significant relationship with Fe_p content. Relationships in the Bf and Bfc horizons were quite similar, with a correlation between Fe_p+Al_p and SOC that was less important than in the B/C horizons (Table 5-3c). In Bf horizons, despite a low Fe_p content ($1.10 \pm 0.98\%$), Fe_p explained an important portion of the variation in BC and SOC contents. In Bf and Bfc horizons, correlations between Fe_p content and

SOC or BC contents were very similar. SOC content explained a large portion of the variation in BC content in Bfc horizons, and slightly less in Bf (Table 5-3c). It is interesting to note that while Fe_p+Al_p content in Bfc explained 64.7% of the variation in SOC content (67% in Bf horizons), Fe_p content only explained 47.2% of the variation (against 64.3% in Bf horizons); Fe_p content represented 34% of total sesquioxide content in Bfc vs. only 23% in Bf (Table 5-1). This was further related to differences in BC/SOC ratios in these two horizons: ratios were lower in Bfc than in Bf horizons (Table 5-1).

Sand content was always negatively related to SOC and BC contents whereas the fine fraction had a positive relationship with them. But the strength of the correlations varied among horizons (Table 5-3d). The Ae horizons contained significantly less sand ($63.9 \pm 16.7\%$) and more silt ($30.7 \pm 14.2\%$) than podzolic Bfc horizons (sand = $79.4 \pm 11.8\%$; silt = $15.3 \pm 9.1\%$). Total C content was significantly higher in Bf ($1.60 \pm 0.87\%$) and Bfc ($3.76 \pm 2.52\%$) than in other horizons, and Bfc bulk density was significantly lower ($0.92 \pm 0.28 \text{ g cm}^{-3}$) than the Ae ($1.29 \pm 0.16 \text{ g cm}^{-3}$) or C horizons ($1.40 \pm 0.19 \text{ g cm}^{-3}$). Bfc horizons contained significantly more BC ($0.13 \pm 0.11\%$) than C horizons ($0.01 \pm 0.01\%$). All horizons had clay contents in the same range (5.1–6.6%, Table 5-1), but in Ae horizons, SOC and BC contents were only correlated to clay content (Table 5-3d). SOC content explained a fair portion of the variation in BC content, in the same order of what occurred in the Bf horizons. In the latter, SOC content was not significantly correlated to any of the particle size fraction. On the other hand, variations in BC were partially explained by sand and silt contents (Table 5-3d).

In Bfc horizons, SOC and BC contents were not significantly correlated to any of the particle size fractions. In B/C horizons, BC content was correlated to the fine fraction. SOC content was only correlated to clay content but in the same order as BC content (Table 5-3d). In C horizons, SOC content explained only a small portion of the variation in BC content, the weakest relationship between these two in all the soil profile. SOC content was correlated to the fine fraction; mainly silt but also clay (Table 5-3d). BC content had a similar pattern, but the strength of the relationship was much weaker: with the fine fraction, the coefficient of determination was only 13%. It is important to notice that BC contents in the C horizons were very low ($0.01 \pm 0.01\%$), and very close to detection limits for the elemental analyzer. Therefore these results should be considered with caution.

To facilitate comparison of BC stocks among profiles, we summed BC stocks in the top 30 cm. For the 23 soil profiles considered, 83% of total BC stock was on average present in these first 30 cm. However in three profiles, the first 30 cm represented only half of the total stocks, demonstrating the importance of sampling at greater depth. Finally, for a few horizons, coarse BC particles (> 2 mm) significantly contributed to total BC stocks of the horizon in a few (< 5) instances (e.g., the highest value was 22% of the total BC stocks for profile 11; Table 5-A.1).

There was no relationship between SOC stocks in the mineral and in the organic parts of the profile. Total forest floor thickness was positively correlated to total SOC stocks (Table 5-3b), but there was no significant relationship

between total SOC stocks and total depth of the soil profile. There was no relationship between forest floor BC stocks and BC stocks in the mineral soils.

5.3.3. *Fractionated podzolic B horizons*

There were significant differences in C content among horizons and fractions (Figure 5-5). In Bhf(c) horizons, carbon in unprotected POM was significantly higher than protected carbon in POM and fine fraction, representing almost 50% of the carbon. In Bf horizons, carbon in the unprotected POM was significantly lower than the protected carbon in POM, and lower (but not significantly) than protected carbon in fine fraction. In B/C horizons, there was significantly less carbon in unprotected POM than in protected POM; and there was significantly less carbon in protected POM than in fine fraction. Proportion of carbon in protected POM was not significantly different among the three horizons (26.9–36.7%). Proportion of carbon in unprotected POM was significantly higher in Bhf(c) than in B/C horizons, and inversely proportion of carbon in fine fraction was significantly higher in B/C than in Bhf(c) horizons. Except for one sample (which always appeared as an outlier in terms of SOC content, light fraction (w/w) = 18% total horizon), the light fraction in these podzolic horizons represented less than 5% of the total weight of the horizon. However the contribution of the light fractions to the unprotected POM was significantly higher in B/C horizons ($64 \pm 11\%$) than in the two podzolic horizons ($36 \pm 17\%$ in Bhf(c); $34 \pm 31\%$ in Bf).

There was no significant difference in BC content among horizons and fractions (Figure 5-6) but some trends were apparent. The contribution of BC to SOC in the coarse unprotected POM was more important in B/C than in Bhf(c) which in turn, was higher than in Bf. In B/C horizons, the contribution of BC to SOC in silt and protected POM were very similar and lower than in unprotected POM. Inversely in Bf and Bhf(c), BC/SOC was highest in the silt fraction. In Bf horizons, BC/SOC in protected POM was higher than in coarse unprotected POM, whereas the two were similar in Bhf(c) horizons.

When looking at the bulk (non-fractionated) horizons, the contribution of BC to SOC was higher in Bf than in Bhf(c), which in turn, was higher than in B/C horizons. In the latter, variability in BC/SOC ratio was very important.

5.4. Discussion

5.4.1. SOC and BC storage in the mineral soil

SOC and BC stocks

In this study, mineral SOC stocks averaged $5.6 (\pm 3.6) \text{ kg C m}^{-2}$, while mineral BC stocks were $0.25 (\pm 0.16) \text{ kg C m}^{-2}$ (Table 5-4). Stocks are in the same range as those reported for the surface mineral soil (A + 5 first cm of B horizons) of Alaskan black spruce forests (Kane et al., 2010), with $3.3 (\pm 0.5)$ and $5.5 (\pm 0.9) \text{ kg C m}^{-2}$ in the mineral horizons of south facing and north facing slopes, respectively. In the same study, BC stocks of $0.26 (\pm 0.001)$ and $0.14 (\pm 0.04) \text{ kg BC m}^{-2}$ were observed for the same south and north facing forests. In podzols from Siberian Scots pine forests, Czimczik et al. (2005) reported 0–1 m

mineral SOC stocks of 1.3–1.8 kg C m⁻². Their corresponding BC stocks were even lower at 0.16–0.25 g BC m⁻². The difference in stocks could originate from smaller BC production in these forests: Siberian Scots pine forests are a less productive ecosystem than the black spruce forests we studied. Guggenberger et al. (2008) obtained BC stocks of 0.16–1.40 kg BPCA-C m⁻² in permafrost soils of Northern Siberian forest tundra. Variability in BC stocks in that study is much more important than the one we observed and may be explained by differences in fire behavior between Quebec boreal black spruce forests and Northern Siberian forest tundra. In temperate and tropical ecosystems with soils similar to the Humo-Ferric Podzols of our study, Eckmeier et al. (2010) reported much greater mineral SOC stocks of 24.1–33.9 kg C m⁻², and mineral BC stocks of 0.63–1.72 kg BPCA-C m⁻² in three Cryptopodzols of Swiss chestnuts (*Castanea sativa*) forests. In Hawaiian volcanic soils, under C3 trees and C4 grasses, Cusack et al. (2012) observed mineral (0–30 cm) SOC stocks of 2–30 kg m⁻², and BC stocks of 0.3–5 kg m⁻². The differences in stocks observed with these two studies are likely the consequence of greater BC production: the Swiss Cryptopodzols are affected by frequent fires; and in the Hawaiian sites, there has been an increasing fire frequency and intensity (associated with sugarcane burning) since 1930 following changes in land use.

Mechanisms of SOC and BC stabilization

While it clearly dominated the entire soil profiles, the sand fraction only contributed to about one third of total SOC storage in podzolic horizons. Similar

SOC distribution patterns have been observed in podzolic horizons from Prince Edward Island (Sorge et al., 1994). In this study, the authors reported that the SOM in sand fraction had a different composition than in fine fraction, and revealed the significant role of intra-molecular SOM bonds in the stabilization of OM in Bf horizons. Correlation analyses support the hypothesis of SOC and BC stabilization in organo-metallic or organo-mineral complexes (Tables 5-5c, 5-5d). The contribution of each protection mechanism varies among horizons, suggesting that different storage mechanisms apply to them. Because of their high SOC content ($6.79 \pm 2.28\%$) and a relatively high contribution of BC to SOC ($3.9 \pm 1.3\%$), Bhf horizons stored the greatest amount of BC, followed by Bf horizons (Table 5-1). In Bfc horizons, organo-metallic complexes appear to be preponderant, and results from the fractionation confirmed the limited organo-mineral associations in these horizons. SOC and BC are mostly in the unprotected POM or in organo-metallic complexes. In Bf horizons, SOC is in organo-metallic complexes in the protected POM, or associated with the fine fraction. BC is stabilized in organo-mineral complexes (dominated by silt) and in organo-metallic complexes in the protected POM (and/or maybe only with iron oxides or Fe^{3+}). In B/C horizons more SOC is associated with the fine fraction (organo-mineral complexes dominated by clay) but there is still some SOC stabilization in organo-metallic complexes in the protected POM. BC does not appear to be associated to organo-metallic complexes – or only rarely – but is found in the coarse unprotected POM and in organo-mineral complexes with the fine fraction. BC and SOC contents have the weakest relationship in these deep horizons. In podzolic B

horizons at least, BC seemed to associate preferentially with iron rather than with aluminum. Eckmeier et al. (2010) reported the opposite trend in Cryptopodzols. This could be linked to differences in podzolization processes between our humo-ferric podzols and their Cryptopodzols (related to e.g., vegetation, climate, parent material, etc.).

These mechanisms of BC stabilization may be essential to BC accumulation. Kane et al. (2010) observed some differences in the composition of the BC present in organic and mineral horizons; in surficial organic horizons, BC was more condensed, hence more resistant to degradation, whereas BC present in mineral horizons was less aromatic, hence less resistant to degradation. The authors suggested that BC stabilization in the mineral horizons could be the result of physical protection by association with fine particles or iron and aluminum oxides.

5.4.2. BC stocks: mineral soil vs. forest floor

Drainage appears as the most important environmental factor driving C storage. In our study sites, changes in drainage related to topographic positions have been showed to influence C stocks in the organic layers through OM accumulation (Boiffin and Munson, 2013; Soucémariadin et al., submitted). In the mineral soil, the influence of drainage on C stocks seems less important (but this could be due to our limited sample size – $n = 23$; Figure 5-4). Drainage has previously been determined as a key control of soil C storage in the Canadian

boreal (e.g., Harden et al., 1997; Preston et al., 2006). Here we demonstrate that drainage is a determinant environmental factor in BC storage.

Total SOC stocks averaged $11.1 (\pm 4.9) \text{ kg C m}^{-2}$ (Table 5-4), which is comparable to the average value reported for Canadian Humo-Ferric Podzols (12.8 kg C m^{-2} ; (Sanborn et al., 2011). Total BC stocks averaged $0.85 (\pm 0.39) \text{ kg C m}^{-2}$ (Table 5-4). Average SOC stocks were evenly distributed between organic and mineral horizons. On the other hand, BC stocks were significantly greater in the forest floor, which contained on average 70% of total BC stocks.

One possible reason for the discrepancy between mineral and organic BC stocks is that the deep organic horizon (H + historical BC) is impermeable compared to the upper F layer. This could impede BC transfer to the mineral soil. The positive correlations between mineral BC and SOC stocks and the H + historical BC thickness ($R^2 \approx 25\%$) emphasize the importance of this organic layer for these stocks.

In organic horizons of Alaskan black spruce forests, Kane et al. (2010) reported C stocks that were in the same range as ours with $4.1 (\pm 0.6) \text{ kg C m}^{-2}$ in south facing forests, and $5.7 (\pm 0.6) \text{ kg C m}^{-2}$ in north facing forests; SOC in the forest floor therefore represented 51–56% of total stocks. But as opposed to our study, BC stocks in surface mineral soils (A + 5 first cm of B horizons) were higher ($0.34 \pm 0.09 \text{ kg C m}^{-2}$) than in organic soils ($0.17 \pm 0.07 \text{ kg C m}^{-2}$). This could be due to the presence of the H + historical BC layer at our sites (absent in the Alaskan sites). In Podzols of Siberian Scots pine forests, Czimeczik et al. (2005) made very different observations. In sites affected by low and medium fire

frequency, SOC stocks in the forest floor were comparable to stocks in the mineral soil (depth > 1 m). However in sites affected by high fire frequency, 96% of total SOC was found in mineral soils. For all sites, 99% of total BC stocks was contained in forest floors. Guggenberger et al. (2008) reported total (forest floor + up to 0.9 m depth) SOC stocks of 5–95 kg C m⁻² and total BC stocks of 0.02–3.44 kg BPCA-C m⁻². Contribution of the organic/moss layer to these total stocks was minimal (4.9–11.9%). The authors explained the larger BC stocks in some part of the catchment as the result of either larger input or longer BC residence time. Combustion of BC by subsequent fires is probably less likely in such ecosystems.

With the anticipated increasing fire severity linked to climate change (e.g., Flannigan et al., 2009; Wotton et al., 2010), BC stocks in Quebec boreal black spruce forests could be in jeopardy. More severe fires will consume a greater amount of forest floor and even possibly will oxidize part of the H + historical BC layer, thereby threatening as much as 70% of the overall BC pool. It seems unlikely that all BC produced during these severe fires will stay on site, since wind and leaching will certainly displace part of it. The remaining BC could be transferred to the mineral soil or could be stabilized within the surficial organic layer as new moss grows and forest floor develops on top of it during post-fire recovery. Czimczik and Masiello (2007) concluded that BC accumulation requires a high enough fire frequency; however, Czimczik et al (2005) showed that extremely high fire frequency greatly reduced the organic horizons (hence, SOC

and BC stocks), and mineral BC stocks if greater, were not significantly different from BC stocks in mineral soils exposed to medium and low fire frequency.

5.5. Conclusions

This study provides much needed estimates about BC pools in Quebec boreal black spruce forests. Although the majority of BC stocks was found in forest floors, mineral horizons stored a non-negligible reservoir that amounted to 12–46% of the total stocks. Podzolic Bhf and Bf horizons contained most of the mineral BC stocks. Physical fractionation shed some light on possible BC storage mechanisms in these soils. Association with organo-metallic complexes appeared as the dominant mechanism at least for podzolic horizons. Further fractionation studies with measurement of pyrophosphate-extractable iron and aluminum in fractions would help to more fully elucidate BC stabilization processes. Finally, carbon dating in the mineral soil, as well as in the historical BC layer could give further insight on the importance of past fire severity for total BC stocks.

Tables and Figures

Table 5-1. Mean physical and chemical properties of different mineral horizons, including particle size distribution, BC, SOC, pyrophosphate-extracted Al, Fe and total sesquioxides contents. Standard deviations from the means are presented in parentheses (n = 14–29). na: not available.

	Ae		Bf		Bfc		B/C^a		C	
sand (%)	63.9	(16.7)	69.9	(18.7)	79.4	(11.8)	66.6	(16.6)	71.2	(19.7)
silt (%)	30.7	(14.2)	23.5	(14.5)	15.3	(9.1)	27.1	(13.6)	24.1	(17.1)
clay (%)	5.5	(4.2)	6.6	(6.1)	5.3	(3.3)	6.3	(5.1)	4.7	(5.2)
BC (%)	0.08	(0.07)	0.06	(0.05)	0.13	(0.11)	0.03	(0.02)	0.01	(0.01)
SOC (%)	0.53	(0.34)	1.55	(0.87)	3.95	(2.55)	0.48	(0.32)	0.17	(0.16)
BC (% SOC)	14.8	(5.9)	4.1	(2.3)	2.9	(1.8)	5.9	(4.7)	5.6	(11.2)
BC (% OC) ^b	17.9	(8.3)	4.3	(2.5)	3.1	(1.9)	6.6	(5.5)	8.6	(24.7)
Al _p (%)	na		3.65	(2.33)	7.34	(3.27)	1.97	(0.63)	na	
Fe _p (%)	na		1.1	(0.98)	3.77	(2.41)	0.71	(1.09)	na	
Fe _p +Al _p (%)	na		4.74	(3.07)	11.11	(5.03)	2.68	(1.37)	na	

^a: only the sample presenting bright colors (chroma \geq /4) were analyzed for

sesquioxides; ^b Relative abundance of BC: OC was calculated by subtracting BC from SOC (Cusack *et al.* 2012)

Table 5-2. Influence of zones of homogeneous fire cycle and climatic conditions and stand types (black spruce- vs. jack pine-dominated stands) on (a) particle size distribution and pH of mineral horizons, and on POD Index and on (b) SOC and BC stocks of soil profiles. Standard deviations from the means are presented in parentheses (horizons: n = 15–76; profiles: n = 4–5). nd: not determined.

(a)	sand (%)		silt (%)		clay (%)		pH		POD Index	
	black spruce	67	(18)	27	(15)	6	(5)	4.4	(0.7)	nd
jack pine	80	(14)	17	(13)	4	(2)	4.6	(0.8)	nd	
North-Shore	81	(12)	14	(11)	5	(2)	4.3	(0.8)	20.5 (10.9)	
Saguenay & Ashuapmushuan	73	(12)	22	(11)	5	(3)	4.2	(0.7)	28.6 (10.3)	
West Baie-James	62	(18)	31	(14)	8	(7)	4.6	(0.7)	23.8 (22.2)	
Chibougamau	73	(21)	22	(18)	5	(5)	4.5	(0.6)	6.7 (4.4)	
East Baie-James	69	(15)	27	(14)	4	(1)	4.6	(0.8)	7.5 (7.3)	

(b)	mineral stocks (kg C m ⁻²)		organic stocks (kg C m ⁻²)		total stocks (kg C m ⁻²)	
	<i>SOC</i>					
all (n = 23)	5.6	(3.6)	5.5	(2.6)	11.1	(4.9)
black spruce	6.2	(4.1)	5.5	(2.3)	11.7	(5.2)
jack pine	4.3	(1.8)	5.5	(3.4)	9.8	(4.1)
North-Shore	9.9	(7.0)	5.1	(2.7)	14.9	(8.3)
Saguenay & Ashuapmushuan	6.1	(2.2)	7.8	(3.3)	14.0	(4.3)
West Baie-James	3.8	(0.7)	4.9	(2.3)	8.7	(2.8)
Chibougamau	4.2	(0.8)	4.6	(2.5)	8.8	(2.7)
East Baie-James	4.5	(1.9)	4.8	(1.5)	9.3	(2.3)
<i>BC</i>						
all (n = 11)	0.24	(0.14)	0.61	(0.31)	0.85	(0.39)
black spruce	0.26	(0.16)	0.71	(0.34)	0.97	(0.44)
jack pine	0.21	(0.10)	0.43	(0.17)	0.64	(0.16)
North-Shore	0.30	(0.29)	0.77	(0.18)	1.06	(0.47)
Saguenay & Ashuapmushuan	0.29	(0.00)	0.42	(0.10)	0.70	(0.09)
West Baie-James	0.17	(0.07)	0.57	(0.57)	0.75	(0.64)
Chibougamau	0.20	na	0.47	na	0.67	na
East Baie-James	0.24	(0.18)	0.71	(0.23)	0.96	(0.34)

Table 5-3. Pearson and non-parametric rank correlation analyses between SOC, BC and various soil parameters for (a) all horizons; (b) soil profiles; (c) podzolic B horizons; (d) individual horizons. Unless otherwise indicated, values are Spearman ρ ; significance is indicated as follows: * $p < 0.05$, ** $p < 0.01$ and *** $p < 0.001$. nd: not determined; NS: not significant.

(a) all horizons (n = 107)					
bulk density					
C content	-0.697***				
BC content	-0.502***	0.715***			
pH	nd	-0.459***	-0.649***		

(b) soil profiles (n = 23)					
mineral SOC stocks					
mineral total BC stocks ^a	0.597**				
Fe _p +Al _p max content	NS	NS			
B horizons thickness	0.580**	NS	nd		
H horizon thickness	0.534**	0.499*	nd	nd	
total forest floor thickness	NS	NS	nd	nd	0.573**

(c) All podzolic B horizons (n = 48)					
Fe _p content					
Al _p content	nd				
Fe _p +Al _p content	nd	nd			
C content	0.866***	0.836***	0.915***		
BC content	0.613***	0.368*	0.495**	0.697***	
Bf horizons (n = 18)					
Fe _p content					
Al _p content	nd				
Fe _p +Al _p content	nd	nd			
C content	0.802***	0.672**	0.818***		
BC content	0.822***	NS	0.474*	0.793***	
Bfc horizons (n = 23)					
Fe _p content					
Al _p content	nd				
Fe _p +Al _p content	nd	nd			
C content	0.687***	0.687***	0.804***		
BC content	0.633**	0.448*	0.606**	0.861***	

B/C horizons (n = 7)

Fe _p content					
Al _p content	nd				
Fe _p +Al _p content	nd	NS			
C content	NS	0.836** ^b	0.929* ^b		
BC content	NS	NS	NS	NS	

(d)

Ae horizons (n = 23)

sand content					
silt content	nd				
clay content	nd	nd			
BC content	NS	NS	0.564**		
C content	NS	NS	0.601**	0.797***	

Bf horizons (n = 17)

sand content					
silt content	nd				
clay content	nd	nd			
BC content	-0.569*	0.478	NS		
C content	NS	NS	NS	0.772**	

Bfc horizons (n = 21)

sand content					
silt content	nd				
clay content	nd	nd			
BC content	NS	NS	NS		
C content	NS	NS	NS	0.866***	

B/C horizons (n = 14)

sand content					
silt content	nd				
clay content	nd	nd			
BC content	-0.676** ^b	0.539* ^b	0.696**		
C content	NS	NS	0.670**	NS	

C horizons (n = 29)

sand content					
silt content	nd				
clay content	nd	nd			
BC content	-0.361	0.376*	0.364		
C content	-0.644**	0.611**	0.429*	0.525**	

^a: includes stocks from fine-earth fraction (≤ 2 mm) and coarse BC particles (> 2 mm); ^b: Pearson correlation

Table 5-4. BC and SOC stocks in organic and mineral horizons, and complete soil profiles.

total stock (kg C m⁻²)		
	BC	(n = 11)^a
organic	0.61	0.31
mineral	0.24	0.14
total	0.85	0.39
	SOC	(n = 23)
organic	5.49	2.61
mineral	5.59	3.63
total	11.08	4.86

^a Only the profiles for which BC content had been estimated in organic horizons were considered here

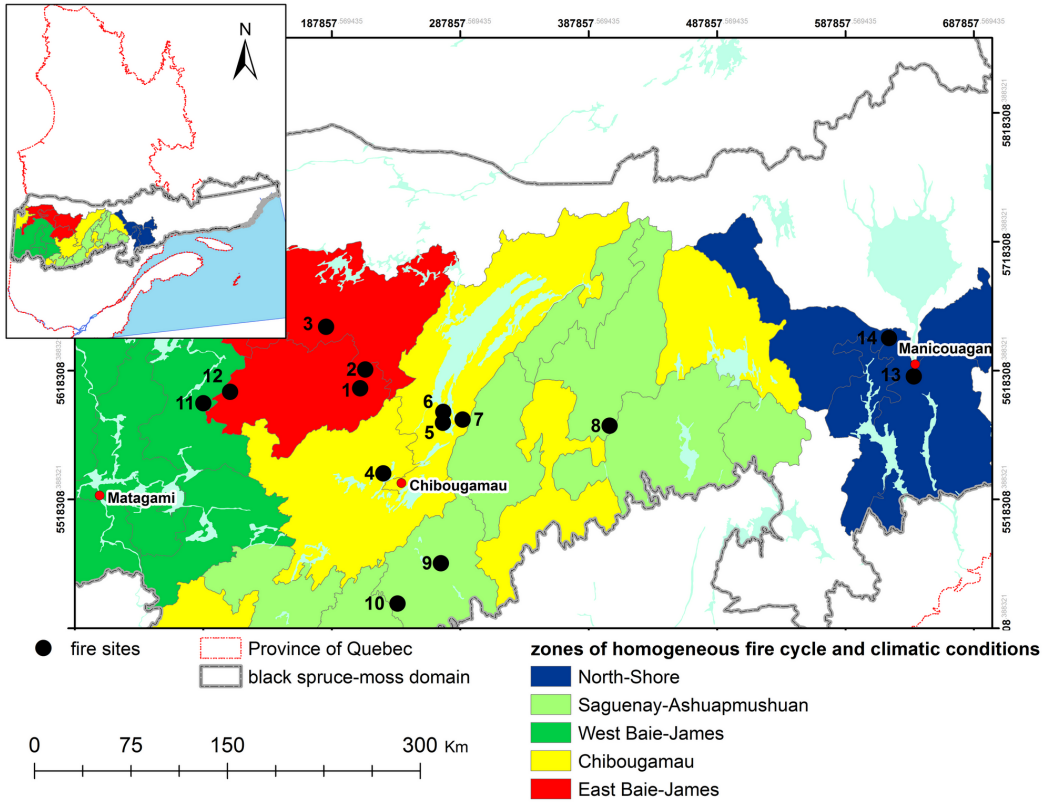


Figure 5-1. The 14 fire sites and their corresponding 5 zones of homogeneous fire cycle and climatic conditions.

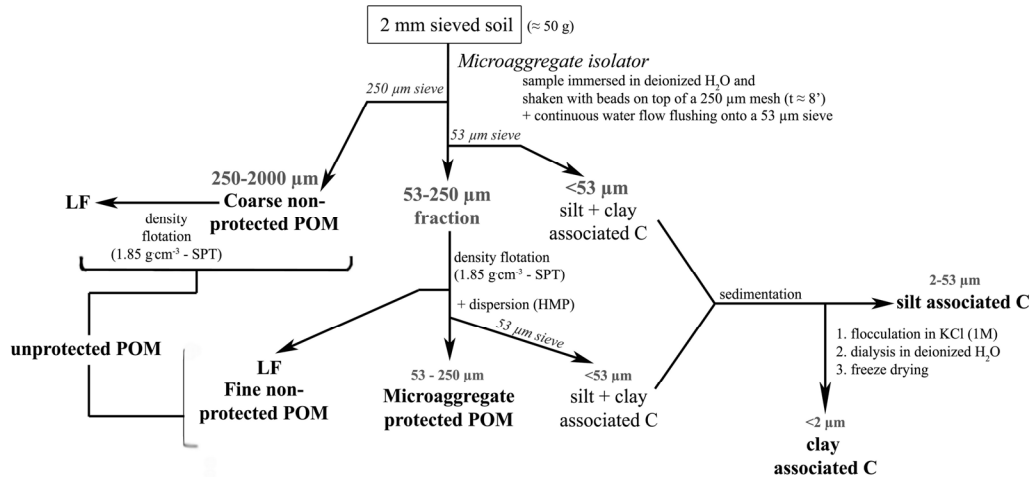


Figure 5-2. Fractionation scheme used to separate the podzolic B horizons into six fractions: coarse (250–2000 μm) particulate organic matter (POM), coarse light fraction (< 1.85 g cm⁻³; 250–2000 μm), fine sand and micro-aggregates POM (53–250 μm), fine light fraction (< 1.85 g cm⁻³; 53–250 μm), silt (2–53 μm) and clay (< 2 μm). SPT: sodium polytungstate; HMP: sodium hexametaphosphate (0.5% solution).

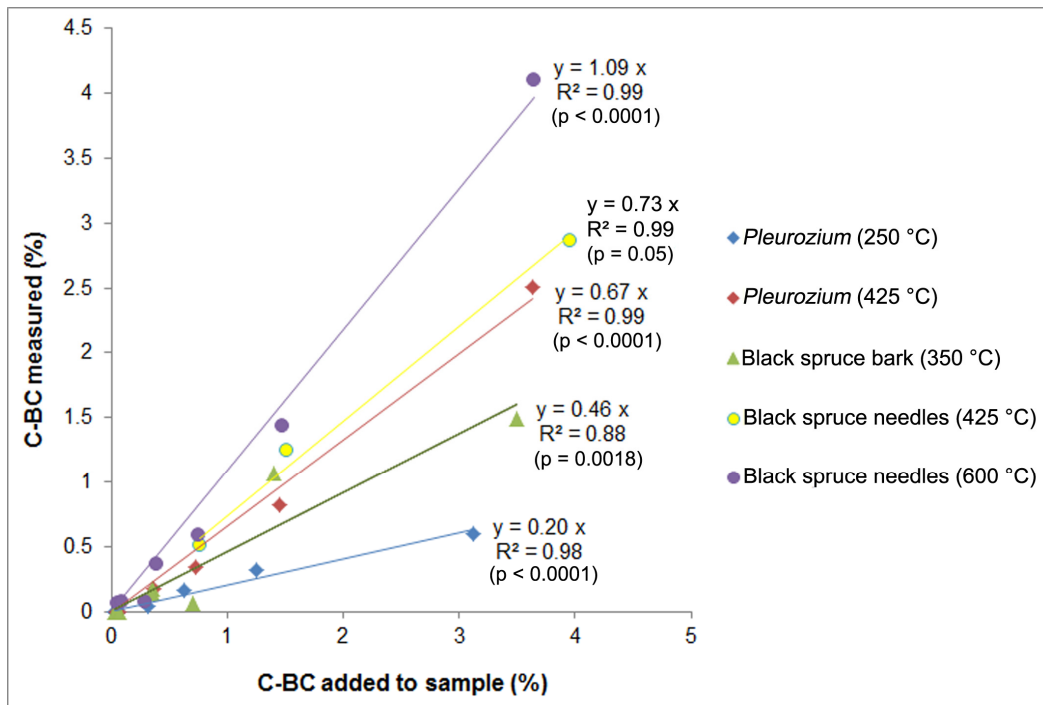


Figure 5-3. Relationship between C-BC added to sample and C-BC measured with the KDM method from BC produced at various temperatures (250–600 °C) from *Pleurozium* and black spruce fuel.

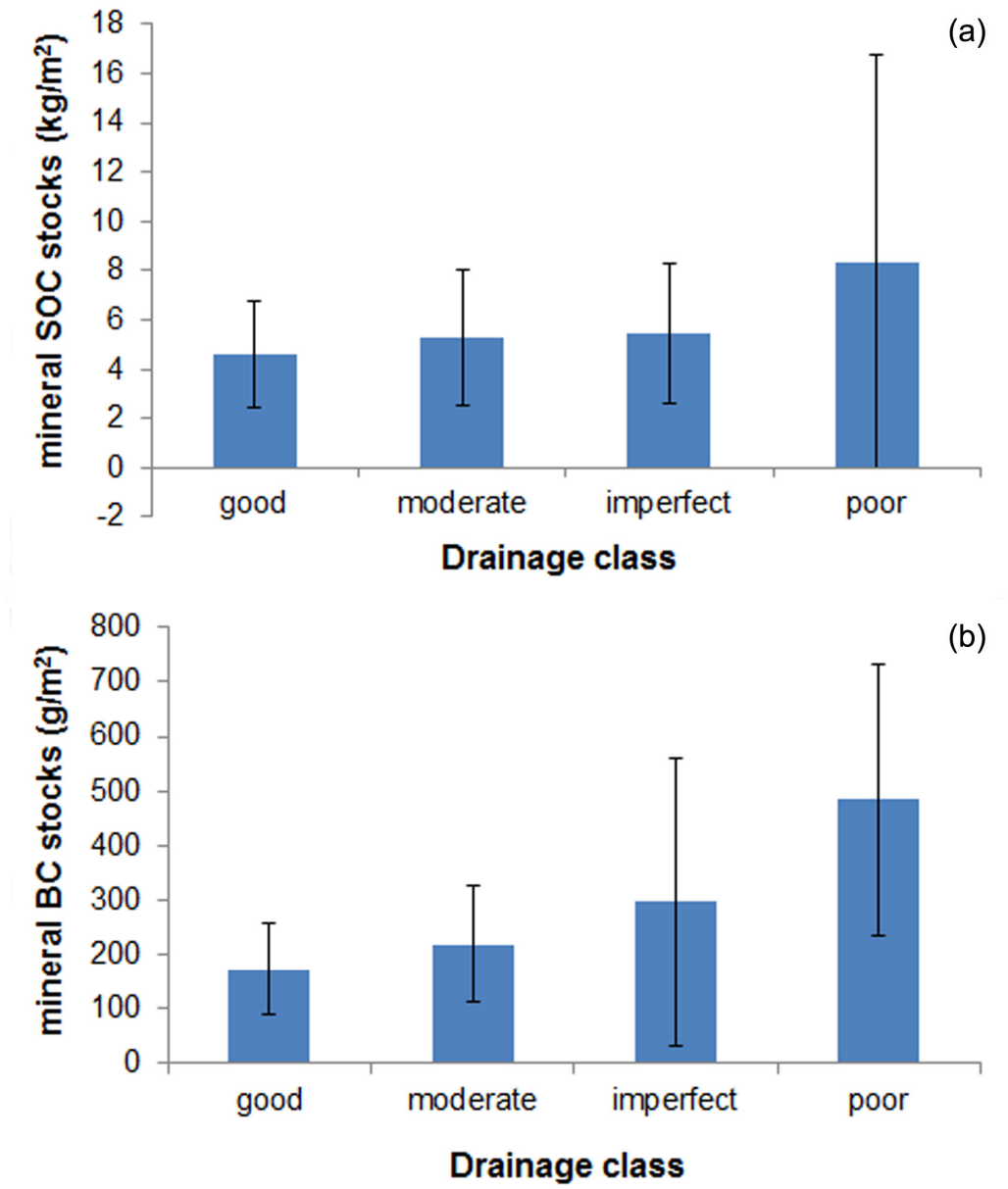


Figure 5-4. Influence of drainage on (a) SOC (kg C/m²) and (b) BC (g C-BC/m²) stocks. Values are mean \pm standard deviation.

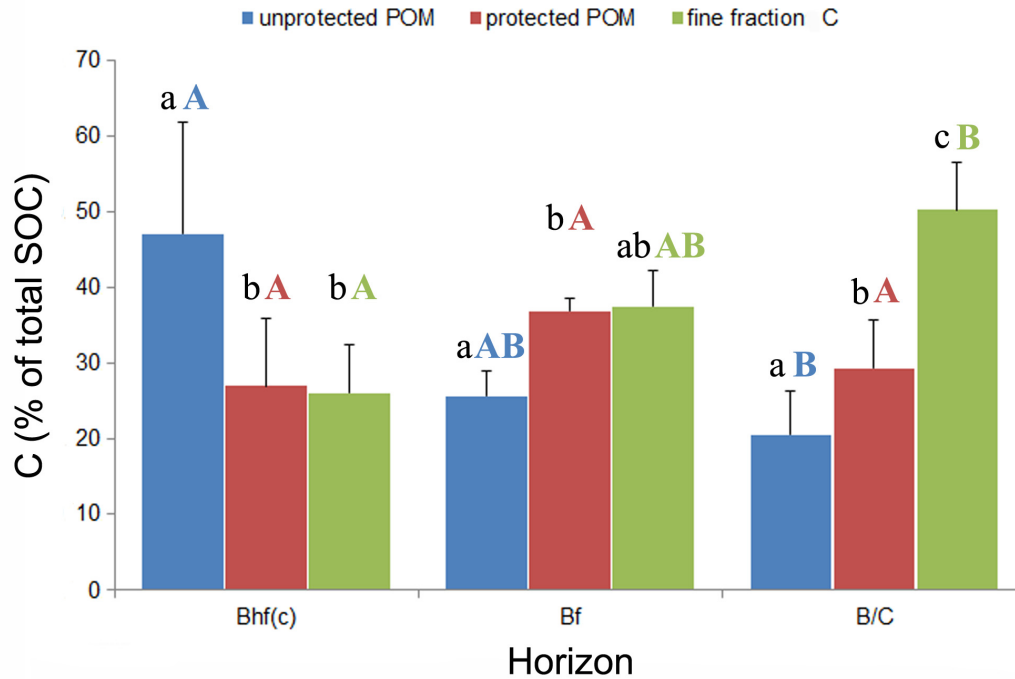


Figure 5-5. Carbon distribution (% of total SOC) in podzolic horizons (n = 11). Three horizons types (Bhf(c), Bf, and B/C) and three following fractions were considered: unprotected POM (coarse POM + light fractions), protected POM (fine sand + micro-aggregates) and fine fraction carbon (silt + clay). Different lower case letters indicate significant differences among fractions for a given horizon; different upper case letters indicate significant differences among horizons for a same fraction.

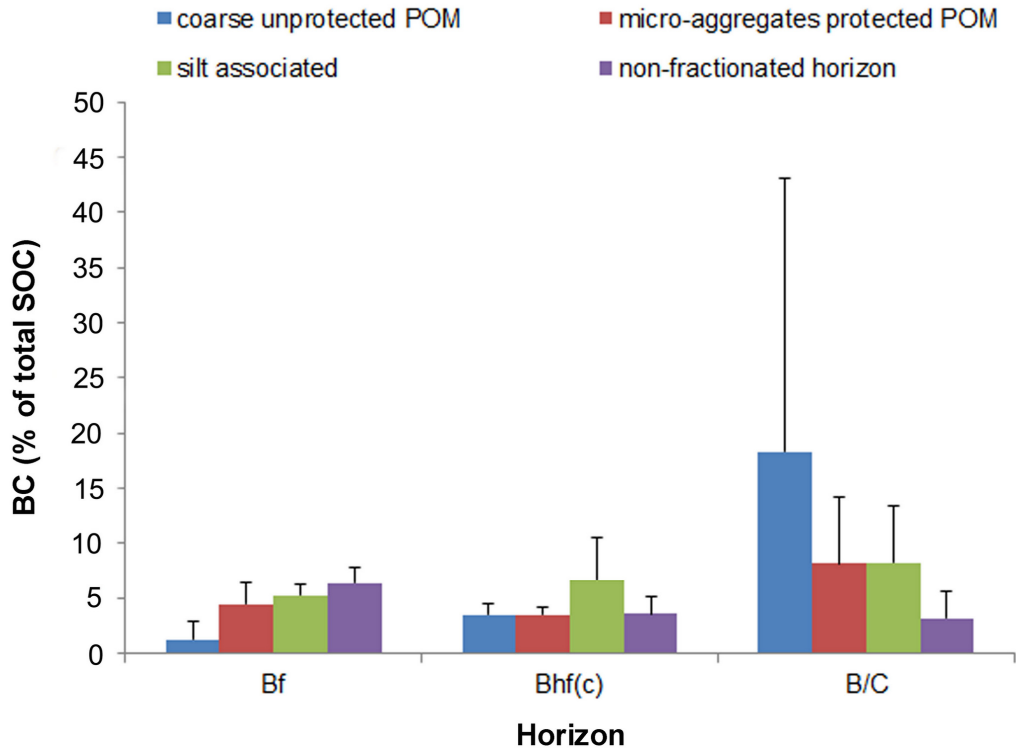


Figure 5-6. Distribution of BC (% of total SOC) in fractionated podzolic horizons (n = 11). For comparison, the non-fractionated horizon is represented.

List of References

- Bélanger, N. and Pinno, B.D., 2008. Carbon sequestration, vegetation dynamics and soil development in the Boreal Transition ecoregion of Saskatchewan during the Holocene. *Catena*, 74:65-72.
- Bergeron, Y., Gauthier, S., Flannigan, M.D. and Kafka, V., 2004. Fire regimes at the transition between mixedwood and coniferous boreal forest in northwestern Quebec. *Ecology*, 85:1916-1932.
- Boiffin, J. and Munson, A.D., 2013. Three large fire years threaten resilience of closed crown black spruce forests in eastern Canada. *Ecosphere*, 4(5):56.
- Bond-Lamberty, B., Peckham, S.D., Ahl, D.E. and Gower, S.T., 2007. Fire as the dominant driver of central Canadian boreal forest carbon balance. *Nature*, 450:89-92.
- Buurman, P. and Jongmans, A.G., 2005. Podzolisation and soil organic matter dynamics. *Geoderma*, 125:71-83.
- Carrier, A., 1996. Contribution de l'imagerie satellitaire NOAA à la cartographie des grands feux de forêt du Québec boréal : 1972 à 1994. Maîtrise en ressources renouvelables, Université du Québec à Chicoutimi, Chicoutimi.
- Chabot, M., Blanchet, P., Drapeau, P., Fortin, F., Gauthier, S., Imbeau, L., Lacasse, G., Lemaire, G., Nappi, A., Quenneville, R. and Thiffault, E., 2009. Le feu en milieu forestier. In: Manuel De Foresterie (2^{ème} Édition). Ordre des ingénieurs forestiers du Québec. Éditions MultiMondes, Québec., pp. 1037-1090.
- Cusack, D.F., Chadwick, O.A., Hockaday, W.C. and Vitousek, P.M., 2012. Mineralogical controls on soil black carbon preservation. *Global Biogeochem. Cycles*, 26:2019.
- Cyr, D., Gauthier, S. and Bergeron, Y., 2007. Scale-dependent determinants of heterogeneity in fire frequency in a coniferous boreal forest of eastern Canada. *Landscape Ecol.*, 22:1325-1339.

- Czimczik, C.I., Schmidt, M.W.I. and Schulze, E., 2005. Effects of increasing fire frequency on black carbon and organic matter in Podzols of Siberian Scots pine forests. *Eur. J. Soil Sci.*, 56:417-428.
- Czimczik, C.I. and Masiello, C.A., 2007. Controls on black carbon storage in soils. *Global Biogeochem. Cycles*, 21.
- Eckmeier, E., Egli, M., Schmidt, M.W.I., Schlumpf, N., Nötzli, M., Minikus-Stary, N. and Hagedorn, F., 2010. Preservation of fire-derived carbon compounds and sorptive stabilisation promote the accumulation of organic matter in black soils of the Southern Alps. *Geoderma*, 159:147-155.
- Flannigan, M.D., Krawchuk, M.A., de Groot, W.J., Wotton, B.M. and Gowman, L.M., 2009. Implications of changing climate for global wildland fire. *Int. J. Wildland Fire*, 18:483-507.
- González-Pérez, J.A., González-Vila, F.J., Almendros, G. and Knicker, H., 2004. The effect of fire on soil organic matter - a review. *Environ. Int.*, 30:855-870.
- Guggenberger, G., Rodionov, A., Shibistova, O., Grabe, M., Kasansky, O.A., Fuchs, H., Mikheyeva, N., Zrazhevskaya, G. and Flessa, H., 2008. Storage and mobility of black carbon in permafrost soils of the forest tundra ecotone in Northern Siberia. *Global Change Biol.*, 14:1367-1381.
- Hammes, K., Torn, M.S., Lapenas, A.G. and Schmidt, M.W.I., 2008. Centennial black carbon turnover observed in a Russian steppe soil. *Biogeosciences*, 5:1339-1350.
- Harden, J.W., O'Neill, K.P., Trumbore, S.E., Veldhuis, H. and Stocks, B.J., 1997. Moss and soil contributions to the annual net carbon flux of a maturing boreal forest. *J. Geophys. Res.*, 102:28,805-28,816.
- Harden, J.W., Trumbore, S.E., Stocks, B.J., Hirsch, A., Gower, S.T., O'Neill, K.P. and Kasischke, E.S., 2000. The role of fire in the boreal carbon budget. *Global Change Biol.*, 6:174-184.

- Hatten, J.A. and Zabowski, D., 2009. Changes in soil organic matter pools and carbon mineralization as influenced by fire severity. *Soil Sci. Soc. Am. J.*, 73:262-273.
- Hockaday, W.C., Grannas, A.M., Kim, S. and Hatcher, P.G., 2006. Direct molecular evidence for the degradation and mobility of black carbon in soils from ultrahigh-resolution mass spectral analysis of dissolved organic matter from a fire-impacted forest soil. *Org. Geochem.*, 37:501-510.
- Kalra, Y.P. and Maynard, D.G., 1991. *Methods manual for forest soil and plant analysis*. Information Report, NOR-X-319E:116.
- Kane, E.S., Kasischke, E.S., Valentine, D.W., Turetsky, M.R. and McGuire, A.D., 2007. Topographic influences on wildfire consumption of soil organic carbon in interior Alaska: Implications for black carbon accumulation. *J. Geophys. Res.*, 112.
- Kane, E.S., Hockaday, W.C., Turetsky, M.R., Masiello, C.A., Valentine, D.W., Finney, B. and Baldock, J.A., 2010. Topographic controls on black carbon accumulation in Alaskan black spruce forest soils: implications for organic matter dynamics. *Biogeochemistry*, 100:39-56.
- Kasischke, E.S. and Stocks, B.J., 2000. Fire, Climate Change, and Carbon Cycling in the Boreal Forest. 138:461.
- Kasischke, E., 2000. Boreal ecosystems in the global carbon cycle. In: E. Kasischke and B. Stocks (Editors). *Fire, Climate Change, and Carbon Cycling in the Boreal Forest*. Springer-Verlag, New-York, pp. 19-30.
- Kurth, V.J., MacKenzie, M.D. and DeLuca, T.H., 2006. Estimating charcoal content in forest mineral soils. *Geoderma*, 137:135-139.
- Lefort, P., Leduc, A., Gauthier, S. and Bergeron, Y., 2004. Recent fire regime (1945-1998) in the boreal forest of western Quebec. *Ecoscience*, 11:433-445.

- McKeague, J.A., 1967. An evaluation of 0.1 M pyrophosphate and pyrophosphate-dithionite in comparison with oxalate as extractants of the accumulation products in Podzols and some other soils. *Can. J. Soil Sci.*, 47:95-99.
- Neff, J.C., Harden, J.W. and Gleixner, G., 2005. Fire effects on soil organic matter content, composition, and nutrients in boreal interior Alaska. *Can. J. For. Res.*, 35:2178-2187.
- Périé, C. and Ouimet, R., 2008. Organic carbon, organic matter and bulk density relationships in boreal forest soils. *Can. J. Soil Sci.*, 88:315-325.
- Preston, C.M., 2009. Biogeochemistry: Fire's black legacy. *Nature Geosci*, 2:674-675.
- Preston, C.M., Bhatti, J.S., Flanagan, L. and Norris, C.E., 2006. Stocks, chemistry, and sensitivity to climate change of dead organic matter along the Canadian boreal forest transect case study. *Clim. Change*, 74:223-251.
- Preston, C.M. and Schmidt, M.W.I., 2006. Black (pyrogenic) carbon in boreal forests: a synthesis of current knowledge and uncertainties. *Biogeosciences*, 3:397-420.
- Robitaille, A. and Saucier, J., 1998. *Paysages Régionaux Du Québec Méridional*. Les Publications du Québec, Sainte-Foy, Québec.
- Rodionov, A., Amelung, W., Haumaier, L., Urusevskaja, I. and Zech, W., 2006. Black carbon in the zonal steppe soils of Russia. *Z. Pflanzenernähr. Bodenk*, 169:363-369.
- Sanborn, P., Lamontagne, L. and Hendershot, W., 2011. Podzolic soils of Canada: Genesis, distribution, and classification. *Can. J. Soil Sci.*, 91:1-38.
- Saucier, J., Berger, J., D'Avignon, H. and Racine, P., 1994. Le point d'observation écologique: normes techniques.
- Saucier, J., Grondin, P., Robitaille, A. and Bergeron, J., 2001. *Zones De Végétation Et Les Domaines Bioclimatiques Du Québec*. Gouvernement du Québec, Ministère des Ressources naturelles, Québec.

- Schaetzl, R.J. and Mokma, D.L., 1988. A numerical index of Podzol and Podzolic soil development. *Physical Geography*, 9:232-246.
- Six, J., Elliott, E.T., Paustian, K. and Doran, J.W., 1998. Aggregation and soil organic matter accumulation in cultivated and native grassland soils. *Soil Sci. Soc. Am. J.*, 62:1367-1377.
- Six, J., Elliott, E.T. and Paustian, K., 2000. Soil macroaggregate turnover and microaggregate formation: a mechanism for C sequestration under no-tillage agriculture. *Soil Biol. Biochem.*, 32:2099-2103.
- Six, J., Conant, R.T., Paul, E.A. and Paustian, K., 2002. Stabilization mechanisms of soil organic matter: Implications for C-saturation of soils. *Plant Soil*, 241:155-176.
- Soil Classification Working Group, 1998. *The Canadian System of Soil Classification - Third Edition*. 1646 (Revised):187.
- Sorge, C., Schnitzer, M., Leinweber, P. and Schulten, H., 1994. Molecular-chemical characterization of organic matter in whole soil and particle-size fractions of a Spodosol by pyrolysis-field Ionization Mass Spectrometry. *Soil Sci.*, 158:189-203.
- Soucémariadin, L.N., Quideau, S.A., Derek MacKenzie, M.D., Bernard, G.M., Wasylishen, R.E., Total carbon and black carbon stocks in black spruce forest floors from eastern Canada: a quantitative study. *J. Geophys. Res.*, (submitted).
- Wiseman, C.L.S. and Püttmann, W., 2006. Interactions between mineral phases in the preservation of soil organic matter. *Geoderma*, 134:109-118.
- Wotton, B.M., Nock, C.A. and Flannigan, M.D., 2010. Forest fire occurrence and climate change in Canada. *Int. J. Wildland Fire*, 19:253-271.

Chapter 6. Conclusions

6.1. Main research objectives

This study aimed to determine the amount and fate of black carbon in podzolic soils of fire-affected Quebec black spruce forests, according to variable fire severity. In chapters 2 and 3, the principal objective was to characterize black carbon chemical and physical properties and to assess how the latter are influenced by formation conditions, in relation to fire severity. Maximum temperature emerged as the most influential factor, although charring duration and the presence of oxygen during pyrolysis also affected BC properties under specific conditions. A relative increase in fire severity on the forest floor resulted in a more condensed fresh BC layer. Chapter 4 presented results from the investigation of total carbon and black carbon stocks, as well as their distribution within the forest floor. This part of the study highlighted the importance of environmental factors such as slope position and aspect, as well as stand type (black spruce- vs. jack pine-dominated canopy vegetation) on carbon storage in Quebec black spruce forest floors after low severity fires. It also demonstrated the importance of the deepest layer of the forest floor for the organic BC stocks. Presenting an abrupt boundary with the underlying mineral soil, this horizon constitutes a mix of humified forest floor (H) and historical black carbon, and it contains most of the BC stocks. In chapter 5, the focus was switched to the mineral soil and possible black carbon stabilization mechanisms were investigated. Black carbon stocks in different parts of the soil profiles were also compared.

6.2. Specific research questions

The work presented in chapter 2 aimed to assess the influence of formation conditions on BC chemical and physical properties. Thermal treatment turns organic matter into BC. In this chapter I showed that thermal treatment had a significant influence on both the chemical and physical properties of BC originating from various types of fuel. Results obtained from artificially-produced BC confirmed the importance of maximum temperature, fuel type, duration of charring and abundance of oxygen as factors influencing BC composition and physical properties. As for the chemical properties, the type of fuel was most important for temperatures $< 250\text{ }^{\circ}\text{C}$ and up to $350\text{ }^{\circ}\text{C}$. Then, the main fuel components – namely cellulose, hemicelluloses and lignin – started to degrade and the maximum temperature became the dominant forming factor. The charring duration I selected affected the composition at both low ($250\text{ }^{\circ}\text{C}$) and high ($\geq 600\text{ }^{\circ}\text{C}$) temperatures. The presence of oxygen affected BC composition mainly at low temperature, i.e. $250\text{ }^{\circ}\text{C}$, and resulted in accelerated alkyl C degradation. The H content and yield of BC were the two attributes most sensitive to other formation factors besides maximum temperature. With increasing temperature, I observed a decrease in yield, although at $250\text{ }^{\circ}\text{C}$, the presence of oxygen also provoked a drastic decrease in yield. With increasing thermal treatment, the precursor materials underwent increasing condensation (aromatization), and the resulting BC acquired some resistant properties: they became more intrinsically stable, i.e., less susceptible to degradation. MT was the

most influential factor with respect to physical properties. There was an important increase in BC porosity (specific surface area and total pore volume) with the more severe thermal treatments. Nevertheless, BC physical features appeared to also be under the control of the type of fuel. There was a huge heterogeneity within this reference set; I was able to place BC samples on the BC continuum and to relate changes in elemental composition (atomic ratios) and specific surface area to temperature thresholds of the thermal treatment. Moss-derived BC presented distinctive chemical and physical properties; knowing the large carbon input this type of fuel represents in black spruce ecosystems (Harden et al., 1997; Harden et al., 2000; Yu et al., 2002), this finding is particularly valuable.

In Quebec black spruce forests, most 2005–2007 wildfires took place early in the fire season. Using the results from the previous chapter, I showed here that these wildfires produced forest floor BC characterized by a low aromatic:O-alkyl carbon ratios, i.e., displaying a relatively low degree of aromatization. The BC chemical properties were related to fire severity, a relative increase in fire severity inducing an increase in aromatization. But overall, the aromatic content of the BC formed by these early season wildfires was low when compared to the range of known values (e.g. atomic H/C and O/C ratios) along the BC continuum: BC samples were part of transition and amorphous chars. These results indicate limited thermal degradation and suggest a low intrinsic potential for recalcitrance. The low porosity of the analyzed samples confirmed the low temperature of formation. Overall, this chapter's results are representative of BC produced under relatively low fire severity at the soil level. They provide insight on the type of

BC that would be produced in the scenario where early season fires were to become dominant. Furthermore, variations in fire severity are still expected to occur with global warming (especially with an increase in occurrence of large fire years), at least until the end of the 21st century in Quebec. Finally, these results can help inform carbon modeling efforts for black spruce boreal forests by providing key information on the influence of low fire severity on relative recalcitrance of BC pools, as well as on the post-disturbance regeneration potential of these forests.

In chapter 4, I demonstrated that wildfires affect the quantity and quality of forest floors present in Quebec black spruce forests. Fire appeared to be a driving factor of the carbon cycle in these forests. First, complete combustion was influenced by environmental features, including slope position and aspect. Second, fire affected part of the remaining C stocks through production of more or less condensed black carbon, as shown in the previous chapter. The recent wildfires that affected my study sites were characterized by an overall low fire severity at the forest floor level. They left part of the carbon pool and much of the historical black carbon legacy intact, with the persistence of the H + historical BC layer, as well as part of the F horizon, which on occasion constituted a substantial BC reservoir. This chapter revealed that in Quebec black spruce forests, fire history, and specifically fire severity history, seemed to control BC stocks in the forest floors, as the H + historical BC layer contained the biggest BC reservoir in most profiles. In this chapter I also highlighted the need to define a standard method for BC quantitation in forest floor samples that would be as accurate but

less time consuming than ^{13}C NMR spectroscopy. This improved knowledge on BC pools is urgently needed in fire-affected ecosystems where organic materials represent a large part of the carbon pool.

In chapter 5, I looked at SOC and BC stocks in the mineral soil, and used the results from chapter 4 to compile total stocks for these podzolic soils. Here I provide much needed estimates about BC pools in Quebec boreal black spruce forests. Although the majority of BC stocks was found in forest floors, mineral horizons stored a non-negligible reservoir that amounted to 12–46% of the total stocks. Podzolic Bhf and Bf horizons contained most of the mineral BC stocks. Physical fractionation shed some light on possible BC storage mechanisms in these mineral soils. Overall, the patterns of BC accumulation in mineral soils were similar to those of SOC. Association with organo-metallic complexes appeared as the dominant mechanism at least for podzolic horizons.

6.3. Research implications

Boreal forest soils represent a massive carbon pool, whose future is at risk with the global warming associated with climate change. Currently, the world's boreal forests are considered as an overall carbon sink but regional differences have already emerged. Whether global warming will be enough to turn these forests into carbon sources through an increase in decomposition is not clear yet and contradictory results have been presented. However climate change has already started to alter disturbance regimes and this could constitute the biggest threat to the huge carbon stocks present in the thick boreal forest floors. In North

American boreal forests, changes in fire regimes resulting from climate change are of particular importance.

The effects of variations in fire regimes on BC production and stocks in boreal forests and how this could affect the carbon balance has not received much attention yet. The three large fire years that took place in Quebec boreal black spruce forests in 2005–2007 provided a unique opportunity to address this question.

The work in chapters 2 and 3 was designed to study the influence of formation conditions on BC chemical and physical properties. Chapter 2 highlights the importance of temperature on BC properties. These results made it possible to reconstruct formation conditions of the BC layer produced by the 2005–2007 wildfires in chapter 3. The work in chapter 3 also reveals that fire severity and BC chemical properties are related: an increase in fire severity on the forest floor results in a more condensed BC, hence less likely to be further decomposed. The early season wildfires selected in this study produced slightly condensed BC, which reflect only the low end of the fire severity spectrum. Nevertheless, these results can help inform carbon modeling efforts for black spruce boreal forests by providing key information on the influence of low fire severity on relative recalcitrance of BC pools, as well as on the post-disturbance regeneration potential of these forests. Variations in fire severity will likely persist in the near future especially if mega-fires become more frequent (Girardin et al., 2013), and at least part of the black spruce-feathermoss domain will experience the same fire conditions as the stands in the present study. In these first two chapters, I tried to

determine if BC inherent increased degree of aromatization would be more likely to protect it from a “fast” degradation than organic matter that was not thermally-altered. In the event of global warming alleviating the current environmental constraints on SOM decomposition in boreal ecosystems, it appears that the chemical properties of BC produced under low fire severity are similar enough to unburned forest floor that both will decompose at the same rate.

But if quality matters, the size of the BC stocks is also likely to make a difference in terms of overall carbon balance. Hence, in the last two chapters I focused on BC stocks present in these forests and how they are distributed. Chapter 4 and 5 reveal the importance of forest floor for BC stocks. The organic horizons and more specifically the almost ubiquitous presence of the H + historical BC layer is the most important soil characteristic in these forests, and what is likely to set apart Quebec black spruce forests from other boreal forests of the world in terms of BC storage. If mineral soils constitute a significant SOC pool, storing half of the total SOC present in fire-affected podzolic soils of Quebec black spruce forests, BC stocks are very dependent on the persistence of at least part of the forest floor, and specifically of the deep H + historical BC layer. Because they are concentrated in the forest floor, BC stocks are very sensitive to fire severity. A generalized increase in fire severity in Quebec black spruce forests implies higher BC temperatures of formation, which would likely generate very condensed BC, hence BC more resistant to microbial degradation. But this would also notably jeopardize total BC stocks. Finally, additional factors, such as a potential shift in species dominance from black spruce to jack pine in

these forests (Boiffin and Munson, 2013) could threaten both SOC and BC stocks. SOC and BC accumulation under jack pine is indeed much reduced compared to black spruce stands as suggested by results from chapter 4.

6.4. Study limitations and future research perspectives

The work presented in this thesis highlights the importance of BC to the carbon cycle in boreal forests soils, but it constitutes only a first step. BC stocks estimates for the Quebec black spruce forests were produced for the first time but our limited sample size did not allow to observe significant differences associated with forest types, climate, topography, or fire frequency on organic and mineral BC stocks. These factors are likely to influence BC pools, based on their known influence on SOC stocks. A more intensive study aiming at setting apart the relative influence of the various environmental factors is an essential step to a better understanding of BC storage in Quebec black spruce forests. It is also primordial for modeling purposes.

Moreover the samples in this study were collected in sites affected by early season fires, which caused fire impacts on the forest floor that were on the low side of the severity spectrum. Sampling in sites exposed to high severity fires, i.e. where most of the forest floor has been consumed by fire, would be a requirement to properly understand how BC stocks depend on fire severity and predict the future evolution in BC stocks in Quebec boreal black spruce forests with climate change.

Lastly there was a BC pool that we did not consider in these burned stands: the snags. The latter are covered with burned bark, i.e., BC, and represent a substantial BC pool, which gets added to the soil pool overtime – more or less quickly – as more bark shedding and/or windthrow occur. BC present on the snags has different characteristics from forest floor BC (especially in the case of early season fires because of the disconnection of fire behavior in the canopy and in the forest floor). The BC snags pool clearly constitutes a significant contribution in the carbon balance of fire-affected forests and deserves some attention.

The problem of BC quantification has been tackled for a few years now, but the answer to the question “what is the best method to quantify BC?” is still up for debate. The problem of BC quantitation in forest floor is also particularly highlighted in chapter 4. I was able to determine BC content in the various forest floors layers by running the molecular mixing model on the ^{13}C NMR DP spectra data. This method of BC quantitation for organic samples is not only accurate but also flexible, with the possibility to calibrate the molecular model for different ecosystems and various scenarios of fire severity by choosing the degree of the aromatization of the BC estimated. Both for characterization and quantification ^{13}C NMR spectroscopy thus proved to be informative and effective but access to a spectrometer and acquisition times are hindering the likelihood of ^{13}C NMR spectroscopy to become routine analysis. Specifically, acquisition times are prohibitive when analyzing a large number of samples.

Further ^{13}C NMR experiments, including spectral editing techniques, could also be conducted on these samples. The non-quaternary suppression (NQS) technique, also called dipolar dephasing, has often been used in characterization studies of char (e.g., Smernik et al., 2000; Knicker et al., 2005; Brewer et al., 2009) or organic matter (e.g., Smernik and Oades, 2001; Cao et al., 2011). This relatively straightforward technique allows quaternary carbon atoms to be distinguished from those with one or two directly-bonded protons. The NQS pulse sequence uses a time period when the proton decoupling is switched off. During this time, the signals due to carbon nuclei with shorter spin-spin relaxation times (T_2) such as methane and methylene carbons, decay rapidly and only carbons not directly attached to hydrogens and carbons from methyl groups contribute significantly to the spectrum (Axelson, 2012).

Regarding the BC stored in the H horizon, radiocarbon dating of the historical BC layer would help to confirm the hypothesis that BC in this layer has been accumulated over several fire cycles. This could provide some insight on how frequently very high severity fires occurs in the black spruce-feathermoss domain. Radiocarbon dating in the mineral soil, could give further insight on the actual BC storage in podzolic B horizons. Dubois et al. (1990) showed that organic matter contained within podzolic horizons turns over rapidly (a few years up to 420 ± 120 years), and it would be interesting to test if BC residence time is somewhat longer. Further, fractionation studies with measurement of pyrophosphate-extractable iron and aluminum in fractions would also help to more fully elucidate BC stabilization processes.

6.5. Conclusion

BC plays a significant role in carbon sequestration in Quebec boreal black spruce forests as it represents a significant part of the carbon stocks present. It accumulates in these forests, principally in the forest floors. BC properties and stocks are under the influence of fire severity. Under low fire severity in the forest floor, a good portion of the SOC stocks persists and BC stocks remain mostly unaffected in Quebec black spruce forests. Global warming associated with climate change constitutes a serious threat for both SOC and BC storage, through modification of fire regimes. The increase in frequency of large fires years could trigger a shift in species dominance from black spruce to jack pine. Black spruce promotes forest floor accumulation, hence C storage but also BC storage through the presence of the H + historical BC layer, whereas jack pine-dominated stands are generally associated with limited C and BC storage. In these stands BC stocks are also more likely to get consumed by successive fires.

List of references

- Axelsson, D.E., 2012. Solid State Nuclear Magnetic Resonance. A Practical Introduction, 1st Edition. MRI_Consulting, Lexington, KY.
- Boiffin, J., Munson, A.D., 2013. Three large fire years threaten resilience of closed crown black spruce forests in eastern Canada. *Ecosphere* 4(5):56.
- Brewer, C.E., Schmidt-Rohr, K., Satrio, J.A., Brown, R.C., 2009. Characterization of biochar from fast pyrolysis and gasification systems. *Environmental Progress & Sustainable Energy* 28, 386-396.
- Cao, X., Oik, D.C., Chappell, M.A., Cambardella, C.A., Miller, L.F., Mao, J., 2011. Solid-state NMR analysis of soil organic matter fractions from integrated physical-chemical extraction. *Soil Science Society of America Journal* 75, 1374-1384.
- Dubois, J.M., Martel, Y.A., Nadeau, D., Côté, L., 1990. Les ortsteins du Québec: Répartition géographique, relations géomorphologiques et essai de datation. *The Canadian Geographer* 34, 303-317.
- Girardin, M.P., Ali, A.A., Carcaillet, C., Gauthier, S., Hély, C., Le Goff, H., Terrier, A., Bergeron, Y., 2013. Fire in managed forests of eastern Canada: Risks and options. *Forest Ecology and Management; The Mega-fire reality* 294, 238-249.
- Harden, J.W., O'Neill, K.P., Trumbore, S.E., Veldhuis, H., Stocks, B.J., 1997. Moss and soil contributions to the annual net carbon flux of a maturing boreal forest. *Journal of Geophysical Research* 102, 28,805-28,816.
- Harden, J.W., Trumbore, S.E., Stocks, B.J., Hirsch, A., Gower, S.T., O'Neill, K.P., Kasischke, E.S., 2000. The role of fire in the boreal carbon budget. *Global Change Biology* 6, 174-184.
- Knicker, H., Totsche, K.U., Almendros, G., González-Vila, F.J., 2005. Condensation degree of burnt peat and plant residues and the reliability of solid-state VACP MAS ¹³C

NMR spectra obtained from pyrogenic humic material. *Organic Geochemistry* 36, 1359-1377.

Smernik, R.J., Skjemstad, J.O., Oades, J.M., 2000. Virtual fractionation of charcoal from soil organic matter using solid state ^{13}C NMR spectral editing. *Australian Journal of Soil Research* 38, 665-683.

Smernik, R.J., Oades, J.M., 2001. Solid-state ^{13}C -NMR dipolar dephasing experiments for quantifying protonated and non-protonated carbon in soil organic matter and model systems. *European Journal of Soil Science* 52, 103-120.

Yu, Z., Apps, M.J., Bhatti, J.S., 2002. Implications of floristic and environmental variation for carbon cycle dynamics in boreal forest ecosystems of central Canada. *Journal of Vegetation Science* 13, 327-340.

Appendices

Table 2-A.1. Details of the charring experiments including the maximum temperature (MT), charring duration and the pyrolysis type (partial or complete); na: not available

MT (°C)	75	75	250	250	250	425	425	425	600	600	600	800
charring duration (h)	24	24	24	12	24	6	6	12	0.5	0.5	6	0.5
pyrolysis type ^a	T	SB	T	SB	SB	T	SB	SB	T	SB	SB	SB
Black spruce bark	na		na			na						
Black spruce needles			na			na				na		
Black spruce branch			na			na			na			
<i>Rhododendron g.</i>	na		na			na			na			
<i>Pleurozium</i>	na											
<i>Sphagnum</i>	na											

^a T (tin): partial pyrolysis; SB (sand-bath): complete pyrolysis

Table 2-B.1. Results from ^{13}C NMR direct polarization (DP) and variable-amplitude cross polarization (VACP) experiments, including spin counting (C_{obs} , where 100% indicates a fully quantitative spectrum) and the relative intensity (% total spectral area) of carbonyl C, aromatic and phenolic C, O-alkyl C and alkyl C.

Fuel	MT	DP- C_{obs}	Carbonyl	DP			Carbonyl	VACP		
				Aromatic & phenolic	O-alkyl	Alkyl		Aromatic & phenolic	O-alkyl	Alkyl
	(°C)	(%)		(% total spectral area)				(% total spectral area)		
<i>Sphagnum</i>	250	84.1	10.6	61.3	7	21.1	5.6	60.4	7.2	26.7
<i>Sphagnum</i> ^a	250	92	15.1	78.4	2	4.5	13.9	75.8	4.1	6.2
<i>Sphagnum</i>	350	78.1	3.8	74.6	5	16.6	1.8	75.2	4.9	18.1
<i>Sphagnum</i>	425	80	6.5	83.4	-0.8	10.9	0.5	82.2	4.3	13
<i>Sphagnum</i>	600	74.6	5.5	89.6	-1.9	6.9	1.4	88.3	1	9.3
Black spruce branch	75	77.5	6.7	26.9	58.5	8	1.3	18.4	71.4	9
Black spruce branch	250	88.7	8.5	46.2	23.5	21.8	3.3	41	34.9	20.8
Black spruce branch	350	68.2	3.8	74.4	4.6	17.2	1.2	71.7	7.3	19.8
Black spruce branch	425	121.2	5.4	80.9	3	10.8	0.8	82.7	3.4	13.1
Black spruce branch	600	94.3	4.2	83.6	1.9	10.2	0.6	85	2.5	11.9

^a BC produced in a tin (presence of oxygen).

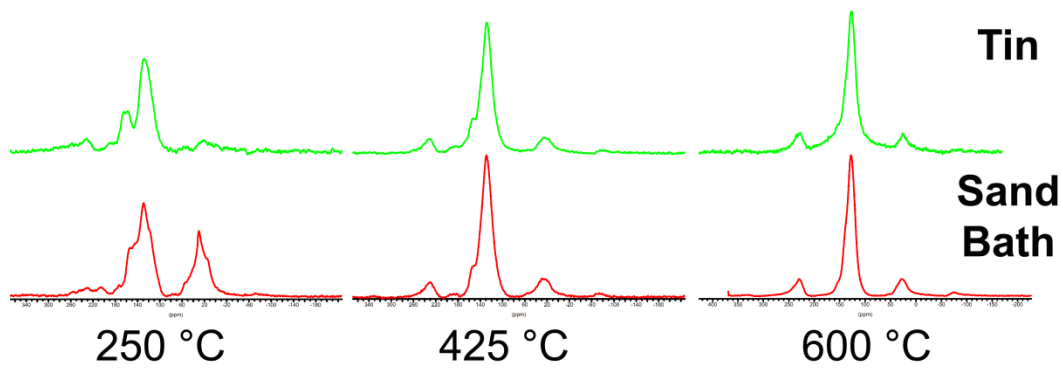


Figure 2-C.1. ¹³C VACP NMR spectra of *Sphagnum* BC produced at three MTs (250 °C; 425 °C; 600 °C) under two different pyrolysis treatments (partial O₂ – tin – and no O₂ – sand bath).

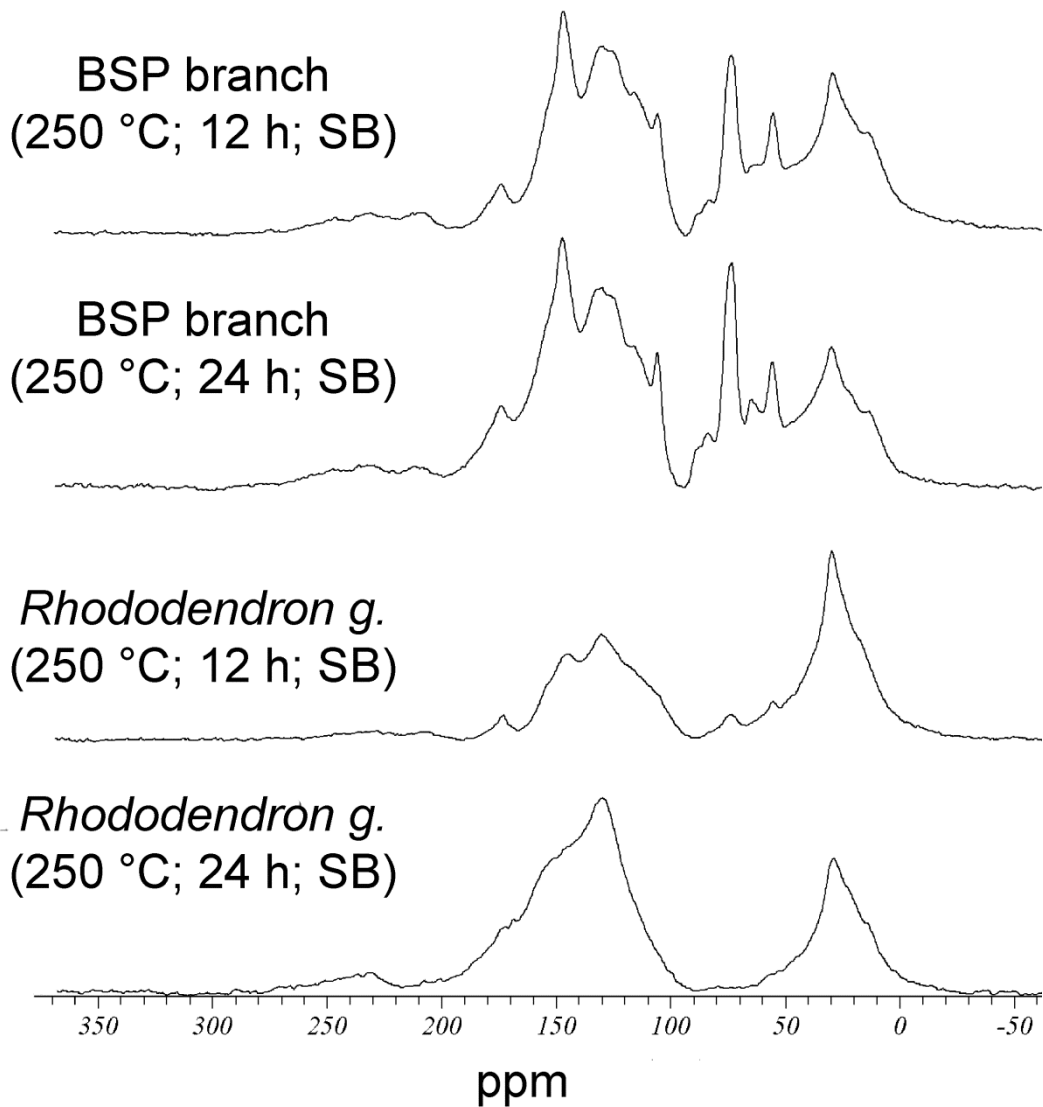


Figure 2-C.2. ^{13}C VACP NMR spectra of black spruce (BSP) branch and *Rhododendron groenlandicum* BC produced at 250 °C with two charring durations (12 h vs. 24 h) under full pyrolysis (sand bath – SB).

Table 3-A.1. Results of the spin counting obtained with a DP experiment for a subset of BC produced by wildfire. C_{obs} represents the amount of carbons that were observed, a C_{obs} of 100 % indicating a fully quantitative spectrum. For comparison, the fire severity, evaluated on the microsite where the BC was sampled, is provided.

sample	DP-Cobs	severity
fresh BC #246	90.78%	low (class 0)
fresh BC #266	82.38%	intermediate (class 2)
fresh BC #128	65.83%	high (class 5)

Table 4-A.1. Characteristics of the 23 soil profiles and their fire site.

ID soil profile	fire site	latitude (°N)	longitude (°W)	altitude (m)	zone ^a	Fire cycle (yrs)	MAP ^b (mm)	MAT ^c (°C)	drainage class	stand type ^d	slope position	aspect	fire year	mean pre-fire stand age (yrs) ^e
1	8	50°19'40.9"	72°03'02.2"	531	Saguenay & Ashuapmushuan	> 500	950	-0.5	Moderately well drained	JP	upslope	W	2005	84 (22)
2	8	50°18'31.1"	72°04'20.5"	482	Saguenay & Ashuapmushuan	> 500	950	-0.5	Moderately well drained	BSP	midslope	W	2005	84 (22)
3	9	49°16'59.0"	73°54'23.1"	384	Saguenay & Ashuapmushuan	> 500	950	-0.5	Moderately well drained	JP	midslope	S	2005	99 (49)
4	9	49°19'31.7"	73°53'27.3"	413	Saguenay & Ashuapmushuan	> 500	950	-0.5	Well drained	JP	midslope	E	2005	99 (49)
5	10	49°04'07.9"	74°21'04.4"	446	Saguenay & Ashuapmushuan	> 500	950	-0.5	Poorly drained	BSP	midslope	S	2007	83 (5)
6	14	50°50'28.2"	68°59'08.0"	461	North-Shore	> 1000	1100	-1.25	Poorly drained	BSP	depression	W	2007	115 (30)
7	14	50°49'51.0"	68°59'53.9"	479	North-Shore	> 1000	1100	-1.25	Poorly drained	BSP	upslope	NW	2007	115 (30)
8	13	50°33'57.0"	68°49'56.8"	456	North-Shore	> 1000	1100	-1.25	Well drained	JP	upslope	N	2005	81 (19)
9	13	50°34'58.1"	68°46'16.5"	428	North-Shore	> 1000	1100	-1.25	Moderately well drained	BSP	upslope	W	2005	81 (19)
10	7	50°21'32.0"	73°42'01.0"	385	Chibougamau	200–500	950	-1.25	Well drained	JP	midslope	S	2006	109 (8)
11	7	50°21'44.7"	73°42'33.4"	397	Chibougamau	200–500	950	-1.25	Well drained	JP	midslope	SE	2006	109 (8)
12	6	50°23'29.3"	73°57'38.2"	387	Chibougamau	200–500	950	-1.25	Moderately well drained	BSP	toe	E	2006	99 (51)
13	6	50°20'06.6"	73°55'25.6"	412	Chibougamau	200–500	950	-1.25	Moderately well drained	BSP	midslope	NW	2006	134 (23)
14	1	50°36'08.7"	74°46'29.0"	405	East Baie-James	< 200	830	-1.75	Moderately well drained	BSP	midslope	NW	2005	78 (7)

15	1	50°36'06.4"	74°46'59.5"	411	East Baie-James	< 200	830	-1.75	Moderately well drained	BSP	downslope	E	2005	78	(7)
16	2	50°42'57.7"	74°46'49.0"	382	East Baie-James	< 200	830	-1.75	Moderately well to imperfectly drained	BSP	midslope	ENE	2005	94	(28)
17	3	50°59'27.7"	75°13'27.3"	342	East Baie-James	< 200	830	-1.75	Well to moderately well drained	BSP	downslope	W	2007	72	(7)
18	3	50°58'45.0"	75°13'25.7"	347	East Baie-James	< 200	830	-1.75	Moderately well drained	BSP	downslope	SW	2007	72	(7)
19	4	49°58'41.5"	74°34'31.4"	385	Chibougamau	200–500	950	-1.25	Moderately well drained	BSP	midslope	W	2007	103	(27)
20	12	50°31'02.8"	76°20'59.0"	303	West Baie-James	> 500	825	-1.25	Moderately well drained	BSP	downslope	NW	2005	74	(7)
21	12	50°30'44.0"	76°21'11.4"	301	West Baie-James	> 500	825	-1.25	Imperfectly drained	BSP	depression	NW	2005	74	(7)
22	11	50°29'31.0"	76°33'21.0"	288	West Baie-James	> 500	825	-1.25	Moderately well drained	JP	upslope	W	2007	106	(2)
23	11	50°28'39.2"	76°34'31.2"	299	West Baie-James	> 500	825	-1.25	Moderately well drained	BSP	depression	W	2007	106	(2)

^a zones of homogeneous fire cycle and climatic conditions; ^b mean annual precipitation; ^c mean annual temperature; ^d stand type: black spruce-dominated (BSP) vs. jack pine-dominated (JP); ^e data (mean and associated SD) from Boiffin and Munson (2013)

Table 4-B.1. Assignment of ^{13}C NMR signal intensity in the spectral regions associated with the char component of the molecular mixing model (default and adjusted models) and their properties; na: not available.

Spectral region (ppm)	MMM	MMM version	
	char	MMM-1 class 5 fresh BC	MMM-2 lab-BC
0–45	0	17	0.8
45–60	1.7	3.8	-0.9
60–95	1.8	13.2	3.7
95–110	5.3	5.2	6.7
110–145	72.1	34.9	83.8
145–165	15.2	14.2	6.2
165–215	3.9	11.6	-0.3
Proportion of char in the sample (%) – estimated by default Baldock MMM	100	53.85	97.1
Fuel		duff	BSP needles
Maximum temperature (°C)	Adjusted using 9 charcoal spectra obtained by J. Skjemstad for a variety of materials	na	600
Duration of charring (h)		na	0.5
Conditions of pyrolysis ^a		SB?	Tin
C content ^b (%)		57.9	78.6

^a partial pyrolysis = tin; full pyrolysis = SB; ^b on a dry weight, ash-free basis

Table 4-C.1. Results of Pearson and non-parametric rank correlation analyses (n = 15).

variable 1	variable 2	Pearson ρ	Spearman rank ρ	p	R ²
BC _{DP+MMM} ^a	C content		0.585	0.0002	0.34
	H/C atomic ratio		-0.897	***	0.80
	PI ^b (DP)	-0.873		***	0.76
	DoA ^c (DP)		0.992	***	0.98
	BC _{DP+MMM-1}	0.964		***	0.93
	BC _{DP+MMM-2}	0.998		***	1.00
BC _{DP+MMM-1}	BC _{CP+MMM-1}	0.936		***	0.88
	BC _{DP+MMM-2}	0.946		***	0.89
BC _{DP+MMM-2}	BC _{CP+MMM-2}		0.922	***	0.85
DoA ^c (CP)	DoA ^c (DP)		0.936	***	0.88
PI ^b (CP)	PI ^b (DP)	0.977		***	0.95

^a BC as percentage of total SOC; ^b Polarity index calculated from ¹³C NMR (CP) or (DP) data; ^c Degree of aromatization calculated from ¹³C NMR (CP) or (DP) data

Table 4-D.1. Results from ^{13}C NMR direct polarization (DP) and variable-amplitude cross polarization (VACP) experiments, including spin counting (Cobs, where 100% indicates a fully quantitative spectrum), the relative intensity (% total spectral area) of alkyl C, N-alkyl and methoxyl C, O-alkyl C, di-O-alkyl C, aromatic C, phenolic C, and amide and carboxyl C, as well as the degree of aromatization and the polarity index.

sample	DP									
	DP- C _{obs} (%)	Alkyl	N-Alkyl / Methoxyl	O- Alkyl	Di-O- Alkyl	Aromatic	Phenolic	Amide / Carboxyl	DoA ^a	Polarity Index ^b
	(% total spectral area)									
P22 fresh BC	82.6	17.6	3.2	23.1	7.1	20.6	10.8	17.6	0.62	1.20
P22 F	82.2	24.6	4.7	30.3	8.6	12.1	7.6	12.1	0.29	1.33
P22 H + historical BC	80.5	13.3	2.0	8.3	4.8	38.8	13.9	18.9	1.85	0.61
P22 historical BC	92.7	5.3	1.1	4.2	3.3	54.6	14.1	17.3	4.94	0.42
P16 fresh BC	86.2	19.5	3.7	33.4	7.0	13.3	6.4	16.6	0.31	1.76
P16 F	89.9	18.1	4.2	30.3	9.4	14.4	8.3	15.3	0.37	1.58
P16 H + historical BC	103.0	11.5	1.2	7.2	4.6	44.0	14.3	17.3	2.38	0.50
P4 fresh BC	89.1	17.4	4.4	35.9	9.8	13.1	6.8	12.7	0.29	1.85
P4 H + historical BC	82.2	19.9	3.6	17.5	6.0	24.9	10.7	17.5	0.76	0.90
P9 H + historical BC	82.1	19.7	4.8	15.9	5.0	26.3	10.4	17.9	0.81	0.86
P19 fresh BC	84.3	12.5	2.5	12.5	7.5	35.0	15.0	15.0	1.43	0.70
P19 H + historical BC	94.7	17.5	5.0	22.5	7.5	20.0	10.0	17.5	0.57	1.22
P8 H + historical BC	84.9	12.5	2.5	17.5	5.0	35.0	12.5	15.0	1.27	0.74
P2 F	94.7	20.1	2.8	17.1	6.2	24.7	10.8	18.3	0.77	0.96
P23 H + historical BC	77.0	19.1	2.5	13.4	5.0	30.5	12.0	17.6	1.07	0.71

VACP									
sample	Alkyl	N-Alkyl / Methoxyl	O- Alkyl	Di-O- Alkyl	Aromatic	Phenolic	Amide / Carboxyl	DoA ^a	Polarity Index ^b
(% total spectral area)									
P22 fresh BC	18.1	5.1	46.1	9.8	13.9	3.5	3.5	0.22	1.86
P22 F	21.4	5.7	45.3	8.6	7.9	3.2	8.0	0.14	2.16
P22 H + historical BC	25.8	6.2	25.6	5.8	25.6	5.5	5.5	0.49	0.76
P22 historical BC	17.8	4.8	14.5	4.7	45.3	6.8	6.1	1.24	0.46
P16 fresh BC	20.7	9.3	45.3	8.3	5.6	3.1	7.7	0.10	2.48
P16 F	21.3	9.0	53.1	10.2	6.8	0.6	-1.1	0.08	2.26
P16 H + historical BC	18.5	4.8	28.2	6.9	28.7	8.0	4.8	0.63	0.84
P4 fresh BC	13.8	2.7	53.4	10.7	9.5	3.0	6.9	0.15	3.00
P4 H + historical BC	23.7	5.8	35.4	8.4	17.6	4.4	4.7	0.30	1.21
P9 H + historical BC	25.4	7.5	30.4	5.2	15.1	5.2	11.2	0.30	1.26
P19 fresh BC	20.7	7.5	35.7	8.1	19.0	4.9	4.1	0.33	1.29
P19 H + historical BC	23.3	7.9	40.3	7.5	10.8	3.4	6.6	0.18	1.71
P8 H + historical BC	19.3	4.9	35.0	6.6	19.9	5.7	8.6	0.39	1.29
P2 F	22.0	5.1	36.7	6.4	13.2	5.7	11.0	0.27	1.55
P23 H + historical BC	21.2	4.2	25.0	4.8	19.8	9.5	15.6	0.53	1.11

^a degree of aromatization (DoA) defined by ratio of (aromatic C) to (aliphatic + O-containing C) from ¹³C NMR spectra data (i.e. ratio of the [165–110 ppm]/[110–0 ppm] regions); ^b Polarity Index defined by ratio of (carboxyl and amide C + O/N-alkyl C) to (phenolic C + aromatic C + alkyl C) from ¹³C NMR spectra data (i.e. ratio of the [(215–165) + (110–45) ppm]/[(160–110) + (45–0) ppm] regions)

Table 5-A.1. Characteristics of the 23 soil profiles and their fire site, including BC stocks (in fine-earth; coarse particles; total).

soil profile	fire site	latitude (°N)	longitude (°W)	altitude (m)	zone ^a	Fire cycle (yrs)	MAP ^b (mm)	MAT ^c (°C)	drainage class	POD Index ^d	soil type ^e	stand type ^f	soil BC stock (g C·m ⁻²)	BC stock from coarse BC particle (g C·m ⁻²)	total BC stock (kg C·m ⁻²)
1	8	50°19'40.9"	72°03'02.2"	531	Saguenay & Ashuapmushuan	> 500	950	-0.5	Moderately well drained	12	humo-ferric PODZOL	JP	141.3	0.0	0.14
2	8	50°18'31.1"	72°04'20.5"	482	Saguenay & Ashuapmushuan	> 500	950	-0.5	Moderately well drained	28	ferro-humic PODZOL	BSP	250.5	0.0	0.25
3	9	49°16'59.0"	73°54'23.1"	384	Saguenay & Ashuapmushuan	> 500	950	-0.5	Moderately well drained	40	humo-ferric PODZOL	JP	290.2	1.2	0.29
4	9	49°19'31.7"	73°53'27.3"	413	Saguenay & Ashuapmushuan	> 500	950	-0.5	Well drained	32	humo-ferric PODZOL	JP	285.6	0.0	0.29
5	10	49°04'07.9"	74°21'04.4"	446	Saguenay & Ashuapmushuan	> 500	950	-0.5	Poorly drained	31	humo-ferric PODZOL	BSP	602.9	61.4	0.66
6	14	50°50'28.2"	68°59'08.0"	461	North-Shore	> 1000	1100	-1.25	Poorly drained	32	humo-ferric PODZOL	BSP	584.9	2.0	0.59
7	14	50°49'51.0"	68°59'53.9"	479	North-Shore	> 1000	1100	-1.25	Poorly drained	20	humo-ferric PODZOL	BSP	199.6	0.0	0.20
8	13	50°33'57.0"	68°49'56.8"	456	North-Shore	> 1000	1100	-1.25	Well drained	6	humo-ferric PODZOL	JP	89.1	0.2	0.09
9	13	50°34'58.1"	68°46'16.5"	428	North-Shore	> 1000	1100	-1.25	Moderately well drained	24	ferro-humic PODZOL	BSP	504.5	1.8	0.51
10	7	50°21'32.0"	73°42'01.0"	385	Chibougamau	200–500	950	-1.25	Well drained	2	humo-ferric PODZOL	JP	178.5	0.0	0.18
11	7	50°21'44.7"	73°42'33.4"	397	Chibougamau	200–500	950	-1.25	Well drained	8	humo-ferric PODZOL	JP	105.2	28.8	0.13
12	6	50°23'29.3"	73°57'38.2"	387	Chibougamau	200–500	950	-1.25	Moderately well drained	3	humo-ferric PODZOL	BSP	352.6	0.0	0.35

13	6	50°20'06.6"	73°55'25.6"	412	Chibougamau	200–500	950	-1.25	Moderately well drained	13	humo-ferric PODZOL	BSP	193.4	0.0	0.19
14	1	50°36'08.7"	74°46'29.0"	405	East Baie-James	< 200	830	-1.75	Moderately well drained	4	humo-ferric PODZOL	BSP	150.7	21.1	0.17
15	1	50°36'06.4"	74°46'59.5"	411	East Baie-James	< 200	830	-1.75	Moderately well drained	2.5	humo-ferric PODZOL	BSP	101.8	0.0	0.10
16	2	50°42'57.7"	74°46'49.0"	382	East Baie-James	< 200	830	-1.75	Moderately well to imperfectly drained	20	humo-ferric PODZOL	BSP	443.1	40.6	0.48
17	3	50°59'27.7"	75°13'27.3"	342	East Baie-James	< 200	830	-1.75	Well to moderately well drained	3	humo-ferric PODZOL	BSP	148.5	0.0	0.15
18	3	50°58'45.0"	75°13'25.7"	347	East Baie-James	< 200	830	-1.75	Moderately well drained	8	humo-ferric PODZOL	BSP	131.3	0.0	0.13
19	4	49°58'41.5"	74°34'31.4"	385	Chibougamau	200–500	950	-1.25	Moderately well drained	7.5	ferro-humic PODZOL	BSP	204.6	0.0	0.20
20	12	50°31'02.8"	76°20'59.0"	303	West Baie-James	> 500	825	-1.25	Moderately well drained	12	humo-ferric PODZOL	BSP	148.6	4.7	0.15
21	12	50°30'44.0"	76°21'11.4"	301	West Baie-James	> 500	825	-1.25	Imperfectly drained	20	humo-ferric PODZOL	BSP	108.2	0.0	0.11
22	11	50°29'31.0"	76°33'21.0"	288	West Baie-James	> 500	825	-1.25	Moderately well drained	56	ferro-humic PODZOL	JP	166.9	2.1	0.17
23	11	50°28'39.2"	76°34'31.2"	299	West Baie-James	> 500	825	-1.25	Moderately well drained	7	ferro-humic PODZOL	BSP	248.8	1.3	0.25

^a zones of homogeneous fire cycle and climatic conditions; ^b mean annual precipitation; ^c mean annual temperature; ^d (calculated) using the definition from Schaetzl and Mokma (1988); ^e Canadian Soil Classification; ^f stand type: black spruce-dominated (BSP) vs. jack pine-dominated (JP).